NASA Tech Briefs

National Aeronautics and Space Administration

July/August 1986
Volume 10 Number 4

Kennedy Space Center: The Work Continues

Artificial intelligence and robotics: giving machines the ability to sense, reason and act.

Much as it may hurt to think so, many things might be done better by independently functioning machines than by humans. Certain tasks may require superhuman precision or speed, or need to be done where humans can't go. Martin Marietta is creating systems that combine the ability to sense, reason and take action—to function autonomously and intelligently. And we are exploring ways to put them to work on a variety of tasks.

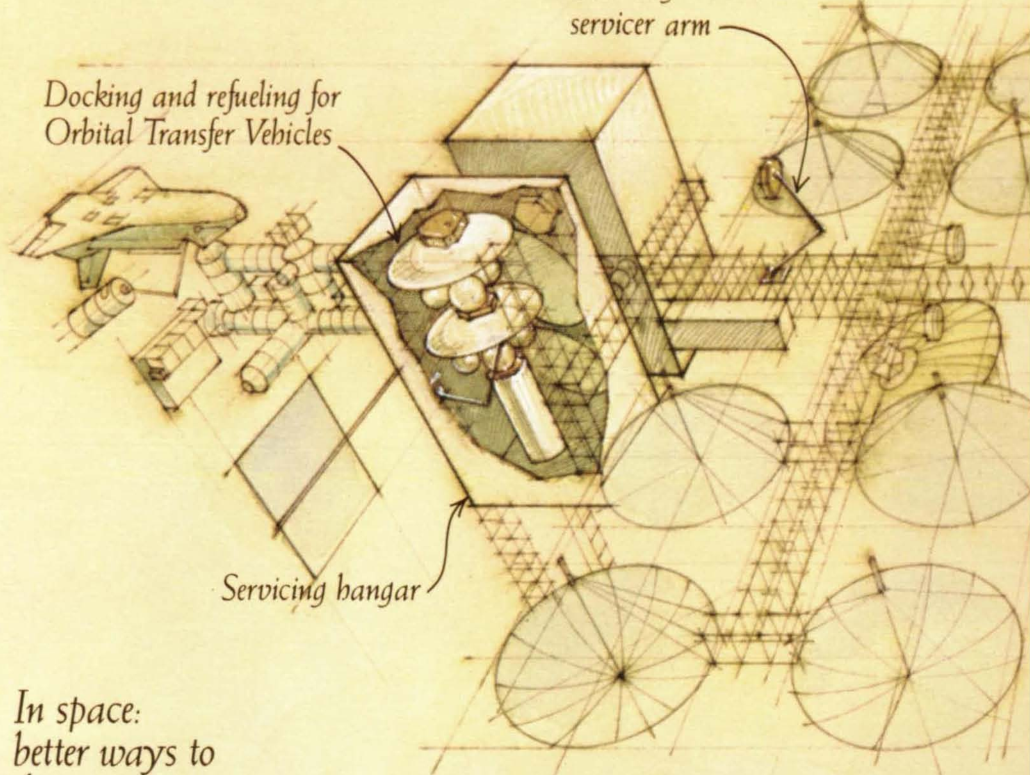

In space: better ways to do servicing.

NASA's manned space station and orbiting satellites will require the use of many robotic devices driven by artificial intelligence.

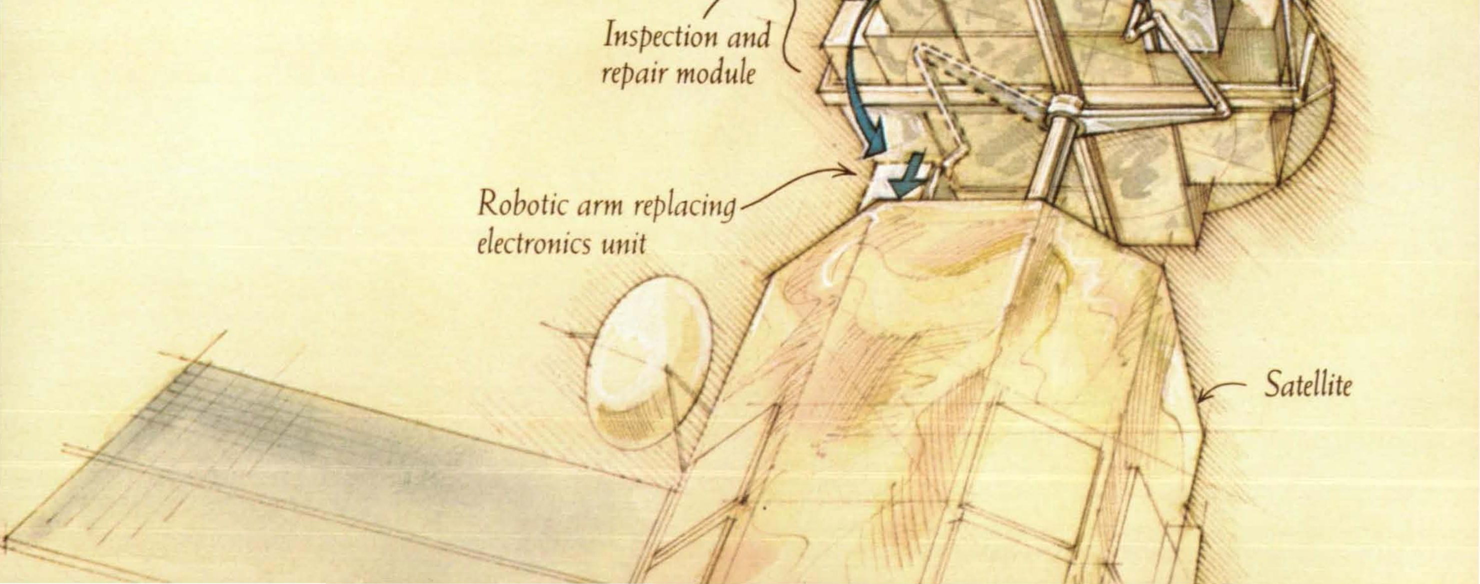

NASA Tech Briefs

National Aeronautics and
Space Administration

JULY/AUGUST 1986
Volume 10 Number 4

BPA

Special Features and Departments

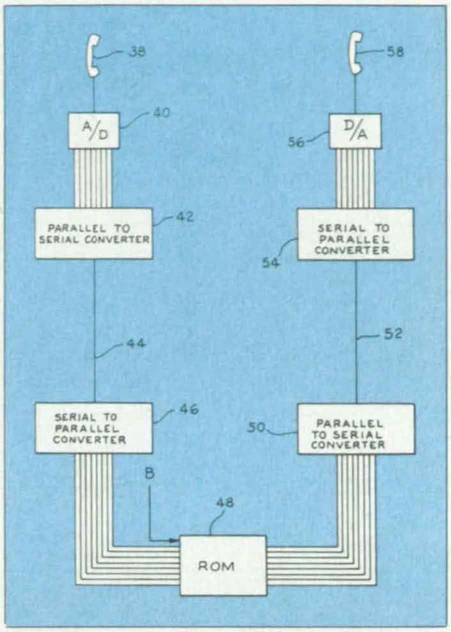

A newly patented telephone conference calling system is one of NASA's latest inventions...page 149.

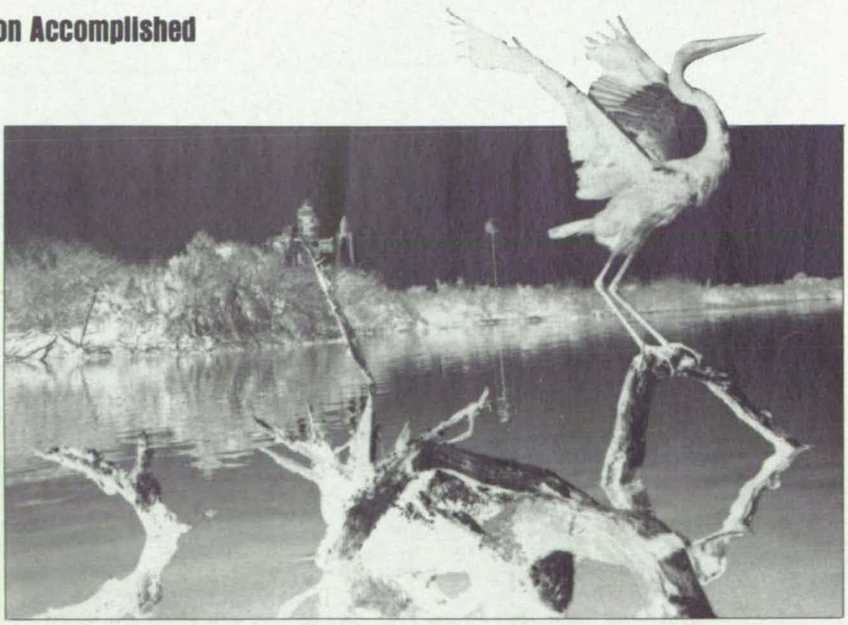

In addition to being the nation's spaceport, Kennedy Space Center is part of a national wildlife refuge—home to this blue heron...page 12.

Technical Section Thumb Index

Thumb Index
Technical Section

NASA Tech Briefs, ISSN 0145-319X, copyright © 1986 in U.S., is published bi-monthly by Associated Business Publications, Inc., 41 E. 42nd St., New York, NY 10017-5391. The copyrighted information does not include the individual Tech Briefs which are supplied by NASA. Editorial, sales, production and circulation offices at 41 E. 42nd Street, New York, NY 10017-5391. Subscriptions for non-qualified subscribers in the U.S., Panama Canal Zone, and Puerto Rico, $50.00 for 1 year; $100.00 for 2 years; $150 for 3 years. Single copies $15.00. Remit by check, draft, postal or express orders. Other remittances at sender's risk. Address all communications for subscriptions or circulation to NASA Tech Briefs, 41 E. 42nd Street, New York, NY 10017-5391. Application to mail at second-class postage rates is pending at New York, NY 10017 and additional mailing offices.

POSTMASTER: please send address changes to NASA Tech Briefs, 41 E. 42nd Street, Suite 921, New York, NY 10017-5391.


PEELING THE LASER BEAM DOWN TO ITS CORE.

AT&T Bell Laboratories scientists have generated a beam from a diode laser with a frequency spectrum 1,000,000 times narrower than that of today's most advanced commercial semiconductor lasers.

Part of a record-breaking coherent lightwave system, this laser 'peels away' a tremendous number of unwanted frequencies that can clutter up a beam—to create a lightwave so pure, its frequency variance is limited to 1 part in 40 billion. The equivalent of one drop of ink in a million-gallon, Olympic-size swimming pool.

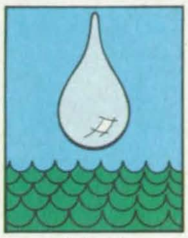

A drop in 40,000,000,000

Purity Has Its Rewards

The new narrow-spectrum laser is the key element in a coherent lightwave communications system that increases the information-carrying capacity of an optical fiber, as well as the distance over which an unboosted laser beam can be received.

Increased capacity comes from dramatically increasing the number of individual laser beams that can be sent through a fiber's best transmission window.

Each laser in a coherent system produces an exceptionally stable, pure wavelength—allowing thousands of non-interfering wavelengths to travel side-by-side on a fiber. (Only a handful of beams can be combined using today's commercial semiconductor lasers.)

Dial 'M' For Movie

In the future, the capacity of coherent transmission could allow us to send 10 million conversations—or 10 thousand digital TV channels—simultaneously, on a single fiber.

Or, using the full capacity of a fiber, a coherent system could dump a movie like 'Gone with the Wind' into a home memory unit in one second flat. Or deliver Beethoven's '5th' in less than a 50th of a second.

Making A Little Go A Longer Way

Increasing capacity is important in an age of rapidly expanding information needs. But so is reducing costs—in this case, by nearly doubling the distance an unboosted signal can be received.

A newly developed AT&T coherent lightwave receiver contains its own narrow-spectrum laser. The beam from this laser reinforces the transmitted signal as it detects it—a technique only possible with two such pure beams.

Using this receiver, AT&T has achieved a laboratory transmission record of nearly 100 miles at a data rate of 1 billion pulses per second.

We Don't Keep The Future Waiting

Coherent lightwave transmission is just one of the ways AT&T is working toward the high-capacity, high-speed integrated networks of the future.

Meanwhile, we're bringing tomorrow closer with leading-edge lightwave systems we're building today.

AT&T this year introduced a commercial lightwave system—the FT Series G—designed to operate at up to 1.7 billion bits per second, a rate that permits the transmission of 24 thousand simultaneous calls on a single pair of fibers.

And by 1988, we'll have installed the first transatlantic and transpacific lightwave systems to Europe and the Far East—systems capable of transmitting 40 thousand simultaneous conversations on two pairs of fibers.

Clearly, whether on land or underseas, AT&T is lighting the way in lightwave. And peeling the laser beam is part of it.

AT&T

The right choice.

NASA Tech Briefs

National Aeronautics and Space Administration

BPA

NASA Tech Briefs:

Published by ....**Associated Business Publications**
Editor-in-Chief/Publisher ....**Bill Schnirring**
Managing Editor ..............................**R.J. Laer**
Associate Editor ....**Judith Mann**
Assistant Editor ....**Elena Nacanther**
Technical Advisor ....**Dr. Robert E. Waterman**
Art Director ....**Melanie Gottlieb**
Assistant Art Director ....**Michelle Schmitz**
Production Manager ....**Rita Nothaft**
Traffic Manager ....**Joe Pramberger**
Circulation Manager ....**Anita Weissman**
Fulfillment Manager ....**Elizabeth Kuzio**
Controller ....**Neil B. Rose**

Technical Staff:

Briefs prepared for National Aeronautics and Space Administration by **Logical Technical Services Corp.**, NY, NY
Technical Editor ....**Ted Selinsky**
Art Director ....**Ernest Gillespie**
Managing Editor ....**Theron Cole, Jr.**
Administrator ....**Elizabeth Texeira**
Chief Copy Editor ....**Pamela Touboul**
Staff Editors ....**James Boyd, Larry Grunberger, Jordan Randjelovich, George Watson**
Graphics ....**Luis Martinez, Huburn Profitt, Joe Renzler**
Editorial & Production ....**Lorne Bullen, Leonard Dalfino, Bill Little Frank Ponce, Ivonne Valdes,**

NASA:

NASA Tech Briefs are provided by the National Aeronautics and Space Administration, Technology Transfer Division, Washington, DC:
Administrator ....**Dr. James C. Fletcher**
Assistant Administrator for Commercial Programs ...**Isaac T. Gillam IV**
Acting Director Technology Utilization Division ......**Henry J. Clarks**
Publications Manager ....**Leonard A. Ault**

Associated Business Publications
41 East 42nd Street, Suite 921
New York, NY 10017-5391
(212) 490-3999
President ....**Bill Schnirring**
Executive Vice President ....**Frank Nothaft**
Vice President—Sales ....**Wayne Pierce**
Vice President ....**Patricia Neri**

Advertising:

New York Office: (212) 490-3999
Vice President—Sales ....**Wayne Pierce**
Sales Manager ....**Robin DuCharme**
Account Executive ....**Dick Soule**
Advertising Executive ....**Carol-Lynne Cox**
Advertising Assistant ....**Erving Dockery, Jr.**

Los Angeles Office: (213) 477-5866
Account Executive ....**Robert Bruder**

FAIRCHILD CONTROL SYSTEMS DEVELOPED THE STANDARDIZED SPACECRAFT REFUELING COUPLING

Until now, the useful life of a spacecraft has been limited by the quantity of propellant and other consumables on board at launch. At Fairchild today, that's being changed. The first steps toward indefinite spacecraft utility are being taken through the development of the Standardized Refueling Coupling. Under the auspices of the NASA Johnson Space Center, Fairchild is working to make spacecraft serviceability a reality. The Standardized Refueling Coupling will allow payloads like TRW's Gamma Ray Observatory to be resupplied with hydrazine in orbit. Designed to be safe for manual servicing, the Standardized Refueling Coupling is easily adapted to automated operation. If your future involves serviceable spacecraft, contact Fairchild Control Systems Company to learn how the Standardized Refueling Coupling can make the future happen.

FAIRCHILD
CONTROL SYSTEMS COMPANY

Fairchild Control Systems Company
1800 Rosecrans Avenue
Manhattan Beach, California 90266
Tel: (213) 643-9222
Telex: 910-325-6216

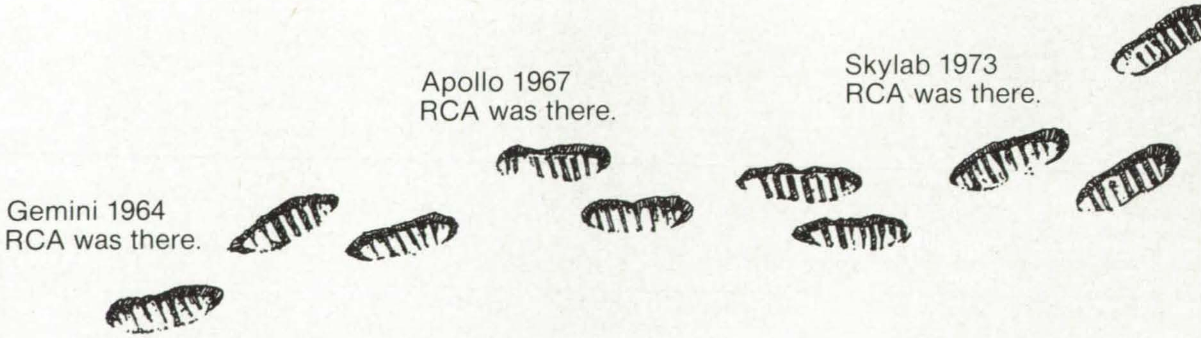

RCA has the track record.

Tracks on the path to Space Station. Since 1964, RCA has been there – a key factor in every NASA manned space project.

Along the way, we've left some large footprints of our own:

- Outstanding ability to integrate communications and tracking systems.
- Outstanding ability to deliver on forecasts — costs as well as schedules.
- Outstanding ability to work productively with NASA colleagues.
- Outstanding ability to perform under pressure — RCA systems have never failed in flight.

As part of the McDonnell Douglas team, we look forward to a major role

Editorial Notebook

Once Upon A Time In A Land Far Away. . .

It's dollars to doughnuts that if Gutenberg had invented the printing press a couple of centuries earlier, there'd have been a *Palos Post* or a *Barcelona Times* editorial questioning Queen Isabella's sanity. I can see it now.

Is This Trip Necessary?

BARCELONA, April 30, 1492—Racked with a deficit left over from the Crusades, plus the heavy burden the recently completed Moorish wars have placed upon the treasury, our Good Queen Isabella has seen fit to underwrite the peregrinations of an itinerant Genoan boat bum who can't even get the support of his own government.

Why? To find a new route to the Indies . . . a place we can reach perfectly well by land! First, he's an odds-on favorite to fall off the edge of the earth. Second, even if he doesn't fall off, it doesn't mean we're going to discover any new routes. Third, there are far more pressing projects. We've got an Inquisition to fund. Our fight with the Moors won't be finished until every last one has been converted.

Moreover, national defense is paramount. Our enemies hound our flanks . . . and one of them will probably capture Columbus's entire expedition anyway.

We would be better off increasing our subsidy of the Flat Earth Society and leaving the trailblazing to the Dutch, or any other nation foolish enough to pursue it. If The Throne feels it must pursue the matter, it should send unmanned craft on such a dangerous expedition.

Not Again!

PALOS, March 15, 1493—Crepuscular Chris is back, with the Santa Maria wrecked and the Nina badly damaged. Just as we predicted, no benefits. His new route to the Indies ends up in an uncivilized area of the boondocks which is inhabited by naked savages to whom the wheel is big news. Their mechanical ability is exceeded only by their artistic expression, which seems to consist of painting their bodies with mud before eating each other. And they smell just as good as you'd expect.

And he has the gall to want 17 more ships to go on another expedition? Columbus's ventures are a hole in the water into which our Good Queen is determined to throw money. It is high time Ferdinand brought her to her senses and determined a sensible policy for Spanish exploration. The monarchy should assign the Navy a goal that justifies risking lives at sea. Resuming the old policy is not the way to learn from the Nina and Santa Maria disasters. The loss of these ships is the right occasion to free the Navy from its aimlessness and at long last give its engineers another project worthy of its skill . . . an Armada, for example.

Columbus Mismanagement Mounts Into Millions

SANTANDER, January 12, 1499—Columbus, his contractors, and staff (some of whom are his family) have wasted millions of Spanish doubloons on the Indian expeditions, despite warning after warning from Empire courtiers that these losses were occurring through bad management. Not only was the entire first settlement wiped out by Indians, but the current Hispaniola settlement seethes with discontent because of poor food, poor living conditions, and inept native labor that produces far less gold than Columbus had promised. It is obvious that his vainglorious project will never be commercially viable.

Experts inside and outside the Empire say such faulty administration procedures have severely hurt the Spanish exploration program. The Admiral of the Mosquitos has brought the Empire only the discovery of lands of vanity and delusion which have been the ruin of many a Spanish gentleman. It is at least heartening to know that Bobadilla is investigating the whole mess and has sent Cornucopia Chris and his brothers back to Spain in chains for a full accounting.

• • •

The news media's job is to jump quickly on the news and report it. Disaster and blame sell a lot more papers and television time than the technological breakthroughs that enhance our daily lives, though the latter outnumber the former exponentially. We can't change that, but we can remind the media and our elected representatives of the benefits we all have derived and will continue to derive from the space exploration process.

We estimate that we have received about 8,000 feedback cards since we privatized *Tech Briefs*. I've read almost all of them, and they are a spur and a delight. Your positive reinforcement makes us all proud, and your suggestions spur us to improve what you have overwhelmingly affirmed is already an excellent product. In all the thousands of comments I have read, I don't remember a dozen that were really negative. Many of you have said that what we're doing should be more widely known. We're trying to make sure that happens; we've increased circulation over 50% in the past 18 months, and we're growing every day.*

The news media and Congress have been eager enough to point out everything that's wrong with NASA. Your comments show that you know well the work NASA has done and continues to do right. Keep the comments coming to us, but more importantly, share them with your local media and your elected representatives. Your input is important. □

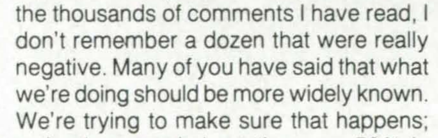

* Look for a bonus this year . . . an extra issue. NTB's *Computer Preview '87* will look at NASA's software and hardware at headquarters, at each of the field centers, and at COSMIC.

Product/Research Developments®

Fourth of a series

General

This series of advertisements is presented in the interest of providing information that may help you do your job for the U.S. Government better and more economically.

Today, with *budget-cutting* a common objective, we would like to highlight a few of the newer breakthroughs in 3M's line of more than 40,000 products that might be especially effective in helping you realize significant savings in your operations.

Moreover, the Federal Systems Department/3M stands ready to help you expedite procurement.

A silver lining

A special 3M silver film has been developed with a capacity for *95% specular reflectivity* — the highest reflectivity of any material currently available.

This "silver lining" is the secret of *Silverlux*™ Fluorescent Reflectors, which can be installed easily in existing fluorescent fixtures. Because of their remarkable reflectivity they allow optimum lighting with as few as *half* the normal number of fluorescent lamps.

With the cost of office lighting running 40% to 60% of the average office energy budget, half the number of lamps, half the ballasts, and half the energy consumption mean big savings.

In addition, where air conditioning accounts for significant energy usage, the reduced lighting wattage with *Silverlux* Fluorescent Reflectors means less heat and correspondingly lower air conditioning requirements.

Storage savings

3M optical media make possible economies on a scale unimaginable only a few years ago.

For example, a 1.2 gigabyte *3M* Optical Disk stores as much information as *thousands* of five-and-a-quarter-inch floppy disks. That's 1,200,000,000 bytes.

This high packing density means not only big savings in storage space, but also even bigger savings in retrieval time, since time spent searching out and inserting disks is cut by factors in the hundreds and thousands.

3M has developed several types of optical disk for industrial audio, video, and data storage and retrieval. *Read-Only Discs* (*3M* "CD-ROM", or new *3M* "OROM" for high-performance computer applications) are for mass replication of large data bases and software packages. *Write-Once Optical Disks* are user-recordable, and provide for storage of permanent documents such as medical, military, and law-enforcement records.

And among our latest breakthroughs, *3M Erasable Optical Disks* use a laser to read, write, erase, and write again.

These versatile disks store large amounts of data, and also let you change and update information quickly, easily, and economically.

3M engineers will be pleased to work with you directly to develop any special application you may envision for the exciting new technology of the optical disk.

Cut costs two ways

Surprising as it may seem, *one* 3M product can cut *both* your heating *and* your air conditioning bills.

Through a patented 3M technology, *Scotchtint*™ *Plus* Window Film cuts heat loss through windows by 20% to 48%, and also rejects 60% to 77% of the sun's intense heat — before it even enters your building.

On average, for every 100 square feet of sun-lit glass covered with *Scotchtint Plus* Window Film you can save *one ton* of air conditioning.

And your people feel cooler in summer, warmer in winter (even next to windows), and are protected from glare — factors likely to significantly improve their productivity.

Durable and attractive, *Scotchtint Plus* Window Film is available in a variety of densities and colors.
(Contract number: GS-00F-79368)

Conclusion

3M is a pioneer and world leader in a wide range of disciplines and technologies.

From photographic film to magnetic tape to optical media.

And expert in the fields of precision coatings, optics, polymer chemistry, and adhesives.

If you need to reduce costs and improve productivity, 3M may have a solution for you.

For more information just call 800-328-1684 toll free (or 800-792-1072 in Minnesota). Descriptive literature will be mailed to you without cost or obligation. Or if you wish, a 3M representative will call you for an appointment at your convenience.

Just call **800-328-1684**
(In Minnesota 800-792-1072)

Silverlux, 3M, and *Scotchtint* are registered trademarks of 3M.

3M hears you. . .

Federal Systems Department/3M
1101 Fifteenth Street, N.W.
Washington, D.C. 20005

3M

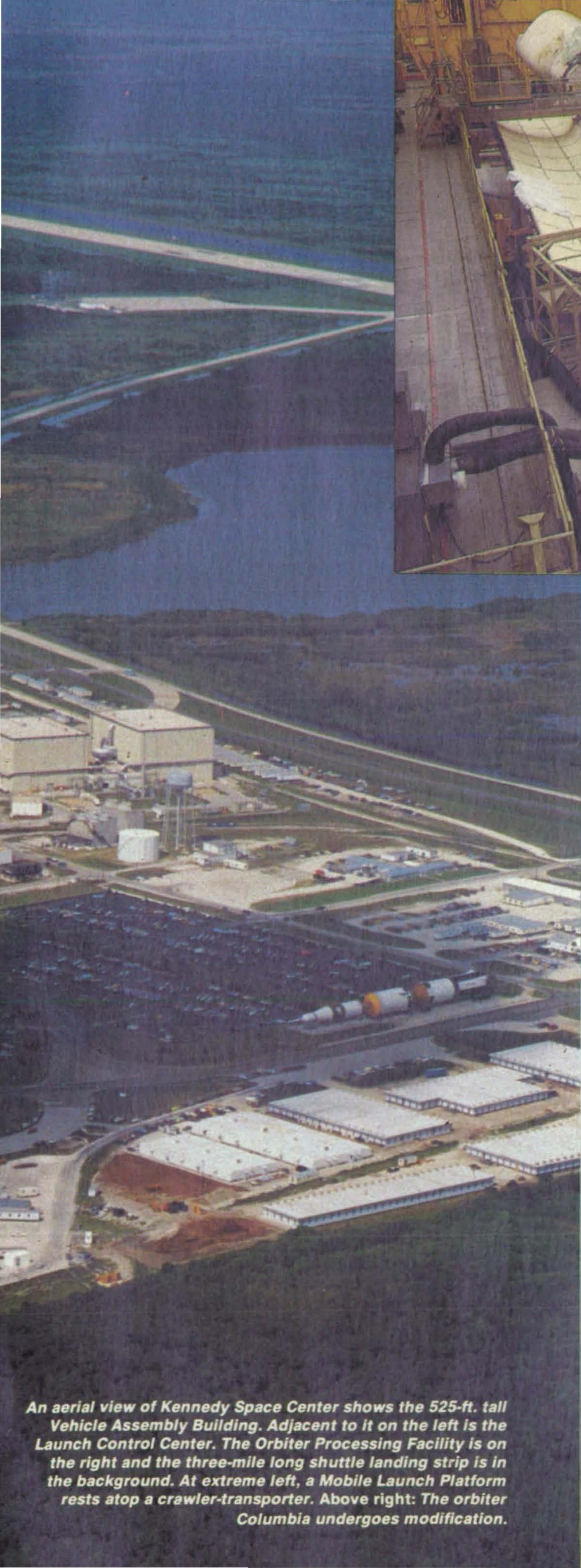

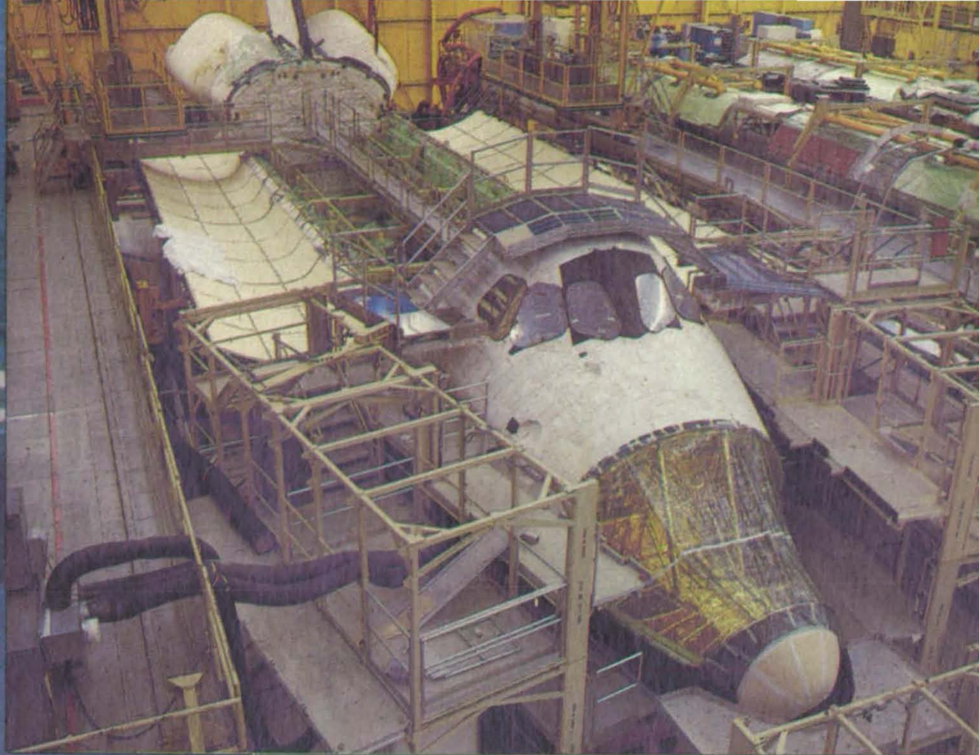

An aerial view of Kennedy Space Center shows the 525-ft. tall Vehicle Assembly Building. Adjacent to it on the left is the Launch Control Center. The Orbiter Processing Facility is on the right and the three-mile long shuttle landing strip is in the background. At extreme left, a Mobile Launch Platform rests atop a crawler-transporter. Above right: The orbiter Columbia undergoes modification.

Kennedy Space Center:

Gateway to the Last Frontier

In the Orbiter Processing Facility at Kennedy Space Center, teams of technicians move briskly up and down stairs and across walkways. A PA system crackles in the background, and overhead the orbiter Columbia rests in the high bay, her sweeping dimensions obscured by support structures and equipment housings. Minus her main engines, nose cone, elevons and assorted other components, Columbia looks strangely vulnerable—not at all the paragon of 20th-century aerospace technology. For an instant one glimpses the irreducible simplicity of the flying machine, an image quickly swept away by the awesome sophistication of the totality. Up close, the shuttle is a technological proof that the whole is greater than the sum of its parts.

The atmosphere in the Orbiter Processing Facility is charged. Technicians, some of them clad in lint-free caps, coveralls and booties—"bunny suits" in the vernacular—attend to the maintenance and modification needs of the premiere orbiter. Columbia's wings are being reinforced and strengthened, "beefed up" so that the next time she flies, she'll be capable of carrying heavier payloads. Her delicate electronic systems are inspected and tested, again in preparation for her next spaceflight.

It's a far cry from business as usual, but it's business nonetheless at the John F. Kennedy Space Center. The next shuttle launch may be at least a year away, but there's work to be done and schedules to be met just the same. ►

Kennedy

Establishing Capabilities

Launching space vehicles has been the focus of activity on Cape Canaveral for over 35 years. Beginning with captured German V-2 rockets in the early 1950s, the launch litany progresses through Redstone, Thor, Atlas, Scout, Centaur, Jupiter, Delta, Titan and Saturn rockets, culminating with the space shuttle.

Nearly every expansion in launch capability has been accompanied by a new launch pad or some other form of facilities expansion. NASA's Launch Operations Center, which was formally established at the Cape in 1960, has grown up quickly. Originally a field office of the Marshall Space Flight Center, the Launch Operations Center was tasked with handling NASA affairs at the Cape. It was given full NASA field center status in 1962, and renamed for the late John F. Kennedy in 1963. With the advent of the Apollo program, expansion at Kennedy Space Center gained momentum. Facilities multiplied fivefold, expanding inland off the Cape proper to adjacent Merritt Island.

Today, Kennedy Space Center covers 88,000 acres on the east coast of central Florida. Complex 39, the centerpiece of the Apollo-era expansion, includes a number of new facilities, among them the mammoth Vehicle Assembly Building (VAB), which is visible from a distance of several miles and reportedly encompasses the largest enclosed space in the world. The 525-ft.-tall VAB was designed to accommodate the long and lean Saturn/Apollo vehicle, and today it is used to mate the shuttle orbiter with its 15-story external fuel tank and solid rocket boosters.

Other Complex 39 facilities include three mobile launcher platforms, upon which the shuttle systems are assembled before being moved to the launch pads, 39A and 39B. Both pads were built for Apollo launches, and their fixed service structures and other ground support equipment were modified for the shuttle program.

The job of moving the assembled shuttle system to the pad for launch is accomplished by crawler-transporters roughly the size of baseball diamonds. The crawler-transporters are powered by two diesel engines and move forward on four double sets of Caterpillar-like metal belts. Each tread of the metal belts weighs a ton, and fully loaded with the shuttle, the crawler-transporter weighs a whopping 3½-million tons.

Needless to say, it's not a quick sprint from the VAB to the launchpad. The trip takes nearly all day and progresses at the rate of one-half mph. Computer-controlled hydraulics keep the crawler's surface, and the shuttle system, level during the three-mile march to the pad. ►

All but the operational areas of Kennedy Space Center are part of the Merritt Island National Wildlife Refuge.

MTS® TestingNews
Materials Testing Edition
Vol. IV, No. 9

The MTS 810: Versatile Test Automation Beyond a PC

The New MicroProfiler™ Provides Added Flexibility to Material Testing

Automation. The new MTS 810 material testing system now offers a new automation package called MicroConsole™ PLUS. This desk-top controller comes with special software packages—the result of 20 years of material-testing experience. The test control and data acquisition capabilities are several steps beyond a commercial PC.

The software is MTS System's special version of BASIC. The language is interactive and friendly, to give you versatility and flexibility. MicroConsole PLUS hardware includes a powerful microcomputer with 512 Kbytes memory, Winchester plus floppy disc drives, printer and more. You can get application software from fracture mechanics through tensile testing and more. Send for details.

NEW VERSATILITY. The 810's new MicroProfiler digital waveform generator adds versatility and flexibility to testing. This microprocessor-based unit generates and stores an array of test profiles (56 Kbytes RAM storage), blocks (up to 90) and stores nine test programs WITHOUT THE NEED FOR A COMPUTER and with very high resolution.

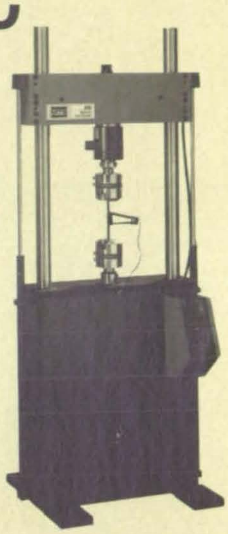

MTS 810 Load Frame

Now it's easier to perform tests like tension, compression, bend, fatigue and fracture. Easy operation—pushbutton selection of 3 modes—programmed, direct and remote. An 18 bit digital-to-analog converter gives you high resolution. And you can select 1 of 9 rates at the touch of a button from a remote location.

The unique performance of the MTS MicroProfiler allows you to perform material tests which cannot be done with an ordinary function generator. Easy installation—nearly immediately operable. Send for more details.

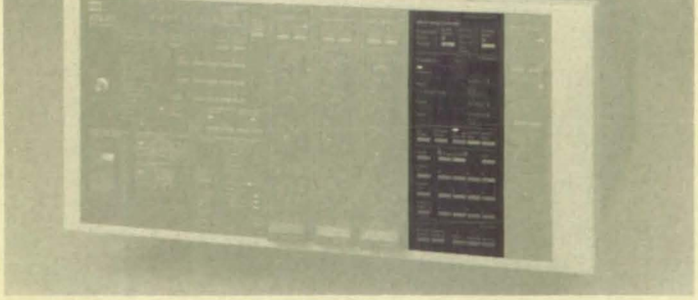

The MicroProfiler™ is the clear dark area in this photo of the MTS 458.20 MicroConsole™

Circle Reader Service #

MicroProfiler™ Waveform Examples

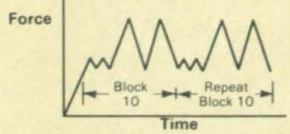

Figure 1. Block Cycle Test for Flight Simulation.

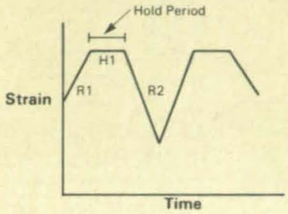

Figure 2. Strain Cycle Creep Typical of Power Generation Test Applications.

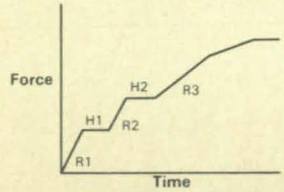

Figure 3. Waveform Used for Civil Engineering Structure/Materials.

Free Extensometer Catalog describes broad test capabilities

This 24-page catalog details the variety of tests which MTS Extensometers can help you perform, such as fracture, bend, fatigue and tension/compression. New products also are described, such as: clip-on gage for testing in hostile environments; averaging axial and biaxial-axial extensometers; axial-torsional extensometers and more. Send now for this information-filled catalog.

Circle Reader Service #

Rock, soil, ice, concrete test capabilities in free brochure

If you do GeoTechnical testing, this informative source book can answer questions about test systems and specialized equipment: triaxial cells, in-vessel instrumentation, pore fluid subsystems and more. Read how these systems and MTS automation can control stress and strain of your geomechanic specimen, take data and control environments in a triaxial cell.

Circle Reader Service #

MTS®
MTS SYSTEMS CORPORATION
BOX 24012, MINNEAPOLIS, MINNESOTA 55424
TELEPHONE 612-937-4000 TELEX 29-0521 MTS SYSTEM ENPE
FAX 612-937-4515

Circle Reader Action No. 418

Kennedy

Applying Technology

Beyond the rockets, launchpads, buildings and ground support hardware, a wealth of related technology has grown up around the launch activities at the Cape. While much of it was developed to meet the specific requirements of assembling, integrating, testing and launching spacecraft, the technology spans a broad range of disciplines, from inorganic coatings that preserve launch structures to programming languages and expert systems.

Computer systems and software development is one area where NASA deserves and in fact receives a good deal of credit. During the '70s, NASA and its contractors advanced a new generation of fail-safe software for the shuttle's on-board computer system. At Kennedy Space Center, advances in networking capability and in software development combined to form the Launch Processing System, an elaborate computer universe that automatically performs the bulk of shuttle checkout and launch functions.

Kennedy Space Center's innovative Common Data Buffer System was developed to provide the communication interfaces necessary to maximize the parallel processing capabilities of some of the system's newer computers. The flexible data buffer system allows many different brands and varieties of computers to interact in an efficient and error-free manner, greatly enhancing the speed with which shuttle checkout, testing and launch operations take place.

Another computer systems development tied to the shuttle era is GOAL, one of the first near-English programming languages. GOAL was developed to avoid the translation problems that can arise between the engineers who develop shuttle checkout and test procedures, the programmers who encode them, and the technicians who perform the actual operations. Using GOAL, engineers were able to write their own procedures into the software, and from there they could be followed through directly by technicians.

A KSC technician inspects the thermal tiles on Discovery's wing.

The computer systems development that took place at Kennedy Space Center throughout the '70s and early '80s was designed to provide specific responses to the equally specific questions posed by the implementation of the new space transportation system. Questions such as how do you process and control the shuttle? how do you integrate the largest distributed computer system in the world? and how do you circumvent the translation problems between systems engineers and technicians were addressed through applied technology development projects.

In the '80s, technology applications projects continue to command a great deal of attention and effort at Kennedy Space Center. The focus is on the development of technology-intensive (as opposed to manpower-intensive) methods for assembling, servicing, testing and launching the space shuttle. The ultimate goal of these projects is to reduce to number of ground operations man-hours per space shuttle flight by 50%, at the same time reducing shuttle turnaround time substantially.

Expanding the Technical Base

Kennedy Space Center's Robotics Applications Development Laboratory is conducting studies to determine where the implementation of robotic systems could reduce the number of man-hours needed to assemble, service and test the shuttle prior to launch. Different time-critical, hazardous and repetitive labor-intensive operations that could potentially be handled partially or completely by automated robotic systems have been identified, and these are currently being evaluated by laboratory personnel. Time-critical applications include the assembly of the space vehicle and the external tank, and the installation and integration of payloads. The application of robotic systems to hazardous tasks focuses on the loading and unloading of the hypergolic and cryogenic propellants that fuel the shuttle. A number of repetitive tasks, such as spot welding, that could eventually be performed by robots are being studied as well.

Kennedy's Robotics Applications Development Laboratory is currently equipped with an electrically driven, ASEA robot composed of a six-axes arm with interchangeable end-effectors or "hands." It is controlled by a user-friendly computer brain that allows it to carry out its functions autonomously, rather than being teleoperated by a person. The prototype robot will supply the baseline data upon which more complex tasks and integrated "smart" robotic systems can be developed. It is expected that both the space station and the next generation space transportation system will rely heavily on robotics and other automated systems, so beyond its immediate applications orientation, the Robotics Application Development Labora- ►

GS00K85AGS0047

THE ONLY NUMBER YOU NEED TO KNOW FOR ALL YOUR INDUSTRIAL VIDEO NEEDS.

When you come to Panasonic® for your industrial video requirements you're getting more than the world's largest selection of video components and accessories. You're also getting the quality and reliability that has long been a trademark of Panasonic.

Production

For sophisticated productions Panasonic has just what you need. Including a wide variety of single-tube and three-tube cameras as well as special-effects generators and ½" and ¾" editing systems.

For documentation, there are a variety of lightweight cameras and portable VHS recorders and camcorders. All with features to make documentation simple and fast. Like One-Touch Recording, Automatic White Balance and Auto-Focus.

Distribution

For your video networks Panasonic offers a multitude of VHS recorders and players. There are even video decks and monitors combined in a single unit. And of course you can find a large selection of both black and white and color monitors.

Surveillance

For your security and surveillance operations Panasonic offers a wide choice of CCTV components. Choose from Vidicon and Newvicon® cameras in both color and black and white. There are small and ultra-durable solid-state color and black and white cameras, time-lapse VCRs and, of course, monitors in virtually every size and every configuration.

By now it should be clear: there's only one name you need to know in industrial video. Panasonic.

For more information and your copy of the Authorized Communications Schedule Price List contact your local Panasonic Industrial Video dealer or call (703) 486-5533 (FTS: (202) 486-5533) or write to Government Marketing Dept., Panasonic AVSG, Suite 901, 1215 Jefferson Davis Highway, Arlington, VA 22202-4302.

Panasonic
Industrial Company

Circle Reader Action No. 380

Technicians at KSC's Orbiter Processing Facility install Spacelab in the shuttle cargo bay.

tory is coordinating intercenter work on these future projects.

Artificial intelligence, particularly knowledge-based expert systems, is another technology Kennedy Space Center is developing in the interest of streamlining and improving assembly, servicing, test and launch operations. Activities in this area focus on control and monitor expert systems and information management expert systems.

Development of the LOX expert system for controlling, monitoring and real-time diagnostics of KSC's liquid oxygen loading system began in 1983. The LOX system was to have gone on-line in the firing room in November 1986, but owing to the current shuttle stand-down, this date has been postponed.

In the meantime, other expert systems are being developed, using IBM AT's and Symbolics computers. KATE, the knowledge-based automatic test equipment project, uses LES (the on-line launch-pad environment expert system) as a baseline for its automated hardware testing and control system. KATE is capable of a variety of functions, including multiple command control, multiple failure diagnosis and adaptive learning through reading and observation. The system is designed to identify failed test system components, determine alternate solutions that will allow the test to proceed, and restore the process by commanding the activation of redundant components.

EMPRESS, the expert mission planning and replanning scheduling system, is designed to capture the expertise of those individuals who plan, construct and maintain shuttle mission schedules. EMPRESS is a subset of a larger planning system in that it deals specifically with payloads manifested to fly on the shuttle. EMPRESS defines the time, resource and task requirements associated with particular payloads, and determines how particular payloads fit into the overall scheme of mission planning.

The near-term goals of Kennedy Space Center's artificial intelligence, expert systems, and robotics development and applications programs involve upgrading the shuttle processing systems and software that have, in the space of a decade, become antiquated. The long-term goal is to create the ultimate paperless management system for the space shuttle. Multiple, interactive expert systems will perform checkout, test and launch procedures of vehicles that have been assembled, fueled and serviced in part by robots.

The proposed space station poses another set of unique questions to Kennedy Space Center. What is the appropriate programming language for user interface? How can artificial intelligence and expert systems be applied to streamline space station assembly, checkout, test and operational procedures? What roles can best be performed by robots and other automated systems?

Again, Kennedy Space Center's expertise in developing and applying innovative technology will be called upon to answer the unique and task-specific questions that arise at the edge of the last frontier.

Finally, though, there is no question regarding what will be Kennedy Space Center's most pressing task in the months ahead. Restoring the space shuttle program to safe and regular operational capacity is a national priority, and Kennedy's role in this process will be vital. All things considered, the people at Kennedy Space Center are optimistic. The somber aura that descended in the wake of the Challenger accident has begun to dissipate, and while a subdued and sober quality is still very much in the air, the atmosphere there is charged with the combination of determination, perseverance and vision that makes spaceflight possible in the first place. □

A Head To Head Comparison

OF WIDEBAND INSTRUMENTATION RECORDERS

Before someone sells you a lab quality wideband instrumentation recorder, we'd like you to ask a simple question—What about tomorrow?

Is the machine that's fine for today's task flexible enough for next month's project? Next year's?

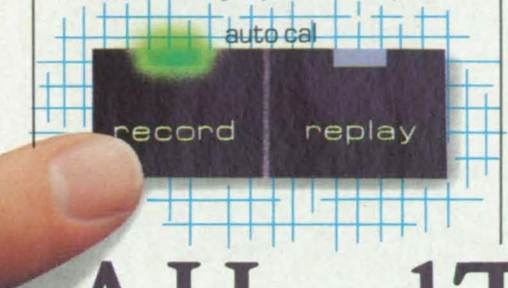

What about reliability and calibration?

Not to mention a close look at the bottom line—including the value of your time.

So, when you're shopping for a wideband instrumentation recorder, look for today *and* tomorrow.

Then look at Racal's Storehorse. See who really measures up.

BE PUSHY, CALIBRATE AND EQUALIZE 42 CHANNELS IN 6 MINUTES

No other recorder in Storehorse's class lets you automatically calibrate and equalize up to 42 channels. (In fact, most require you add an extra cabinet to even *get* 42 channels.)

Every signal channel adjustment—from bias and record currents to replay equalization, is fully automatic. To IRIG Standards.

What does that mean to you?

Well, first of all, you save an incredible amount of time. And what would you rather do—set up tests, or run them?

What's more, automatic equalization guarantees optimal record and replay characteristics—even from machine to machine. You get flat frequency response and correct phase performance on every replay.

ADVANCED MONITORING AND METERING

An onboard Video Display Unit saves your time for more important things than hand holding your instrumentation. Because it displays automatic problem diagnostics.

The VDU also lets you easily monitor signal, machine and tape status. And you can even make non-standard adjustments quickly and easily.

IEEE 488 AND RS232 INTERFACES

Sure the others can handle IEEE 488 and RS232, after you add the extra-cost interfaces.

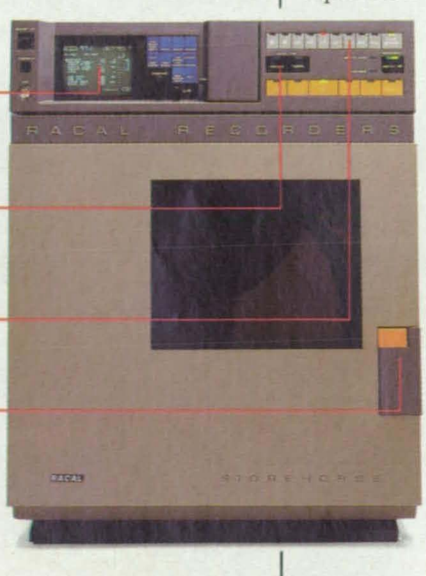

VDU constantly monitors recording and machine parameters.

Calibrate and equalize 42 channels in 6 minutes.

15/32 to 120 inches/second, 2 to 42 tracks.

Automatic lockout and positive cabinet pressure all but eliminates dust contamination.

With Storehorse they come built in. That gives you remote access to all deck functions and signal channel parameters.

	Racal Storehorse	Honeywell 101	Sabre 9
Calibration Equalization	Fully Automatic Record Calibration and Replay Equalization	Manual Calibration and Equalization with Internal Verification	Manual Calibration and Equalization with Internal Verification
Tape Path	Planar Transitition Device, No Tape Twist and Stretch	Traditional Approach with Tape Twist and Stretch	Traditional Approach with Tape Twist and Stretch
Remote	IEEE 488 & RS232 Access to all Deck Functions and Signal Channel Parameters	IEEE 488 *or* RS232, with Limited Selection of Functions	IEEE 488 *or* RS232, Single Option Only
Size	Up to 42 Record/Reproduce Channels in One Portable Housing	Additional Chassis Required	Additional Chassis Required

ROADWORTHY

Best of all, the lab quality, automatic flexibility of Storehorse is portable. With 28 channels or more, it comes in a cabinet just about half the size of the other guys.

If you've got a use for up to 42 automatically calibrated and equalized channels, with nearly unlimited interface capability, all in a portable package, call Shirley at Racal.

And find out why only Storehorse measures up.

RACAL

Racal Recorders Inc.
4 Goodyear Street,
Irvine, CA 92714 USA
Tel: (714) 380 0900
Outside Calif. Toll Free:
(800) 847 1226

New Product Ideas

New Product Ideas are just a few of the many innovations described in this issue of *NASA Tech Briefs* and having promising commercial applications. Each is discussed further on the referenced page in the appropriate section in this issue. If you are interested in developing a product from these or other NASA innovations, you can receive further technical information by requesting the TSP referenced at the end of the full-length article or by writing the Technology Utilization Office of the sponsoring NASA center (see page 29). NASA's patent-licensing program to encourage commercial development is described on page 29.

Retractable Sun Shade

A mechanism that unfurls a blanket to form an arched canopy, developed for Space Shuttle missions, can be adopted to the shading of greenhouses, swimming pools, and boats. A window-shade type spring roller contains a tough, opaque polyimide blanket, which is taken up by a rotating cylindrical frame and held over the area to be shaded (see figure). When the roller motion is reversed, the blanket is drawn by its return spring back into the spring roller. Powered manually or by an electric motor, the drive roller can be stopped at any point to provide partial shade instead of full shade.
(See page 94.)

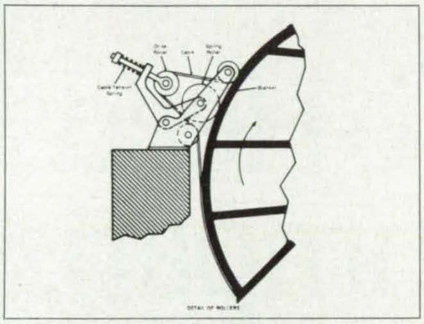

Filter Bed of Packed Spheres

A proposed filter would be constructed from densely packed spheres restrained by screens (see figure). Hollow gas-filled plastic or metal spheres would normally be used. These can be manufactured within a 10-percent diameter tolerance. Normally, all the spheres in a filter would be of the same nominal diameter. The dimensions and surface coatings of the spheres would be selected to provide the desired physical and chemical properties. Such a filter could be used as a sieve to pass only particles smaller than a given size or to retain particles larger than that size. In the case of cells or other biological materials, the new filter may be preferable to older screen-type filters, which can damage the cells or other filtrate particles.
(See page 140).

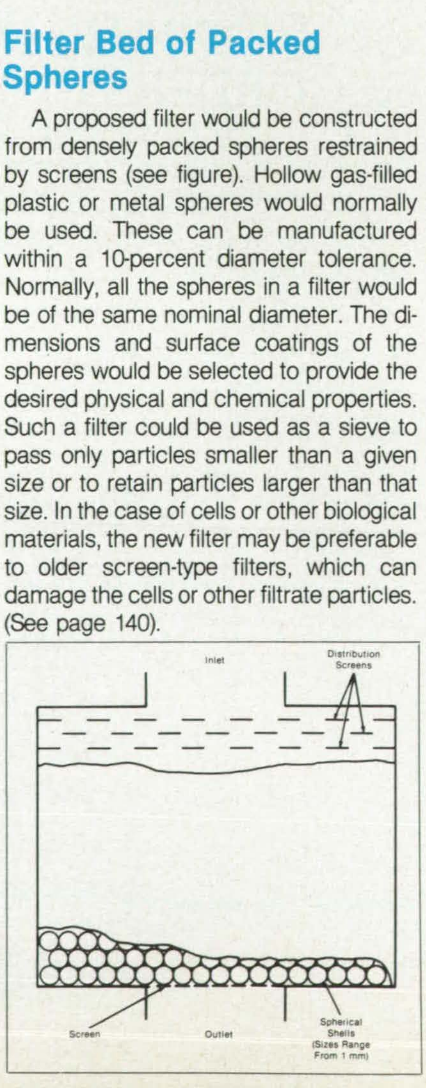

Hydraulic Shutdown Monitor

A simple modification enables a commercial electronic load controller to be used in an electromechanical system for load monitoring and overload shutdown. A four-pole, double-throw switch is added to the front panel of the controller to disable the tracking-error and endpoint-error circuitry yet still retain the overload-detection capability. In the "disable" position, the added switch overrides functions of the controller that would prevent automatic shutdown on overload during friction tests (see figure). In the "operate" position, the switch allows the controller to operate in its normal fashion. Previously, it was necessary to use adjustable-voltage-level detection equipment connected with cables to the hydraulic "dump" or shutdown circuitry in the controller.
(See page 30).

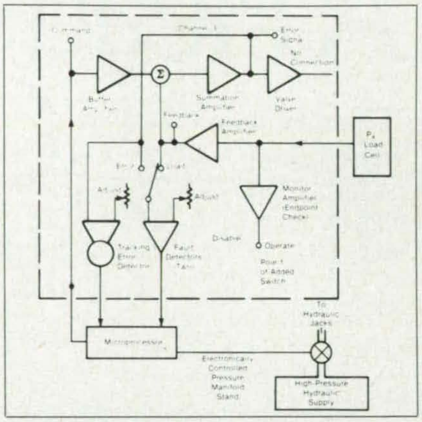

Tailorable Infrared Sensing Devices

A proposed infrared sensing device using a Ge_xSi_{1-x}/Si strained-layer superlattice may offer enhanced detection sensitivity and could be tailored for a specific cutoff wavelength over the range from 2.7 to about 50 μm. The device (see figure) includes a large number of alternating thin layers of Ge_xSi_{1-x} and Si deposited on a silicon substrate by molecular-beam epitaxy. When an electric field is applied across the stack, it acts as a detector for infrared photons. Such a structure could find a wide range of applications in robotics, space exploration, and terrestrial surveillance.
(See page 36).

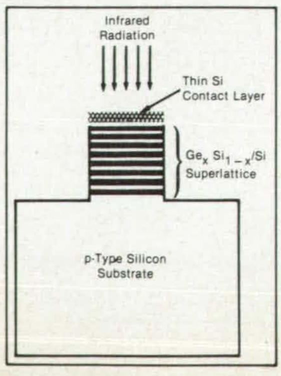

Semiconductor Laser With Two-Dimensional Beam Steering

The proposed modification of a monolithic semiconductor injection laser capable of one-dimensional electronic beam steering should enable the deflection of its beam in a second direction. Such a laser chip could provide beam pointing or raster scanning for applications in optical communications, data processing, image scanning, and optical ranging. Two-dimensional electronic steering of the beam would be achieved by adding electrode (contact) 3 to a laser (see figure) that was previously capable of one-dimensional beam steering. The laser beam would come out of the page in the z direction from the p-type base region. (See page 37).

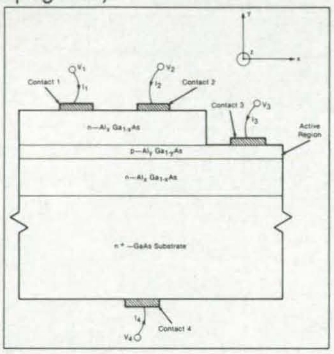

Cleaning of Liquid N_2O_4

A technique developed for cleaning of liquid N_2O_4 may be adaptable to the cleaning of a variety of industrial fluids, including fuels. Metal nitrate impurities are precipitated from N_2O_4 by cooling the N_2O_4 in a heat exchanger and then passing it through a hydraulic pump. The precipitate is then removed by a fine membrane filter (see figure). This process, used in filling the facility storage tank, is repeated several times by the recirculation of the stored N_2O_4 to remove as much of the nitrates as possible. This system typically lowers the iron content in liquid N_2O_4 from as high as 5.0 parts per million to about 2.0 or fewer parts per million. (See page 103).

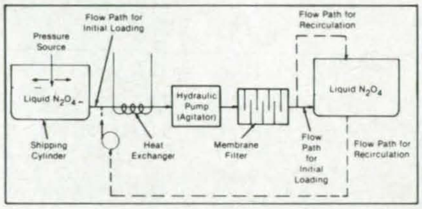

Interferometer for Observing Compressible Flow

A new optical interferometer (see figure) enables the instantaneous visualization of compressible fluid flows. Because it is relatively immune to vibration, the unit is well suited to the observation of flows over models in large wind tunnels. By noting the relationships between fringe shifts, refractive indices, and densities, an experimenter can map the flow-field density contours. The interferometer can give a quantitative, time-resolved characterization of the flow field and has been demonstrated by producing images of the flow around a candle, a propane torch, a heated cylinder, and an oscillating airfoil in a wind tunnel.
(See page 60).

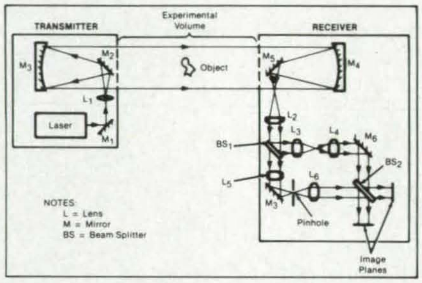

NO OTHER POSITIONING SYSTEMS OFFER SO MUCH FOR SO LITTLE.

Simply the best: every system delivers 0.1 micron or 0.25 arc second resolution, at high speed, for 20% less money than the competition.

What you see here is a four-axis UNIDEX™ XI motion controller, coupled with a 200 Series ACCUDEX® XZθ stage. It is just one positioning system out of thousands from Aerotech. Four other UNIDEX models, for up to six axes of motion, are available—along with five series of linear stages (travel up to 1 meter) and rotary stages (diameters up to 305 millimeters), accommodating payloads up to hundreds of kilograms.

These systems and their components have all been designed, engineered and manufactured by Aerotech and are suitable for use in any environment from clean rooms and small labs to large, high throughput industrial situations. Yet these fine-resolution, high-speed Aerotech positioning systems cost 20% (or more) less than their slower, less precise competitors.

Complete technical information is available. Contact Aerotech, Inc., 101 Zeta Drive, Pittsburgh, PA 15238—phone 412-963-7470.

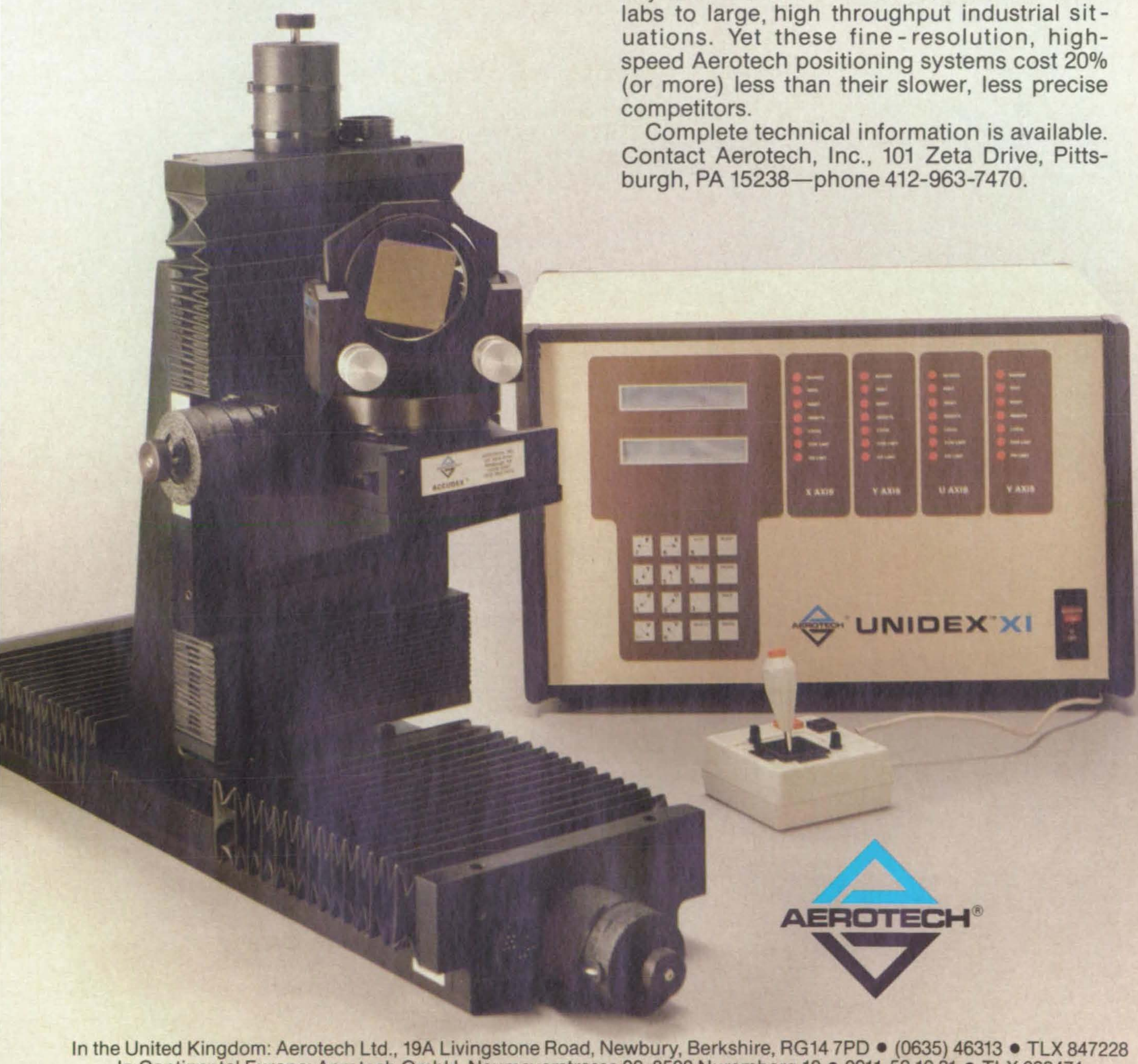

In the United Kingdom: Aerotech Ltd., 19A Livingstone Road, Newbury, Berkshire, RG14 7PD • (0635) 46313 • TLX 847228
In Continental Europe: Aerotech GmbH, Neumeyerstrasse 90, 8500 Nuremberg 10 • 0911-52 10 31 • TLX 622474

Circle Reader Action No. 310

AT-39734

APTEC RUNS VAX TO THE MAX

Now VAX/VMS™ systems can handle high-performance real-time data at 24 Mbyte/sec I/O. The VAX can be host to powerful, high-speed peripherals—and get up to 24 MB/sec throughput. Result: exceptionally fast and productive systems that easily meet realtime data acquisition and processing needs.

Only the Aptec I/O Computer makes this possible. By offloading VAX I/O tasks, it extends system capabilities and performance, while assuring optimal use of peripherals. Modular and expandable, Aptec provides a cost-effective path to multiple array processor—even multiple VAX systems, with virtually no I/O degradation on even the biggest systems.

Key to offloading the VAX is Aptec's 32-bit bus structure. With a 24 MB/sec aggregate bandwidth, it handles I/O by direct communication between peripherals and Aptec mass memory.

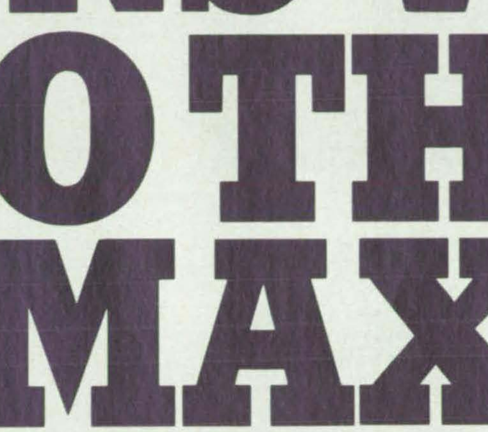

Aptec also interfaces to high-speed peripherals such as the Ibis 1400 disk system with up to 10 MB/sec data transfer rates.

Aptec frees the VAX for other tasks and frees you from frustrating host holdups. Our extensive software supports powerful languages such as FORTRAN, STAPLE and Microcode; and familiar tools, including software drivers for array processors, A/D converters, disk and tape storage devices; all within a FILES-11™ environment.

Find out how Aptec runs VAX to the max—into new dimensions of realtime processing. Call toll-free: 1-800-552-7832. OEM arrangements are available. Aptec is a participant in Digital Equipment Corporation's Cooperative Marketing Program.

Aptec Computer Systems
P.O. Box 6750
Portland, OR
97228-6750
(503) 626-9000
Telex 467167

APTEC SYSTEMS

TEAM UP APTEC AND VAX/VMS FOR HIGH PERFORMANCE REALTIME SOLUTIONS

Circle Reader Action No. 314

New Alloy for Glass-to-Metal Seals

A new alloy — composed of about 60 percent iron, 40 percent nickel, and traces of six other elements — has a low coefficient of thermal expansion, $1.9 \times 10^{-6}(°F)^{-1}$ [$3.4 \times 10^{-6}(°C)^{-1}$]. Because the coefficient is close to that of KG-33 (or equivalent) glass, the alloy can be used in glass-to-metal seals without introducing excessive residual stresses. In addition, the alloy has potential for other applications in which low thermal expansion is important; for example, mechanical measuring devices and precise sliding parts that must function over wide temperature ranges. The alloy was developed as a replacement for Kovar (or equivalent) Fe/ NiCo alloy in a ferrule-and-tube assembly (see figure).
(See page 100).

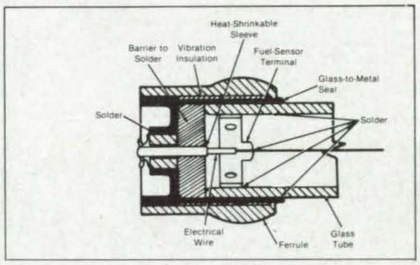

Liquid Scavenger for Separator/Pump

A pump for hydrogen has been modified to remove moisture that condenses in the impeller stage and shunt it back to the earlier centrifugal separator stage for removal. Normally, the separator stage removes water droplets from an incoming mixture of hydrogen gas, water droplets, and water vapor. In the unmodified pump, however, additional condensation sometimes occurs in the pump stage. The moisture-removal problem was solved by adding a shallow circumferential groove and a small exit hole to the impeller chamber (see figure). The circumferential groove leads to an exit hole near the high-pressure outlet. As the impeller disk (not shown) rotates, it flings water droplets that have condensed in the pump toward the groove. Aerodynamic drag drives the water around the groove to the exit hole. (See page 92).

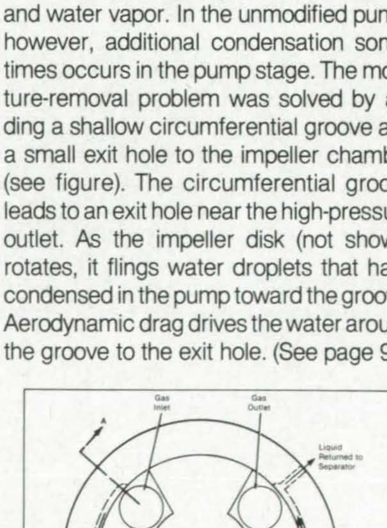

Centrally-Rupturing Squib-Closure Disks

An improved squib rupture disk would insure that the squib explosion is directed toward the center of a combustion chamber. This can obviate the use of oversize squib units that can cause undesirably large impulses. In the new design (see figure), the center of the rupture disk contains a cruciform indentation in which the thickness is reduced to about 0.5 mil (0.013 mm). This reduces the strength of the center of the rupture disk in the same manner as that of the pull tabs on beverage cans; therefore, the disk will fail predictably in the center, causing a predictable flow of combustion products toward the center of the combustion chamber. (See page 93).

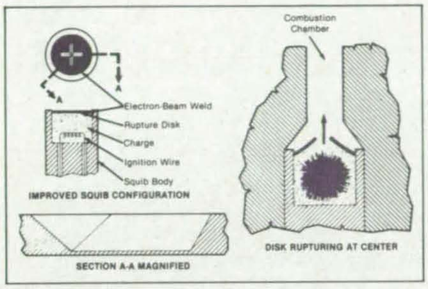

Omnivector Probe Measures Airflow

A probe (called an omnivector anemometer) has a fixed-position sensing element capable of simultaneously measuring steady and unsteady velocity head and flow direction of a moving fluid over a complete 360-degree angle in two-dimensional flow. The sensing element of the omnivector anemometer (see figure) is mounted on the end of a support tube, which is necessary for inserting the sensing element into the flow field. The main element of the anemometer is a drag body consisting of a cylindrical tube upon which are mounted eight miniature strain gages near the base and electrically connnected in the form of two four-arm Wheatstone bridges.
(See page 84).

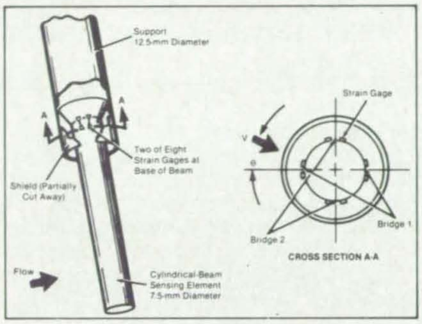

Hydraulic-Leak Detector for Hidden Joints

An indicator reveals leaks in hidden fittings on hydraulic lines. It allows fast inspection of joints without disassembly and can be used in aerospace, petroleum, chemical, nuclear, and other hydraulic applications where removing covers for inspection is impossible, difficult, or time-consuming.

The indicator consists of a wick wrapped at one end around the joint to be monitored (see figure). The wick, made of Kevlar (or equivalent) aramid sleeving, absorbs hydraulic fluid leaking from the joint and transmits it to the opposite end where it is visible to an inspector. At the end of the wick is a bulb filled with fibrous insulation to make the fluid more evident as a discoloration of the outside end of the wick.
(See page 102).

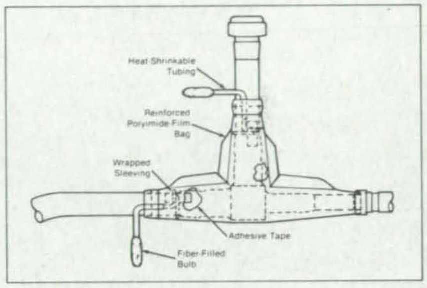

HOW YOU CAN BENEFIT FROM NASA's TECHNOLOGY UTILIZATION SERVICES

If you're a regular reader of TECH BRIEFS, then you're already making use of one of the low- and no-cost services provided by NASA's Technology Utilization (TU) Network. But a TECH BRIEFS subscription represents only a fraction of the technical information and applications/engineering services offered by the TU Network as a whole. In fact, when all of the components of NASA's Technology Utilization Network are considered, TECH BRIEFS represents the proverbial tip of the iceberg.

On the following pages, we've outlined NASA's TU Network—named the participants, described their services, and listed the individuals you can contact for more information relating to your specific needs. We encourage you to make use of the information, access, and applications services offered by NASA's Technology Utilization Network. You can save time and money by doing so.

HOW YOU CAN UTILIZE NASA'S

Industrial Applications Centers

A nationwide network offering a broad range of technical services, including computerized access to over 100 million documents worldwide.

You can contact NASA's network of Industrial Applications Centers (IACs) for assistance in solving a specific technical problem or meeting your information needs. The "user friendly" IACs are staffed by technology transfer experts who provide computerized information retrieval from one of the world's largest banks of technical data. Nearly 500 computerized data bases, ranging from NASA's own data base to Chemical Abstracts and INSPEC, are accessible through the nine IACs, which are located throughout the nation. The IACs also offer technical consultation services and/or linkage with other experts in the field.

You can obtain more information about these services by calling or writing the nearest IAC. User fees are charged for IAC information services.

Aerospace Research Applications Center (ARAC)
Indianapolis Center for Advanced Research
611 N. Capitol Avenue
Indianapolis, IN 46204
Dr. F. Timothy Janis, Director
(317) 262-5003

Kerr Industrial Applications Center (KIAC)
Southeastern Oklahoma State University
Station A, Box 2584
Durant, OK 74701
Tom J. McRorey, Director
(405) 924-6822

NASA Industrial Applications Center
823 William Pitt Union
University of Pittsburgh
Pittsburgh, PA 15260
Paul A. McWilliams, Executive Director
(412) 624-5211

NASA/Southern Technology Applications Center
State University System of Florida
307 Weil Hall
Gainesville, FL 32611
J. Ronald Thornton, Director
(904) 392-6760

NASA/UK Technology Applications Center
University of Kentucky
109 Kinkead Hall
Lexington, KY 40506-0057
William R. Strong, Director
(606) 257-6322

NERAC, Inc.
Mansfield Professional Park
Storrs, CT 06268
Daniel U. Wilde, President
(203) 429-3000

North Carolina Science and Technology Research Center (NC/STRC)
Post Office Box 12235
Research Triangle Park, NC 27709
J. Graves Vann, Jr., Acting Director
(919) 549-0671

Technology Application Center (TAC)
University of New Mexico
Albuquerque, NM 87131
Stanley A. Morain, Director
(505) 277-3622

NASA Industrial Applications Center (WESRAC)
University of Southern California
Research Annex
3716 South Hope Street
Room 200
Los Angeles, CA 90007
Radford G. King, Acting Director
(213) 743-6132
(800) 642-2872 (CA only)
(800) 872-7477 (toll-free US)

If you represent a public sector organization with a particular need, you can contact NASA's Application Team for technology matching and problem solving assistance. Staffed by professional engineers from a variety of disciplines, the Application Team works with public sector organizations to identify and solve critical problems with existing NASA technology.

Technology Application Team
Research Triangle Institute
P.O. Box 12194
Research Triangle Park, NC 27709
Doris Rouse, Director
(919) 541-6980

A SHORTCUT TO SOFTWARE:

COSMIC®

An economical source of computer programs developed by NASA & other gov't. agencies.

Software developed by the U.S. government may be applicable to your needs. To tap this valuable resource, contact COSMIC, NASA's Computer Software Management and Information Center. Approximately 1100 computer programs and related documentation comprise the current library. New and updated programs are announced regularly in NASA Tech Briefs' Computer Programs section, and COSMIC publishes an annual software catalog.

More information about COSMIC's services can be obtained by calling or writing:

COSMIC®
Computer Services Annex
University of Georgia
Athens, GA 30602
John A. Gibson, Director
(404) 542-3265

HOW YOU CAN ACCESS TECHNOLOGY TRANSFER SERVICES AT NASA FIELD CENTERS:

Technology Utilization Officers & Patent Counsels

Each NASA Field Center has designated a Technology Utilization Officer and a Patent Counsel to facilitate technology transfer between NASA and the private sector.

If you need further information about new technologies presented in NASA Tech Briefs, you should request the Technical Support Package (TSP) that accompanies the brief. In the event that a TSP is not available, you can contact the Technology Utilization Officer (TUO) at the NASA Field Center that sponsored the research. The TUO can arrange for expert assistance in applying the technology by putting you in touch with the people who developed it.

If you want additional information about the patent status of a particular technology or are interested in licensing a NASA invention, contact the Patent Counsel at the NASA Field Center that sponsored the research. Be sure to refer to the NASA reference number at the end of the tech brief.

Ames Research Center
Technology Utilization Officer:
Laurance A. Milov
Mail Code 204-10
Moffett Field, CA 94035
(415) 694-5761
Patent Counsel:
Darrell G. Brekke
Mail Code 200-11
Moffett Field, CA 94035
(415) 694-5104

Goddard Space Flight Center
Technology Utilization Officer:
Donald S. Friedman
Mail Code 702-1
Greenbelt, MD 20771
(301) 286-6242
Patent Counsel:
John O. Tresansky
Mail Code 204
Greenbelt, MD 20771
(301) 286-7351

Lyndon B. Johnson Space Center
Technology Utilization Officer:
William Chmylak
Mail Code AL32
Houston TX 77058
(713) 483-3809
Patent Counsel:
Marvin F. Matthews
Mail Code AL3
Houston, TX 77058
(713) 483-4871

John F. Kenedy Space Center
Acting Technology Utilization Officer: Thomas M. Hammond
Mail Stop PT-TPO-A
Kennedy Space Center, FL 32899
(305) 867-3017
Patent Counsel:
James O. Harrell
Mail Code PT-PAT
Kennedy Space Center, FL 32899
(305) 867-2544

Langley Research Center
Technology Utilization Officer:
John Samos
Mail Stop 139A
Hampton, VA 23665
(804) 865-3281
Patent Counsel:
Howard J. Osborn
Mail Code 279
Hampton, VA 23665
(804) 865-3725

Lewis Research Center
Technology Utilization Officer:
Daniel G. Soltis
Mail Stop 7-3
21000 Brookpark Road
Cleveland, OH 44135
(216) 433-5567
Patent Counsel:
Gene E. Shook
Mail Code 60-2
21000 Brookpark Road
Cleveland, OH 44135
(216) 433-5753

Jet Propulsion Laboratory
Technology Utilization Manager:
Norman L. Chalfin
Mail Stop 201-110
4800 Oak Grove Drive
Pasadena, CA 91109
(818) 354-2240

NASA Resident Office-JPL
Technology Utilization Officer:
Gordon S. Chapman
Mail Stop 180-801
4800 Oak Grove Drive
Pasadena, CA 91109
(818) 354-4849
Patent Counsel:
Paul F. McCaul
Mail Code 180-801
4800 Oak Grove Drive
Pasadena, CA 91109
(818) 354-2734

George C. Marshall Space Flight Center
Technology Utilization Officer:
Ismail Akbay
Code AT01
Marshall Space Flight Center, AL 35812
(205) 544-2223
Patent Counsel:
Leon D. Wofford, Jr.
Mail Code CC01
Marshall Space Flight Center, AL 35812
(205) 544-0014

National Space Technology Laboratories
Technology Utilization Officer:
Robert M. Barlow
Code GA-10
NSTL Station, MS 39529
(601) 688-1929

NASA Headquarters
Technology Utilization Officer:
Leonard A. Ault
Code IU
Washington, DC 20546
(202) 453-1920
Assistant General Counsel for Patent Matters: Robert F. Kempf
Code GP
Washington, DC 20546
(202) 453-2424

IF YOU HAVE A QUESTION...

NASA Scientific & Technical Information Facility

If you have a general or specific question about NASA's Technology Utilization Network or its services and documents, you can contact the STI facility for assistance. The STI staff can answer your questions, supply documents and provide referrals to meet your needs. You can use the feedback card in this issue to contact STI directly.

NASA Scientific and Technical Information Facility

Technology Utilization Office
P.O. Box 8757
BWI Airport, MD 21240
Walter M. Heiland, Manager
(301) 859-5300, Ext.242, 243

Electronic Components & Circuits

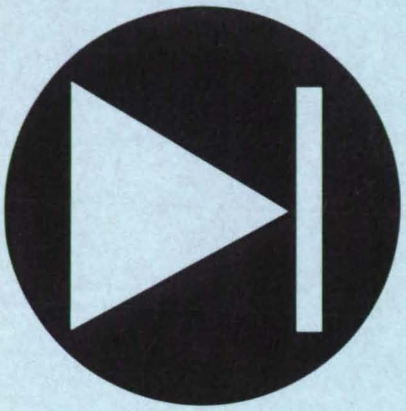

Hardware, Techniques, and Processes

Books & Reports

Hydraulic Shutdown Monitor

Adding a switch allows inappropriate control actions to be overridden.

Lyndon B. Johnson Space Center, Houston, Texas

A simple modification enables a commercial electronic load controller to be used in an electromechanical system for load monitoring and overload shutdown. A four-pole, double-throw switch is added to the front panel of the controller to disable the tracking-error and endpoint-error circuitry yet still retain the overload-detection capability. Previously, it was necessary to use adjustable-voltage-level detection equipment connected with cables to the hydraulic "dump" or shutdown circuitry in the controller.

During a friction test, for example, the

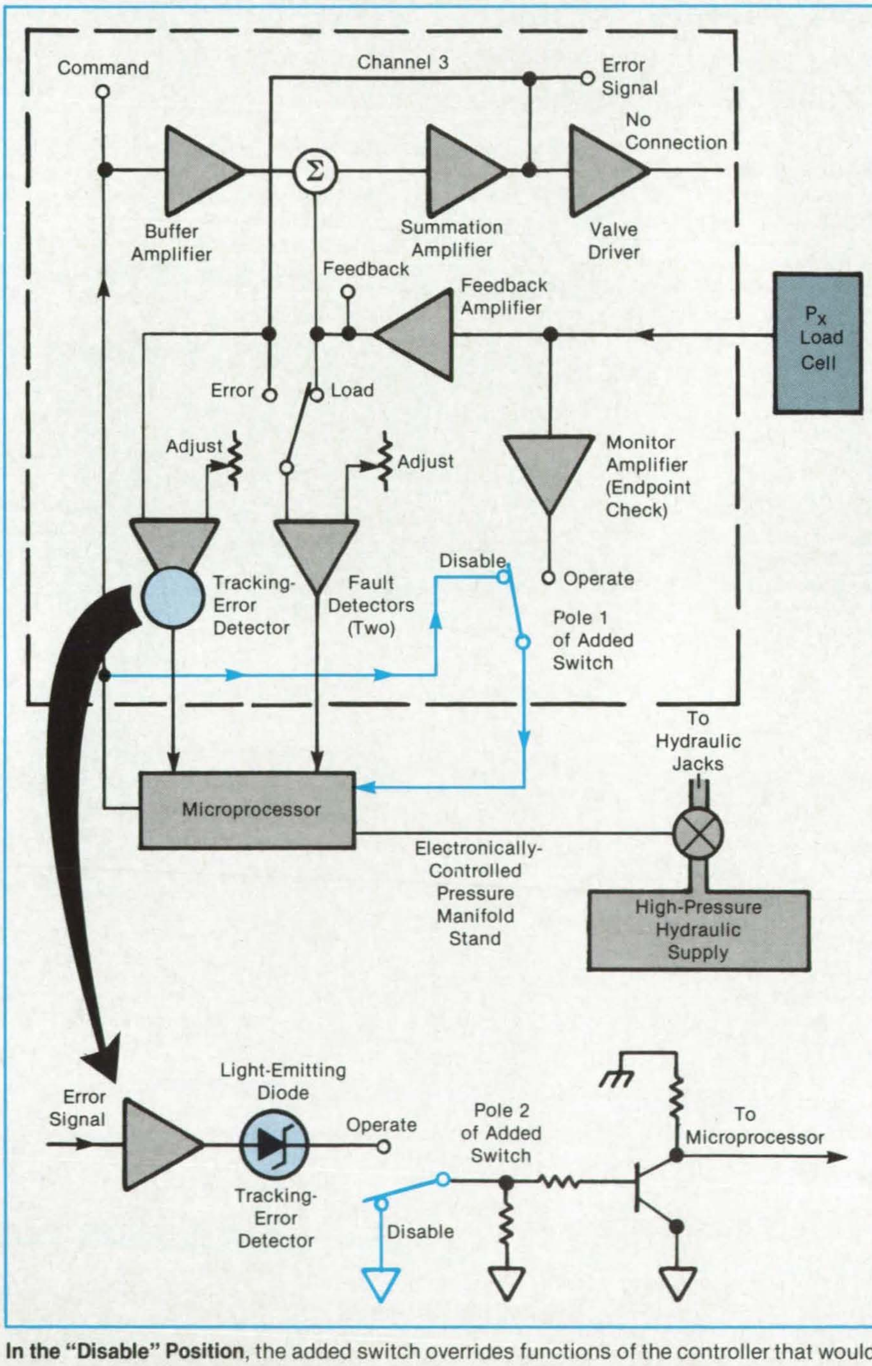

In the "Disable" Position, the added switch overrides functions of the controller that would prevent automatic shutdown on overload during friction tests. In the "operate" position, the switch allows the controller to operate in its normal fashion.

IN A MATTER OF SECONDS, THE NEW TEK 2467 CAN SAVE WEEKS OF TROUBLESHOOTING.

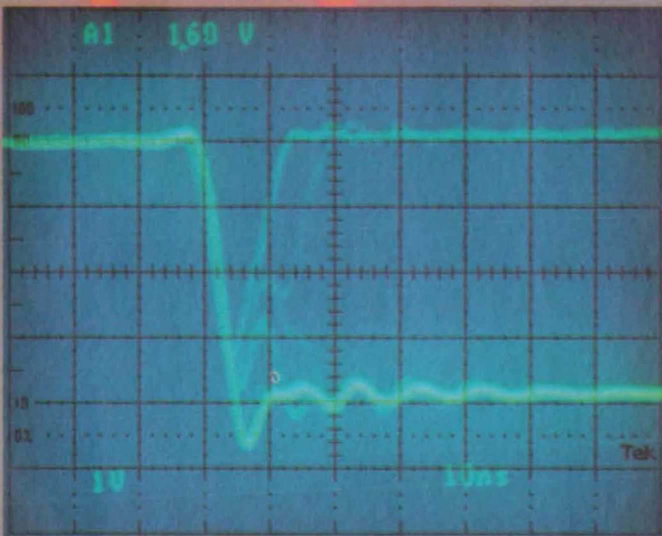

Now. See what you've always needed to see with a portable scope. (Above) Tek's new 2467 Transient Intensifying Oscilloscope, with its exclusive microchannel-plate CRT, highlights the infrequent metastability of a flip-flop output. (Below) The same metastability is invisible on a conventional high-speed scope.

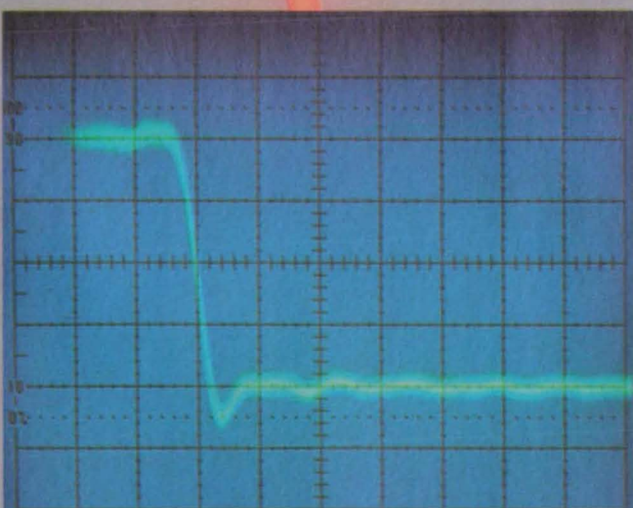

Don't be stymied by elusive glitches, pulses and single-shot events.

Our new 350 MHz Transient Intensifying Oscilloscope reveals invisible signals that escape detection by any other portable instrument. An approximate 100-fold increase in *visual* writing rate translates high-speed, single-shot phenomena and low-repetition-rate signals into easily-seen displays—in normal room light and at sweep speeds as fast as 500 ps/div.

Discover marginal conditions you don't even know exist. Now designers and test engineers can quickly identify circuit or system faults caused by infrequent metastability, asynchronous noise, crosstalk or erratic timing-margin violations—even if they occur only once in a million normal operations.

Not only can you shorten time to market, you can deliver more reliable new products.

To see the Tek 2467 in action, or to order, contact your Tek Sales Engineer. Or call the Tek National Marketing Center, 1-800-426-2200. In Oregon, call collect, (503) 627-9000.

To rent a Tek 2467 for a trial evaluation, contact an authorized Tektronix rental company:

Continental Resources, Inc.
(800) 323-2401 Nationwide
(312) 860-5991 Illinois

Electro Rent Corporation
(800) 423-2337 Nationwide
(800) 232-2173 California

General Electric Company
(800) GE-RENTS

GENSTAR Rental Electronics, Inc.
(800) 227-8409 Nationwide
(800) 331-3440 California

McGrath RentCorp
(415) 568-8866

Telogy, Inc.
(800) T-E-L-O-G-Y-Inc.

U.S. Instrument Rentals, Inc.
(800) 824-2873

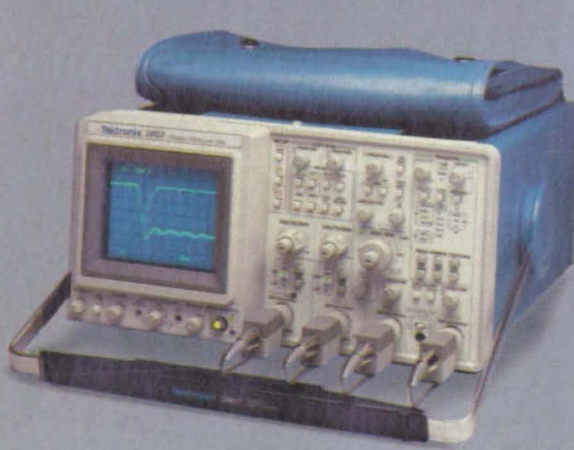

Tektronix®
COMMITTED TO EXCELLENCE

Circle Reader Action No. 359

specimen is stroked in the x direction while it is subjected to a load in the y direction. Data-acquisition equipment records loads in the x and y directions, P_x and P_y, respectively, and divides P_x by P_y to determine the coefficient of friction. It is necessary to monitor P_x and shut down the hydraulic pressure when P_x exceeds a predetermined value, thus preventing damage to the specimen or to the test equipment. The unmodified controller, however, would perceive an increase in P_x as an "endpoint-check" error or a "tracking" error, and its logic circuits would instruct the test machine to hold its commanded load instead of shutting it down.

The addition of the switch to the P_x channel of the controller disables the endpoint-error and the tracking-error circuits (see figure). This allows the controller to use its fault-detection circuits to dump the hydraulics in case of a P_x overload while allowing tests to continue on other channels with full endpoint and tracking control.

Pole 1 of the switch puts the command signal (which orders the load on the specimen) on the endpoint-check line (which monitors the load on the specimen) to the controller microprocessor. Thus, when the microprocessor compares the command signal with the endpoint-check signal, it finds agreement between the two and does not generate an endpoint-error signal.

Pole 2 of the switch grounds the base of the tracking-error output transistor. This prevents the tracking-error circuit from causing a hold-to-load signal to be sent to the test machine.

Pole 3 of the switch (not shown) turns on an "errors disabled" indicator on the front panel. Pole 4 (not shown) changes a meter switch from the "monitor ouput" line to the "command" line. Neither of these two poles affects the controller function: They are included for the operator's benefit only.

This work was done by Scott T. Fleming and Douglas B. Harrington of Rockwell International Corp. for **Johnson Space Center.** *For further information, Circle 56 on the TSP Request Card.*
MSC-20796

Controlling a Four-Quadrant Brushless Three-Phase dc Motor

The motor drives or brakes regeneratively on command, in either direction.

Marshall Space Flight Center, Alabama

A control circuit (see figure) commutates the windings of a brushless, three-phase, permanent-magnet motor operating from a dc power supply. With a single analog command voltage, the controller makes the motor accelerate, drive steadily, or brake regeneratively, in a clockwise or counterclockwise direction. The controller is well suited for use with energy-storage flywheels, actuators for aircraft-control surfaces, cranes, industrial robots, and other electromechanical systems requiring bidirectional control or sudden stopping and reversal.

Position sensors placed on the shaft provide signals that indicate the position of the rotating magnets with respect to the stationary windings. These signals are square waves that differ from each other in phase by 120°. The high interval of each position signal determines when the switching transistors of the corresponding winding are turned on.

At any given instant, winding current is being conducted by only one pair of diagonally-located switching transistors. The transistor-pair configuration changes every 60 electrical degrees of shaft rotation. For example, when the shaft position enters the first 60° (electrical) of winding A while moving clockwise in the accelerating motor mode, current is conducted through Q_1, windings A and B, and Q_5. During the second 60°, Q_5 is turned off, and the current path is through Q_1, windings A and C, and Q_6.

Resistors R_1, R_2, and R_3 provide feedback voltages proportional to the winding currents. These current-feedback signals are alternately sampled during 120° intervals, inverted as necessary, and compared with the current-command signal

You'll find CTS hybrids where precise performance is an absolute...

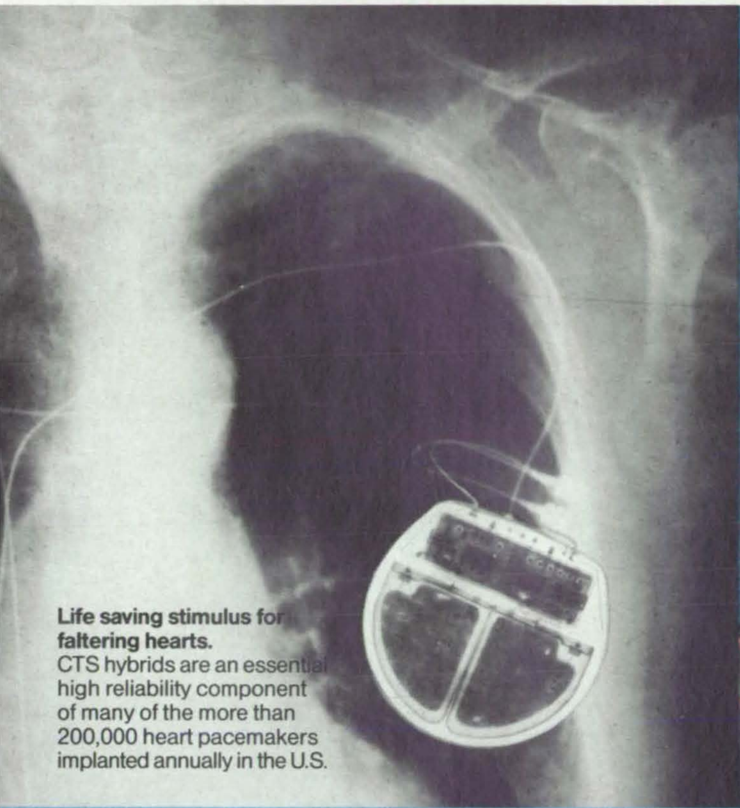

Life saving stimulus for faltering hearts.
CTS hybrids are an essential high reliability component of many of the more than 200,000 heart pacemakers implanted annually in the U.S.

Precise missile guidance.
State-of-the-art guidance systems such as those on the Navy "Harpoon" missile rely upon CTS hybrids for extraordinary quality and exacting performance.

CTS Custom Hi-Rel hybrids have established an enviable record of proven reliability for over 20 years. They withstand the harshest environments, typically exceeding MIL-STD -883 and MIL-M-38510 standards. Additional tests are performed, as required, to achieve the degree of reliability needed for specialized operating environments. CTS is equipped to meet *your* microcircuit needs—from scientific engineering and circuit design through volume production, including total in-process inspection and final QA verification.

With unmatched thick and thin film hybrid manufacturing capability, CTS produces Hi-Rel hybrids in volume quantities with no sacrifice in reliability.

Write today for an 8-page brochure detailing our capabilities in Thick and Thin Film Hybrid Technology. Contact: CTS Corporation, 1201 Cumberland Avenue, West Layfayette, IN 47906. (317) 463-2565.

CIRCLE NO. **350**

Heart pacemakers from Cordis incorporate CTS Hi-Rel circuits
Cordis Corporation could not consider anything less than precise performance in the circuitry of their Gemini automatic DDD pacer. Cordis scientists selected this CTS Hi-Rel hybrid to meet their exacting needs. Other critical, high volume medical applications include insulin shock detectors, CAT scanners, heart and blood pressure monitors and neurostimulators.

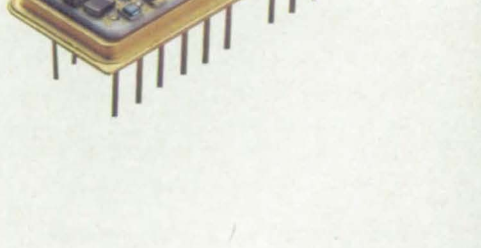

CTS means Reliability

CTS CORPORATION • ELKHART, INDIANA

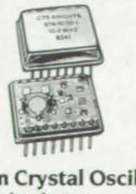

Custom Crystal Oscillator with multiple integrated functions. Phone: (815) 786-8411
CIRCLE NO. 351

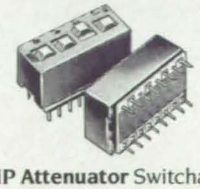

DIP Attenuator Switchable attenuator in standard DIP package.
Phone: (317) 463-2565
CIRCLE NO. 375

Series CCXO-140 Leadless Chip Carrier crystal oscillator for surface mounting.
Phone: (815) 786-8411
CIRCLE NO. 376

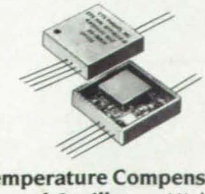

Temperature Compensated Crystal Oscillators High stability and reliability.
Phone: (815) 786-8411
CIRCLE NO. 377

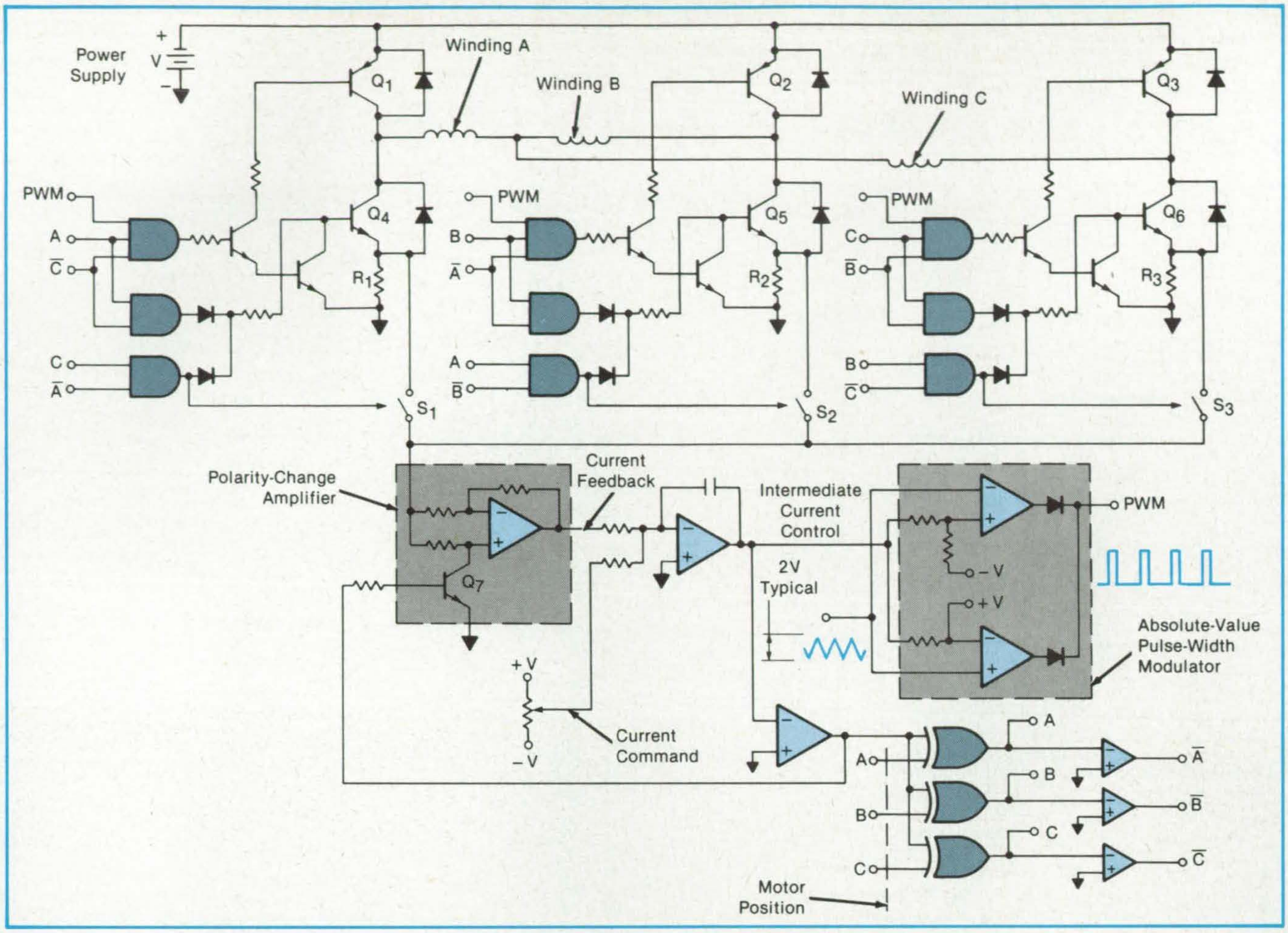

With this **Motor-Control Circuit**, a three-phase permanent-magnet motor is made to accelerate or brake regeneratively in either direction by setting the magnitude and polarity of the current-command voltage.

(regardless of its polarity) to obtain an intermediate negative-feedback current-control signal. In the absolute-value pulse-width modulator (PWM), the intermediate signal is compared with a triangular wave of about 10 kHz. The resulting PWM output is a train of pulses, the durations of which are varied to turn the switching transistors on and off at intervals intended to produce the commanded current.

The lower transistor in each pair (for example, Q_4 for winding A) is turned on during the 120° that begin 60° after the cessation of the "on" period of the upper transistor of that pair. In addition, the lower transistor is turned off and on during the 120° when the upper transistor is being turned on and off, respectively.

The turn-on and turn-off times for each transistor are determined according to the current command and to the shaft position, direction of rotation, current, and back-electromotive force of the motor, as measured by the position and current sensors. For example, a current-command signal of one polarity causes acceleration or turning against a load in a clockwise direction, or braking from counterclockwise rotation, possibly followed by reversal into clockwise rotation. A current-command signal of the opposite polarity produces similar effects in the opposite directions.

In acceleration, the appropriate transistor pairs are connected in the sequence of pulses as the circuit attempts to maintain the commanded current from the supply to the motor. In braking, the motor acts as a generator, and the transistor pairs are connected in the pulse sequence as the circuit attempts to maintain the commanded current from the motor as it feeds power back to the supply. As the braking motor slows toward a stop, the back-electromotive force is no longer sufficient to maintain the commanded current: At that point, the circuit begins to feed current from the supply to the motor to continue the braking by maintaining the commanded current. Eventually, the motor may stop and begin to accelerate in the opposite direction. Thereafter, the circuit continues to maintain the commanded current, with the difference that the pulse sequence moves in the opposite direction among the windings, corresponding to the opposite motor rotation.

This work was done by Frank J. Nola of **Marshall Space Flight Center**. *For further information, Circle 48 on the TSP Request Card.*

This invention is owned by NASA, and a patent application has been filed. Inquiries concerning nonexclusive or exclusive license for its commercial development should be addressed to the Patent Counsel, Marshall Space Flight Center [see page 29]. Refer to MFS-28080.

Tailorable Infrared Sensing Devices

Proposed devices would consist of Ge_xSi_{1-x}/Si strained-layer superlattices on silicon.

NASA's Jet Propulsion Laboratory, Pasadena, California

A proposed infrared sensing device using a Ge_xSi_{1-x}/Si strained-layer superlattice may offer enhanced detection sensitivity and could be tailored for a specific cutoff wavelength over the range from 2.7 to about 50 μm. Such a device could be fabricated on a silicon substrate together with sophisticated very-large-scale integrated circuitry, making it useful for a wide range of applications related to robotics, space exploration, and terrestrial surveillance.

The device (see Figure 1) includes a large number of alternating thin layers of Ge_xSi_{1-x} and Si. Such a structure can be grown using molecular-beam epitaxy; in the future, such other growth techniques as chemical vapor deposition might be used.

Figure 2 illustrates the energy-band diagram of a Ge_xSi_{1-x}/Si superlattice with a high concentration of dopant under an electrical bias voltage. The energy gap of Ge_xSi_{1-x} is lower than that of Si by an amount $\Delta E(x)$, which depends on the germanium content, x. As the superlattice gets richer in germanium, its energy gap decreases monotonically from that of silicon (1.1 eV) to that of germanium (0.66 eV). Although the lowest value of $\Delta E(x)$ can be zero (when $x = 0$), in practice the lowest ΔE depends on the temperature and for a practical device could be about 0.01 to 0.05 eV, depending on operating conditions; thus the new device could operate at wavelengths up to 50 μm. Good-quality Ge_xSi_{1-x}/Si superlattices with $x < 0.5$ grown by molecular-beam epitaxy already have been demonstrated; and theory indicates that in the future, high-quality superlattices with the full range of x (from 0 to 1) can be grown.

The mechanism of the new device is similar to that of the silicide Schottky-barrier detector, with the silicide film being replaced by the heavily-doped Ge_xSi_{1-x} semiconductor layer. A photon of energy greater than $\Delta E(x)$ excites a hole from the valence band of Ge_xSi_{1-x} to that of Si. The hole then drifts to the cathode under the influence of the applied electric field. Since the device has many charge-separation barriers, its detection sensitivity should be greatly enhanced. The device could be operated in an avalanche mode, under which the gain should be high and the response time very short.

This work was done by Li-Jen Cheng of Caltech for **NASA's Jet Propulsion Laboratory**. *For further information, Circle 52 on the TSP Request Card.*

Inquiries concerning rights for the commercial use of this invention should be addressed to the Patent Counsel, NASA Resident Office-JPL *[see page 29].* *Refer to NPO-16607.*

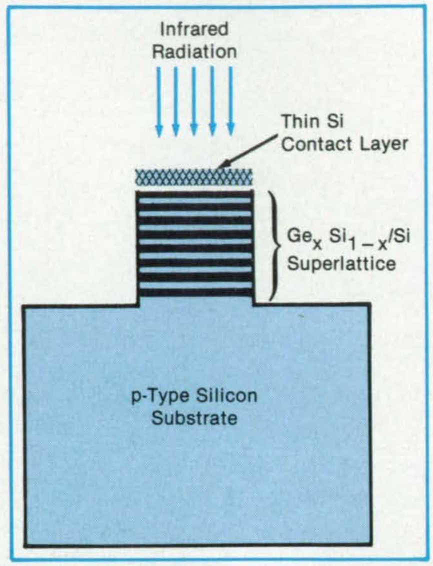

Figure 1. **Alternating Layers of Ge_xSi_{1-x} and Si** are deposited by molecular-beam epitaxy. When an electric field is applied across the stack, it acts as a detector for infrared photons.

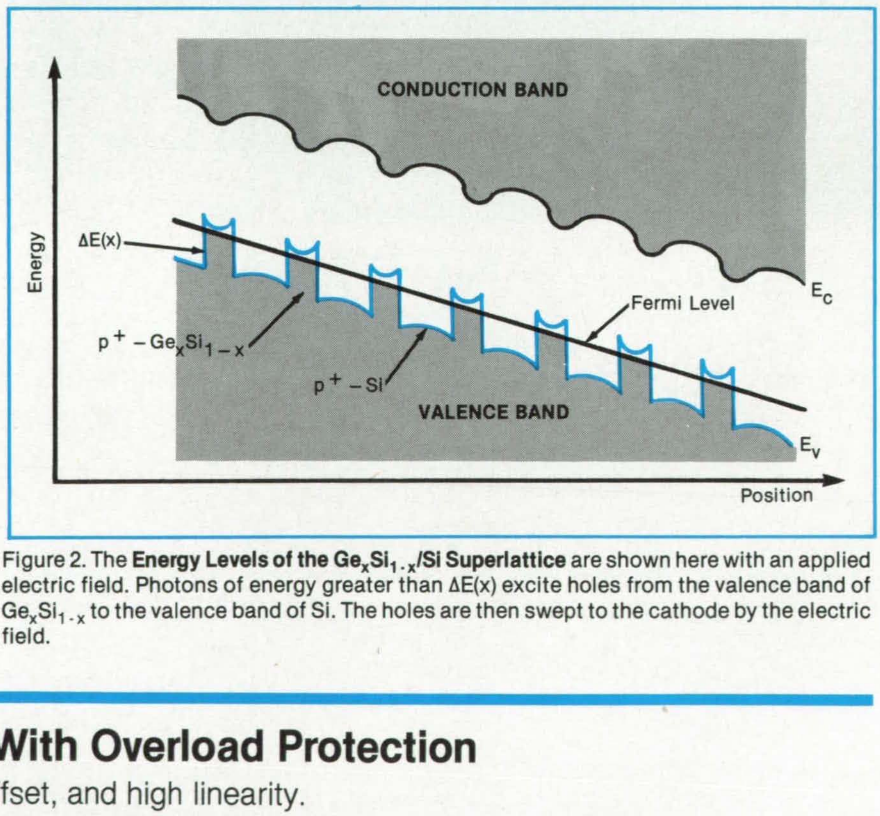

Figure 2. The **Energy Levels of the Ge_xSi_{1-x}/Si Superlattice** are shown here with an applied electric field. Photons of energy greater than $\Delta E(x)$ excite holes from the valence band of Ge_xSi_{1-x} to the valence band of Si. The holes are then swept to the cathode by the electric field.

Electrometer Amplifier With Overload Protection

Circuit features low noise, input offset, and high linearity.

Ames Research Center, Moffett Field, California

A prototype dc amplifier designed for use with an ion detector has features that are desirable in general laboratory and field instrumentation. The circuit is assembled from commercially available integrated circuits.

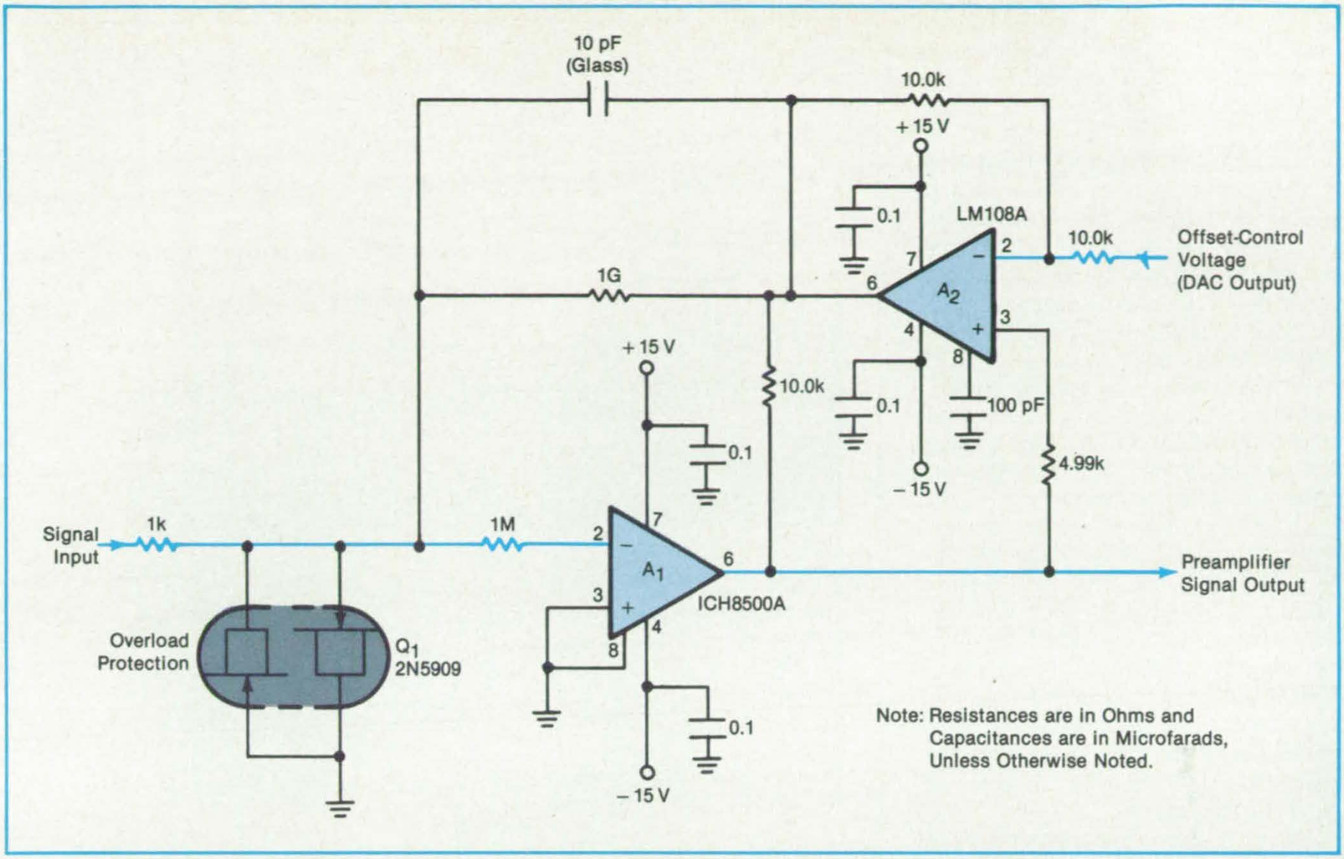

The **Input Preamplifier** includes input-overload protection and a nulling circuit to subtract a dc offset from the output.

The critical part of the circuit is the preamplifier (see figure), which is basically a current amplifier. The current is fed to the inverting input of operational amplifier A_1. The feedback loop keeps the input resistance low, maintaining the input voltage within millivolts of ground.

The preamplifier is protected from excessive input signals of either polarity by the 2N5909 junction field-effect transistor (JFET). While a pair of anti-parallel-connected diodes might suffice in a less sensitive application, the JFET is used here because it is a low-leakage, low-capacitance unit. With the millivolt normal input levels, leakage through the JFET is not significant.

A nulling circuit makes it possible to set the preamplifier output voltage to zero at a fixed low level (up to $\pm 10^{-8}$ A) of the input current. (This level is called the standing current and corresponds to the zero-signal level of the instrumentation.) The opposing (offset) current is generated in the 10^9-Ω feedback resistor to buck the standing current.

The offset current is set by thumbwheel-switch control inputs to a digital-to-analog converter (DAC). The DAC output is subtracted in A_2 from the signal output, and the difference signal at the output of A_2 is the voltage that develops the bucking current. This somewhat complex nulling arrangement produces less shot noise than would be produced by simply feeding a bucking current directly to the preamplifier input.

Different current ranges are reached by feeding the preamplifier output to low- and high-gain amplifier chains. To reduce noise, each chain includes a 1.5-Hz corner active filter. The amplifier operates with a linear output over the range of ± 10 V for input signals ranging from $\pm 10^{-13}$ to $\pm 10^{-8}$ A. The total noise generated in the circut is equivalent to an rms input-current variation of about 10^{-3} A.

This work was done by Fritz H. Woeller of **Ames Research Center** *and R. M. Alexander of TRW, Inc. For further information, Circle 44 on the TSP Request Card.*

Inquiries concerning rights for the commercial use of this invention should be addressed to Patent Counsel, Ames Research Center [see page 29]. Refer to ARC-11457.

Semiconductor Laser With Two-Dimensional Beam Steering

An added electrode provides steering in a second direction.

NASA's Jet Propulsion Laboratory, Pasadena, California

The proposed modification of a monolithic semiconductor injection laser capable of one-dimensional electronic beam steering should enable the deflection of its beam in a second direction. Such a laser chip could provide beam pointing or raster scanning for applications in optical communications, data processing, image scanning, and optical ranging.

To deflect the laser beam in a given plane, the charge density in the active region that emits the light must have a gradient in that plane along the direction perpendicular to the emitted light. Deflection occurs because the charge gradient affects the waveguide properties of the laser. The proposed laser geometry shown in the figure should provide control of such gradients in two perpendicular directions.

Conceptually, the four-terminal device is a combination of an npn transistor and a laser fabricated in AlGaAs. (It could also be fabricated in such other atomic systems as GaAsP.) As in the existing version of this device, the beam is scanned in the x-z plane by variation of the ratio or of the magnitudes of I_1 and I_2 (or of $V_1 - V_4$ and $V_2 - V_4$). However, the addition of electrode 3 to the transistor base region should enable the control of the vertical charge distribution, which affects the beam axis in the y-z plane.

The amount of beam steering achievable would be determined experimentally. In the one-dimensional case, beams have been steered by ±2 beam widths in the x-y plane. There is a tradeoff between the amount of steering in the y-z plane and the laser threshold current. For large beam deflections, the active region must be relatively thick (at least 1 μm) and must have an aluminum content similar to that in the cladding layers.

This work was done by Joseph Katz of Caltech for **NASA's Jet Propulsion Laboratory.** *For further information, Circle 77 on the TSP Request Card.*
NPO-16031

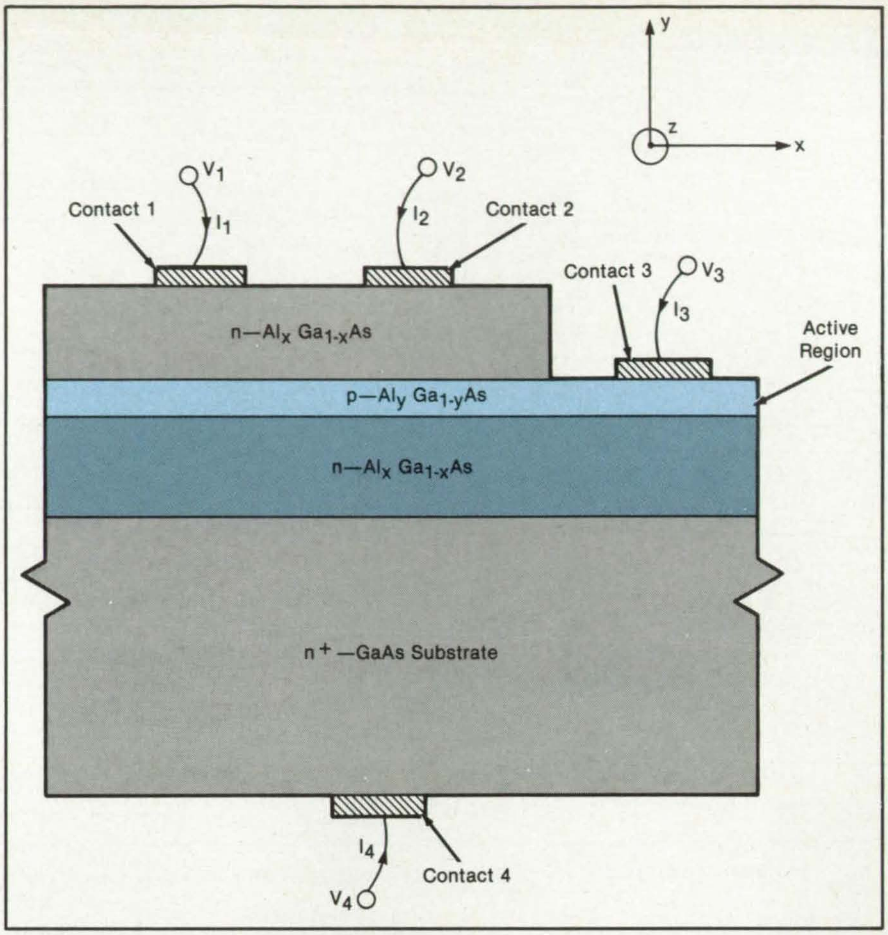

Two-Dimensional Electronic Steering of the beam from a proposed semiconductor injection laser would be achieved by adding electrode 3 to a laser that was previously capable of one-dimensional beam steering. The laser beam would come out of the page in the z direction from the p-type base region.

MOSFET Power Controller

High current and voltage are controlled remotely.

Lewis Research Center, Cleveland, Ohio

The availability of high-voltage MOSFET's that have low "on" resistance is the enabling factor in developing improved remote power controllers (RPC's). To demonstrate the capabilities of these devices, they were used to build an RPC that would withstand 1,000 V and switch 25 Adc. One of the unique features of this RPC (see figure) is that it uses two banks of parallel-connected MOSFET's in series to provide the required voltage capability. It also has an improved trip circuit.

To insure voltage sharing between the switch banks, low-impedance, gate-drive circuits were used that provided a controlled range for turn on. They are individually trimmable to insure simultaneous switching within a few nanoseconds during both turn on and turn off. The control circuit for each switch bank and the overcurrent trip circuit float independently and are supplied power via transformer T_1 from an inverter. Control of the floating stages is by optocouplers.

At turn on, optocouplers OC_1 are on, clamping pin 2 of U_{102} and pin 3 of U_{101} to the negative rail. This keeps Q_{101} turned off and $Q_{102A\text{-}D}$ conducting. Therefore, power switch $Q_{104A\text{-}J}$ is open. After a delay of 25 ms, OC_1 is turned off, pin 2 of U_{102} is driven high, and $Q_{102A\text{-}D}$ releases the gate circuit of $Q_{104A\text{-}J}$. Pin 3 of U_{101} goes high, generating a controlled ramp to turn $Q_{104A\text{-}J}$ on. The rate of rise of the ramp is controlled by C_{101}. Turn off reverses this process. $Q_{102A\text{-}D}$ is turned on as described above, turning off the 10 parallel MOSFET's, $Q_{104A\text{-}J}$. This can be done in one-half μs. Normal overcurrent tripping with an inverse time delay uses operational amplifiers U_{303A}, U_{303B}, and associated components.

CR_{303} is a 1.22-V precision voltage reference that provides a bias current that subtracts the load-current signal from R_{SH} and R_{306} at the noninverting input of pin 2 of V_{303A}. For normal load current, the R_{305} bias current exceeds the R_{306} load-current signal, and the output voltage of V_{303A}, pin 1 will be at a low level. At high values of load current, C_{302} will be charged through resistor R_{303}. The capacitor integrates the input current above 1.2 per unit, and the voltage at pin 1 of U_{303A} continues to rise until the voltage at pin 5 of U_{303B} reaches 1.22 V. Thus, when the output voltage of the integrator (pin 1

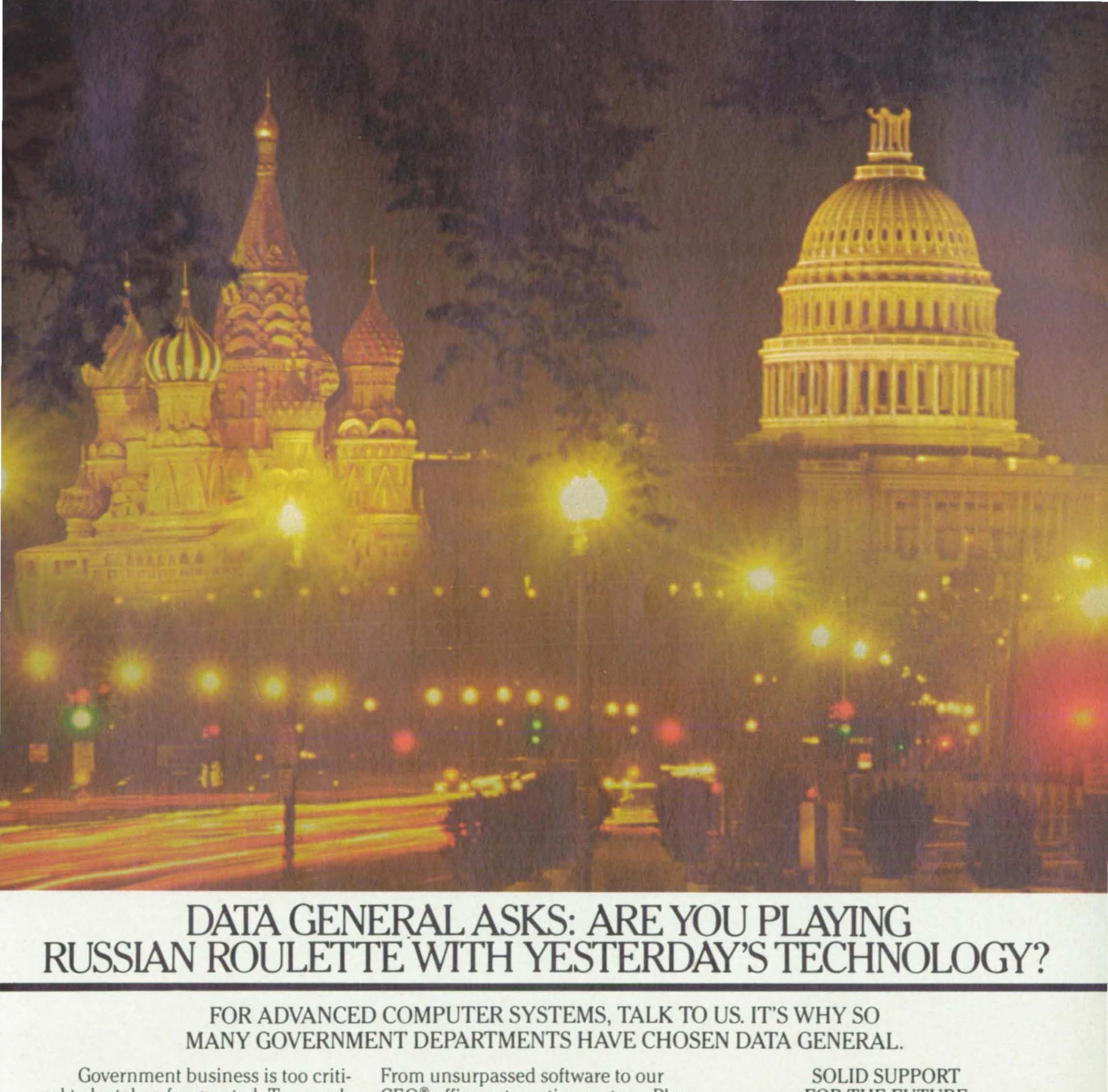

DATA GENERAL ASKS: ARE YOU PLAYING RUSSIAN ROULETTE WITH YESTERDAY'S TECHNOLOGY?

FOR ADVANCED COMPUTER SYSTEMS, TALK TO US. IT'S WHY SO MANY GOVERNMENT DEPARTMENTS HAVE CHOSEN DATA GENERAL.

Government business is too critical to be taken for granted. Too much depends on it.

No wonder nineteen of the top twenty U.S. defense contractors have bought a Data General system. As have all the Armed Services and most major departments of the federal government.

And to date, nearly thirty U.S. Senate offices and committees have chosen Data General.

TODAY'S BEST VALUE

Why such unanimity? Because Data General offers a complete range of computer solutions for government programs, with one of the best price/performance ratios in the industry.

From our powerful superminis to the DATA GENERAL/One™ portable. From unsurpassed software to our CEO® office automation system. Plus complete systems for Ada® and Multi Level Secure Operating Systems, and a strong commitment to TEMPEST.

All Data General systems have full upward compatibility. And because they adhere to international standards, our systems protect your existing equipment investment. We give you the most cost-effective compatibility with IBM outside of IBM—and the easiest to set up and use.

SOLID SUPPORT FOR THE FUTURE

We back our systems with complete service and support. As well as an investment in research and development well above the industry norm.

So instead of chancing yesterday's technology, take a closer look at the computer company that keeps you a generation ahead. Write: Data General, Federal Systems Division, C-228, 4400 Computer Drive, Westboro, MA 01580. Or call 1-800-DATAGEN.

Data General
a Generation ahead.

Circle Reader Action No. 353

of $U_{303A\text{-}O}$) exceeds 1.22 V, pin 7 of U_{303B} goes high, firing SCR_{301}, and causing conduction of OC_3. An amplifier not shown on the figure boosts the OC_3 signal and turns on OC_1. R_{303} is included in the integrating circuit to lower the trip time at higher currents, since the integrating current causes a voltage drop in R_{303}. Thus the voltage on pin 1 of U_{303A} could rise rapidly since some of the voltage would appear across R_{303}. R_{303} is chosen to give instant tripping if the current exceeds three per unit.

A second, faster acting circuit is used for fault protection. It responds only to steep current fronts by sensing a high di/dt developed across the shunt. C_{303} can be considered a short circuit for these rapidly changing currents, which allow V_{SH} to appear across R_{310} and R_{311} in series. Since these resistors are equal, one-half of V_{SH} appears at U_{302}. The polarity of this voltage is negative, and since it is applied to the inverting input of U_{302}, will be driven positive and fire SCR_{301}, which turns on OC_3. Since response to small changes is not desired, a positive voltage is established at pin 3 of U_{302} by CR_{303}, R_{309}, and R_{310}. This positive reference voltage must be overcome by the negative V_{SH} voltage to drive pin 3 of U_{302} negative. Because this positive reference voltage is controlled on pin 3 of U_{302}, the circuit can be made to respond to transient currents of any magnitude. U_{301} is used to modify this reference voltage proportionally to the load current. This enables a smaller change in current to trip the circuit when the steady-state current is near full load.

This work was done by J. T. Mitchell and K. Jones of Westinghouse Electric Corp. for **Lewis Research Center.** *Further information may be found in NASA CR-168041 [N83-21236/NSP], "Kilovolt dc Solid State Remote Power Controller Development."*

Copies may be purchased [prepayment required] from the National Technical Information Service, Springfield, Virginia 22161, Telephone No. (703) 487-4650. Rush orders may be placed for an extra fee by calling (800) 336-4700.
LEW-14112

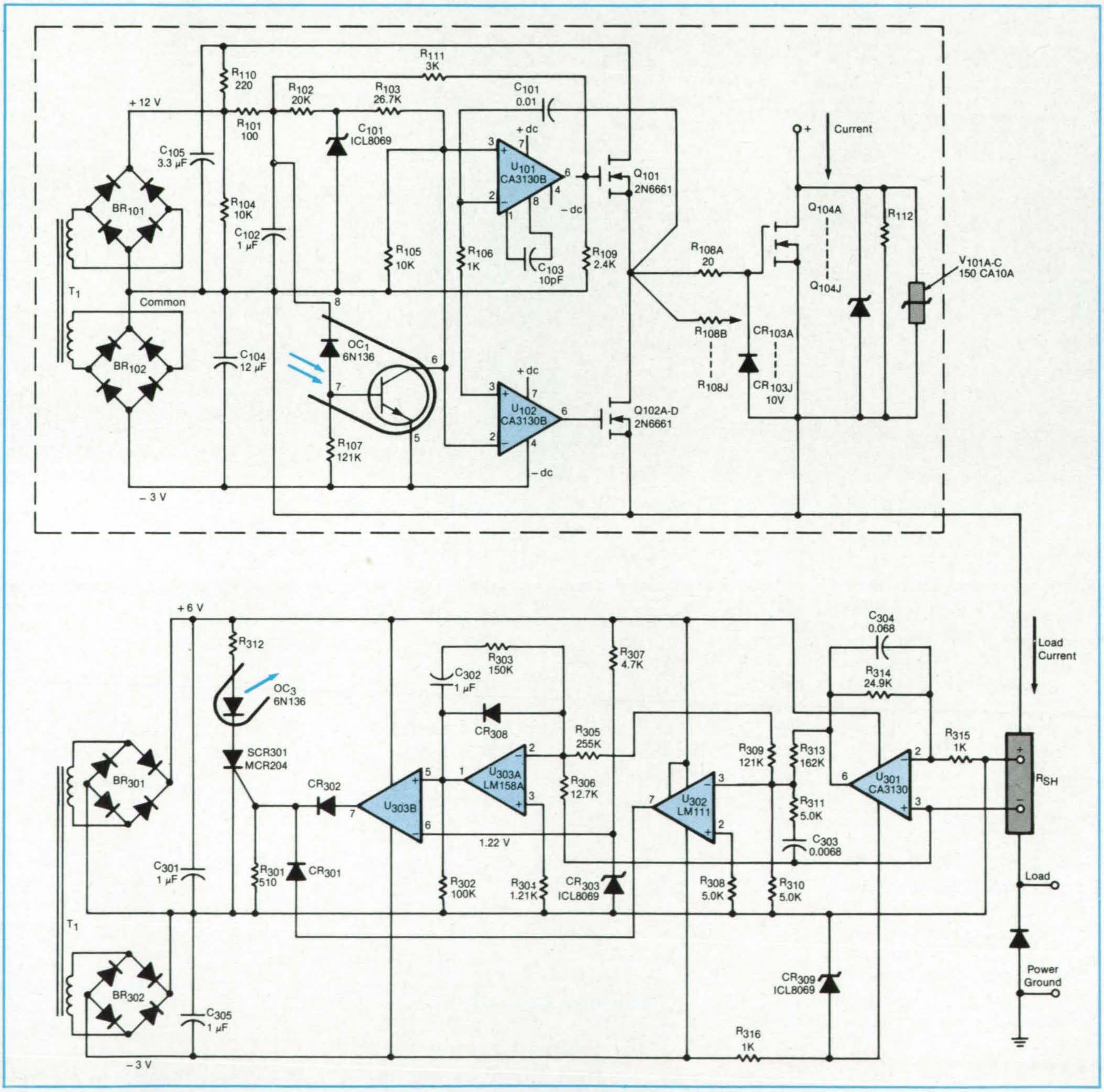

The **Remote Power Controller** includes two series-connected banks of parallel-connected MOSFET's to withstand high current and voltage.

Fast Remote Kilovolt-Power Controller

High power is turned off rapidly in case of overload.

Lewis Research Center, Cleveland, Ohio

A remote power controller (RPC) has been developed with a power-handling capability of 25 A at 1,000 Vdc. The RPC has a programmable characteristic that can trip open to clear a fault within 3 μs. In addition to load switching, overload protection, and status indication, the RPC possesses the following advantages:

- No contact bounce or wear and no arcing;
- Precise open and close times;
- Controlled current transients;
- Consistent, repeatable overload protection over the temperature range; and
- Immunity to high vibration and shock.

The figure shows a fast-acting base-drive circuit and a fast-acting overcurrent-protection circuit. There is also a power converter feeding T_1 and logic circuits that command the RPC on and off. These are of conventional design.

The fast-acting base-drive circuit operates as follows: During normal operation, C_{106} becomes charged because of the few volts dropped across CR_{111}, CR_{113}, and R_{114}. For a fast turnoff, SCR_2 is fired, which allows C_{106} to discharge through SCR_2, R_{116}, and R_{115}. This applies a reverse potential across Q_{101} and Q_{102} emitter/base junctions, which clears the junction of carriers for a fast turnoff.

The three diodes are included in series with R_{114} to obtain a minimum voltage of three diode drops, to work against the drop of SCR_2 and have sufficient voltage left to clear the carriers in Q_{101} and Q_{102}.

In the fast-acting overcurrent-protection circuit, Z_{101} and Z_{102} are connected in a normal inverting threshold/integrator trip circuit. Diode CR_{110} is a 1.22-V precise reference which, along with R_{110} and R_{112}, sets the threshold. At this threshold Z_{101} responds and causes output pin 6 to go high, in turn charging capacitor C_{105} through R_{109}. When the voltage at pin 6 of Z_{101} is greater than the CR_{110} reference voltage, the Z_{102} comparator output at pin 2 becomes positive, firing SCR_1 through CR_{105}. This sequence causes a "slow" trip response from the base-drive circuit, since C_{106} must discharge through CR_{106} in addition to SCR_1. The result is less reverse voltage across the emitter/base junctions of Q_{101} and Q_{102}.

Pin 6 or Z_{101} can reach the reference voltage of 1.22 V by allowing C_{105} to charge to 1.22 V (integrating the current), resulting in an inverse current/time relationship. If the load current reaches 3 per unit (PU), a highly negative voltage tends to be established at pin 2 of Z_{101}; its output pin 6 would be driven suddenly positive. The resulting voltage drop would appear across R_{109}, since C_{105} would be a short circuit. This condition would allow pin 6 to reach above 1.22 V without "waiting" for capacitor C_{105} to charge, which could result in an "instant" tripping.

Resistor R_{109} is chosen for this to occur at 3 PU. Circuits Z_{101} and Z_{102} are relatively slow; this instant tripping would take several microseconds before the output of Z_{102} becomes positive. If this occurs as the result of a short circuit, the current could be well above 5 PU before the tripping is initiated. No action would begin until the current reaches 3 PU, and in the few microseconds of response time of Z_{101} and Z_{102}, the current could be much higher. Therefore, this circuit is not adequate for short-circuit protection without current limiting but is adequate for light overloads.

The current-sensing shunt R_{117} gives a 50 mV drop at a 25 A (1 PU) load. This voltage does not normally appear at pin 3 of Z_{103} because of capacitor C_{103}. However, with a rapidly rising current (e.g., a steep front of current from a short circuit), C_{103} appears as an effective short circuit, and half of the negative shunt voltage appears at pin 3 of Z_{103} (R_{106} and R_{107} are equal and divide the shunt voltage).

Pin 3 of Z_{103} is normally held at +55 mV. Therefore, when a steep front of load current reaches 2.2 per unit, the net voltage at pin 3 of Z_{103} would be zero, since the shunt voltage of −110 mV is divided and exactly neutralizes the +55 mV at the inverting terminal. As the steep front increased beyond 2.2 PU, the output of Z_{102}, a fast operating amplifier, would go positive and fire SCR_1 and SCR_2. This would give a "fast" tripping action as previously described. The tripping action takes less than one microsecond. The remainder of the circuit consists mainly of power supply and logic.

This work was done by P. Hower of Westinghouse Electric Corp. for **Lewis Research Center**. *Further information may be found in NASA CR-168041 [N83-21236/NSP], "Kilovolt DC Solid State Remote Power Controller Development."*

Copies may be purchased [prepayment required] from the National Technical Information Service, Springfield, Virginia 22161, Telephone No. (703) 487-4650. Rush orders may be placed for an extra fee by calling (800) 336-4700. LEW-14111

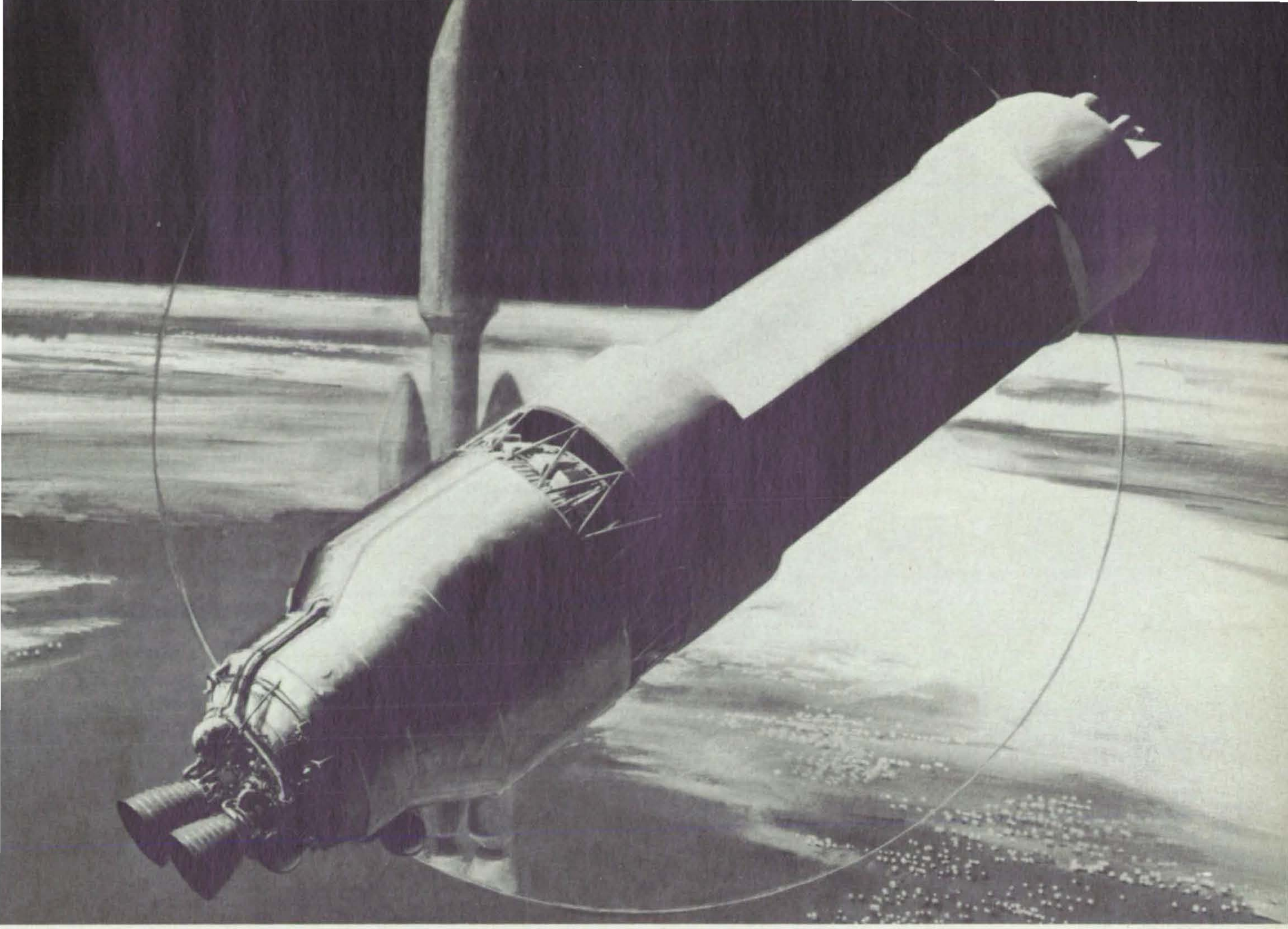

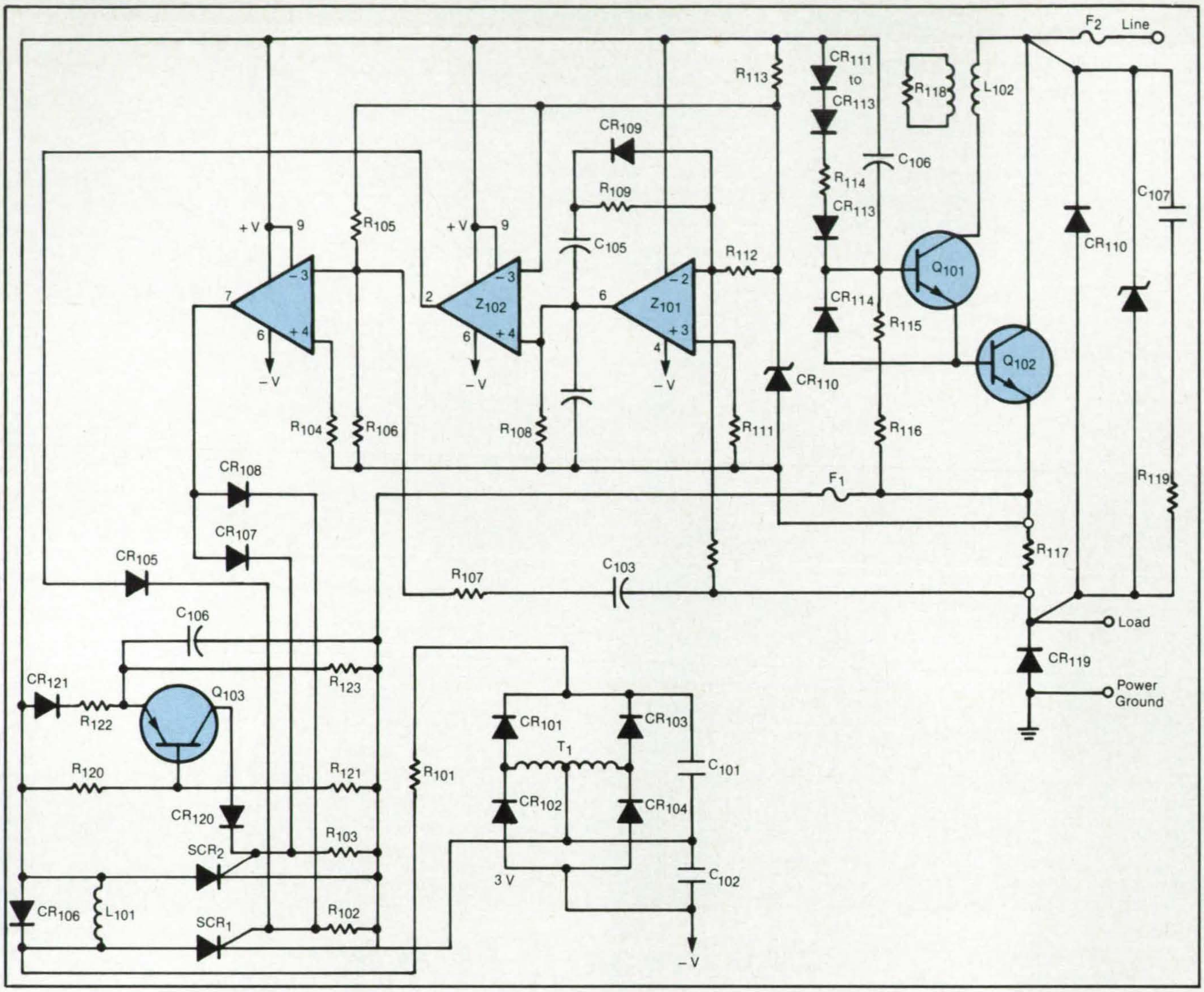

The **Base-Drive and Overcurrent-Protection Circuits** respond rapidly to overcurrent conditions.

Books and Reports

These reports, studies, and handbooks are available from NASA as Technical Support Packages (TSP's) when a Request Card number is cited; otherwise they are available from the National Technical Information Service.

List of Preferred Electronic Parts

Components that have passed stringent qualification tests are tabulated and described.

A preferred parts list tabulates electronic, magnetic, and electromechanical parts for electronic equipment in which reliability is a major consideration. The list presents parts that have qualified for service in critical flight and ground-support applications by NASA's Jet Propulsion Laboratory.

Destructive and nondestructive qualification testing confirmed that the parts are capable of withstanding spacecraft environments without excessive degradation and have stable characteristics during their operating lives. Testing also assessed the effects of electrical, environmental, and mechanical stresses in various levels and time durations.

Each part on this list must undergo a design appraisal in which device construction and processing are examined. This examination provides guidance in the design of screening tests. Approval of the manufacturers' materials, processes, quality control, and engineering and production capabilities are also required for part approval.

Parts included in the list are capacitors, diodes, filters, fuses, magnetic devices, microcircuits, relays, resistors, switches, and transistors. Each category of parts is covered in a separate section. An introduction to each section contains application notes and brief descriptions of the major types of the part. The section on diodes, for example, describes the following types: General-purpose rectifiers, power rectifiers, signal or switching diodes, voltage regulators, special-purpose diodes (microwave, optical, and current-regulating), and silicon-controlled rectifiers and switches.

This work was done by Robert E. Covey, W. Richard Scott, Lawrence M. Hess, George Steffy, and Frank R. Stott of Caltech for **NASA's Jet Propulsion Laboratory.** *Further information may be found in NASA CR-176258 [X86-10015/NSP], "JPL Preferred Parts List."*

Copies may be purchased [prepayment required] from the National Technical Information Service, Springfield, Virginia 22161, Telephone No. (703) 487-4650. Rush orders may be placed for an extra fee by calling (800) 336-4700.
NPO-16028

STOKES® VACUUM

VAC-TECH NEWS

How to stop water vapor from destroying your vacuum system when you're plasma etching.

DRY PLASMA ETCHING SYSTEM
TYPICAL VACUUM SYSTEM SCHEMATIC

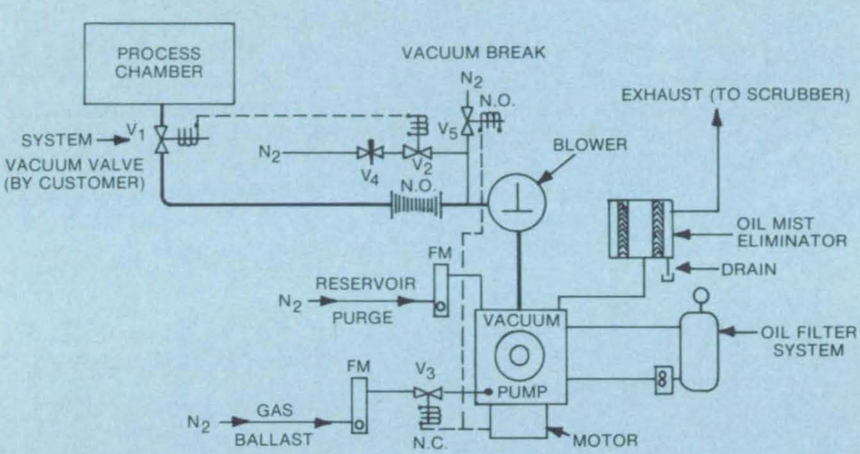

NOTES:
1. ALL NITROGEN GAS BLEEDS—1 PSIG MAXIMUM
2. SYSTEM VALVE V_1 INTERLOCKED WITH VALVE V_2. WHEN V_1 CLOSED V_2 OPEN. WITH V_1 CLOSED & VACUUM SYSTEM IN OPERATION, USE NEEDLE VALVE V_4 TO ADJUST PRESSURE IN MANIFOLD TO 50-100 MICRONS.
3. SOLENOID VALVE V_3 CONNECTED ACROSS MOTOR LEADS, OPENS WHEN PUMP STARTS.
4. FM = FLOW METER
5. SOLENOID VALVE V_5 CONNECTED ACROSS MOTOR LEADS, CLOSES WHEN PUMP STARTS.

Due to the corrosive nature of the gases used and the particulates generated, plasma etching can impose harsh requirements on your vacuum system.

The presence of water vapor makes these conditions even more severe.

To keep your vacuum system performing to its capabilities, you must prevent water vapor from entering the system. If it does, you must remove it quickly.

The following installation and operation procedures will help you keep your system operating smoothly.

The right installation.

Install PVC exhaust piping instead of galvanized or black iron pipe, and an oil mist eliminator to reduce oil loss from the pump.

The exhaust line should be installed so it can easily be disassembled for periodic cleaning and the vacuum manifold must be leak-free.

The right operation.

Operate the vacuum system continuously and make sure the vacuum pump is gas ballasted during processing with a nitrogen flow rate of 1 to 2 L/M.

Purge the reservoir with nitrogen (in humid ambients it may be necessary to increase the nitrogen flow). Do not pump on the process chamber with the vacuum system at blank-off pressure as oil backstreaming may result. When necessary to shut down the vacuum system for over 8 hours, fill gas ballast with nitrogen for at least 4 hours before stopping.

The right maintenance.

Drain the exhaust oil mist eliminator weekly. If oil is clean, it can be reused by returning to the pump. If it is "milky" or cloudy, it should be decanted before returning to pump reservoir. Cleaning interval is determined by the amounts of particulates accumulated.

Monitor differential pressure across the oil filter. Replace element when filter pressure shows a significant increase above baseline pressure. Actual pressures will be determined by your own process.

Open pump reservoir at 2-month intervals to remove sediment from bottom of the reservoir. And when the particulate oil filter elements are used, replace element when filter pressure as shown on the gage is exceeded.

The right vacuum system.

Stokes is America's full-line vacuum components manufacturer so we have the right pumping package for your application. So you don't have to over-design or over-purchase.

If you have a processing design question call or write: Stokes Division, Pennwalt Corporation, 5500 Tabor Road, Philadelphia, PA 19120. 215-831-5400.

Send for free subscription to Vac-Tech News.
Keep up with the latest developments and advanced technology taking place in the vacuum industry. Just call or write and we'll see that you receive each issue.

STOKES
PENNWALT
EQUIPMENT ■ CHEMICALS
HEALTH PRODUCTS

Stokes Division, Pennwalt Corporation
5500 Tabor Road, Philadelphia, PA 19120
Phone: 215-831-5400

Circle Reader Action No. 425

Electronic Systems

Hardware, Techniques, and Processes

Computer Programs

Pilot-Tone System for Mobile Communications

The degrading effects of multipath fading would be reduced.

NASA's Jet Propulsion Laboratory, Pasadena, California

In a proposed mobile communication system called the tone-calibrated technique, a pilot tone provides a phase- and amplitude-calibration reference to enable the coherent demodulation of the signal at the receiver despite fading. The signal received by or from a mobile terminal is severely and rapidly faded due to the motion of the terminal and the propagation of the signal along multiple paths. This fading introduces random amplitude modulation and phase modulation with a bandwidth of twice the Doppler frequency shift.

Under these conditions, it is difficult to extract the carrier from the faded sidebands for use in demodulation. However, if a pilot tone is transmitted along with the rest of the signal, it undergoes the same fading, maintaining the same amplitude and phase relationship with the rest of the signal at the receiver that it had at the transmitter. Thus, it can serve as the carrier reference for demodulation.

The tone-calibrated technique is intended for use with phase-modulated data or telephony systems using Manchester digital pulse-code modulation. Because this kind of modulation has no spectral component at zero frequency, there is a null at the carrier frequency in the middle of the spectrum occupied by the transmitted signal; that is, the transmitted signal is all sidebands and no carrier. The

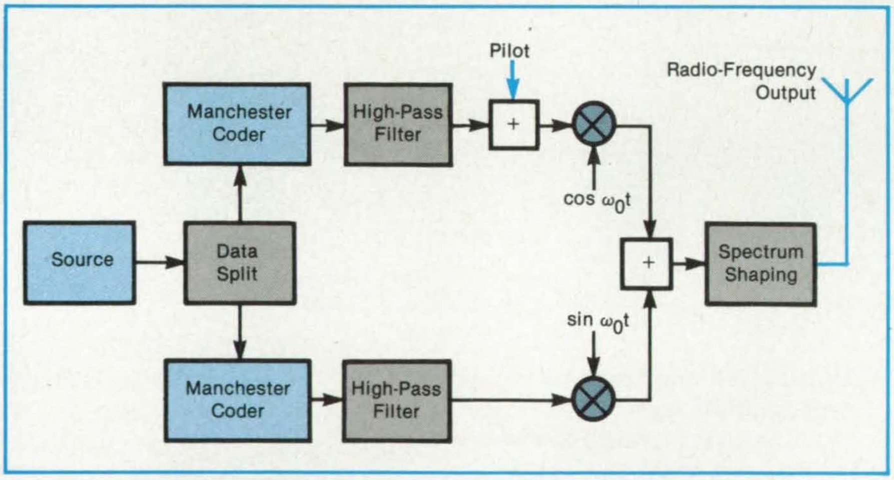

Figure 1. **In the Transmitter,** a Manchester digital pulse code is first high-pass filtered, then used to modulate a carrier. A pilot tone is inserted at the transmitter to provide a fade-compensating calibration tone at the receiver.

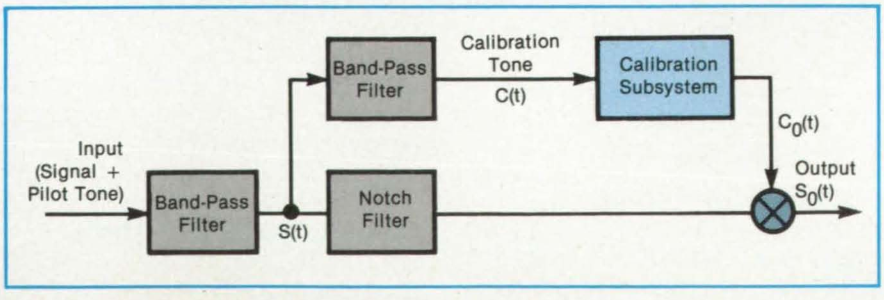

Figure 2. **In the Receiver,** the faded pilot tone is extracted for use in the coherent demodulation of the signal. The faded pilot divided by its amplitude squared is mixed with the faded signal to recover unfaded Manchester pulses.

pilot tone is conveniently inserted at the null frequency and consists of nothing more than a low-power replica of the normally absent carrier.

The low spectral density of the modulation at and near zero frequency makes it possible to suppress the low-frequency components with little adverse effect on the transmission of data. Taking advantage of this, the modulation is fed through a filter (see Figure 1) that passes frequencies above twice the expected Doppler shift. The central null in the transmitted signal is thereby broadened to provide more spectral room for the insertion of the pilot tone. At the receiver, this facilitates the acquisition of the carrier information without interference from the sidebands.

In one branch of the receiver (see Figure 2), the input signal plus pilot tone is notch-filtered to extract the signal. In another branch, the same input is bandpass filtered to strip off the signal and obtain the faded pilot tone. The calibration subsystem divides the faded pilot tone by its estimated amplitude squared, yielding the calibration tone. This calibration tone is mixed with the signal to recover a fade-compensated version of the original modulating signal.

This work was done by Faramaz Davarian of Caltech for **NASA's Jet Propulsion Laboratory.** *For further information, Circle 25 on the TSP Request Card.*

This invention is owned by NASA, and a patent application has been filed. Inquiries concerning nonexclusive or exclusive license for its commercial development should be addressed to the Patent Counsel, NASA Resident Office — JPL [see page 29]. Refer to NPO-16414.

Reduced-Bandwidth Coding for Mobile Communication

Fade-resistant mobile systems would use power and spectrum more efficiently.

NASA's Jet Propulsion Laboratory, Pasadena, California

Balanced coding, an efficient, new digital-coding technique, would reduce the bandwidth and power requirements of mobile communications that use satellite repeaters. The coding technique, intended for a residual-carrier transmission system, would alleviate the fading and spectrum crowding that hamper mobile communications.

The proposed transmission system employs the tone-calibrated technique (TCT). A residual carrier is used in this technique to reduce fading-induced effects and coherently demodulate the received signal. The TCT is potentially efficient in its use of power and of the frequency spectrum.

However, the success of the TCT in reaching its power and bandwidth objectives depends on the way in which the baseband signal is encoded. Because the residual carrier power should not be larger than the minimum power necessary for effective reception, the received tone (the "tone" being the residual carrier) must be free from data-induced interference (self-interference). Therefore, the code should be one that results in a null in the modulation spectrum near zero frequency. Because multipath fading causes the tone to spread in frequency by as much as twice the Doppler frequency, the code must ensure low power density up to the maximum expected Doppler shift. On the other hand, overbroadening should be avoided because it results in gross expansion of the transmission band.

The balanced code gives the requisite low-power band around zero frequency without overbroadening the transmitted signal spectrum. A balanced code contains an equal number of ones and zeros in a word. This characteristic guarantees a spectral null at dc regardless of the code length. The code is constructed by mapping every group of M source symbols into a greater number, N, of channel symbols, N being the number of symbols in a word.

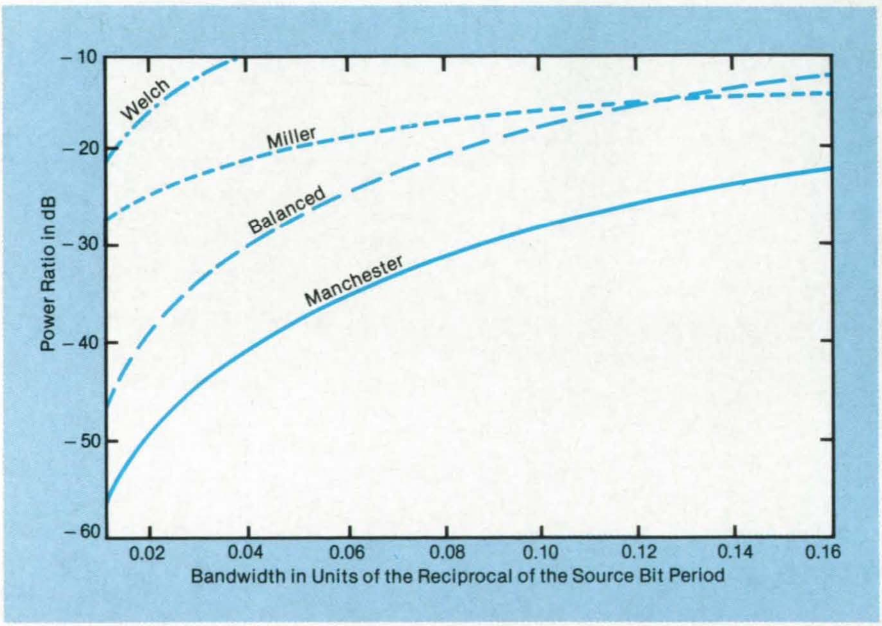

The **Portion of the Total Power** contained within the frequency band from zero to the indicated frequency is plotted for four codes. While the Manchester code has the lowest spectral power density near zero, the balanced code results in less bandwidth expansion at the overall signal.

Of the known codes, the Manchester code (N = 2) gives the lowest spectral density near zero frequency (see figure) but also results in a doubling of the signal bandwidth. For example, for a channel with a maximum Doppler rate of 78 Hz, the Manchester code is the one of choice for a source rate of 1,200 bits per second. The balanced code with N = 6 multiplies the bandwidth by 1½ and outperforms the Manchester code at rates beyond 2,400 bits per second. Although balanced coding adds a small amount of delay to the modulator and requires a slightly more complicated receiver, these are minor disadvantages.

This work was done by Faramaz Davarian of Caltech for **NASA's Jet Propulsion Laboratory.** *For further information, Circle 26 on the TSP Request Card.*

NPO-16447

Your technology needs can't wait this long

At Allied we've cut nature's timetable from centuries to days. We advance the state-of-the-art for single crystal garnet material every day. We have to.

To meet increasingly demanding needs for rods and slabs as solid state laser hosts.

To raise the standard and definition of both quality and size in Czochralski crystal growth and liquid phase epitaxy.

To maintain our leadership in meeting customer needs for Alexandrite, Nd:YAG, GSGG, $LiNbO_3$, GGG, and LPE garnet films.

Let our resources help you take your technology into the 21st Century. Contact Allied Corporation, Synthetic Crystal Products, P.O. Box 31428, Charlotte, NC, 28231, 704/588-2340, Telex 572 573.

We can't wait either.

ALLIED

Circle Reader Action No. 435

Frame-Synchronization-Assisting Module

The main processor is relieved of preliminary computational tasks.

NASA's Jet Propulsion Laboratory, Pasadena, California

An auxiliary data processor does computations related to the synchronization of frames of telemetry data, thereby relieving the main processor of this task. The auxiliary processor, called a frame-synchronization-assisting module (FSAM) sorts through large amounts of data to determine whether they are valid and, if so, how they are configured.

The FSAM searches any data passed to it for four possible types of frame-synchronizing codes. These include the following:

1. True forward (normal bit polarity and order);
2. Complement forward (inverted bit polarity);
3. True reverse (normal bit polarity, reverse bit order); and
4. Complement reverse (inverted bit polarity and order).

The FSAM reports back to the main processor with a 17-word result block. The first 16 words contain relative bit locations of the detected codes, with mode and error information. The 17th word indicates the number (up to eight) of codes that were detected, thereby enabling the user to go directly to word 17 to determine whether a valid correlation has occurred, without having to peruse the first 16 words.

In principle, any number of data may be passed to the FSAM. In practice, the number is determined partly by the user's confidence in finding the desired codes in a data block and partly by the limitations of the interface/host processor. In the present design, a block contains 4K words.

As shown in the figure, all interface and data signals between the FSAM and the main processor pass through the direct-memory-access (DMA) module, which lies directly on the computer bus. The DMA module acts as an interface for all DMA functions and programmed input/output communication with the bus.

Operation begins when the command-word register is loaded under programmed input/output. The command word specifies the type of code, the number of bits in the code, and the allowable errors. Any combination of the four code modes may be selected to conduct a code search. Next, the actual image in memory of the desired code is passed under programmed input/output in two words.

After the three words are loaded, the FSAM automatically sets up to look at incoming data and signals the user via the interface that it is ready to accept data.

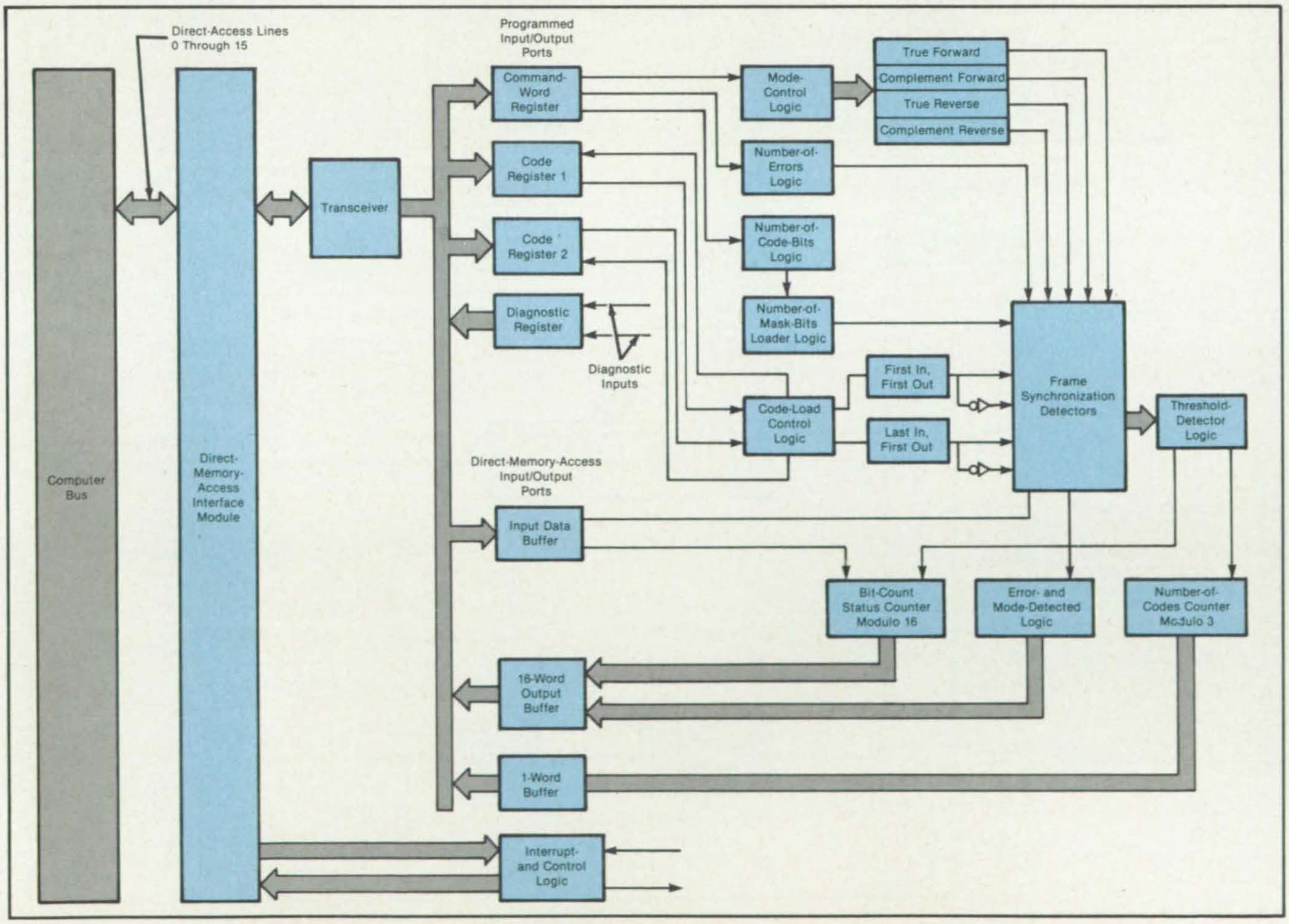

The **Frame-Synchronization-Assisting Module** is connected to the main processor of a computer through a direct-memory-access (interface) module. It examines data in the computer memory to find frame-synchronizing codes.

The data are then passed to the FSAM until the desired number of words has been counted by the word counter in the DMA module. At this point, the module sends a signal that turns off the code-detection function of the FSAM. Under interrupt control, the FSAM indicates, to the user's program, that it is ready to pass the 17-word result block. This completes one cycle, and the FSAM is ready for the next three command words.

This work was done by Carl DeSilveira of Caltech for **NASA's Jet Propulsion Laboratory**. *For further information, Circle 33 on the TSP Request Card.*
NPO-16564

Motor Servoloop With Optical Shaft Encoder

Position and rate feedback signals are derived from a single transducer.

Ames Research Center, Moffett Field, California

A motor control circuit derives shaft-angle and rotation-rate signals from an optical detector. The hybrid digital and analog circuit requires only a few components and has no moving parts.

A simplified block diagram is shown in the figure. The encoder includes an optical detector that emits pulses on lines A and B at intervals of 0.72° (500 pulses per complete revolution). The pulses occur when holes on the encoder disk pass by as the shaft turns. The relative phases of A and B depend upon the sense of rotation: If the shaft rotates clockwise, pulse A occurs before pulse B. The opposite is true for counterclockwise rotation.

The pulses are fed to an up/down counter, which counts them up or down when the rotation is clockwise or counterclockwise, respectively. The output of the counter is fed to a digital-to-analog converter. The converter output is a voltage proportional to the shaft rotation from the angle at which the counter was last reset.

The encoder pulses are also fed to a fixed-pulse-width one shot, thereby producing a pulse train with a frequency proportional to the motor speed. After low-pass filtering, the pulse train becomes a dc voltage proportional to the motor speed.

The analog position and speed signals are fed to an error amplifier along with the position-command voltage. The amplifier output is an error signal that drives the motor in the direction that reduces the error.

This work was done by Steven P. Marascalco of Sperry Rand Corp. for **Ames Research Center**. *For further information, Circle 11 on the TSP Request Card.*

Inquiries concerning rights for the commercial use of this invention should be addressed to the Patent Counsel, Ames Research Center [see page 29]. Refer to ARC-11582.

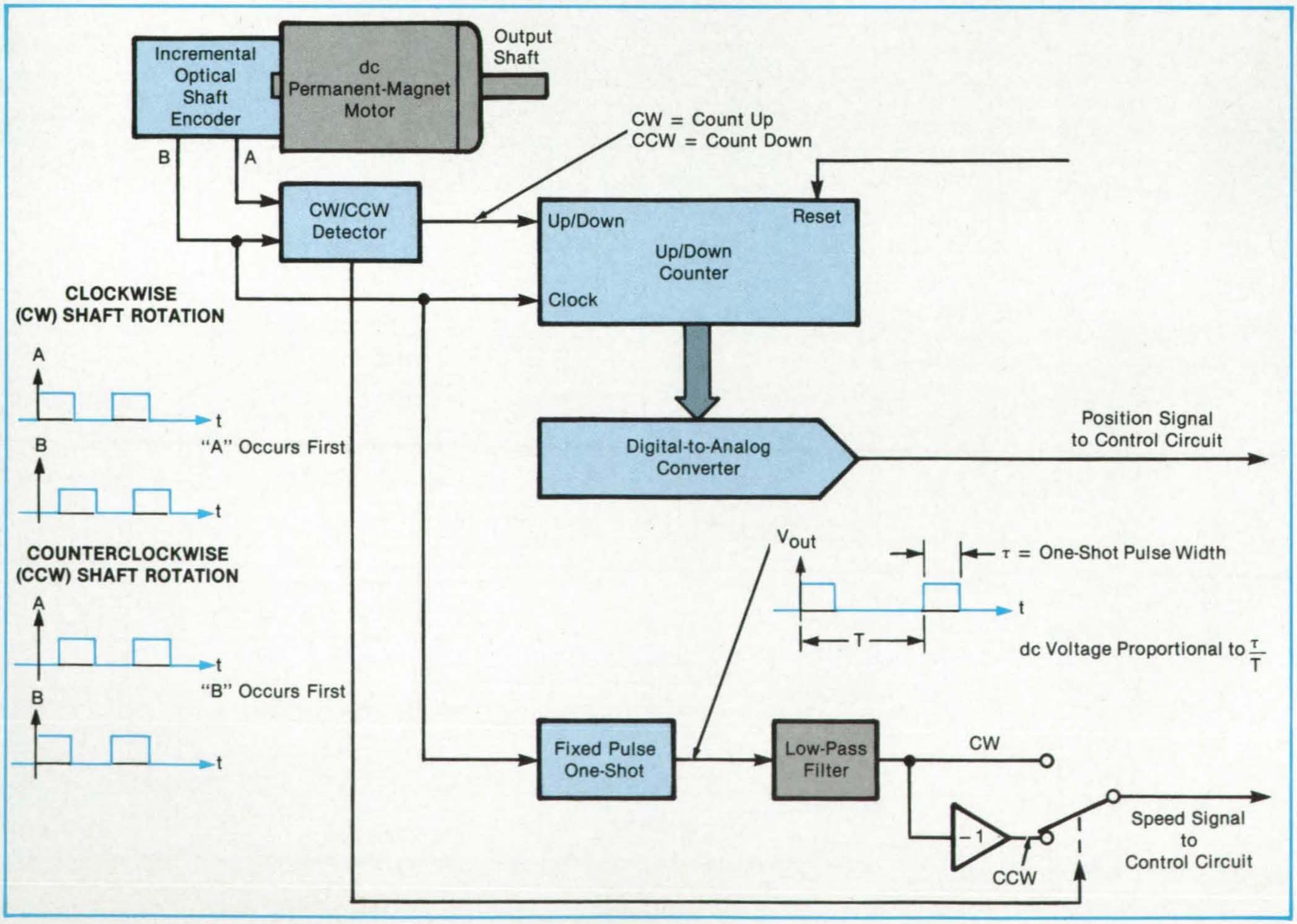

The **Servoloop** generates digital and analog shaft-position and analog shaft-speed signals from the output of an incremental optical encoder. These signals are used in the feedback control of the motor.

Digital Pseudonoise Generator

Numbers would be generated to satisfy a probability distribution.

NASA's Jet Propulsion Laboratory, Pasadena, California

An architecture has been developed for a noise generator based on a pseudorandom number sequence. The concept involves no additions or multiplications; rather, the outputs of a set of feedback shift registers would be combined, bit-by-bit, in accordance with the desired probability distribution. The digital, pseudorandom number output could be fed to a digital-to-analog converter to generate a pseudonoise signal suitable for testing broadband amplifiers.

The output number lies between 0 and 1 and is generated in binary form with N bits. Each less significant bit depends partly on the more significant bits according to conditional probabilities for zeros and ones that satisfy the probability distribution. A binary feedback shift register associated with each bit generates a sequence of zeros and ones. The registers are initialized from values stored in a read-only memory to be linearly independent and appreciably different: This guarantees the quasistatistical independence of the N sequences.

The N shift registers are grouped into three sections (see figure). The exact section includes units that generate the N/3 (or other arbitrarily designated number) most significant bits. Each unit contains a shift-register generator of a uniform random sequence, a logic network, data lines from a random-access memory, and an address line to the memory. The last few stages of each feedback shift register feed into a logic array to get the right proportion of zeros and ones for the specified probability distribution.

In the interpolation section, each unit includes three shift registers for averaging pairs of distributions to obtain approximations of the middle bits. The first N/3 bits, already generated exactly, address the random-access memory through a control that determines the two adjacent conditional probabilities, which can be linearly combined to yield bits (N/3) + 1 through N/2.

The extrapolation section generates the N/2 least significant bits. It is similar to the interpolation section, except that only one parameter is needed in each unit. The frequencies of the least significant

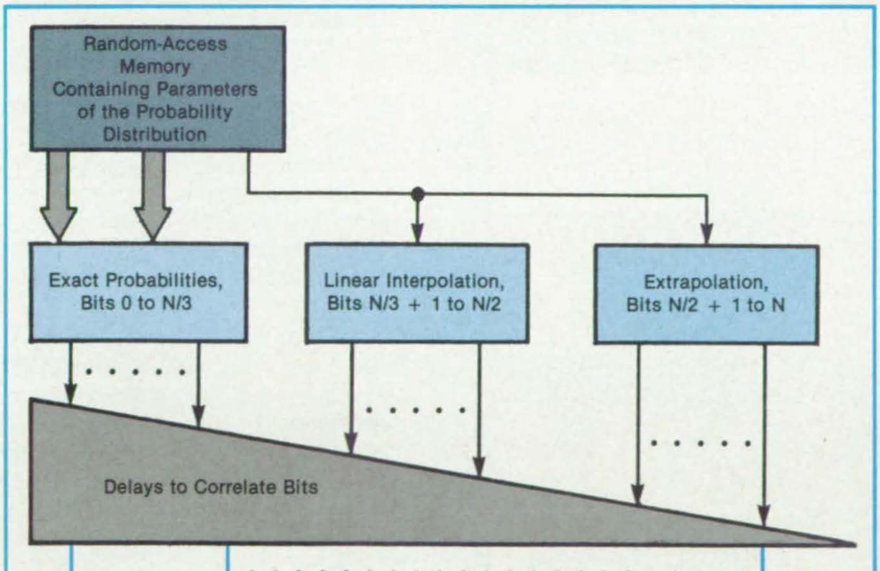

The **Pseudorandom Number Generator** would generate N-bit binary numbers. Three groups of feedback shift registers interconnected according to different schemes, would generate three bit sequences to be combined into the N-bit number sequence. The delays at the output end are necessary for the correlations of the less significant bits with the more significant bits, upon which they partly depend.

bits are shaped from the frequencies of the earlier bits by what amounts, in effect, to an extrapolation of the distribution function.

Because the later bits depend on the earlier ones, there must be delays between the first registers to align the output bits in time. This is only an initial delay: Once the system is in full operation, pseudorandom numbers are produced rapidly, one after another.

The system is to be constructed of complementary metal-oxide semiconductor circuitry. A conceptual system using somewhat fewer than 40,000 transistors would generate 25 × 10^6 random numbers per second, each containing 22 bits. The error (that is, the deviation from a truly random sequence in the desired probability distribution) would be less than 2^{-22}.

This work was done by Arthur Knoebel of Caltech for **NASA's Jet Propulsion Laboratory.** *For further information, Circle 18 on the TSP Request Card.*
NPO-16627

Compensating Function for Antenna Pointing

The mean-square errors of the antenna surface are reduced.

NASA's Jet Propulsion Laboratory, Pasadena, California

A compensating function helps to point a deformable antenna without inducing excessive pointing oscillations or deformations of the reflecting surface. When implemented on a computer in real time, the function enables the calculation of control signals in response to several sensor inputs: The function is devised so that the signals control the torque actuator of the antenna-pointing mechanism in such a way as to reduce or minimize the squares of the errors of the antenna surface over a long time.

The function was developed for an axisymmetric dish antenna made of mesh supported by ribs. The function is obtained by minimizing a performance index, J, given by

$$J=\int_0^{\infty}[q_1\Theta^2+q_2\dot{\Theta}^2+q_3\iint W^2dA+ru^2]dt$$

where t = time, Θ = the angle of rigid-body-rotation error, $\dot{\Theta}$ = rotational speed, W = the displacement of the mesh reflecting surface from the position in which the rigid-body rotation and all elastic deformations are zero, dA = the increment of mesh area (the area integral is taken over the entire mesh), and u = the control torque.

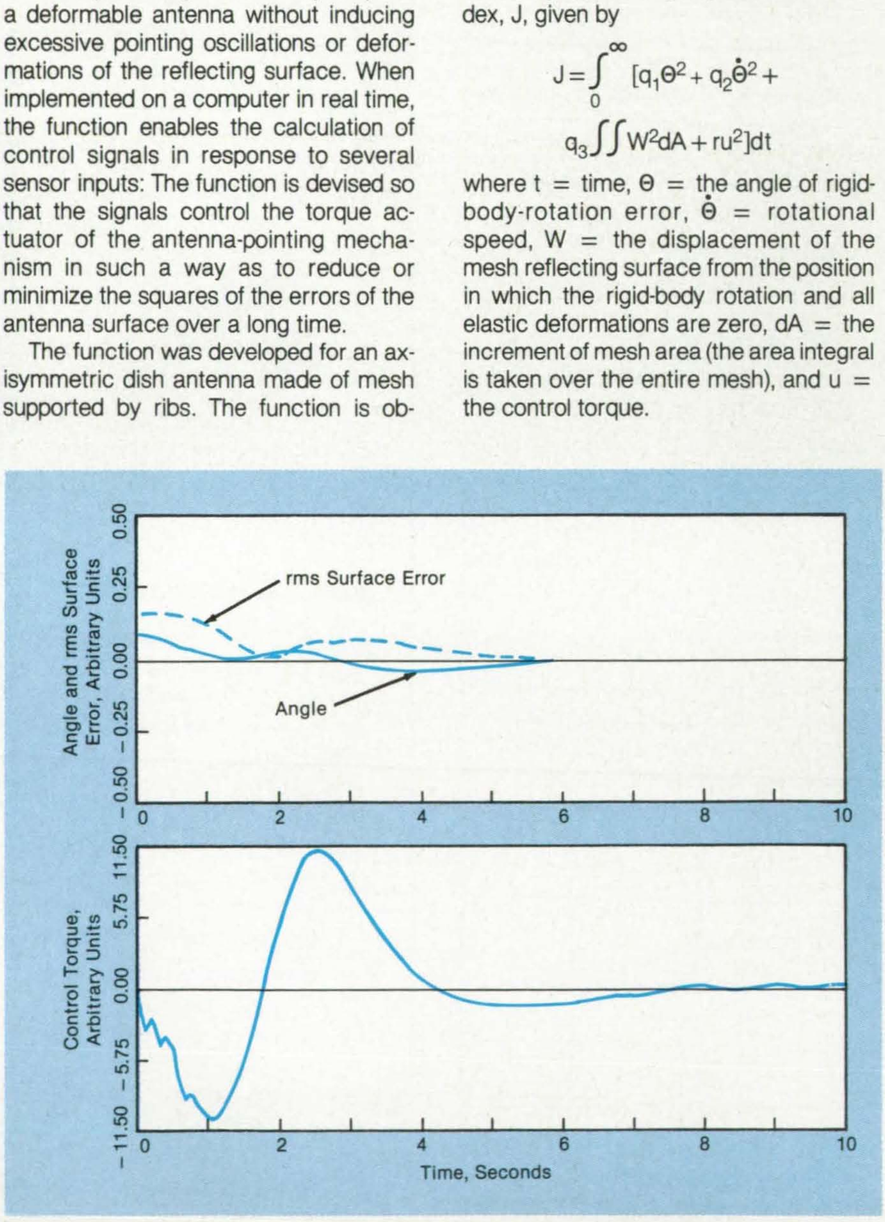

The **Antenna Settles Down** toward zero surface and pointing errors and zero control torque after the imposition of an initial rotation error. The compensating function for this case is derived from a performance index that penalizes the mean-square surface error and the control torque but not the angular overshoot.

The weighting coefficients q_1, q_2, q_3, and r are chosen according to the amounts by which each error is to be mathematically penalized or minimized in the control function. The mean-square surface error weighted by q_3 is the primary term to be minimized, but the minimization of the response time and of the overshoot of the rigid-body angle are also secondary objectives. The combination of weighting coefficients that best achieves these objectives is found by numerical experimentation with the equations that describe a particular system.

Once the weighting coefficients are found, the compensating function, F, is expressed by a matrix equation

$$F = K_n[SI - A_n + B_nK_n + G_nC_n]^{-1}G_n$$

where the subscript n denotes an *n*th order approximation, S = the Laplace-transform complex-frequency variable, I = the identity matrix, K = the control gain, G = the estimator gain, A = the antenna dynamical matrix, B = the control-input matrix, and C = the measurement matrix.

Numerical simulations have been performed for a compensating function having three channels: Channel 1 is from the hub-rotation sensor to the torque actuator. Channels 2 and 3 are from two rib-tip displacement sensors to the torque actuator; these channels have identical transfer functions by virtue of the antenna symmetry. The figure gives results from one of the simulations, showing the responses of the rigid-body error angle, the mean-square surface error, and the control torque as they evolve from an initial rigid-body-rotation error.

This work was done by D. Lewis Mingori and James S. Gibson of the University of California, Los Angeles for **NASA's Jet Propulsion Laboratory.** *For further information, Circle 53 on the TSP Request Card.* *NPO-16616*

Imagine what you could do if your computer could see.

Eikonix® high performance digital imaging cameras give your computer the ability to see. Which in turn gives you the ability to improve the quality of your research, and open new markets.

Easy-to-use Eikonix cameras are compatible with IEEE 488, DEC Q-Bus, Unibus, Multibus and VME bus based systems as well as IBM® PCs. They're the most flexible, cost-effective, reliable, and accurate means available for getting high resolution image data into a computer for analysis, manipulation, display and storage. And they're backed by a team of specialists that provides all the technical support you need for whatever applications you have—worldwide.

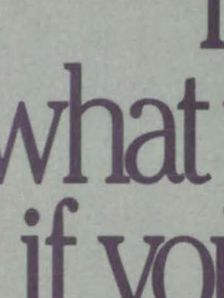

Eikonix high performance digital imaging cameras convert stationary pictures and objects into digital form via a linear sensor array. They offer precise analytical capabilities and highly accurate storage and retrieval for more applications than you can imagine.

Typical applications: Artificial Intelligence ▫ Pattern Recognition ▫ Remote Sensing ▫ Earth Resource Analysis ▫ Color Infrared Imaging ▫ Electron Microscopy ▫ Astrophysics ▫ CAD input ▫ Modeling (2D & 3D) ▫ Circuit Design ▫ Mapping: Radar, Cartographic, Thematic, Utility, Topographic ▫ Medical Imaging: NMR, X-Ray, Ultrasound, PET, Autoradiography, Tomography ▫ Materials Testing: Surface Analysis, Tensilometry.

If you'd like us to focus on your particular application, please call us at (617) 275-5070. If you'd like some literature, simply write to us at Eikonix Corporation, 23 Crosby Drive, Bedford, MA 01730, Telex: 951231.

Illustration of a typical imaging system.

EIKONIX®
A KODAK COMPANY

Visit us at Siggraph '86 Booth #1450

Circle Reader Action No. 356

Airborne Instrumentation Computer System

A modular microcomputer provides real-time data processing and telemetry-interface functions.

Ames Research Center, Moffett Field, California

A programmable instrumentation system links pulse-code-modulation (PCM) telemetry to digital systems on test aircraft. The system, called AICS for airborne instrumentation computer system, also analyzes flight-test data during a flight. A

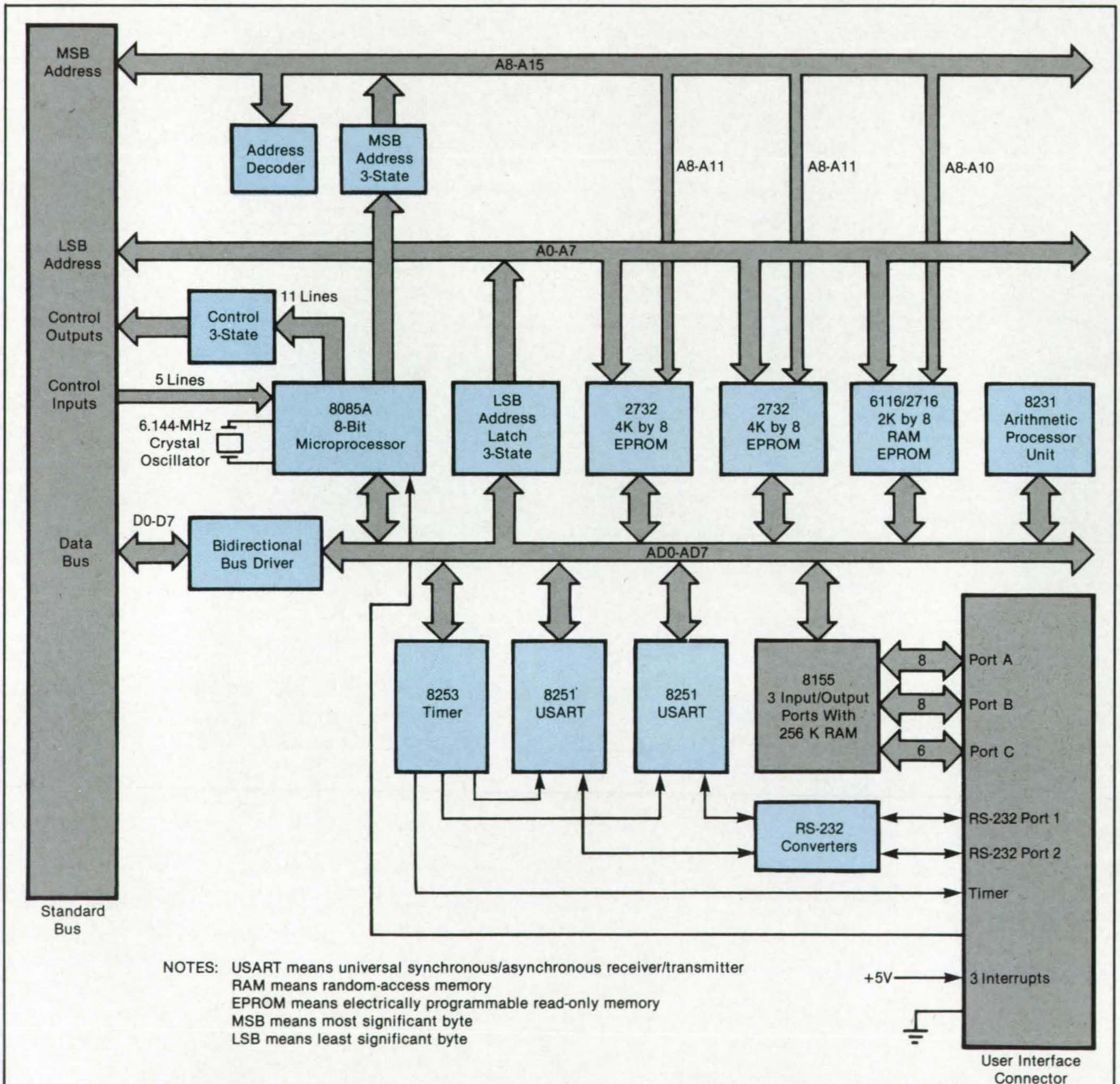

The **Single-Board Microcomputer** in the AICS includes only commercially available VLSI circuits. In typical applications, the power consumption is less than 50 W.

synthesized voice output is also available.

A block diagram of the single-board AICS computer is shown in the figure. The interface to the PCM telemetry system uses two additional printed-circuit cards (not shown). By virtue of its programmability and its use of the STD bus with plug-in cards, the AICS can be quickly adapted to different projects.

The 114-by-165-mm, six-layer computer board plugs into the STD-bus backplane mounted in a 254-by-133-by-140-mm enclosure. The backplane can accommodate six printed-circuit cards.

The computer includes an 8085A 8-bit microprocessor and an 8231 arithmetic processor with a 32-bit internal data path for performing single- and double-precision floating-point arithmetic and scientific calculations.

AICS software is prepared in assembly language on a minicomputer with a relocating cross assembler having macro and subroutine capability. A real-time hardware emulator is used for program testing.

The AICS has been used on an F-15 aircraft as an interface between two digital electronic engine-control computers and a PCM telemetry system. Because of the flexibility of the AICS design, only software modifications and one additional line-receiver card are required to adapt the AICS from the F-15 application to one on an F-111 aircraft with a complex, two-computer control system used to study a variable-camber wing. The AICS has also been used on an OV-1C Mohawk aircraft to test a stall-warning concept, a more complex application that illustrates the potential power of the system.

The interface to the PCM telemetry system can provide up to 16-bit data words. Since the PCM interface must provide a data word on demand within 4 microseconds, asynchronously with other AICS processes, the PCM interface contains a separate 16-bit-word buffer memory with a direct-memory-access controller. To send 16-bit words via a 10-bit-word telemetry system, the interface sends a 10-bit word followed by a 6-bit word for each DMA access.

This work was done by Glenn A. Bever of **Ames Research Center**. *Further information may be found in NASA TM-86036 [N84-20521/NSP], "The Development of an Airborne Instrumentation Computer System for Flight Test."*

Copies may be purchased [prepayment required] from the National Technical Information Service, Springfield, Virginia 22161. Telephone No. (703) 487-4650. Rush orders may be placed for an extra fee by calling (800) 336-4700.

Inquiries concerning rights for the commercial use of this invention should be addressed to the Patent Counsel, Ames Research Center *[see page 29]*. *Refer to ARC-11602.*

VLSI Architectures for Computing DFT's

Simplifications result from the use of residue Fermat number systems.

NASA's Jet Propulsion Laboratory, Pasadena, California

A system of finite arithmetic over residue Fermat number systems enables the calculation of the discrete Fourier transform (DFT) of a series of complex numbers with a reduced number of multiplications. The computer architectures based on this approach are suitable for the design of very-large-scale integrated (VLSI) circuits for computing DFT's. The general approach may not be limited to DFT's; it may also be applicable to the decoding of error-correcting codes and to other transform calculations.

A complex integer can be represented by a pair of residues modulo a Fermat number, F_n, where $F_n = 2^{2^n} + 1$. The ring of residues of integers modulo F_n is designated as Z_{F_n}. The set $Z_{F_n}[i] = \{a + ib | a,b \in Z_{F_n}\}$ contains F_n^2 elements. Over this set, addition is given by

$$(a + ib) + (c + id) = (a + c)_{F_n} + i(b + d)_{F_n}$$

while multiplication is given by

$$(a + ib)(c + id) = (ac - bd)_{F_n} + i(bc + ad)_{F_n}$$

where the subscript F_n denotes the residue of a modulo F_n. An important mapping in this system is specified by $\phi: a + ib \rightarrow [(a + sb)_{F_n}, (a - sb)_{F_n}] = (\alpha, \bar{\alpha})$ where $\alpha = (a + sb)_{F_n}$, $\bar{\alpha} = (a - sb)_{F_n}$, and $s = \pm 2^{2^{n-1}}$.

A recently developed algorithm makes it possible to compute the DFT using the direct sum S_{F_n} of two copies of residue number systems Z_{F_n}. A principal advantage of this algorithm is that a complex multiplication can be done by using similar integer multiplications in two parallel, independent residue channels. Building on this idea, it has been found that a complex-integer DFT can be computed by multiplication modulo a Fermat number in two parallel, independent residue channels.

Such a multiplication over the direct sum of two copies of Z_{F_n} can be used in the implementation of a systolic array of the DFT. A VLSI architecture has been developed for computing the d-point DFT over the direct sum S_M of $Z_{F_{k+j}}$, using two copies of the finite ring $Z_{F_{k+j}}$ for all j. The VLSI processor is composed of d basic cells.

The figure shows an example of this architecture for a four-point DFT in $Z_{17}[i]$. First, the integer complex-number sequence a_n is converted from $Z_{17}[i]$ into $(a_i, \bar{a}_i) \in S_{17}$ for $1 \leqslant i \leqslant 4$ and sent to all the cells simultaneously. Each register is composed of two five-bit subregisters containing $(\alpha, \bar{\alpha})$. Initially, all registers are set at zero. After the input data are entered, the components A_k (in S_{17}) of the DFT are contained in registers B_1 through B_3. The values computed in this manner are shifted sequentially out of register R_0. These values are then converted by the inverse mapping ϕ^{-1} into $\tilde{A}_k = a_k + ib_k$ for $0 \leqslant k \leqslant 3$. Finally, these $\tilde{A}_k$ are returned to the scale of the original complex numbers by $B^{-1} = 1$ for $1 \leqslant k \leqslant 4$.

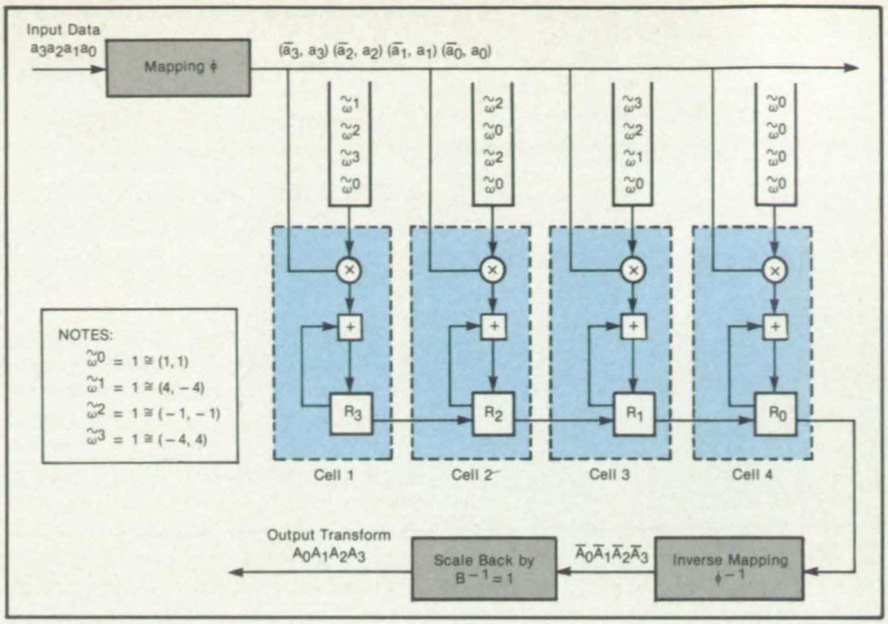

This **Systolic Array** would be used to compute a 4-point DFT over the direct sum, S_{17}, of two copies of Z_{17}. This system is readily implemented in VLSI.

This work was done by Trieu-Kie Truong, Jaw John Chang, In-Shek Hsu, Irving S. Reed, and Ding-Yai Pei of Caltech for **NASA's Jet Propulsion Laboratory**. *For further information, Circle 98 on the TSP Request Card. NPO-16656*

Physical Sciences

Hardware, Techniques, and Processes

Books & Reports

Interferometer for Observing Compressible Flow

Moving pictures show changing flow-field contours.

Ames Research Center, Moffett Field, California

A new optical interferometer enables the instantaneous visualization of compressible fluid flows. Because it is relatively immune to vibration, the unit is well suited to the observation of flows over models in large wind tunnels. By noting the relationships between fringe shifts, refractive indices, and densities, an experimenter can map the flow-field density contours. Since the relationships among the density, pressure, and velocity are fairly well understood theoretically, the interferometer can give a quantitative, time-resolved characterization of the flow field.

The new interferometer (see figure) combines elements of the schlieren and point-diffraction interferometers. The light source would ordinarily be a laser, but, with sufficiently precise optics, an incoherent source can sometimes be used. The light beam is first spatially filtered, expanded by lens 1, then collimated by spherical mirror 3 into a broad beam that crosses the experimental volume. The beam is then focused by mirror 4 and recollimated into a narrower beam by lens 2.

The portion of the beam reflected by beam splitter 1 is focused by lens 3, recollimated by lens 4, and passed on to beam splitter 2. This portion contains the diffraction imposed on the object beam by the experiment. The part of the beam transmitted by beam splitter 1 is focused by lens 5, then passed through a pinhole to remove the experimental diffraction pattern and generate a spherical reference beam.

The reference beam is collimated by lens 6 and recombined with the reflected part of the object beam at beam splitter 2. Both the transmitted and reflected outputs of beam splitter 2 can be used. The recombined beams interfere on the image planes, producing interference fringes that can be observed directly and photographed while the experiment continues.

The interferometer has been demonstrated by producing images of the flow around a candle, a propane torch, a heated cylinder, and an oscillating airfoil in a wind tunnel. Future developments will include the refinement of the optics, the selection of advanced recording media, and quantitative comparisons to holographic interferometry (which does not have real-time capability, unlike the new technique).

This work was done by W. D. Bacnalo and M. J. Houser of Aerometrics, Inc. for **Ames Research Center**. *For further information, Circle 43 on the TSP Request Card.*

Inquiries concerning rights for the commercial use of this invention should be addressed to the Patent Counsel, Ames Research Center *[see page 29].* *Refer to ARC-11549.*

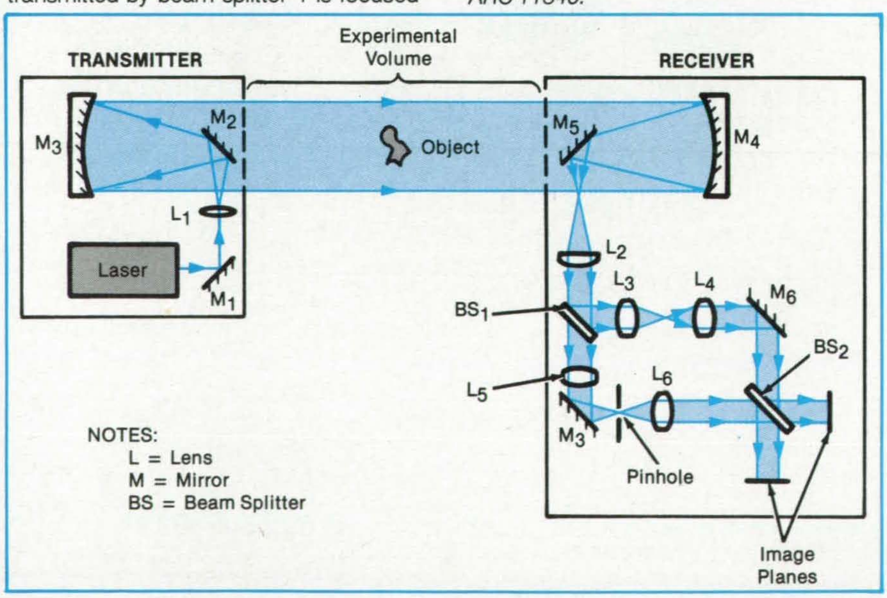

In the **Improved Point-Diffraction Interferometer,** the reference beam is generated by pinhole (point) diffraction at a place in the object beam outside the experimental volume. The object under test is positioned so that its interior or its supporting stand (for which no interferogram is normally required) lies in the shadows of turning mirrors 2 and 5.

Ultrasonic Verification of Metal-Grain Size

The heat treatment of a sample of known material can be measured.

Lewis Research Center, Cleveland, Ohio

Ultrasonic attenuation as a function of frequency can be determined for a metal sample having a known mean grain diameter. It has been demonstrated at the Lewis Research Center that once this function is determined for one sample of a material, it can be scaled to determine the mean grain size of other samples of the material. The results suggest that an ultrasonic approach is viable for verifying the effects of the heat treatments that vary the grain size. Thus, an in situ, nondestructive method is available for verifying the degree and correctness of heat treatment in metals-processing facilities.

Advanced techniques are used for the ultrasonic interrogation of heat-treated metals. It has been shown that the ratio between the wavelength and mean grain diameter is a significant factor in comparing changes in microstructure. This ratio can be used to determine a scale factor between two polycrystalline materials having different mean grain diameters. These results are achieved by determining the attenuation as a function of frequency without reference to any particular scattering mechanism. By this approach, it is unnecessary to associate a particular wavelength with the mean grain diameter. This allows a generalized formulation for scaling the mean-grain-diameter variations among samples of polycrystalline material that has undergone heat treatment.

Representative sets of experimentally-based calibration curves are shown in the figure. The heat treatment of an unknown sample can be verified by comparing its attenuation curve to the calibration set for the material. Possible uses of this technology include nondestructive ultrasonic verification of heat treatments and other online inspection systems.

This work was done by Edward R. Generazio of **Lewis Research Center**. *Further information may be found in NASA TM-83788 [N84-32849/NSP], "The Role of the Reflection Coefficient in Precision Measurement of Ultrasonic Attenuation."*

Copies may be purchased [prepayment required] from the National Technical Information Service, Springfield, Virginia 22161, Telephone No. (703) 487-4650. Rush orders may be placed for an extra fee by calling (800) 336-4700.
LEW-14283

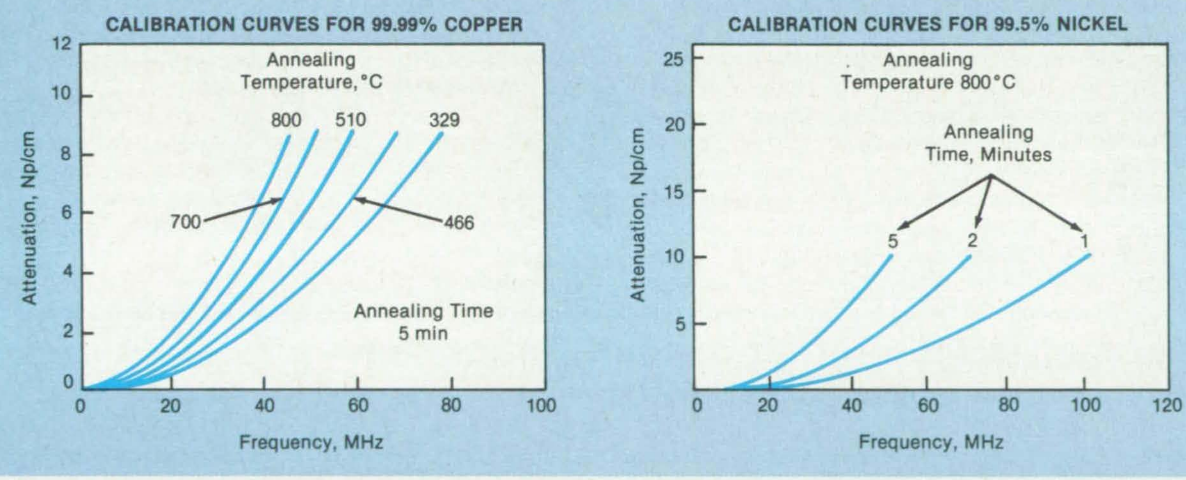

The **Heat Treatment of a Sample** can be verified by comparing its attenuation curve to the set of calibration curves for the sample material.

Solar-Powered Water Electrolyzer

Field trial provides data for an economic assessment.

John F. Kennedy Space Center, Florida

An experimental solar-powered water electrolyzer operates efficiently and with the promise of favorable economics. The electrolyzer produces hydrogen and oxygen from water using solar photovoltaic electricity directly, without conditioning. The hydrogen could be used as an energy-storage medium to be burned when needed to generate heat or electricity for domestic use.

The system consists of a commercial photovoltaic array with a 1-kW peak-power rating and a scaled-down version of a commercial electrolyzer. The electrolysis module consists of 15 cells, each having an effective diameter of 5.19 cm and an allowable current density of 600 mA/cm^2. The electrode area and the number of cells, which determine the current and the voltage demand, respectively, were selected to match the peak

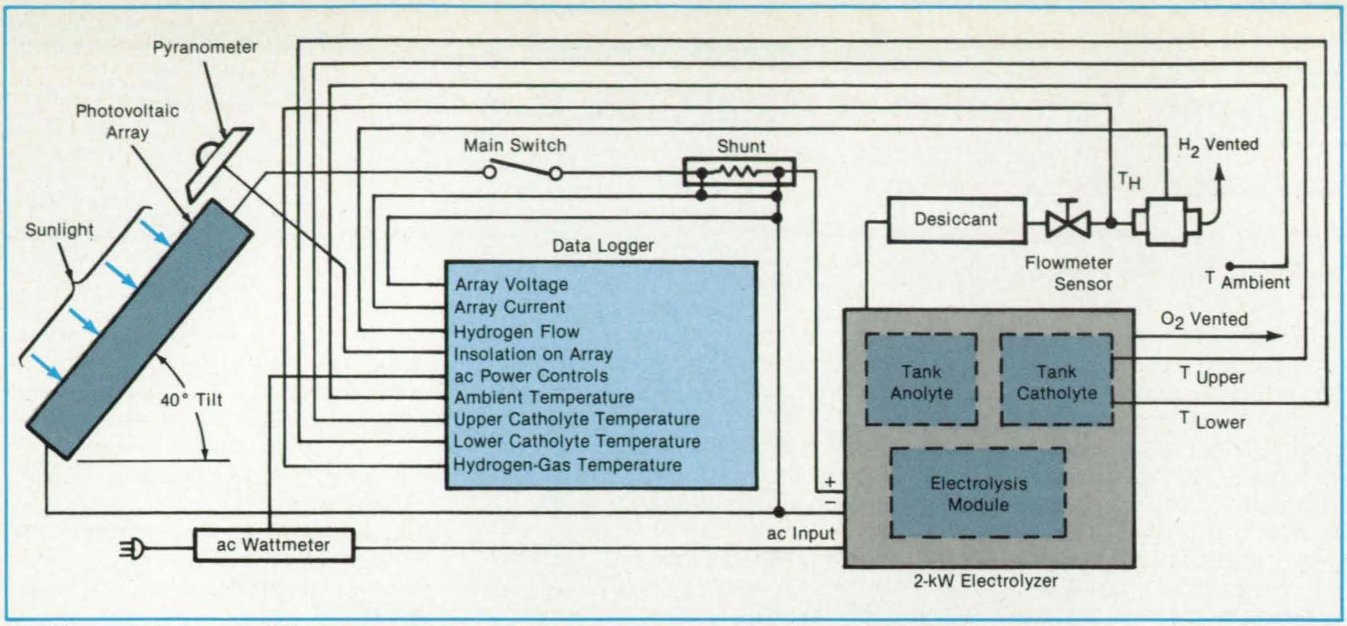

The **Photovoltaic Array and Electrolyzer** were connected to instrumentation, then tested to determine performance under various operating conditions.

power output of the solar array. An asbestos diaphragm separates the anode and the oxygen from the cathode and the hydrogen in each cell. Controls and alarms use commercial ac power distinct from the dc supplied by the photovoltaic cells.

The unit functions with an energy efficiency (the ratio of energy in the hydrogen to that delivered by the solar cells) of about 50 to 75 percent, the exact value depending on the weather and the operating schedule. The overall system efficiency is about 4 percent — a respectable figure in view of the inherent inefficiency of photovoltaic conversion.

The system (see figure) was tested for 3 months in Florida. From the data collected during this trial, an economic analysis was made by extrapolating to a 4-kW residential system. Such a system is expected to produce 500 kWh per month in Florida, on the average. Since the average Florida residence uses about 1,000 kWh per month, or double the output of a 4-kW electrolyzer, this size is appropriate for a basic module.

According to the analysis, the cost of 1 kWh of energy as hydrogen gas would be 73 cents in 1983-84 and only 17 cents in 1995. These costs include allowances for the photovoltaic array, the electrolyzer, maintenance, electrolyte replacement, electrolysis-module replacement, property tax, insurance, and Federal income tax credit. The electrolyzer cost for 1983-84 was based on a production rate of 200 units per year and for 1995 on a rate of 20,000 units per year.

The economics can be improved if a use can be found for the oxygen generated with the hydrogen and its value included in the analysis. In addition, if the hydrogen were used with a fuel cell during cloudy periods and at night, the combined heat from the electrolyzer and fuel cell could provide all the hot water needed for the household.

This work was done by Omar J. Hancock, Jr., of the Florida Solar Energy Center for **Kennedy Space Center**. *For further information, Circle 87 on the TSP Request Card.*

Inquiries concerning rights for the commercial use of this invention should be addressed to the Patent Counsel, Kennedy Space Center [see page 29]. Refer to KSC-11297.

Ellipsometric Monitoring of Film Deposition

Impurities would be detected nondestructively during processing.

NASA's Jet Propulsion Laboratory, Pasadena, California

Ellipsometry has been proposed as a nondestructive method of detecting impurities in films of amorphous silicon during plasma deposition. Because ellipsometry can monitor only the surface layer it "sees," it can monitor the deposition conditions continuously throughout the process, alerting the operator to the need to make adjustments and making it unnecessary to destroy samples in post-deposition analysis. Such monitoring would not disturb the deposition process appreciably.

An ellipsometer — also called more descriptively a spectral polarimeter — measures the polarization of light of a specific wavelength reflected from the surface under observation. The reflected light is generally elliptically polarized. The measured polarization components are used to calculate the real and imaginary parts of the index of refraction, which represent dielectric permeability and absorption, respectively, of the surface material at the given wavelength.

In the proposed system, the surface of a growing amorphous-silicon film would be monitored by an ellipsometer at a wavelength or combination of wavelengths at which the impurity or impurities of interest absorb light strongly. For example, oxygen absorbs strongly in the infrared at a wavelength of about 9 μm, while silicon is nearly transparent at this wavelength. This strong contrast between silicon and oxygen should permit ellipsometric determinations of oxygen content in the amorphous-silicon surface layer.

A conventional ellipsometer has to be modified in several ways before it is incorporated in the proposed system. The visible light source (usually a laser) must be replaced with a suitable infrared or other source for the wavelengths of interest. The instrument must be built into the plasma-deposition chamber, with the light source on one side, the detector on the other. All windows and optical surfaces must be far enough from the plasma to avoid film deposition.

Experiments have shown that the deposition plasma does not affect the polarization. However, optical absorption by the plasma reduces the strength of the reflected light, and radiation from the plasma enters the detector. To decouple the plasma radiation from the reflected light, the light source could be chopped and the detector synchronized with the source.

This work was done by Donald B. Bickler of Caltech for **NASA's Jet Propulsion Laboratory.** *For further information, Circle 2 on the TSP Request Card.* *NPO-16791*

Books and Reports

These reports, studies, and handbooks are available from NASA as Technical Support Packages (TSP's) when a Request Card number is cited; otherwise they are available from the National Technical Information Service.

Convection in a Solidifying Binary Mixture

Temperature and concentration profiles are calculated.

A paper discusses the theory of interrelated problems of heat transfer and material distribution in a solidifying binary alloy. The study expands on earlier work by including more realistic, mathematically complicating physical effects and yet retains a simple geometry and enough simplifying assumptions to make the equations solvable. The study will lead to improved understanding of metal and glass production, material processing in low gravity, and other important material processing problems.

The model of the system is a binary alloy slab of infinite width and finite depth. Heat is removed from the upper and lower slab surfaces by convection, with solidification starting at the lower surface. The solidification front moves up, releasing latent heat of solidification at the interface. The solid and liquid have different densities, causing a volume change and motion of the upper surface during freezing.

There is no mass flow across the upper and lower surfaces. The model does, however, include mass diffusion within the liquid and solid. Because the substance is an alloy, the freezing temperature depends on the composition at the interface, and the model takes this effect into account.

Four governing equations are derived from the standard expressions for time-dependent thermal and mass transport. The first equation expresses the relationship among the liquid temperature and its spatial derivatives, the liquid and solid densities, the interface position, and the thermal diffusivity of the liquid. The second equation relates the solute concentration and and its spatial derivatives in the liquid to the densities, the interface position, and the solute diffusivity in the liquid. The third and fourth equations are conventional expressions for the temperature and solute diffusion in the solid.

The interface conditions include two equations, based on the conservation of mass and energy at the interface. The solid and liquid at the interface are assumed to be at the concentration-dependent equilibrium melting temperature. The thermal boundary conditions at the upper and lower surfaces are expressed by equating the conductive heat fluxes within the adjacent alloy to the convective heat fluxes outside.

Although the governing equations are linear, the interface conditions are not. As a consequence, the coupled equations are nonlinear. One numerical solution method involving a Runge-Kutta integrator fails at low diffusion rates of solids. A second method involves closed-form, analytical solutions and reaches lower diffusion rates (though not as low as desired).

This work was done by B. Antar and F. Collins of the University of Tennessee for **Marshall Space Flight Center.** *For further information, Circle 5 on the TSP Request Card.* *MFS-27092*

Materials

Hardware, Techniques, and Processes

Fire-Resistant Polyimides Containing Phosphorus

The limiting oxygen index is increased.

Ames Research Center, Moffett Field, California

Polyimides having increased fire resistance have been made by reacting 1-[(dialkoxyphosphinyl)methyl]-2,4- and -2,6-diminobenzenes (compound 1 isomers) with such tetracarboxylic dianhydrides as pyromellitic dianhydride (PMDA) and benzophenone tetracarboxylic dianhydride (BPTDA). Copolyimides have also been synthesized from the reactions of compound 1 and m-phenylenediamine with the dianhydrides.

Compound 1 is made from the corresponding (dialkoxyphosphinyl)methyl benzenes by nitration followed by catalytic hydrogenation. The 2,4 and 2,6 isomers are formed in relative amounts of about 9 and 1, respectively. Separation of the isomers is not necessary; the compound 1 isomer mixture can be used as is to make polyimides and copolyimides.

The reaction of the predominant 2,4 isomer with a comonomer and a tetracarboxylic dianhydride is shown in the figure. The copolymer is formed in a two-step polycondensation process. The first step is carried out at 20 to 50 °C in a solvent of dimethyl sulfoxide, N,N-dimethyl formamide, or N,N-dimethyl acetamide. This step produces a polyamic acid in a fast, exothermic reaction.

The second step is cyclodehydration, which can be done thermally or chemically. In the thermal method, the solvent is first removed at 75 °C, and the polymer is then heated at 300 °C in a vacuum for 2 hours. In the chemical method, the water of cyclization is azeotropically removed with benzene or removed by stirring at room

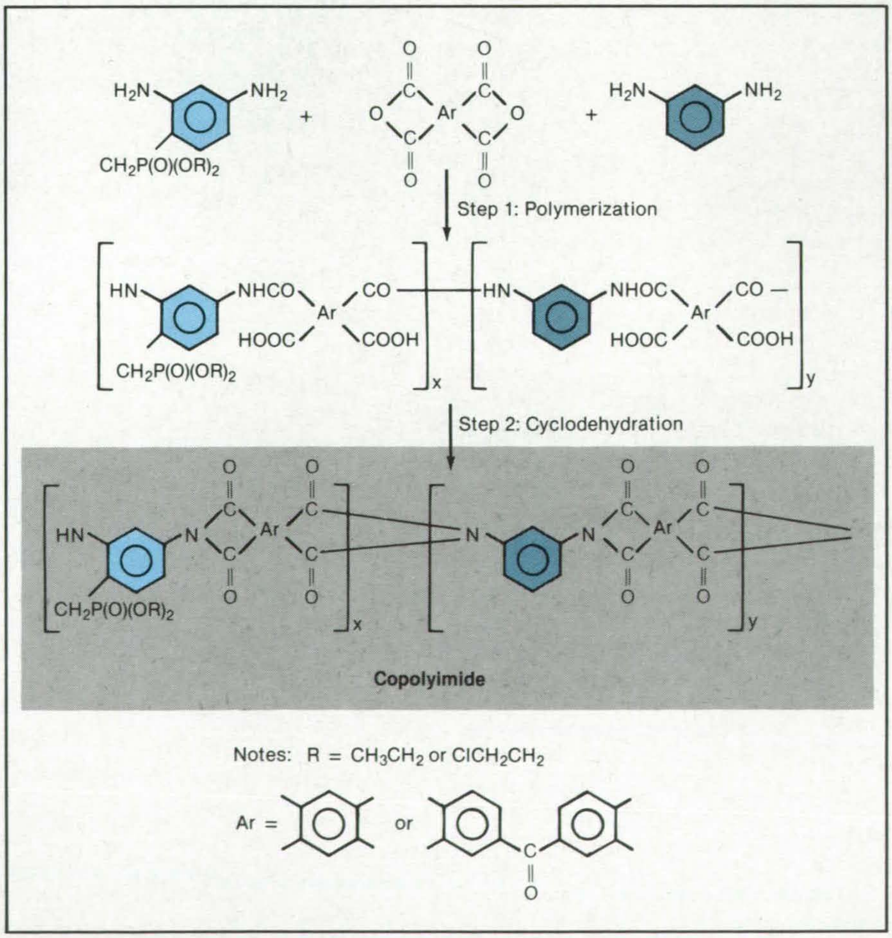

A **Copolyimide With a Group Containing Phosphorus** is synthesized from a 1-[(dialkoxyphosphinyl)methyl]-2,4-diaminobenzene (top, left), m-phenylenediamine (top, right), and a tetracarboxylic dianhydride (top, middle). The copolymer is more fire resistant than the corresponding polyimide without phosphorus.

temperature in acetic anhydride with pyridine as a catalyst. The polymer thus precipitated is heated to 200 °C in a vacuum for 2 hours to complete the cyclization reaction.

Phosphorus-bearing polyimides and copolyimides prepared in this way were compared with the corresponding polyimides without phosphorus, prepared from m-phenylenediamine and PMDA or BPTDA. The glass-transition temperatures were reduced by the incorporation of the (dialkoxyphosphinyl)methyl groups. The molecular weights and thermal stabilities of the copolymers were found to decrease with the increasing concentration of the moieties containing phosphorus. However, the copolyimides containing phosphorus showed considerably more resistance to fire as measured by the limiting-oxygen-index test.

This work was done by John Mikroyannidis of **Ames Research Center**. *For further information, Circle 28 on the TSP Request Card.*

This invention has been patented by NASA (U.S. Patent No. 4,536,565). Inquiries concerning nonexclusive or exclusive license for its commercial development should be addressed to the Patent Counsel, Ames Research Center [see page 29]. Refer to ARC-11522.

Sulfone/Ester Polymers Containing Pendent Ethynyl Groups

Two processes make these high-performance polymers resistant to solvents, without compromising the mechanical characteristics.

Langley Research Center, Hampton, Virginia

A variety of polysulfones and polyesters is commercially available for use in such applications as adhesives, moldings, membranes, and composite matrices. The un-cross-linked forms of these materials are tough and thermoformable but sensitive to certain solvents, especially under load. As a result, these materials are unacceptable for use as resin matrices in composite structures on commercial and military aircraft, where resistance to fluids and paint strippers is an essential

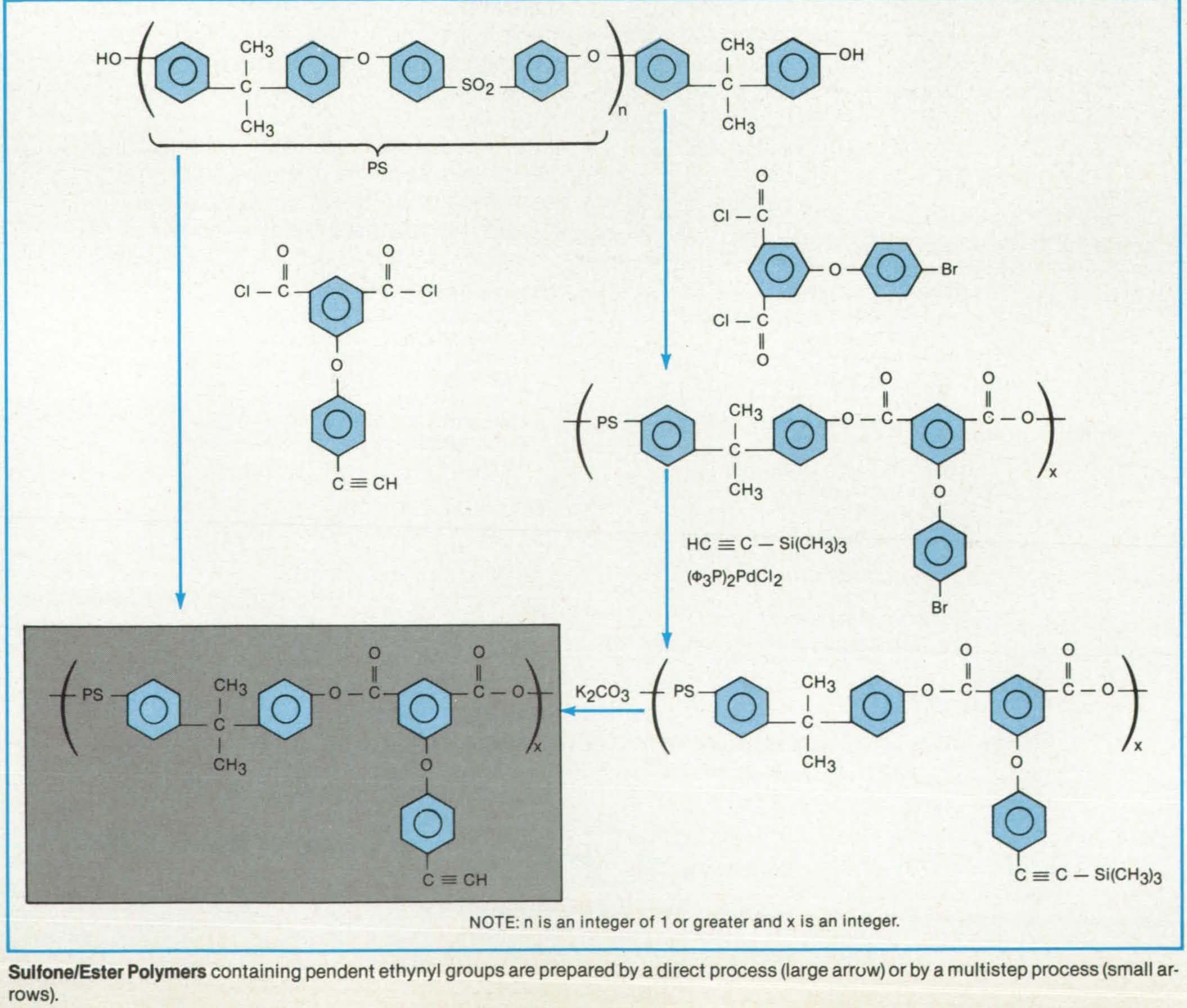

Sulfone/Ester Polymers containing pendent ethynyl groups are prepared by a direct process (large arrow) or by a multistep process (small arrows).

requirement.

Two processes have been developed for preparing an improved class of high-performance polymers. These polymers show improved solvent resistance while retaining high toughness, thermoformability, and mechanical performance. Sulfone/ ester polymers containing pendent ethynyl groups are prepared by a direct or a multistep process. The multistep process involves the conversion of a pendent bromo group to the ethynyl group, while the direct process involves reacting hydroxy-terminated sulfone oligomers or polymers with a stoichiometric amount of 5-(4-ethynylphenoxy) isophthaloyl chloride. The two different processes are shown in the figure.

The preferred direct route is depicted in the left portion of the reaction equation and involves the reaction of hydroxy-terminated sulfone oligomers, also referred to as arylene ether sulfone oligomers, with 5-(4-ethynylphenoxy) isophthaloyl chloride. The multistep route is shown in the right portion of the equation and involves the reaction of hydroxyterminated sulfone oligomers with 5-(4-bromophenoxy) isophthaloyl chloride to form a sulfone/ester polymer containing pendent bromo groups. The bromo groups are displaced by trimethylsilylacetylene using a palladium catalyst followed by cleavage of the trimethylsilyl group to the ethynyl group with a weak base.

The ethynyl-group content and, accordingly, the cross-link density of the cured polymer may be readily controlled in both processes. High ethynyl-group content provides high cross-link density in the cured resin. The material properties of toughness, stiffness, solvent resistance, and processability are also controlled by ethynyl-group content. Polymers containing high ethynyl-group content are generally more difficult to process (less flow due to reactions of the ethynyl groups) than those with lower ethynyl-group content and, when cured, are not as tough as those with lower ethynyl-group content (lower cross-link density). Conversely, cured polymers with higher ethynyl-group content (higher cross-link density) are stiffer (higher modulus) and have better solvent resistance and higher use temperatures.

The synthesis of sulfone/ester polymers containing pendent ethynyl groups can be readily controlled to adjust the chemical composition for use in specific applications. As prepared, the sulfone/ester polymers containing pendent ethynyl groups are readily soluble in a variety of solvents. Solutions can be used to cast films, form coatings, or impregnate reinforcement materials to form adhesive tapes and prepregs. The solvent can be removed, and when the resultant polymer is heated in the range of 200 to 300°C, the ethynyl groups react to provide branching and cross-linking. The cured resin is insoluble, although swelling in certain solvents, depending on the cross-link density, is observed.

The synthesis may also be used to place pendent ethynyl groups onto a variety of polymers in addition to sulfone/ esters. Potential applications for the new sulfone/ester polymers containing ethynyl groups include adhesives, composite resin matrices, moldings, ultrafiltration membranes, protective coatings, and such electrical insulators as thin films for microelectronic circuitry.

This work was done by Paul M. Hergenrother and Brian J. Jensen of **Langley Research Center.** *For further information, Circle 27 on the TSP Request Card.*

This invention is owned by NASA, and a patent application has been filed. Inquiries concerning nonexclusive or exclusive license for its commercial development should be addressed to the Patent Counsel, Langley Research Center (see page 29). Refer to LAR-13316.

Powder Extinguishants for Jet-Fuel Fires

Mixtures of alkali metal dawsonite and metal halide show superior performance.

Ames Research Center, Moffett Field, California

In tests of new dry powder fire extinguishants, mixtures of potassium dawsonite [$KAl(OH)_2CO_3$] with either stannous iodide (SnI_2) or potassium iodide (KI) were found most effective for extinguishing jet-fuel fires on hot metal surfaces (up to 900 °C). These mixtures performed more effectively than either compound alone. This is particularly striking since KI was one of the most effective extinguishants known previously.

Alkali metal dawsonites can be prepared as follows: Equimolar quantities of aluminum hydroxide and an alkali metal hydrogen carbonate powder of particle size less than 90 μm are thoroughly mixed and transferred to an open-topped vessel made of aluminum or other metal that is chemically inert to the ingredients. The vessel is placed in a high-pressure reactor, which is then flushed and pressurized to 120 to 360 psig (830 to 2,500 kPa) with CO_2 gas. The reactor is then quickly heated to 150 to 200 °C and held at that temperature for 1 to 6 hours. After cooling and depressurization, the product is dried in a vacuum oven at 50 °C.

Mechanical mixing of the dawsonite and iodide components is adequate for preparing the extinguishant mixtures. The ingredients should be finely divided, about 250 to 350 mesh (about 62 μm maximum particle size). To ensure that the resultant mixture will pour well, moisture should be driven off from the iodide (either before or after mixing) and the mixture kept in an airtight container. The mixture must be readily pourable so that it will spread rapidly and evenly over the burning surface.

The performance of single compounds and two-component mixtures was evaluated in two tests. In the static test, jet fuel (type JP-4) dripped continuously into an electrically-heated stainless-steel trough. After a flame developed and reached a fairly steady state, the extinguishant powder was applied to the flame while the input of heat and fuel continued. The time the flame took to rekindle was taken as a measure of extinguishant effectiveness.

In the flow test, a fuel leak (such as might occur in aircraft) was simulated by spraying the fuel into a heated duct with air flowing through it. Rekindling time was again taken as the measure of effectiveness.

Static- and flow-test results are shown in the table both for individual compounds and for mixtures containing one aluminum compound and one metal halide. At 900 °C the

FLOW TESTS

DRY CHEMICALS	Grams	Reignition Delay Time, s, at Various Airflows, m/s	
		6 (m/s)	36 (m/s)
(1) KD*	30	>20	0.5
(2) KD + KCl (32%)	10-20	2	>20
(3) KCl (PYROCHEM)	30	<1	0
(3) KCl (SUPER-K)	50	—	20
(4) KD + KI (10%)	20	3	>20
(5) KI	40	<1	0
(6) KD + KI (5%)	20	1	<1
	25	>20	—
(7) KD + KI (9%)	15	<1	<20
(8) KD + KI (18%)	20	<1	>20
(9) KD + SnI_2 (5%)	15	>20	>20
(10) KD + SnI_2 (10%)	15	>20	>20
(11) KD + SnI_2 (20%)	10	>20	>20

Notes: Mixtures 6 to 11 were preheated.
*KD = potassium dawsonite, $KAl(OH)_2CO_3$.

STATIC TESTS

INGREDIENTS	Reignition Delay Time at Noted Temperature,s			
	700 °C	750 °C	800 °C	900 °C
(1) KD		153 ± 15		10 ± 4
(2) KD + SnI_2 (6% I)		520 ± 52		51 ± 3
(3) KD + SnI_2 (6% I)		419 ± 61		50 ± 2
(4) SnI_2 (68% I)	380 ± 80			2 ± 2
(5) KD + KI (7% I)		500 ± 90		13 ± 4
(6) KD + KI (7% I)		>900		50 ± 14
(7) KI (76% I)	>900		16 ± 6	2 ± 2
(8) $Al(OH)_3$		100 ± 30		3 ± 2
(9) $Al(OH)_3$ + SnI_2 (7% I)		204 ± 20		8 ± 1
(10) $Al(OH)_3$ + KI (7% I)		72 ± 3		8 ± 1
(11) $Al(OH)_3$ + KI (8% I)		233 ± 56		—
(12) AlOOH		48 ± 35		None
(13) AlOOH + KI (7% I)		131 ± 7		15 ± 4
(14) Al_2O_3		28 ± 12		None
(15) Al_2O_3 + KI (7% I)		>900		50 ± 12
(16) NaI (85% I)	600 ± 60			3 ± 2
(17) $NaAl(OH)_2CO_3$		296 ± 50	29 ± 5	6 ± 3

Notes: Mixtures 2, 5, 9, and 11 were mechanical mixtures;
mixtures 3, 6, 10, 13, and 15 were preheated.

Fire Extinguishant Test Results show longer reignition delays at the higher test temperatures when mixtures of an alkali dawsonite and a metal halide are used than when either component is used alone. The percentage of iodine by weight in each mixture is shown in parentheses.

mixtures consistently outperformed their individual components. At lower temperatures, both KI alone and mixtures containing KI performed very well.

While these results are very promising, further development work might be required to develop practical systems using the new mixtures. For example, the hygroscopic tendencies of the iodides would have to be considered in designing storage for the mixtures.

This work was done by Robert L. Altman of **Ames Research Center** *and Ludwig A. Mayer and Alan C. Ling of San Jose University. No further documentation is available.*

This invention has been patented by NASA (U.S. Patent No. 4,406,797). Inquiries concerning nonexclusive or exclusive license for its commercial development should be addressed to the Patent Counsel, Ames Research Center [see page 29]. Refer to ARC-11252.

Process for Making Tris(N-methylamino) Methylsilane

This efficient process will aid the production of silicon carbide/silicon nitride fibers.

Marshall Space Flight Center, Alabama

A process for making tris(N-methylamino) methylsilane (TNMAMS) allows this important precursor of silicon carbide/silicon nitride ($Si_xN_yC_z$) fibers to be produced on a large, economically acceptable scale. $Si_xN_yC_z$ fibers are produced by the thermal polymerization of TNMAMS to polycarbosilizane resin, which is then drawn and pyrolyzed. These fibers are 10^6 times as electrically resistive as carbon fibers while having similar mechanical properties; consequently, they are promising replacements for carbon fibers in composite materials in which high conductivity would pose a hazard.

The new preparation of TNMAMS involves the gradual addition, under dry nitrogen, of x moles of dry methyltrichlorosilane to a solution of 10x moles of methylamine in a dry, inert solvent (e.g., petroleum ether). (Water must be excluded because it engages in competing chemical reactions.) During the addition, the temperature is maintained at about −30 °C. The methyltrichlorosilane must be added slowly to insure that the byproduct hydrochloric acid reacts mainly with the excess methylamine (rather than with the product TNMAMS) to produce an insoluble salt.

When the addition is complete, the reaction mixture is warmed to about 40 °C and kept at that temperature for about 60 minutes. The byproduct salts are then removed by filtration. Finally, the solvent is removed by distillation, leaving the TNMAMS, which is a clear liquid at room temperature.

The synthesis was demonstrated in a large-scale reaction starting with 1,150 g (900 ml) of methyltrichlorosilane. After distillation, 673 ml of TNMAMS remained, the yield being 58.6 percent by weight.

This work was done by Johnny M. Clemons, Benjamin G. Penn, and Frank E. Ledbetter III of **Marshall Space Flight Center.** *For further information, Circle 54 on the TSP Request Card.*
MFS-28143

Composite Lightning Rods for Aircraft

Sacrificial tips protect composite parts of modern aircraft.

Langley Research Center, Hampton, Virginia

The problem of protecting aircraft from electrostatic discharges and lightning strikes has stimulated a variety of protective measures including both passive and active dischargers. The problem becomes more severe as insulating composites replace more and more of the Faraday shield inherent in all-metal construction. Also, modern electronics and the practice of entrusting vital flight functions to computers creates a need for protection from electrical charges that can induce disruptive currents in the electronic circuits. The composite, lightweight sacrificial tip with graphite was designed especially to reduce lightning-strike damage to composite parts of aircraft and to dissipate the harmful electrical energy.

Extensive damage is often caused by lightning strikes on the relatively nonconductive composite structures now frequently used for the wings, tails, fuselage, or control surfaces on aircraft. This damage often takes the form of delamination and/or holes (complete burnthrough) in the structural surfaces. When the sacrificial tip is installed in a position protruding from the aft surface of an aircraft part made of composite material, the energy from a lightning strike on the part is dissipated through the tip. These tips are very inexpensive and sacrificial but may be usable for withstanding numerous lightning strikes.

The device consists basically of a slender composite rod fabricated from highly-conductive unidirectional reinforcing fibers in a matrix material. These rods are strategically installed in the trailing edges of such aircraft parts as wings, tails, winglets, control surfaces, and the rearward-most portion of the aft fuselage. The rods faricated thus far were of unidirectional graphite fibers in an epoxy matrix, 5/16 in. (0.8 cm) in diameter and 5½ in. (14 cm) long, tapered approximately the last inch (2.5 cm) down to about 50 percent of the major diameter at the tip. This device has already been installed and used successfully on Langley Research Center's F-106 aircraft.

This work was done by Charles F. Bryan, Jr. of **Langley Research Center.** *No further documentation is available.*

This invention is owned by NASA, and a patent application has been filed. Inquiries concerning nonexclusive or exclusive license for its commercial development should be addressed to the Patent Counsel, Johnson Space Center [see page 29]. Refer to LAR-13470.

Computer Programs

Hardware, Techniques, and Processes

COSMIC: Transferring NASA Software

COSMIC, NASA's Computer Software Management and Information Center, is the one central office established to distribute software that is developed with NASA funding. COSMIC's role as part of NASA's Technology Utilization Network is to ensure that NASA's advanced software technology is made available to industry, other government agencies, and academic institutions.

Because NASA's software development efforts are dynamic and ongoing, new programs and updates to programs are added to COSMIC's inventory on a regular basis. *Tech Briefs* will continue to report information on new programs. In addition, the 1986 edition of the *COSMIC Software Catalog* is available with descriptions and ordering information for available software. Several new programs for control systems/robotics, expert systems, thermal analysis, turbomachinery design, structural analysis, and computer graphics are offered.

For additional information on any programs described in this issue of *Tech Briefs*, circle the appropriate number on the TSP card at the back of the publication. If you don't find a program in this issue that meets your needs, you can call COSMIC directly at (404) 542-3265 and request a review of programs in your area of interest. There is no charge for this information review.

COSMIC®
Computer Services Annex, University of Georgia, Athens, GA 30602; Phone (404) 542-3265
John A. Gibson, Director

Computer Programs

These programs may be obtained at a very reasonable cost from COSMIC, a facility sponsored by NASA to provide tested and reliable software to the public. For information on program price, size and availability, circle the reference number on the TSP and COSMIC Request Card in this issue.

Electronic Systems

Computer Program for Space-Shuttle Testing

The demand on the Space Shuttle general-purpose computers is reduced.

The Space Shuttle has a number of devices which communicate with the general-purpose computers (GPC's) onboard. Because of the small number of GPC's available, using them to test Space Shuttle hardware and associated software is both inconvenient and expensive. The Simulation Testbed and the Scenario Preprocessor (STB&SPP) system reduces the need for use of GPC's in hardware and software development and testing. The system consists of a computer program, the SPP, and a set of utility subroutines, the STB, which incorporates the Interface Simulator (ISIM).

STB&SPP provides a set of utility test routines that may be linked with user-supplied routines into a user-defined, menu-driven test program for sending GPC messages to a device under test and recording the response of the device. It also provides a facility for sending scenarios of GPC messages to a device under test, simulating in real time the timing and updating of messages as normally performed by the GPC. Finally, SBT&SPP provides a symbolic language, the Scenario Language, for constructing scenarios and translating them into an intermediate language suitable for interpretation by the GPC Interface Simulator.

The STB&SPP system is written in FORTRAN V and Assembler for interactive execution and has been implemented on a Data General Eclipse C330 operating under RDOS with 32K words of extended memory configured as a Shuttle avionics test system (SATS), including a serial-world simulator/serial-word modulator (SWS/SWM). The STB&SPP system was developed in 1983.

This program was written by Martin D. Hyman, Gerald H. Fine, and Gerald J. Hollombe of Abacus Programming Corp. for **Johnson Space Center**. *For further information, Circle 118 on the TSP Request Card.*
MSC-20779

Circle Reader Action No. 327

Mechanics

Nonlinear Supersonic Full Potential Analysis

Accurate results are obtained for complex geometries.

The Supersonic Implicit Marching Program (SIMP) applies a numerical method, based on the conservative form of the full potential equation, to the problem of three-dimensional supersonic flows with embedded subsonic regions. The conservative formulation of the problem provides the ability to capture shocks and to assess accurately the impact of sweep, thickness, and lift for conditions where linear theory is unsatisfactory.

SIMP fills the need for a nonlinear supersonic technique that produces accurate results for complex geometries, with efficient use of computational resources as well as minimization of the required level of user sophistication. Sample results have been obtained for a variety of problems, including the Space Shuttle orbiter flow at low supersonic mach numbers, flow over realistic fighter configurations, wake simulations for an arrow wing, and a forebody in sideslip.

This analysis method is based on the full potential equations written to conserve mass across shock waves as well as throughout the flow. A conservative switching scheme is used for the transition from a supersonic marching procedure to a subsonic relaxation algorithm. The technique uses characteristic signal-propagation theory to control density biasing for the treatment of shocks (including embedded shocks) and mixed elliptic/hyperbolic crossflow.

SIMP does not require any specific form of geometry or physical grid system. The separation of the body-fitted grid calculations and the actual analysis allows the verification of the geometry before proceeding with the solution. The input consists of detailed contour geometries and environmental parameters. The output contains the surface pressure and density calculations at every marching step and detailed flow-field information at user-specified cross-section stations.

SIMP is written in FORTRAN 77 for batch execution and has been implemented on a CDC CYBER 170-series computer operating under NOS 1.4, with a central-memory requirement of approximately 260K of 60-bit words. Optional graphic output requires the PLOT10 software package. The SIMP program was developed in 1985.

This program was written by V. Shankar and K. Y. Szema of Rockwell International Corp. for **Langley Research Center.** *For further information, Circle 64 on the TSP Request Card.*
LAR-13413

Calculating Aerodynamic-Stability Derivatives

This program accommodates complicated three-dimensional shapes.

The VORSTAB program was developed to calculate the lateral-directional characteristics of nonplanar wing/body combinations in subsonic flow. VORSTAB mathematically determines the effects of edge-separated vortex flow, including augmented vortex lift, strake-induced downwash, and vortex breakdown.

VORSTAB accepts up to six lifting surfaces, under free-air or ground static conditions. Asymmetrical configurations and curved leading/trailing edges, as well as more traditional configurations, are accommodated by VORSTAB.

The computational method is based on the Prandtl-Glauert equations. VORSTAB represents the wing effect by a vortex distribution, with flow tangency solved through the quasi-vortex-lattice method. The edge-separated vortex flow is represented by Polhamus' method of suction analogy. The effect of vortex breakdown is accounted for by an empirical method. The influence of the fuselage on the flow field is modeled by vortex multiplets distributed along the body centerline.

The VORSTAB input consists chiefly of geometric specifications for the lifting surfaces, edges, flaps, and fuselage. The output includes the lateral-directional stability derivatives for both attached and vortex flow, the angle of attack for vortex breakdown at the trailing edge of a lifting surface, control effectiveness for both longitudinal and lateral-directional control surfaces, the pressure distribution, and the wing bending-moment distribution.

VORSTAB is written in FORTRAN IV for batch execution and has been implemented on a CDC CYBER 170-series computer operating under NOS 1.4, with a central-memory requirement of approximately 145K of 60-bit words. The program was developed in 1984.

This program was written by C. Edward Lan of the University of Kansas Center for Research, Inc., for **Langley Research Center.** *For further information, Circle 65 on the TSP Request Card.*
LAR-13471

Wing-Design Program for Subsonic or Supersonic Speeds

The surface of mildest possible camber is generated.

The WINGDES program provides a wing-design algorithm based on modified linear theory that takes into account the effects of attainable leading-edge thrust. A primary objective of the WINGDES approach is the generation of the surface with the mildest possible camber that will produce drag levels comparable to those attainable with full theoretical leading-edge thrust.

WINGDES provides an analysis as well as a design capability and is applicable to both subsonic and supersonic flows. The optimization can be carried out for an entire wing or for designated leading- and trailing-edge areas, for the design of mission-adaptive surfaces.

WINGDES determines an optimum combination of a series of candidate surfaces, rather than the more-commonly-used candidate loadings. An optimization procedure based on Lagrange's method of undetermined multipliers is used to select a combination of candidate surface shapes to yield minimum drag, subject to restraints on the lift and moment. The input consists of wing-planform and airfoil-section-thickness data and of such operational parameters as the mach number, Reynolds number, and design lift coefficient. The results include the optimized camber-surface ordinates, the pressure-coefficient distributions, and theoretical aerodynamic characteristics.

WINGDES is written in FORTRAN IV for batch execution and has been implemented on CDC 6600 and CDC CYBER-series computers operating under NOS 1.4, with a central-memory requirement of approximately 161K of 60-bit words. The program was developed in 1984.

This program was written by Harry W. Carlson and Kenneth B. Walkley of Kentron International, Inc., for **Langley Research Center.** *For further information, Circle 66 on the TSP Request Card.*
LAR-13315

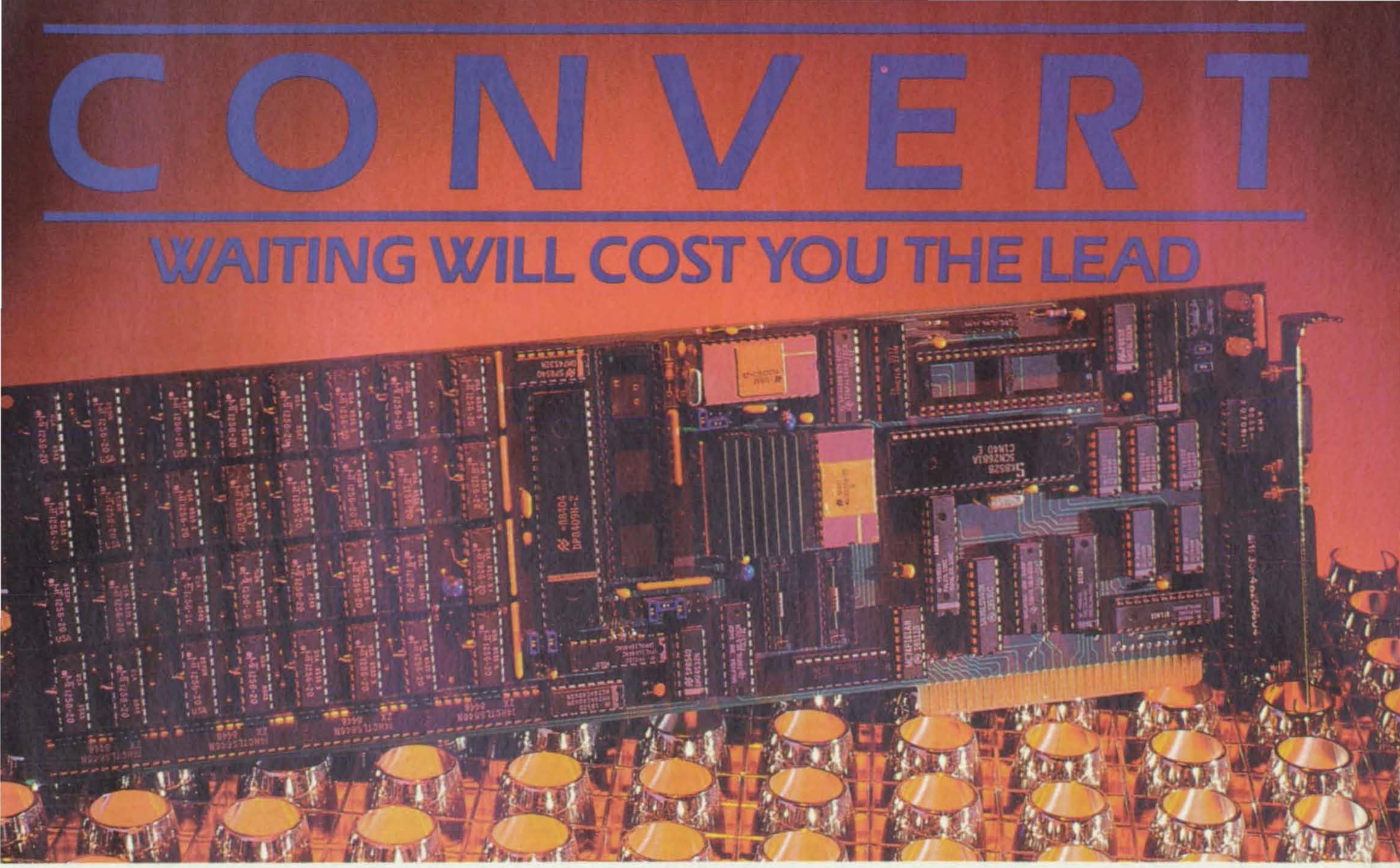

Turn your PC into a powerful 32-bit Super-Mini.

When your PC runs 35 times faster, you outrun the competition. Tired of playing runner-up? Plug a **PM**™ model **DSI-32 Co-Processor** into your personal computer. And easily outrun any XT, AT... even many VAX's.

A completely self-contained 32-bit computer—with floating point processor—on a single PC board, the **PM**™ converts any IBM/PC into a powerful Super-Mini that runs at an incredible 10 MHz, with no wait states. Across the board, it's the fastest board for the money, putting the power and performance of a $150,000 computer in your lap... *for a hundredth of the price!*

Simple to install, in minutes it's up and running compatibly with your standard PC MS/DOS system, without retraining or file conversion. You can port scientific or commercial applications without recoding or restructuring your software to fit Intel's architecture. And you can choose either MS/DOS or Unix at will, without commiting your system to either one.

Why lag behind? Call the 800 number below for a no-risk trial of the **PM**™. And convert your personal computer to a *Personal Mini*. It'll make a convert out of *you*.

- Operates in any PC/XT/AT or compatible.
- Takes only one slot.
- Has National Semiconductor's 32032 processor and 32081 math co-processor both running at 10 Mhz.
- Optional MMU and ICU provide for true demand paging virtual memory up to 15 megabytes.
- DSI memory full 32 bit bus with 1/2/4/8 megabytes on board
- DSI-MS/DOS environment has access to all devices on PC bus.
- The PC's 8088/86/286, used concurrent, handle all I/O and leaves DSI-32 to run uninterrupted.
- Port, mini and mainframe source programs in minutes.
- Includes assembler, linker, and debugger and full documentation.
- Supported by C, Pascal and Fortran-77 compilers ported for Vax/VMS compatibility.
- Two level hardware implemented software protection, custom arrangements negotiable.
- Two serial ports up to 38k baud.
- Hardware and software support for 1 year. Extended hardware/software support available.
- Try our board NOW for no-risk, 30 day Money Back Evaluation Period.

Sieve Benchmark

N*	IBM XT	IBM AT	VAX 750	VAX 780	DSI-32
20,000	35.30	8.13	6.11	3.04	4.52
40,000	351.50	99.71	13.13	6.38	9.07

Float Benchmark

40,000	11.46	17.71	.83	.50	.80

Unix Benchmarks

	DSI-32	VAX 780	VAX 750
O.S. Overhead	3.88	4.4	7.0
C Compiler Test	.55	1.0	1.7
Sieve of Eratosthenes	1.93	1.7	2.4

ECOTECH, INC.®
COMPUTER SYSTEMS

3711 35th Street, N.W.
Washingtin, D.C. 20016
202 244-3858

800 826-2189

Circle Reader Action No. 440

Machinery

Dynamic Tooth Loads for Spur Gears

The program should facilitate the application of high-contact-ratio spur-gear concepts.

As a result of the recent interest in the possible weight saving obtained by using high-contact-ratio gear (HCRG) meshes, a computer program was developed using a time-history, interactive, closed-form solution for the dynamic tooth loads for both low- and high-contact-ratio spur gears. Because the magnitude and variation of the tooth-pair compliance with load position can affect the dynamics and loading significantly and because the tooth-root stressing per load varies significantly with load position, it was desirable to include in the dynamic gear program preprocessors and postprocessors, respectively, for calculating these two important factors. Since the tooth forms for HCRG's deviate appreciably from the tooth forms for conventional low-contact-ratio gears (LCRG's), improved and simplified methods were developed for calculating the compliance and stress sensitivity for three involute tooth forms as a function of load position — a standard LCRG tooth with no undercut and two HCRG teeth with different forms of undercut.

The method developed for calculating the compliance of spur-gear teeth follows to a great extent that developed by Weber and includes three factors: (1) the basic deflection of the tooth as a beam, (2) the deflection of the tooth caused by the fillet and foundation flexibility, and (3) the local deflection caused by the contact between the two teeth. The principal improvement in the compliance analysis was for the fillet/foundation deflection, which was found to be defined by different fillet angles for various load positions, whereas previous studies assumed a given fillet angle of about 75°. The resulting compliance analysis was evaluated by applying it to available test, finite-element, and analytic-transformation results and was found to give compliance results that agreed well with measurement and "exact" analyses.

The method developed for calculating the stress sensitivity is an improved and simplified version of the Heywood analysis. Because the tooth forms for HCRG's deviate appreciably from conventional LCRG tooth forms, the stress-sensitivity analysis had to include most of the factors affecting the stressing. The improved analysis does not assume the peak stress occurs at 30° from the base of the fillet, as the Heywood analysis does, but allows it to be a function of the load position. The sensitivity analysis was found to give results that agreed well with the Heywood and Kelley and Pederson methods, which in turn, have been found to correlate well with test results. Evaluation of the modified Heywood stress-sensitivity analysis showed that its results compared very well with available test, finite-element, and analytic-transformation results.

The formulas contained in the computer program are based on the work done by Heywood, Weber, and O'Donnell for the stress sensitivity and compliance of low- and high-contact-ratio, involute, spur-gear teeth. The parameters used in these formulas require the derivation of the effective fillet length or angle rather than assuming particular values as done by Heywood and O'Donnell. The stress-sensitivity formula is a modified version of the Heywood formula, using simple beam parameters. The compliance formula uses O'Donnell foundation-flexibility factors and Weber's local-contact compliance.

The program is written in FORTRAN IV for use on an IBM 370 computer.

This program was written by R. W. Cornell and W. W. Westervelt of United Technologies Corp. for **Lewis Research Center.** *For further information, Circle 67 on the TSP Request Card.*
LEW-14099

Fabrication Technology

Program for Heat Flow in Welding

The user can predict power requirements and temperature distributions.

This program contains a numerical model of the temperature distribution in the vicinity of a weld. The weld model can be used to produce estimated welding-power requirements, welding-power-loss analysis, heat-affected-zone temperature history, and weld-puddle cross-section plots. The model can be applied to gas/tungsten-arc, plasma-arc, electron-beam, and laser-beam welds on wide plates under steady conditions.

The basic weld model combines a point source on the surface with a line source of heat. One dipole and three quadrupole components can be added at the user's option. Marangoni circulation, surface contamination, and magnetic pumping within the weld puddle can be simulated by use of the multipoles.

The entire program is written in a menu format that includes prompts for such required input as metal-characterization parameters and weld geometries. The program contains default characterization values for four common weld materials. There is extensive plotted output to the screen, including graphs of weld speed versus power, temperature versus distance from the heat source, and weld-puddle cross sections within user-defined boundaries.

The weld model is written in BASIC for interactive execution and has been implemented on a Tektronix WP 1220 series computer operating under TEK SPS with a central-memory requirement of approximately 12K of 16-bit words. This program was developed in 1984.

This program was written by A. C. Nunes, Jr., and M. H. Graham of **Marshall Space Flight Center.** *For further information, Circle 10 on the TSP Request Card.*
MFS-28081

Mathematics & Information Sciences

Program for Generating Graphs and Charts

The user can create and maintain a customized data base and related graphics.

The Office Automation Pilot (OAP) Graphics Database system offers the IBM personal computer user assistance in producing a wide variety of graphs and charts and a convenient data-base system, called a chart base, for creating and maintaining data associated with the graphs and charts. Thirteen different graphics packages are available to the OAP user. Access to each of the graphics capabilities is obtained in a similar manner. The user chooses creation, revision, or chartbase-maintenance options from an initial menu. The user may then enter or modify data displayed on a graphic chart.

The cursor moves through the chart in a "circular" fashion to facilitate data entries and changes. Various "help" functions and onscreen instructions are available to aid the user. The user data are used to generate the graphical portion of the

Circle Reader Action No. 313

chart. Completed charts may be displayed in monotone or color, printed, stored in the chart base on the personal computer, or uploaded to an IBM host computer (if the user's personal computer supports communications).

The thirteen graphics capabilities are divided into three groups: forms, structured charts, and block diagrams. There are eight forms available: (1) bar/line charts, (2) pie charts, (3) milestone charts, (4) resources charts, (5) earned-value analysis charts, (6) progress/effort charts, (7) travel/training charts, and (8) trend-analysis charts. There are three structured charts available: (1) bullet charts, (2) organization charts, and (3) work breakdown structure (WBS) charts. There are two block diagrams available: (1) N × N charts and (2) PERT charts.

Each graphics capability supports a chart base. The OAP graphics data-base system provides the user with an effective means of managing data, which are best interpreted as graphical displays.

The OAP graphics data-base system is written in Microsoft PASCAL for interactive execution on an IBM personal or XT computer with at least 192K of memory, at least one disk drive, and the color graphic adapter and monitor. For printed charts, an Epson printer (or equivalent) is required. Source code for the entire system is available to the user for modification and customizing. An executable disk is also supplied for each of the thirteen graphics capabilities. The system was developed in 1983.

This system was developed by Clarence T. Ackerson of **Goddard Space Flight Center.** *For further information, Circle 32 on the TSP Request Card.*
GSC-12925

Scanning Program

A user can extract tokens from character strings.

The SCAN program uses a scanning algorithm to locate tokens in a line of input data. The tokens can be command words, numbers, data values, labels, and the like. By using the SCAN subroutines, a user can extract tokens from character strings in languages with simple or complex syntax. SCAN has been thoroughly tested and is implemented in NASA's Descent Design System for the Shuttle orbiter. Due to its generality, SCAN should be useful for other programs requiring input scanning.

The SCAN algorithm was developed from digital design concepts and automata theory. The program has three main elements: (1) input and output data, (2) process-control data consisting of a state value and a transition table defining the states for each category of input character, and (3) process logic.

The process logic will retrieve a character, determine the category of the character (letter, digit, delimiter, and the like), use the transition table to assign a new state, and initiate a subprocess, which depends on the new state. The SCAN process accepts a character string as input and will return the leftmost token. The test driver program included with the SCAN subroutine incorporates a loop to extract all tokens in the input line.

SCAN is written in FORTRAN 77 for interactive or batch execution and has been implemented on an HP 9000-series computer operating under UNIX 3.0 with a central-memory requirement of approximately 107K of 8-bit bytes. This program was developed in 1984.

This program was written by William C. Mattison of OAO Corp. for **Johnson Space Center.** *For further information, Circle 30 on the TSP Request Card.*
MSC-20904

Collector-Output Analysis Program

Cross-reference indexes and supplemental information are produced.

The Collector-Output Analysis Program (COAP) is a programmer's aid for analyzing the output produced by the UNIVAC collector (MAP processor). COAP was developed to aid in the design of segmentation structures for programs with large memory requirements and numerous elements but is of value in understanding the relationships among the components of any program.

COAP provides a comprehensive set of alphabetized cross-reference tables describing the relationship between elements, external references, external symbols, common blocks, and collector-defined tags. Supplemental information concerning memory requirements and allocation, common banks, undefined external references, unused elements, and unused external symbols is also provided. COAP input consists of a file containing the L-option collector print listing. If this file also contains the R-option collections of a segmented program, information on each of the relocatable elements is provided.

COAP is written in FORTRAN 77 for batch execution and has been implemented on a UNIVAC 1100-series computer operating under EXEC 8 with a central-memory requirement of approximately 65K of 36-bit words. This program was developed in 1984.

This program was written by Dave R. Glandorf and Robert F. Phillips II, of Lockheed Engineering and Management Services Co., Inc., for **Johnson Space Center.** *For further information, Circle 75 on the TSP Request Card.*
MSC-20866

Language and Program for Documenting Software Design

Accurate records are kept, and errors are detected more readily.

Effective, efficient communication is an essential element of the software development process. The Software Design and Documentation Language (SDDL) provides an effective communication medium to support the design and documentation of complex software applications. SDDL supports communication among all the members of a software-design team and provides for the production of informative documentation on the design effort.

Even when an entire development task is performed by one individual, it is important to document communication explicitly among the various aspects of the design effort, including concept development, program specification, program development, and program maintenance. SDDL ensures that accurate documentation will be available throughout the entire software life cycle. SDDL offers an extremely valuable capability for the design and documentation of complex programming efforts ranging from scientific and engineering applications to data management and business systems.

Throughout the development of a software design, the SDDL-generated software-design document always represents the definitive word on the current status of the continuing, dynamic design/development process. The document is easily updated and readily accessible in a familiar, informative form to all members of the development team. This makes the software-design document an effective instrument for reconciling misunderstandings and disagreements in the development of design specifications, engineering-support concepts, and the software design itself.

Use of the SDDL-generated document to analyze the design makes it possible to eliminate many errors that might not be detected until coding and testing are attempted. The SDDL processor program translates the designer's creative thinking into an effective document for

For 25 years, DCS has been shaping the future of telemetry.

4784 Bit Synchronizer

- IEEE-488 interface
- Soft decision AGC
- 10 MBPS Operation
- 1 DB of theoretical
- Card changeable for later upgrades
- Remote terminal or computer entry

We look to tomorrow with new products like this:
The DCS model 4784 PCM Bit Synchronizer is an upgraded version of an already proven design. This state-of-the-art telemetry data processing component is capable of handling serial PCM bit streams which have been degraded by noise, base line instabilities, or jitter. The 4784 utilizes a synchronous clock to reconstruct and normalize data to NRZ-L. Both filter/sample and integrate/reset detection techniques are available, providing optimum performance under varying operating conditions.

5001 PCM Decommutator

- Multiple program format storage
- Programmable bit synchronizer
- Integral PCM simulator
- Diagnostic self-test
- Remote terminal or computer entry

We continue to pioneer better ways to serve our customers.
The DCS model 5001 PCM Decommutator utilizes the most recent developments in microprocessor technology, and brings these capabilities to the field of high bit rate PCM. A dedicated microprocessor within the Decommutator interfaces with a front panel keyboard and a 16-digit alpha/numeric display. The panel displays program parameters, or data, under control of the keyboard. Up to 30 formats may be saved in nonvolatile storage.

At DCS, we always support our customers with fast, on-call maintenance in your shop or ours.

6010 High Speed Frame Synchronizer

- 30 MBPS bit rate
- ECL technology
- Adaptive pattern recognition
- Auto polarity recognition

Future advances in telemetry are being designed today.
The DCS model 6010 High Speed PCM Frame Synchronizer represents one of the most technologically advanced instruments of its kind in the industry today. It is capable of handling data rates of up to 30 MBPS utilizing an adaptive frame sync strategy consisting of search, check, and lock; based on four sequential, correct and incorrect patterns. Auto polarity inverts the incoming data when a compliment of the frame synchronization pattern is detected. The 6010 and soon to be released, 4785 Bit Synchronizer are the forerunners of a whole new family of products now in advanced stages of design.

1455 Research Blvd.,
Rockville, Maryland 20850
Tel. (301) 279-8798 Twx. (710) 828-9785
8291 Westminster Ave., Suite 150,
Westminster, California 92683 Tel. (714) 894-4471 Twx. (910) 596-1802

DATA-CONTROL SYSTEMS
where the customer still comes first!

DCS
A CompuDyne Company

communication. The processor performs as many automatic functions as possible, thereby freeing the designer's energy for the creative effort.

Document formatting includes graphical highlighting of structure logic, the accentuation of structure escapes and module invocations, logic-error detection, and special handling of title pages and text segments. The SDDL-generated document contains software-design summary information, including module-invocation hierarchy, module cross-reference, and cross-reference tables of user-selected words or phrases appearing in the document.

The basic forms of the method are module and block structures and the module-invocation statement. A design is stated in terms of modules that represent problem abstractions that are complete and independent enough to be treated as separate problem entities. Blocks are lower level structures used to build the modules. Each of both kinds of structure may have an initiator part, a terminator part, an escape segment, or a substructure.

The SDDL processor program is written in PASCAL for batch execution on an IBM 370-series computer under OS. The PASCAL version of SDDL was developed in 1981 and last updated in 1984.

This program was written by Henry Kleine and Thomas M. Zepko of Caltech for **NASA's Jet Propulsion Laboratory.** *For further information, Circle 70 on the TSP Request Card.*
NPO-16511

Fitting Polynomial Equations to Curves and Surfaces

A program finds least-squares fits for functions of two independent variables.

FIT is a computer program for interactively determining least-squares polynomial equations that fit user-supplied data. FIT will approximate a given y = f(x) with a polynomial and plot the resulting curve. FIT also includes a method for computing the polynomial equation of a surface fit to data that are described by a function of two independent variables, y = f(x,z). Computer graphics are provided to allow the user to evaluate the shape characteristics of the calculated fit. The interactive graphical and editing capabilities in FIT enable the user to control the polynomial equations to be fitted to data arising from most practical applications.

FIT requires data values for the dependent variable y and the independent variable x (also z for surface fits). A weighted-least-squares solution determines the polynomial coefficients for the independent variable x. For surface fits or "crossplots" of two variables, the calculated x coefficients are then treated as dependent-variable values across z.

The user can specify the order of polynomial; alter weighting factors; edit the input data; view customized plots with defined labels, grids, reference lines, and scaling; and save the plotting parameters in a file for future use. FIT is menu-driven and includes a HELP facility.

FIT is written in FORTRAN and COMPASS for interactive execution and has been implemented on a CDC CYBER 170-series computer operating under NOS with a central-memory requirement of approximately 146K (octal) of 60-bit words. FIT requires a Tektronix terminal with PLOT-10 software to support its full graphics capability. This program was developed in 1984.

This program was written by P. Douglas Arbuckle, Steven M. Sliwa, and Sherwood H. Tiffany of **Langley Research Center** *and Marie-Louise Roy of Kentron International, Inc. For further information, Circle 36 on the TSP Request Card.*
LAR-13457

Structured Design Language for Computer Programs

This language can be used at all stages of program development.

The BOX language was developed to provide for improved productivity in designing, coding, and maintaining computer programs. BOX is a structured design language that can be used from the earliest conceptual design stage through the final coding.

At the design stage, comments are used to define the logical structure of the code in terms of functional boxes. In the coding stage, statements from an intermediate language like FORTRAN are used to implement the functions described in the comments, and condition lines are added to relate the required logic to program variables. The branching logic required by the structures is automatically generated from these conditional lines and the comments that define the structures. The usual FOR, WHILE, and UNTIL loops and the IF-THEN-ELSE and CASE structures are implemented in a consistent and explicit way.

The BOX system is written in FORTRAN 77 for batch execution and has been implemented on an HP 9000 series computer operating under HP-UX. The current BOX system uses FORTRAN 77 as the intermediate language. The BOX system was developed in 1982 and last updated in 1985.

This program was written by Walter H. Pace, Jr., of TRW, Inc., for **Johnson Space Center.** *For further information, Circle 31 on the TSP Request Card.*
MSC-20917

Workspace Program for Complex-Number Arithmetic

The existing APL language is empowered to manipulate complex numbers.

Complex-variable methods provide analytical tools invaluable for applications in mathematics, science, and engineering. The advent of computers significantly streamlined the bulk of manipulations involved in complex-number methods. APL is a computer-programming language with powerful matrix-handling capabilities, but it has no built-in complex-arithmetic functions. COMPLEX is a workspace program designed to empower APL with complex-number capabilities.

Functions available in COMPLEX include addition, subtraction, multiplication, and division; trigonometric and hyperbolic functions; natural and general logarithms; and such other functions as power, root, and modulus. Still other functions can be programmed by building on existing functions.

A program is converted to complex-number arithmetic by replacing +, −, *, /., etc., with the appropriate COMPLEX operators. The user assigns complex values to the desired variables, usually in a matrix of 2*N, where N is the number of complex variables.

COMPLEX is written in APL for use with interactive or batch programs and has been implemented on a Honeywell Sigma-series computer operating under CP-V with a central-memory requirement of approximately 6K bytes. This workspace program was developed in 1985.

This program was written by Marshall C. Patrick and Leonard W. Howell, Jr., of **Marshall Space Flight Center.** *For further information, Circle 23 on the TSP Request Card.*
MFS-28111

Estimating Prices of Products

Company-wide or process-wide production can be simulated.

The Improved Price Estimation Guidelines (IPEG) program provides a simple yet accurate estimate of the price of a manufactured product. The IPEG program facilitates sensitivity studies of price estimates at considerably less expense than would be incurred by the Standard Assembly-line Manufacturing Industry Simulation, SAMIS, program [see "Solar Array Manufacturing Industry Simulation" on page 446 of *NASA Tech Briefs*, Vol. 4, No. 3, Fall 1979 (NPO-14747)]. A difference of less than 1 percent between the IPEG and SAMIS price estimates has been observed with realistic test cases.

The IPEG simplification of SAMIS allows the analyst with limited time and computing resources to perform a greater number of sensitivity studies than with SAMIS. Although the IPEG program was developed for the photovoltaic industry, it is readily adaptable to any standard assembly-line type of manufacturing industry.

The IPEG program estimates the annual production price per unit. The input data include the costs of equipment, space, labor, materials, supplies, and utilities. Production on a company-wide basis or a process-wide basis can be simulated. The IPEG input file can be generated by SAMIS or may be prepared by the user. Once the IPEG input file is prepared, the original price is estimated, and sensitivity studies may be performed.

The IPEG user selects a sensitivity variable and a set of values. IPEG will compute a price estimate and a variety of other cost parameters for every specified value of the sensitivity variable. The IPEG program is designed as an interactive system; it prompts the user for all required information and offers a variety of output options.

The original IPEG program is written in SIMSCRIPT II.5 for interactive execution and has been implemented on an IBM 370-series computer with a central-memory requirement of approximately 300K of 8-bit bytes. The original IPEG program was developed in 1980. The IPEG/PC program is written in TURBO PASCAL for execution on an IBM PC computer under DOS 2.0 or above with at least 64K of memory. The IBM PC color display and color graphics adapter are needed to use the plotting capabilities in IPEG/PC. The IPEG/PC program was developed in 1984.

This program was written by Robert W. Aster, Robert G. Chamberlain, Silvino C. Zendejas, Thomas S. Lee, and Shan Malhotra of Caltech for **NASA's Jet Propulsion Laboratory.** *For further information Circle 4 on the TSP Request Card.*
NPO-16583

Mechanics

Hardware, Techniques, and Processes

Books & Reports

Computer Programs

Ultrasonic Inspection Near Small Bores

A portable, lightweight instrument finds small cracks near internal surfaces.

Marshall Space Flight Center, Alabama

A portable ultrasonic probe makes it possible to inspect for hidden cracks near the insides of narrow tubes. Using the pulse-echo technique, the instrument can detect cracks as small as 0.015-in. (0.38-mm) deep. It can be used for nondestructive inspection of other hard-to-reach places where conventional large transducers will not fit or where it is difficult to apply coupling liquid for contact ultrasonic testing.

The probe is connected to conventional ultrasonic inspection equipment through a flexible tube. The probe and tube are inserted in the part to be inspected (see figure). At its tip, the probe holds an ultrasonic transducer — a piezoelectric crystal in a stainless-steel case. The case centers the crystal in the part to be inspected and dispenses acoustic coupling liquid from orifices. A damping material isolates the transducer acoustically from the probe tube. The probe tip and the damping material are made of Emerson and Cuming resin 2057 (or equivalent) cured with Catalyst 9 (or equivalent).

The probe tube, made of polytetrafluoroethylene or a similar material, can bend around corners in the part. It carries coupling liquid from the probe handle to the transducer and serves as a conduit for electrical wires between the transducer and the external ultrasonic equipment. Coupling liquid is supplied through a port in the handle from a syringe or from a pressurized line. The diameter of the transducer is tailored to the size of tube under inspection.

After inserting the probe in the part, the test operator pushes the syringe plunger on the handle to inject the coupling liquid. The operator then slowly withdraws the probe while rotating it, thereby ultrasonically scanning the inside wall over the length of the tube.

This work was done by Ronald G. Parent of Rockwell International Corp. for **Marshall Space Flight Center.** *No further documentation is available.*
MFS-29024

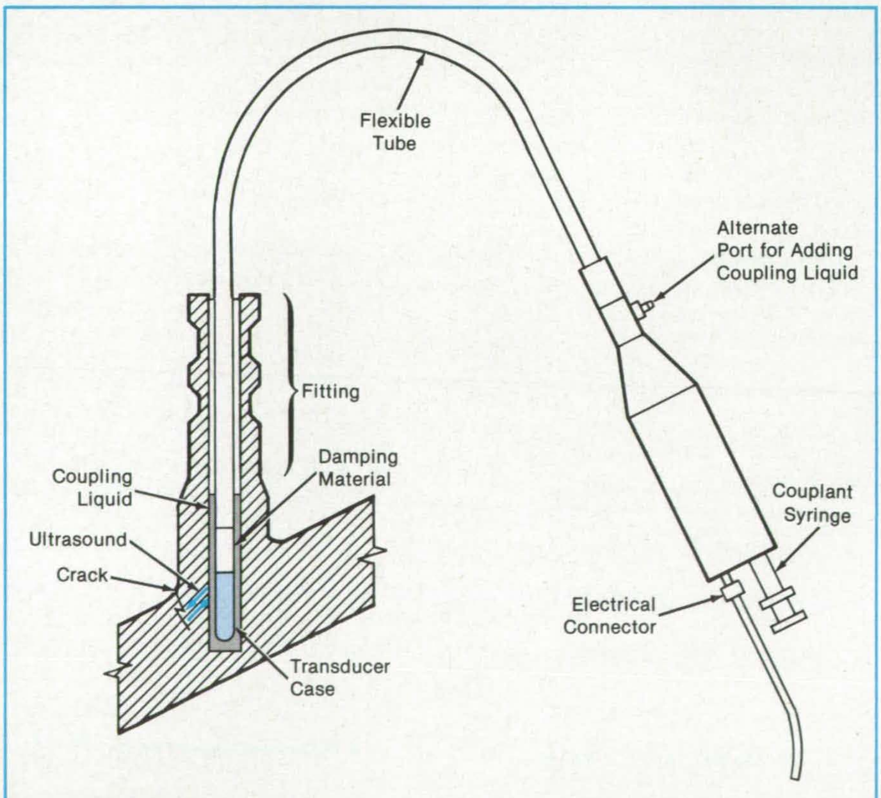

The **Ultrasonic Probe Inspects** the bore of a tubelike fitting. The ultrasonic instrument makes it unnecessary to disassemble the fitting to check for cracks. A precise orientation of the transducer with respect to the part is not necessary for detecting cracks.

Beta Backscatter Measures the Hardness of Rubber

Specimens can be thinner than those used on conventional mechanical testers.

Lyndon B. Johnson Space Center, Houston, Texas

A nondestructive testing method determines the hardness, on the Shore scale, of room-temperature-vulcanizing silicone rubber. The method measures backscattered beta particles; the backscattered radiation count is directly proportional to the Shore hardness.

Ordinarily, a durometer is used to measure the Shore hardness of a resilient material. However, reliable durometer measurements can be made only when the specimen is at least 0.25 in. (6.4 mm) thick. The backscatter technique can be used on specimens as thin as 0.02 in. (0.5 mm). For example, it might be used to test the postcure hardness of thin silicone rubber gaskets and seals.

The backscatter-measuring system includes a thallium-204 beta-particle emitter, a Geiger-Müller tube, a test stand, and a computer for data processing and control. The emitter is housed in a platen and is encased, with the tube, in the upper part of the test stand (see figure). When the test stand is placed on the rubber specimen, its weight makes the rubber bulge into the slot in the apex of the platen. The amount of bulging increases as the hardness of the rubber decreases.

Beta particles from the thallium isotope pass through the slot and bombard the specimen. The Geiger-Müller tube detects the radiation scattered back from the specimen. The more the specimen bulges, the more it directs the backscattering away from the Geiger-Müller tube and the fewer the radiation counts recorded. Conversely, the greater the hardness, the greater the radiation count. The relationship between the hardness and the Geiger-Müller count rate is nearly linear except at very low rates.

The test set is calibrated with a specimen, the Shore hardness of which is known from a mechanical durometer test. Then a specimen of unknown hardness is tested, and its radiation count is recorded. The count is compared with that for the known sample to find the Shore hardness of the unknown.

This work was done by Edward T. Morrissey and Frank N. Roje of Rockwell International Corp. for **Johnson Space Center**. *For further information, Circle 78 on the TSP Request Card.*
MSC-20991

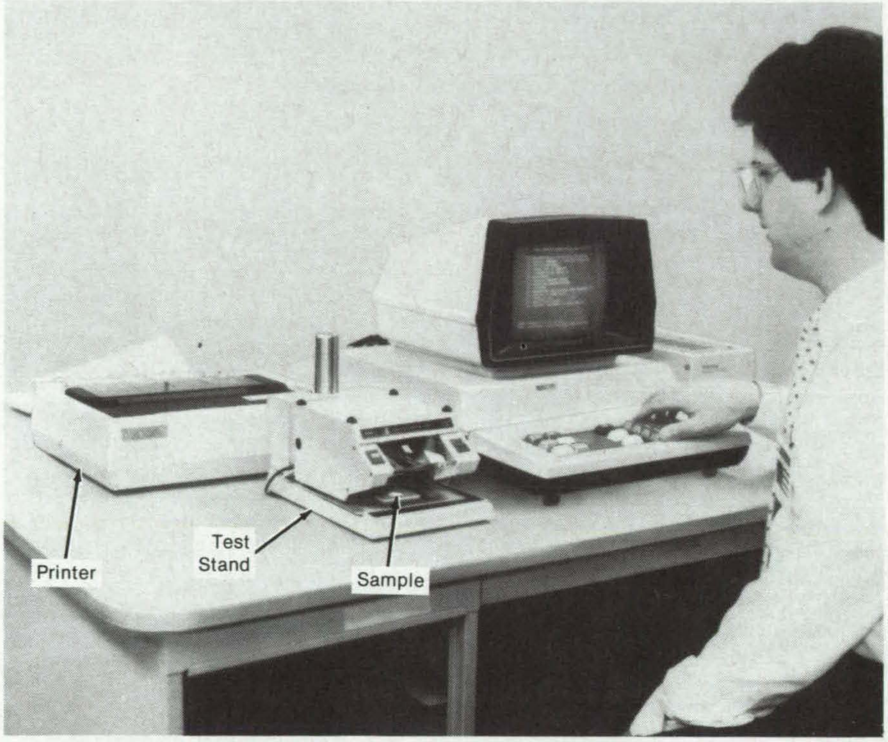

TESTING SYSTEM WITH SAMPLE IN PLACE

The **Hardness Test Setup** consists of a commercial beta-backscattering system. The backscattering technique is usually used to measure the thicknesses and compositions of coatings on the basis of chemical properties. Here, it is used to measure hardness.

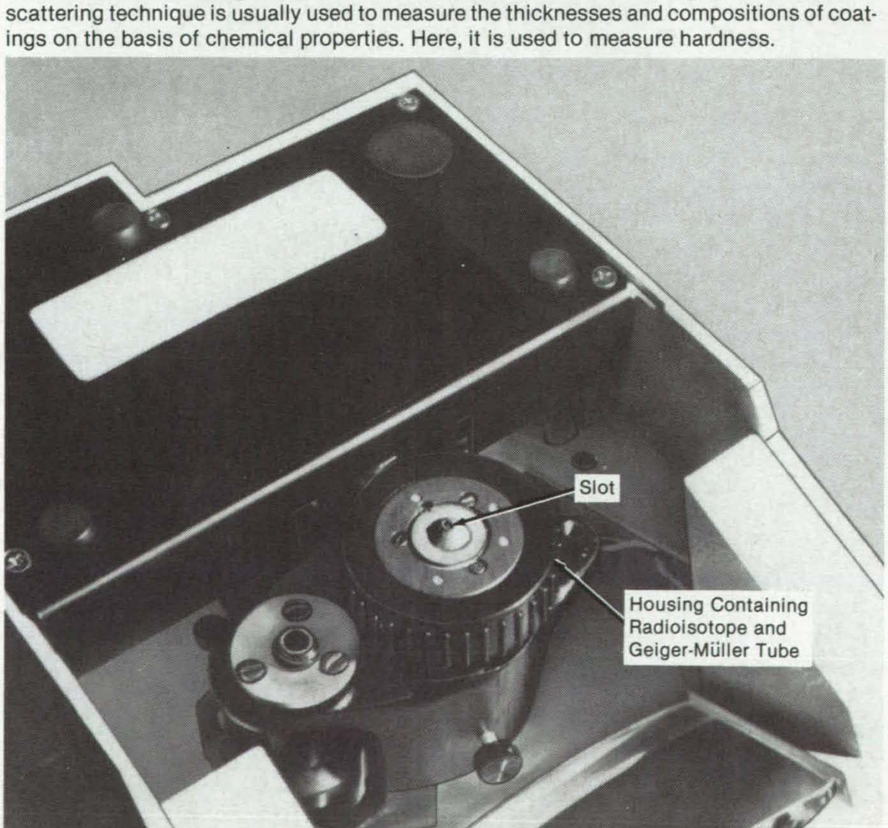

BETA-BACKSCATTERING HEAD
(Turned Upside Down for Visibility)

The Inland Motor Team Philosophy: Enhance While Simplifying—Specify Direct-Drive.

Inland Motor is the original manufacturer of direct-drive, frameless, DC torque motors. Although we've been providing these high-performance motion control solutions for more than 30 years, many designers don't fully realize the principles behind these motors—or their remarkable potential.

All Parts Dedicated To Motion

As illustrated in Figure 1, a direct-drive, frameless motor has no housing, no shaft and no bearings. It's comprised of three major components: stator, rotor and brush-ring (or sensor assembly for brushless motors). A frameless motor becomes an integral part of the host machine and relies upon the existing bearing structure for its support. Often, the unusual geometry—and extraordinary performance—of a frameless motor is the only solution to a challenging motion control problem.

Direct-drive motors eliminate the unwanted backlash, cogging and compliance associated with the gears, belts and couplings used in non-direct systems. This *direct* attachment of the frameless motor allows the designer to apply torque precisely where it is needed in the mechanism, rather than at some remote location.

Direct-drive motors have very high torque-to-inertia ratios *at the load*—where it really counts. The ratio indicates how responsive the system will be to commands for rapid stops and starts. In a geared system, the reflected torque is proportional to the gear ratio while inertia is reflected as the square of the gear ratio. One clear advantage of direct-drive motors is a torque-to-inertia ratio better by a factor equal to the gear ratio under consideration.

Designed To Be Predictable

Our DC torque motors are designed to be predictable. (See Figure 2.) We go to great lengths to preserve linearity over the full range of operation. From the lowest excitation through peak level, output torque is directly linear with respect to current load. Thus, stability and response criteria do not change with respect to load.

Plus, frameless DC motors grant economy of space. We use the finest magnetic materials when designing our motors, which allows us to pack a great deal of "muscle" into a very small package. Furthermore, since the motor rests on existing bearings and shaft, redundant parts are eliminated.

Figure 1 shows that frameless motors have a hole through their center. For many customers, this space is crucial for cable runs, waveguides or optics. Frameless motors free up the center axis so it can be used for other purposes.

Selection of a Direct-Drive Motor

Direct-drive motors often operate near to zero speeds as they precisely control positon or angular rate. For this reason, these unique motors cannot be measured by conventional standards such as horsepower. Rather, the primary figures of comparison for torque motors are peak torque, motor constant and physical size. The following criteria are the basis on which our engineers can quickly define a motor suitable for your requirements.

Maximum Torque—sum of all torque seen by the motor; encompasses acceleration torque, friction, windage and viscous losses.
Maximum Speed.
Maximum Power Point—where the highest product of torque and simultaneous speed occur.
Duty Cycle.
Power Budget—available DC voltage and current.
Ambient Temperature.
Operating Environment.
Size Restrictions—allowed O.D., I.D. and axial length.

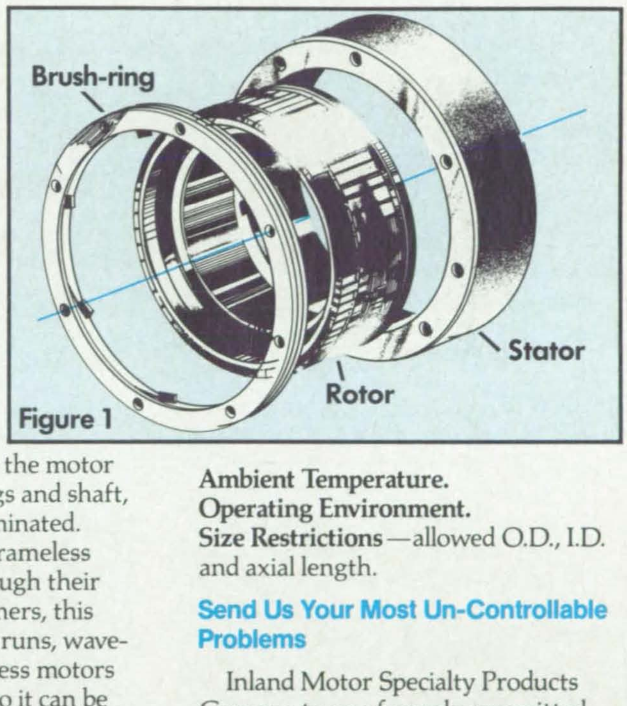

Figure 1

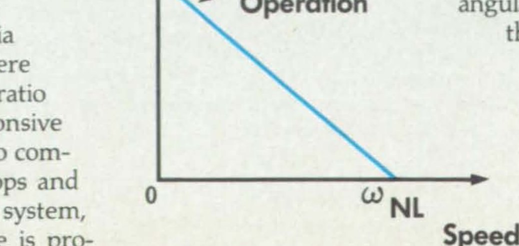

Figure 2

Send Us Your Most Un-Controllable Problems

Inland Motor Specialty Products Group: a team of people committed to delivering solutions to your most challenging motion control problems. Let us show you how responsive our direct-drive motors—and our organization—can be.

INLAND MOTOR
KOLLMORGEN CORPORATION
SPECIALTY PRODUCTS GROUP
501 First St. Radford, VA 24141
703/639-9045 TWX: 710-875-3740

Omnivector Probe Measures Airflow

The probe outputs are direct measures of perpendicular velocity components.

Lewis Research Center, Cleveland, Ohio

A probe (called an omnivector anemometer) has been designed and tested that has a fixed-position sensing element capable of simultaneously measuring steady and unsteady velocity head and flow direction of a moving fluid over a complete 360-degree angle in two-dimensional flow.

One of the problems in experimental fluid mechanics is the difficulty of providing flow probes capable of operating over a wide range of flow direction, including flow reversals. In some situations (such as stall and surge of jet-engine compressors), changes in flow direction take place very rapidly. These problems have been overcome with the development of this new omnivector anemometer.

The sensing element of the omnivector anemometer (as shown in Figure 1) is mounted on the end of a support tube, which is necessary for inserting the sensing element into the flow field. The main element of the anemometer is a drag body consisting of a cylindrical tube upon which are mounted eight miniature strain gages near the base and electrically connected in the form of two four-arm Wheatstone bridges (see cross section A-A). The strain gages, which form the arms of the two bridges, are arranged around the tube so as to provide the X and Y components of the drag force due to the moving fluid. The square root of the sum of the squares of the output of the bridges (E_1 and E_2) is proportional to the velocity head (one half times the fluid density times the square of the fluid velocity), and the ratio of the two outputs (E_2/E_1) is the tangent of the flow angle, Θ, (see Figure 2). If the variation in fluid density is negligible, the fluid velocity may be obtained from the computed value of the velocity head.

The natural frequency of the probe tested (sensing element length of 500 mm, wall thickness of 0.1 mm, and with a 1.5-mm-thick end cap) was 1.5 kHz, so the probe can be used for unsteady measurements to about 0.5 kHz.

This work was done by L. N. Krause and G. C. Fralick of **Lewis Research Center.** *No further documentation is available.*
LEW-13830

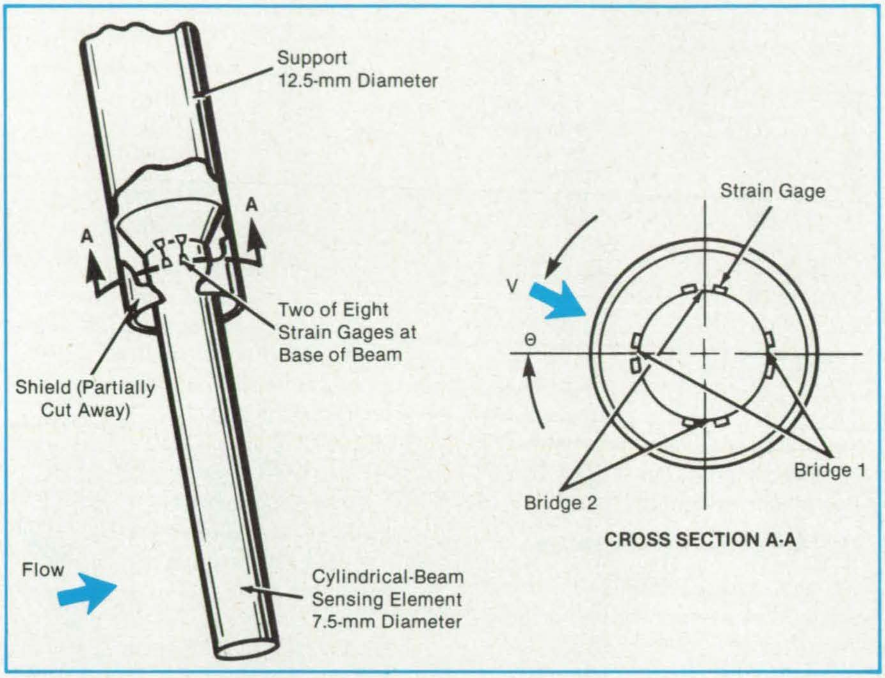

Figure 1. The **Omnivector Anemometer** includes a cylindrical sensing element with eight strain gages. The gages, connected in two Wheatstone bridges, sense the two perpendicular components of flow across the cylinder.

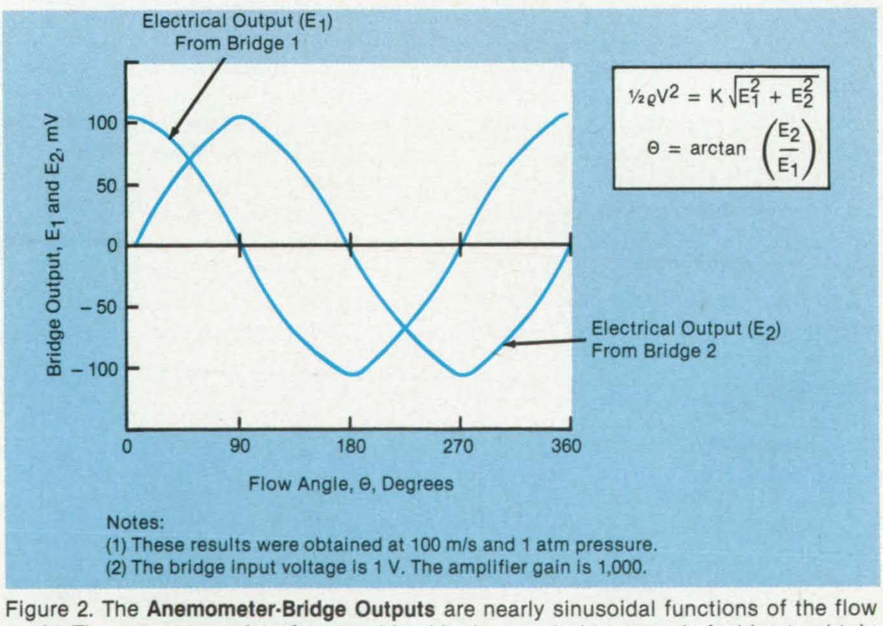

Figure 2. The **Anemometer-Bridge Outputs** are nearly sinusoidal functions of the flow angle. The outputs are therefore combined in the usual trigonometric fashion to obtain the magnitude and direction of the flow.

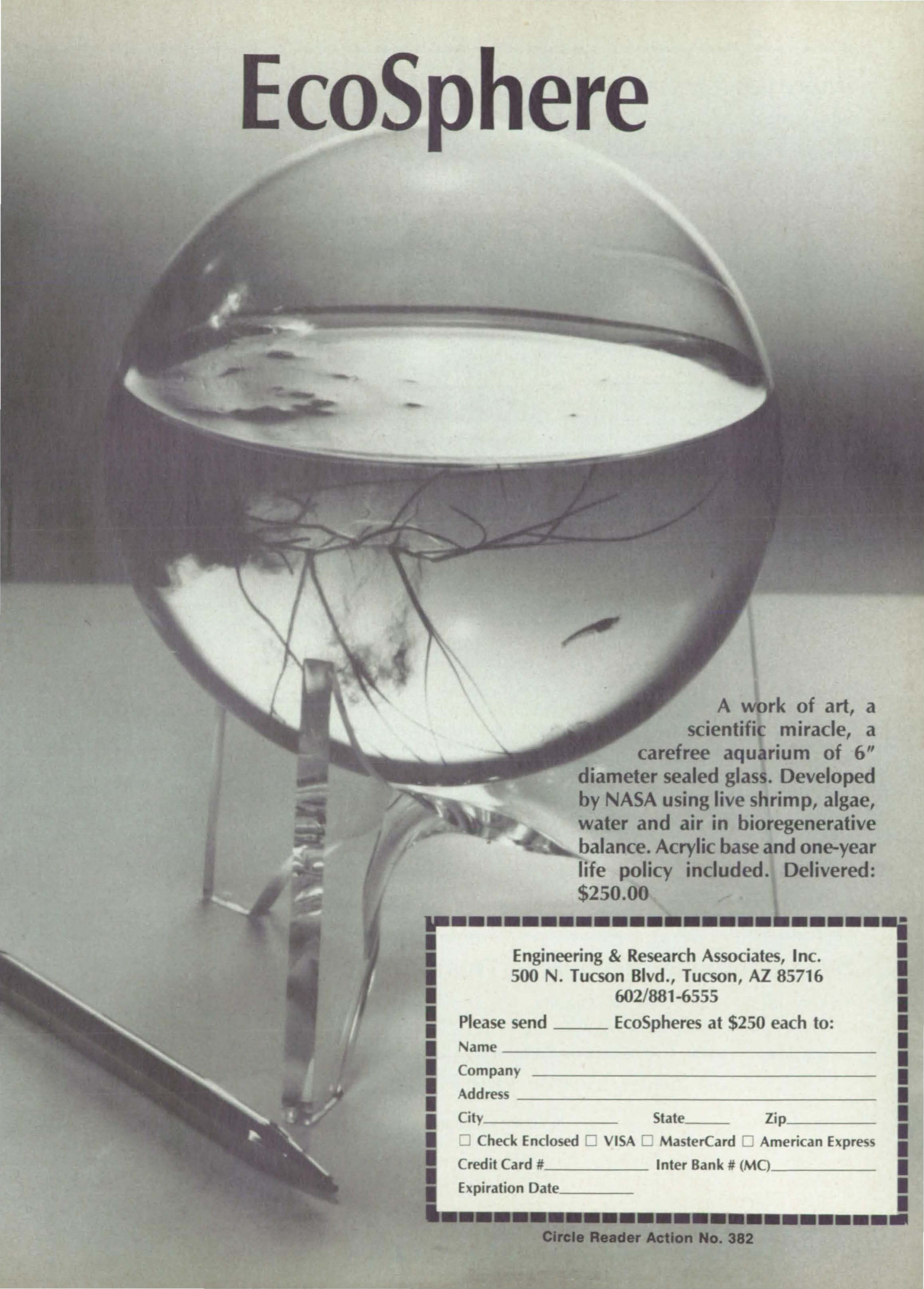
EcoSphere
A work of art, a scientific miracle, a carefree aquarium of 6" diameter sealed glass. Developed by NASA using live shrimp, algae, water and air in bioregenerative balance. Acrylic base and one-year life policy included. Delivered: $250.00
Engineering & Research Associates, Inc.
500 N. Tucson Blvd., Tucson, AZ 85716
602/881-6555
Please send _____ EcoSpheres at $250 each to:
Name
Company
Address
City State Zip
☐ Check Enclosed ☐ VISA ☐ MasterCard ☐ American Express
Credit Card # Inter Bank # (MC)
Expiration Date
Circle Reader Action No. 382

Improved Technique for Finding Vibration Parameters

Filtering and sample manipulation reduce noise effects.

Lyndon B. Johnson Space Center, Houston, Texas

An analysis technique improves the extraction of vibrational frequencies and damping rates from measurements of the vibrations of a complicated structure. The technique is based on a statistical method for analyzing vibrational data but is less susceptible than an earlier version is to errors induced by noise and by the presence of multiple modes.

The structural vibrations are measured by accelerometers, the outputs of which are digitized at a frequency high enough to cover all the modes of interest. The mathematically-reconstructed vibrational acceleration, $\ddot{z}$, is expressed as a sum of N damped, sinusoidal vibrational modes, namely:

$$\ddot{z}(t) \equiv \sum_{n=1}^{N} \ddot{z}_n(x,y)\exp\left(-\beta_n + i\omega_n\right)t$$

where t is time, x and y represent spatial coordinates, and $\ddot{z}_n$, β_n, and ω_n represent the acceleration amplitude, damping coefficient, and frequency, respectively, of the *n*th mode. The coherence function, Γ^2, gives a measure of how closely the reconstructed and measured accelerations differ, and is expressed by

$$\Gamma^2 = 1 - \frac{\sum(\ddot{Z} - \ddot{z})^2}{\sum \ddot{Z}^2}$$

where $\ddot{Z}$ is the measured acceleration and the sum is taken over all the digitized measurements obtained during the sampling interval.

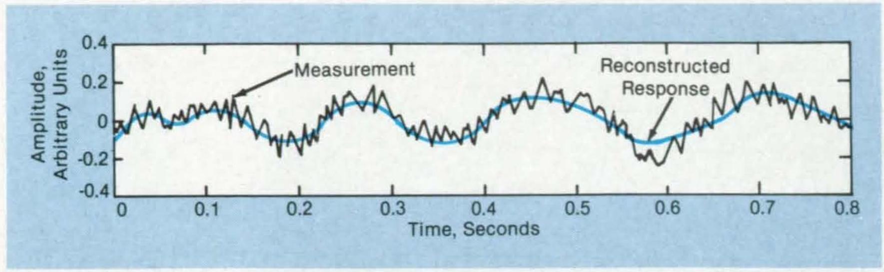

Simulated Accelerometer Measurements at a point on a structure (in this case, the Space Shuttle) were taken after an excitation at 6.25 Hz. The measurements are noisy, but the vibrational response reconstructed from the measurements shows little noise.

To eliminate aliased data from vibrational responses above the Nyquist frequency, the mode shapes are compared to predicted ones with natural frequencies below the maximum frequency of interest; those with low correlations are discarded. Next, pools of damping rate/vibration frequency pairs having nearly equal values (thus representing the same mode) are formed. The pairs with the highest Γ^2, mode-shape correlations, and modal confidence factors are selected for the final acceptance test.

The candidate modal components that have survived to this point are subjected to a computation of the increment of multiple coherence that occurs when each previously unaccepted component is combined with the previously accepted ones. The one that yields the highest increment is accepted. This procedure is repeated until the subsequent increments of the coherence value decrease to less than 1 percent of the previous coherence value or until all the candidate modes are accepted.

The measurement data often contain noise (see figure) and multiple simultaneous modes. While this usually poses no serious obstacle to finding the modal frequencies, it often leads to significant errors in the modal damping rates; which is unacceptable, because accurate damping rates are necessary for the prediction of flutter in large, complicated structures.

Of the various ways of processing the measurements to reduce the effects of noise, the ones that work best include digital low- or band-pass filtering, the manipulation of modal starting times, the selection of sample sizes, and combinations of these. Use of the improved method on a set of vibrational measurements from the Space Shuttle, for example, raised the level of coherence from previous values below 50 percent to values between 90 and 99 percent.

This work was done by Lowell V. Andrew and Charles C. Park of Rockwell International Corp. for **Johnson Space Center**. *For further information, Circle 85 on the TSP Request Card.*
MSC-20901

Synchronously Deployable Truss Structures

The structure is lightweight, readily deployed, and has reliable joints.

Langley Research Center, Hampton, Virginia

Deployable beam structures are required for many applications aboard the proposed space station as well as for uses in other artificial satellites. These structures must pack efficiently for launch into orbit and must deploy reliably upon command. A new truss concept, designated as the "pac truss," has been developed to rectify many of the shortcomings of previous designs, including the need for a complex deploying mechanism.

As shown in the figure, the truss beam has four longeron members located at the corners of the rectangular cross section. A series of battens and diagonals connects the longerons together at joints or nodes. The cross section is maintained by a section diagonal, and the orientations of the section diagonals alternate 90° from node to node. All members connect at nodes in such a way that only two node types are required.

For deployment, each diagonal has a midlength hinge that opens the member, permitting the diagonals and battens to rotate about simple clevis-type hinges at the nodes. The deployment of all members occurs in a synchronous manner; therefore, the beam deploys simultaneously in length and width. During deployment, the diagonal opens to the fully extended straight position, and the midlength hinge is locked by a latch, thus locking the model in the fully deployed position.

Truss-beam deployment can be accomplished by a number of methods. Since deployment is synchronous, an astronaut can deploy a long truss beam or large platform simply by hand deployment of a single bay. Also, structures of this type could be deployed in free flight by the controlled release of stored energy in torsional springs at selected hinges located throughout the structure. The same double-folding technique used in the beam model is applicable to flat planar trusses, allowing structures of large expanse to be folded into compact packages and to be deployed for space-platform applications. The unique folding arrangement of the members also permits the preattachment of instrumentation and utility cables to the longeron members without degradation of packaging or deployment.

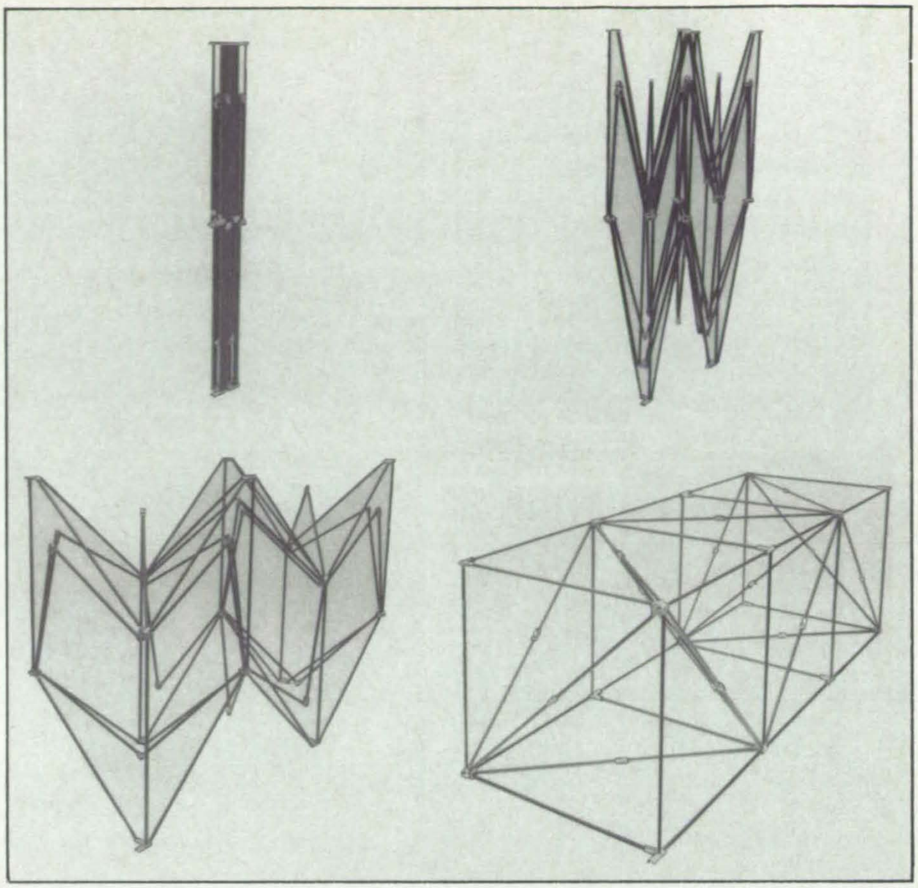

The **"Pac Truss" Features Easy Deployment** without the need for complex mechanisms.

This work was done by Marvin D. Rhodes of **Langley Research Center** *and John M. Hedgepeth of Astro Research Corp. No further documentation is available.*

Inquires concerning rights for the commercial use of this invention should be addressed to the Patent Counsel, Langley Research Center [see page 29]. Refer to LAR-13490.

Detecting Foreign Particles in Wind Tunnels

A simple scratch test tells whether particles, which could distort results, were present in a test.

Lyndon B. Johnson Space Center, Houston, Texas

A polished metal surface is used to detect abrasive foreign particles in an airflow test chamber such as a wind tunnel. Scratches and dents from such particles are readily apparent on the metal surface. Because it is impractical, if not impossible, to filter out all foreign particles, at least the detector can be used to provide evidence of particles in cases in which they are suspected of distorting the experimental results.

The detector was developed for tests of the abrasion resistance of flexible insulation blankets. When blankets partially disintegrated in wind-tunnel tests, there was no way of knowing whether the damage was caused only by the fast airflows or was also influenced by entrained particles. Now, when a detector indicates that particles were present in a test, the results can be interpreted accordingly.

The insulation specimen to be tested is mounted in a frame made of a lightweight silica insulating material (see figure). The frame protects the edges of the specimen. The frame contains holes for the detectors. Each detector consists of a plug of the same material as that of the frame, covered by a layer of Inconel* (or equivalent) nickel-alloy foil 0.001 in. (0.025 mm) thick.

The materials in the detector plug can easily withstand high temperatures. The detector can also be used in tests of paints and coatings to determine whether abrasive particles are present.

(*Inconel is a registered trademark of the Inco family of companies.)

This work was done by Howard L. Sharp, Peter A. Hogenson, and Wendall D. Emde of Rockwell International Corp. for **Johnson Space Center.** *For further information, Circle 81 on the TSP Request Card.*
MSC-20850

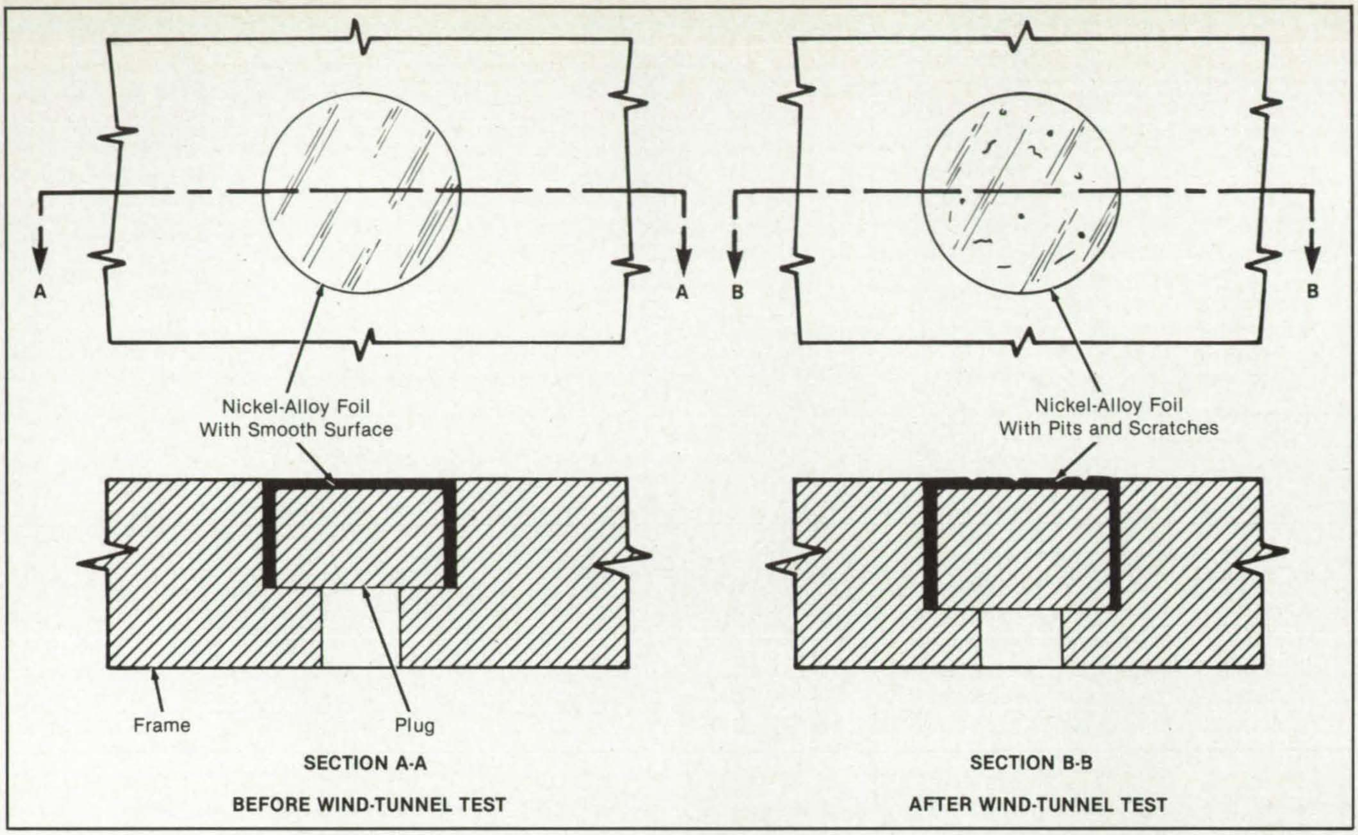

Small Pits and Scratches on a metal foil indicate that abrasive particles struck the surface during a wind-tunnel test.

Monitoring Temperatures Indirectly in Cooled Combustors

Temperature measurements are taken on the outside walls.

Marshall Space Flight Center, Alabama

A proposed noninvasive monitoring of the temperatures on the inner surface of the combustion liner of a cooled combustor could help increase liner life, thereby increasing combustor reliability and performance. This technique could be used in furnaces, reactors, jet engines, rocket engines, stationary turbines, combustors, and heat exchangers.

Typically, the coolant flows more or less parallel to the long axes of the individual channels (see figure), with very little lateral mixing.

The heating of the combustion liner is typically nonuniform, with overheated streaks (selectively hot and heat-damaged areas) developing lengthwise on the linear surface. These streaks in turn cause increased heating of the coolant along the corresponding channel, selectively reducing the cooling action of the fluid downstream of this location. This in turn causes the longitudinal section of the liner to overheat still further.

The problem is particularly acute when the coolant is a gas, because, as

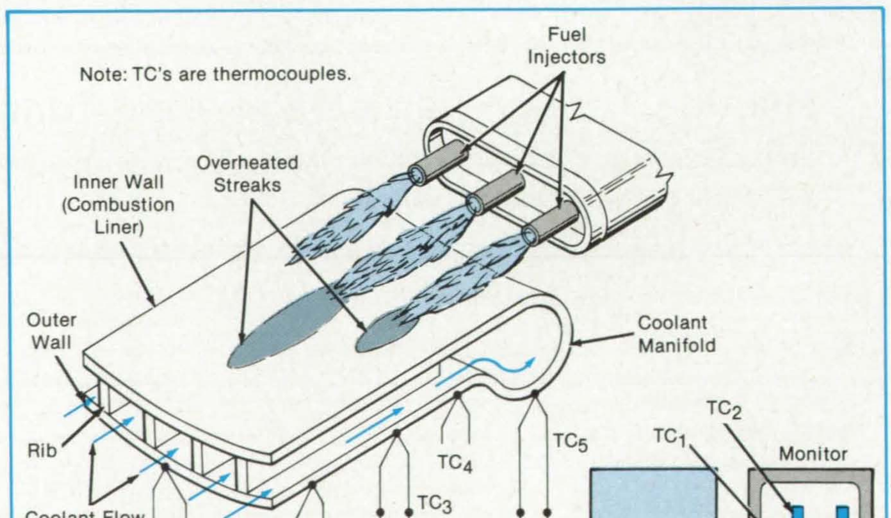

The **Growth of Internal Overheating Streaks** could be monitored using the output from an array of thermocouples on the outside wall of the combustor. Computer analysis of this output would indicate the temperature pattern on the combustor lining.

its temperature is significantly increased, its density and hence its mass flow rate is significantly decreased. Eventually the streaks may be the sites of fatigue, cracking, splitting, and ultimately the loss of coolant through the wall. If unchecked, such damage could lead to overall failure.

To locate and monitor these developing overheating streaks, an array of wire-type thermocouples would be placed at various points along the length and the circumference of the outside wall of the combustor and insulated to prevent heat loss to the environment. Because this technique is noninvasive, a large number of thermocouples can be used. The outer wall would be heated indirectly by heat transferred from the combustion lining via the cooling fluid; the temperature pattern in the outer wall would correspond to the pattern in the liner, being modified and displaced in a predictable manner by the coolant flow.

The output of the thermocouple array would be passed to a computer, which would use the appropriate heat-transfer theory to infer a temperature profile of the combustor lining. This output could be presented in any format, including a graphical display with colors and could be continuously recorded.

The use of these data would enable timely liner maintenance or overhaul. It could also guide adjustments; for example, by changing the sizes of the coolant orifices or passages or by changing the fuel-injection mixture ratio in the combustion chamber to retard or prevent the growth of heating streaks.

This work was done by W. R. Wagner of Rockwell International Corp. for **Marshall Space Flight Center**. *No further documentation is available.*
MFS-29061

Measurement of Dynamic Bolt-Stress

Modification of a static technique gives a complete stress cycle history.

Marshall Space Flight Center, Alabama

An ultrasonic method provides a record of the changing stresses in dynamically loaded bolts; for example, those in vibrating machines, ground vehicles, and aircraft. The method makes available the history of stress cycles, from which the fatigue state and remaining bolt life can be inferred.

Unlike the strain gauges bonded with epoxy to bolt shanks, the ultrasonic sensors are not extremely delicate and are not easily damaged when bolts are removed after testing. The ultrasonic method therefore eliminates laborious and time-consuming replacement of damaged strain gauges. Moreover, it gives true stress measurements rather than the torque or strain measurements.

The new method employs a modified static ultrasonic bolt extensometer. The ultrasonic transducer mounted on a bolt is modified so that it transmits and receives ultrasound pulses at much higher repetition rates. The high data sampling rate yields high-frequency dynamic stress measurements.

This work was done by Sarkis Barkhoundarian of Rockwell International Corp. for **Marshall Space Flight Center.** *No further documentation is available.*
MFS-29058

Books and Reports

These reports, studies, and handbooks are available from NASA as Technical Support Packages (TSP's) when a Request Card number is cited; otherwise they are available from the National Technical Information Service.

Determining Chaotic Instabilities in Mechanical Systems

Theoretical developments may enable the suppression of chaotic structural motions.

A report discusses the theory of chaotic instabilities in mechanical systems having many degrees of freedom. Chaotic motions occur in systems characterized by nonlinearities. These include bilinear springs, unilateral constraints, two-bar linkages, systems with multiple equilibrium states (for example, buckling columns or shells), aeroelastic systems, and structures with feedback control devices. A fully developed theory may enable the prediction, avoidance, and suppression of chaotic vibrations in structures, especially those using dynamic feedback stabilization.

In recent years, researchers have become increasingly aware of the difference between classical and chaotic instabilities. In a classical instability, a small perturbation grows exponentially toward an infinite amplitude. In a chaotic instability, random or aperiodic finite motions are apparently generated by a deterministic system without any random input, and the subsequent trajectories are supersensitive to small changes in the initial conditions.

The classical equations of motion of a system with N degrees of freedom are expressed as the parametrical equations of the trajectory of a point in the corresponding N-dimensional space. (This point represents the instantaneous configuration of the system.) The tangent and normals to the trajectory are then calculated. Assuming that the undisturbed trajectory is known, one can also solve, in principle, the equations for the growth of an infinitesimal initial perturbation in the trajectory. If the perturbation begins to grow exponentially, the motion is chaotic.

It must be emphasized that the chaotic nature of a mathematically predicted motion is the result of inadequacies in the mathematical model. All of the functions on which mechanical theory has been based are assumed to be differentiable as many times as necessary for mathematical convenience. However, the assumption of differentiability is not always physically realistic and is not required by the principles of mechanics nor by the definition of continuity. The behaviors of real systems are not always describable by smooth functions. The prediction of chaotic motion is the mathematical penalty for the unjustifiable assumption of smoothness.

Current efforts are directed toward including nondifferentiable functions in system descriptions so that predicted motions that formerly seemed chaotic become deterministic. The essence of this approach is the search for a noninertial reference frame that oscillates or moves with a nonsmooth transport velocity. The fluctuating components of velocity (for example, turbulence in a fluid) are expressed in the moving reference frame.

The solution of the equations of motion requires the calculation of a feedback function. The Lagrange equations of motion for the fluctuating velocity components are coupled with the feedback differential equations. The solution gives a deterministic description of the motion that formerly seemed chaotic. In the new formulation, the motion is both repeatable and predictable: Small changes in the initial conditions lead to small changes in both the mean and fluctuation velocities.

This work was done by Michail A. Zak of Caltech for **NASA's Jet Propulsion Laboratory.** *To obtain a copy of the report, "Chaotic Instability in Mechanical Systems," Circle 15 on the TSP Request Card.*
NPO-16709

Multishaker Modal Testing

Abstracts summarize time- and frequency-domain component-mode synthesis methods for damped systems.

The abstracts of six papers on vibration analysis and a summary of the contributions and recommendations contained in them are presented in a 14-page report on multishaker modal testing. The collection includes four reports published by the Center for Aeronautical Research, a paper accepted for publication in the journal of the American Institute for Aeronautics and Astronautics, and a paper presented at the Fourth International Conference on Applied Numerical Modeling.

The principal contributions and recommendations reported are the following:

1. A component-mode synthesis method for systems with general viscous damping has been developed. The inclusion of residual attachment modes as well as free-vibration modes increases the convergence rate. Further work to improve the efficiency of this method is recommended.
2. Methods of component-mode synthesis in the frequency domain have been explored. It has been shown that digital Fourier transforms can be used to compute the transient response of a coupled structure.
3. A robust, multi-input, multioutput modal-parameter estimation algorithm requiring little user interaction has been developed for identifying frequencies, damping values, and mode shapes of systems with general viscous damping. It applies to general linear, time-invariant systems. It results in reduced system matrices, which might be very useful in such applications as the control of flexible structures. Other applications of the algorithm should be explored, and the algorithm should be compared with other modal-parameter estimation algorithms, such as the Polyreference algorithm.

This work was done by Roy R. Craig, Jr., of the University of Texas for **Marshall Space Flight Center**. *Further information may be found in NASA CR-178507 [N85-33544/NSP], "Multishaker Modal Testing."*

Copies may be purchased [prepayment required] from the National Technical Information Service, Springfield, Virginia 22161, Telephone No. (703) 487-4650. Rush orders may be placed for an extra fee by calling (800) 336-4700. The report is also available on microfiche at no charge. To obtain a microfiche copy, Circle 83 on the TSP Request Card.
MFS-27132

Fatigue Criterion for System Design

A report discusses principles of structural-life prediction.

A fundamental principle of good design is to recognize that any structure can fail. The structure should be so designed that its failure does not cause personal injury or secondary damage. Once a structure is designed to fail in a benign manner, it then can be designed for finite life so that the overall size, weight, and cost can be reduced and still meet the reliability requirements of the application.

The design of machine elements is based, for the most part, on yield stresses and fatigue-limiting stresses. In addition to the material properties of components, proper consideration must be given to the effects of notches, surface condition, component size, residual stress, temperature, duty cycle, and such environmental factors as corrosive or chemical exposure. For most machine elements, individuals and organizations usually develop design methods based upon engineering fundamentals found in most machine-design texts and upon factors based upon their corporate experience and test data. As a result, it is not too unusual for different organizations or individuals, starting with the same or similar design requirements, to reach dissimilar conclusions or designs while seemingly applying the same fundamental engineering principals to the problem.

Setting aside the subjective, creative aspects of design, there appears to be nonuniformity of data from which numbers and design factors are selected, as well as differences in the computer codes and boundary conditions used in the design process. To compound these difficulties, the fatigue data used to establish fatigue limits are usually of a limited nature, with the conditions under which the data were obtained not adequately defined or reported. Such items as temperature, humidity, number of specimens, specimen size and volume, heat treatment, hardness, surface finish, and life distribution are not given.

The established fatigue limit for much of the reported data is a mean value. From a statistical viewpoint, the median value is equal to or less than the mean. This can be interpreted as meaning that before a fatigue limit is reached there is a probability that 50 percent of the specimens will have failed; that is, even at the fatigue-limit stress, life is finite. Experienced design engineers have recognized this for years, and they have added safety factors to their design procedures usually based on experience. While these procedures are generally adequate, they can result in overdesigned, oversized, overweight, and overcost structures.

A generalized methodology has been developed for structural life prediction, design, and reliability, based upon a fatigue criterion. The life-prediction methodology is based in part on work of W. Weibull, G. Lundberg, and A. Palmgren. The approach incorporates the computed life of elemental stress volumes of a complex machine element to predict system life. The results of coupon fatigue testing are incorporated into the analysis, allowing for life prediction and component or structural renewal rates, with reasonable statistical certainty.

This work was done by Erwin V. Zeretsky of **Lewis Research Center**. *Further information may be found in NASA TM-87017 [N85-27226/NSP], "Fatigue Criterion to System Design, Life and Reliability."*

Copies may be purchased [prepayment required] from the National Technical Information Service, Springfield, Virginia 22161, Telephone No. (703) 487-4650. Rush orders may be placed for an extra fee by calling (800) 336-4700.

LEW-14344

Scuffing and Lubrication of Gears and Bearings

A new Reynolds equation is developed for elastohydrodynamic-lubrication analysis.

Scuffing is a problem encountered in gears and rolling-element bearings. In rolling-element bearings, for example, scuffing is found in the acceleration zones of large, heavily loaded bearings. For these circumstances, inertia effects lead to high sliding speeds. Scuffing is related to lubrication-film thickness failures leading to metal-to-metal contact. High surface stresses lead to rolling-bearing fatigue, and high surface temperatures may cause local melting of the surfaces.

Because the surface temperature can be calculated if the kinematic and surface stresses are known, important parameters to control when one is studying scuffing are the film thickness and the surface stresses. These parameters can be calculated by use of elastohydrodynamic lubrication (EHL) analysis.

A new method was developed to study macro- and micro-EHL, without restriction on the load applied to the contact. Macro-EHL refers to the lubricant-film thickness developed in the inlet zone of the EHL conjuction. Micro-EHL may occur below the asperities and is due to the squeeze or sliding-speed effects in the bearing. Macro-EHL is first studied by use of the classical Reynolds equation (linear viscous-fluid model), and the results are accurate for any applied loads. Under severe conditions (large pressure and high sliding speeds), the lubricant behavior can no longer be considered to be linearly viscous; a nonlinear viscosity model is needed.

A new Reynolds equation takes into account the nonlinear viscous behavior of the fluid. The Reynolds equation and the elasticity equations are solved simultaneously by a system approach and the Newton-Raphson technique. The film thickness, pressure, and shear stress can be obtained without load restrictions. This new method therefore is a very powerful tool that can be used to study scuffing. Using this new approach, the researchers have analyzed stress concentrations near both a bump and a groove in a bearing surface.

This work was done by B. J. Hamrock of **Lewis Research Center** *and L. G. Houpert of the National Research Council. Further information may be found in NASA TM-87097 [N85-34408/NSP], "Elastohydrodynamic Lubrication Calculations Used as a Tool to Study Scuffing."*

Copies may be purchased [prepayment required] from the National Technical Information Service, Springfield, Virginia 22161, Telephone No. (703) 487-4650. Rush orders may be placed for an extra fee by calling (800) 336-4700.

LEW-14364.

Machinery

Hardware, Techniques, and Processes

Books & Reports

Computer Programs

Liquid Scavenger for Separator/Pump

Aerodynamic drag impels condensate along a groove to an exit hole.

Lyndon B. Johnson Space Center, Houston, Texas

A pump for hydrogen has been modified to remove moisture that condenses in the impeller stage. The moisture is returned to the centrifugal separator stage for removal from the system.

Normally, the separator removes water droplets from an incoming mixture of hydrogen gas, water droplets, and water vapor. In the unmodified pump, however, additional condensation sometimes occurs in the impeller stage.

The moisture-removal problem is solved by adding a shallow circumferential groove and a small exit hole to the impeller chamber (see figure). As the impeller wheel rotates, the condensate is forced toward the outer wall of the chamber, where it collects in the groove. Aerodynamic drag impels the water around the groove toward an exit hole located at the high-pressure region of the chamber. The condensate and a small portion of the gas flow through the exit hole into

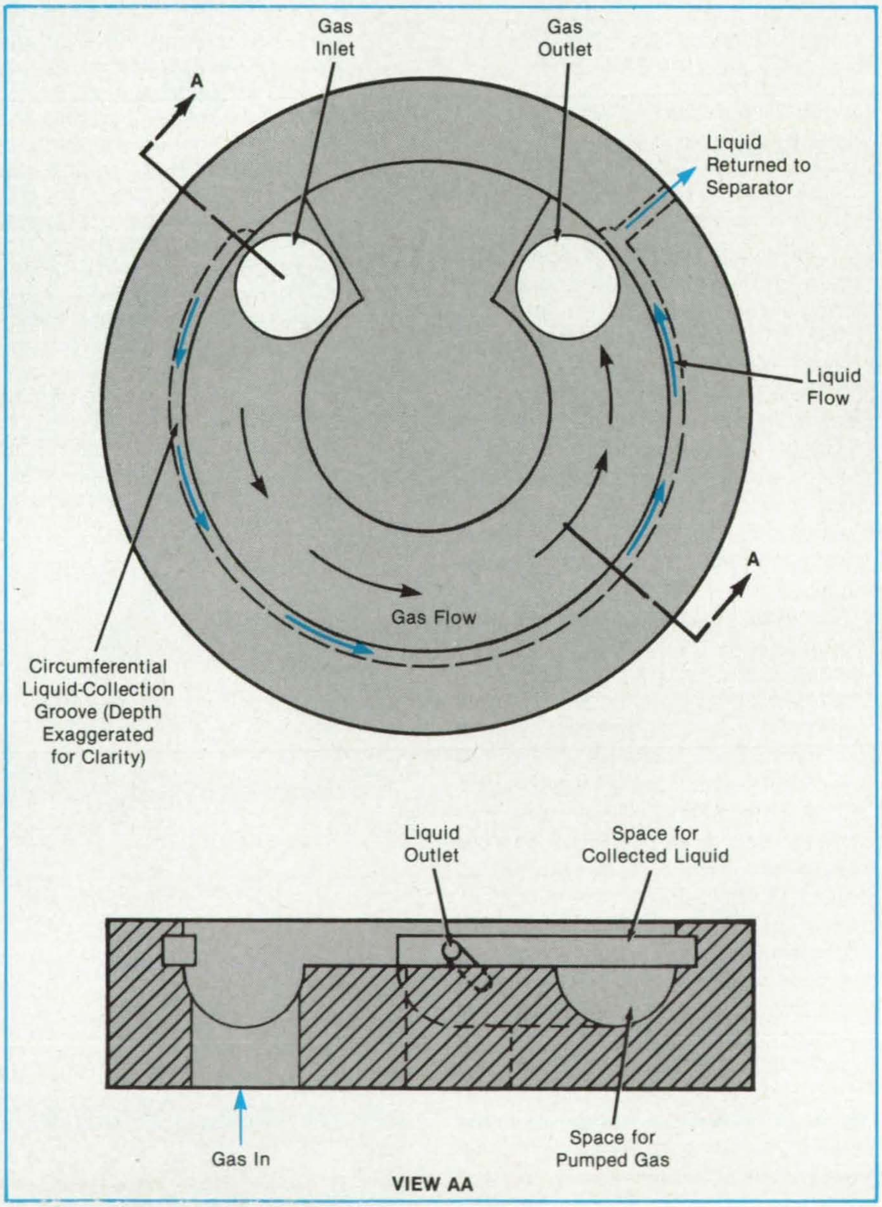

The **Modified Impeller-Pump Housing** has a circumferential groove that leads to an exit hole near the high-pressure outlet. As the impeller disk (not shown) rotates, it flings water droplets that have condensed in the pump toward the groove. Aerodynamic drag drives the water around the groove to the exit hole.

a tube that leads back to the separator stage inlet, which is the point of lowest pressure in the system.

Depending on the impeller tip speed and pressure, droplets as small as 10 μm may be removed. Since the droplets are formed by condensation, the final drop size depends on the pump compression ratio. The higher the ratio, the larger the droplets, and the more water will be removed.

The moisture-removal modification may reduce the effectiveness of pumping, especially with such low-molecular-weight gases as hydrogen. To minimize the loss of pumping pressure, the groove must be as shallow as possible and the exit hole as small as possible consistent with adequate moisture removal. Alternatively, moisture removal could be achieved by using an auxiliary dryer downstream. In deciding which method to use in a given application, the pressure losses for the two methods should be compared.

This work was done by Paul F. Berg of United Technologies Corp. for **Johnson Space Center.** *No further documentation is available.* *MSC-20632*

Centrally-Rupturing Squib-Closure Disks

The rupture-disk design makes squib action more predictable.

NASA's Jet Propulsion Laboratory, Pasadena, California

A proposed squib rupture disk would insure that the squib explosion is directed toward the center of a combustion chamber. This can obviate the use of oversize squib units that can cause undesirably large impluses.

Conventional squibs are fabricated with round, stainless-steel rupture disks, attached to the squib bodies by electron-beam welding (see Figure 1). Each disk has uniform thickness, typically 5 mils (0.13 mm). Because the weakest section in the disk is somewhere in the weld, pressure buildup in the squib invariably causes the disk to fail somewhere along the circumferential weld seam. Consequently, the combustion material is propelled toward the side and hence along the combustion-chamber wall.

It is not possible to predict how large the initial opening will be and what amount of the combustion material will be thrown against the wall of the combustion chamber downstream of the squib. (The maximum pressure developed in the combustion chamber varies randomly from test to test.) In view of this unpredictability, it has become the practice to use oversized squib units.

In the new design (see Figure 2), the center of the rupture disk contains a cruciform indentation in which the thickness is reduced to about 0.5 mil (0.013 mm). This reduces the strength of the center of the rupture disk in the same manner as that of the pull tabs on beverage cans; therefore, the disk will fail predictably in the center.

With this design, the expulsion of combustion material is expected to be uniform and predictable, making it unnecessary to use oversized squib units. Moreover, the flow from the ruptured squib will be directed advantageously toward the center of the combustion chamber.

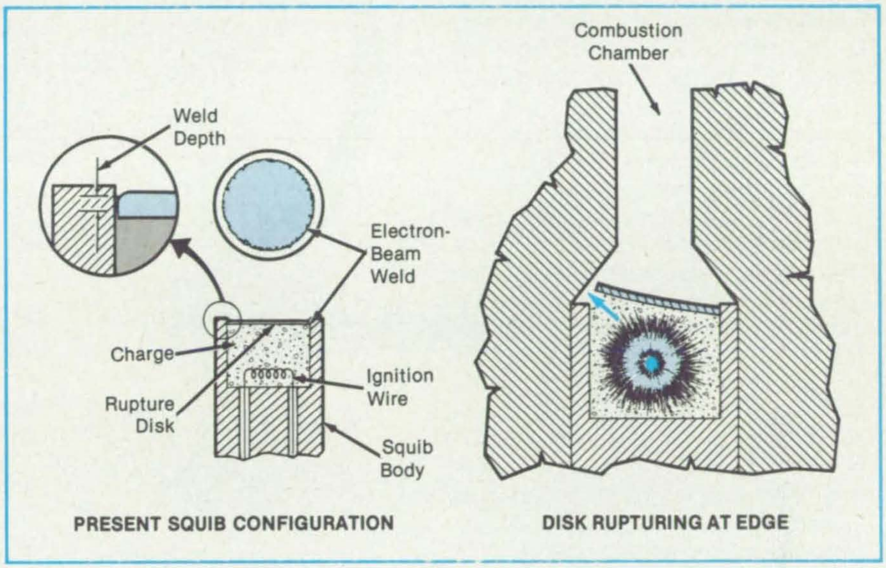

Figure 1. The **Conventional Squib Rupture Disk** fails where it is welded to the squib body, causing an unpredictable flow of combustion products toward the walls of the combustion chamber.

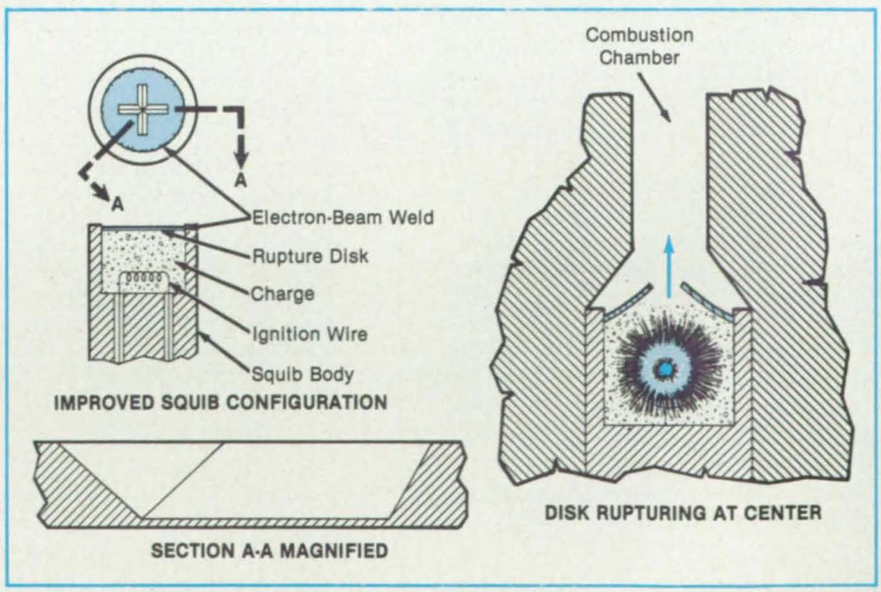

Figure 2. In the **Improved Squib,** failure occurs predictably at the center of the rupture disk, causing a predictable flow of combustion products toward the center of the combustion chamber.

This work was done by Robert Richter of Caltech for **NASA's Jet Propulsion Laboratory.** *For further information, Circle 16 on the TSP Request Card.*
NPO-16707

Retractable Sun Shade

A mechanism unrolls a canopy and rerolls it when shade is no longer needed.

Lyndon B. Johnson Space Center, Houston, Texas

A blanket can be readily unfurled by a mechanism to protect the space it encloses from the Sun. The blanket forms an arched canopy over the space and allows full access to it from below. When shading is not needed, the retracted mechanism stores the blanket compactly. The mechanism was developed for protecting sensitive Space Shuttle payloads from direct sunlight while the cargo-bay doors are open. It can be adapted to the shading of greenhouses, swimming pools, and boats.

To unfurl the blanket, rollers drive cables at the end of a cylindrical frame (see figure). As the frame rotates to the right, it draws the blanket from a spring roller in the manner of a common window shade. The driving cables hold the blanket against the circular members at the ends of the frame. Thus, as the blanket unfurls it assumes the cylindrical shape of the frame. When the roller motion is reversed, the cables rotate the cylindrical frame back to its storage position. At the same time, the blanket is drawn by its return spring back into the spring roller.

The drive roller can be powered manually or by an electric motor. It can be stopped at any point, if desired, to provide partial shade instead of full shade. (In the nearly zero gravity of space, the unfurled blanket does not sag on the frame; on Earth, however, additional radial support may be needed.)

This work was done by Arthur Frank, Silvio F. DeRespinis, and John Mockovciak, Jr., of Grumman Aerospace Corp. for **Johnson Space Center.** *For further information, Circle 29 on the TSP Request Card.*

This invention is owned by NASA, and a patent application has been filed. Inquiries concerning nonexclusive or exclusive license for its commercial development should be addressed to the Patent Counsel, Johnson Space Center [see page 29]. Refer to MSC-20162.

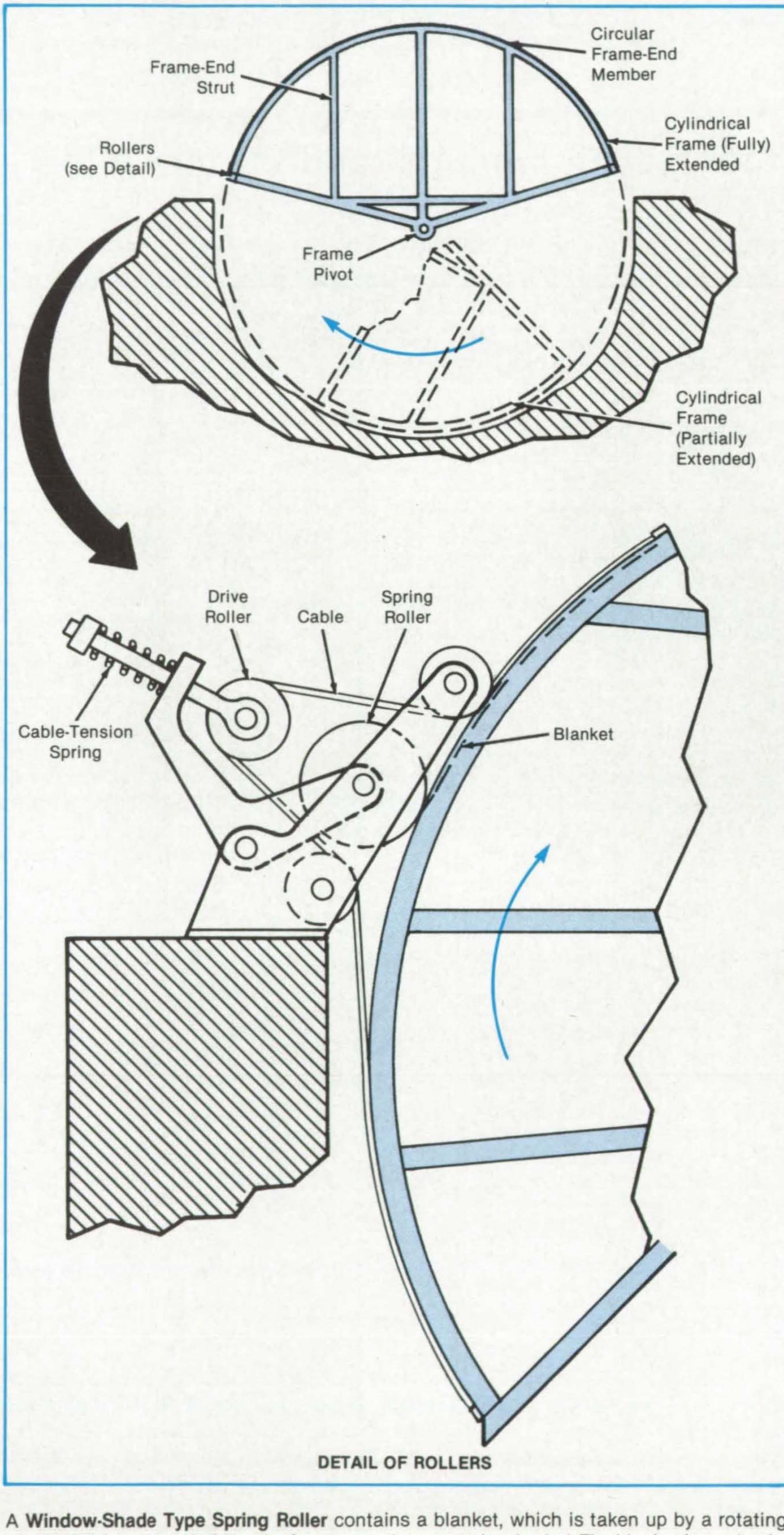

A **Window-Shade Type Spring Roller** contains a blanket, which is taken up by a rotating cylindrical frame and held by the frame over the area to be shaded. The blanket is made of a tough, opaque polyimide material.

Direction-Sensitive Latch

A mechanism eliminates clearance and applies a positive load to a latched member.

Lyndon B. Johnson Space Center, Houston, Texas

A latching mechanism eliminates clearance between itself and a latched member. It is simpler and lighter than previous direction-sensitive latches (also called "vector-sensitive latches"). Like the previous latches, it responds to the direction of forces in determining whether members should be accepted, held in position, or released. However, unlike the previous latches, it eliminates the need for an auxiliary latch to press the mechanism against the latched member for retention. The new mechanism is well suited to operation by automatic control or by a remotely controlled manipulator.

A roller at an apex of the triangular main link of the mechanism contacts a beveled edge on the member to be latched (see figure). With no force applied, the roller and the member remain in this relationship. However, a force applied to the roller in a direction approximately toward the primary member overcomes the frictional force on the latch slider pin, which then slides in a slot in the latch housing. The latch collapses, allowing the secondary member to pass the roller and contact the primary member. The roller then returns to its original position, where it latches the secondary member in place.

There is now a small clearance between the roller and the latched secondary member. The clearance is necesary to allow for dimensional variations in the parts due to manufacturing tolerances and thermal expansion or contraction. However, the clearance must be eliminated after latching so that the latched members are held tightly together. Accordingly, the actuator is designed to exert a force on the yoke, rotating the yoke counterclockwise about the yoke pivot point. This pushes the roller against the secondary member with a force perpendicular to the beveled edge. The clearance is thus taken up, and a retaining force is applied to the latched secondary member.

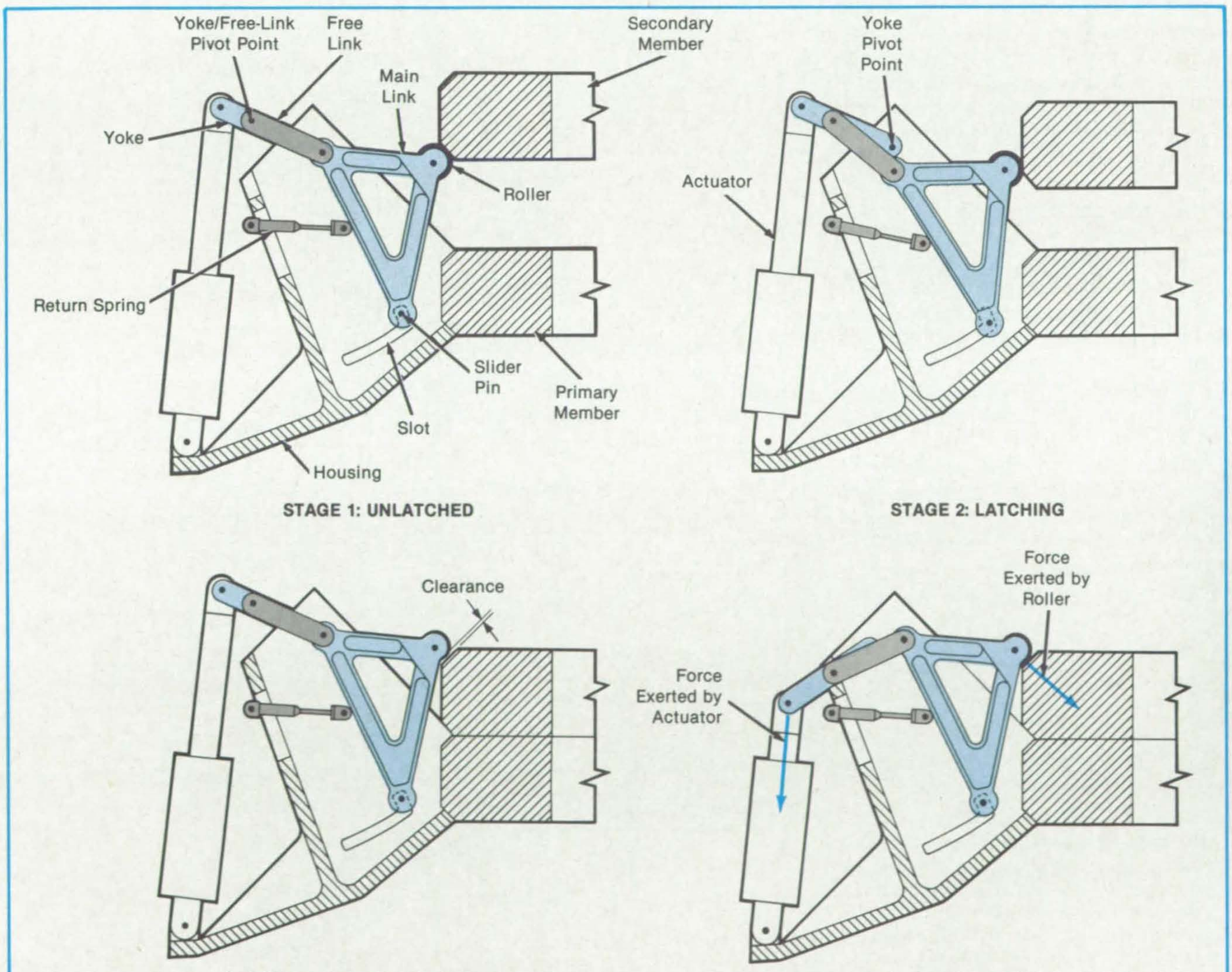

The **Stages of the Latching Process** begin with the application of a downward force to the secondary member, causing it to displace the roller. After the secondary member has passed the roller and joined the primary member, the actuator removes the clearance between the roller and the secondary member.

The secondary member can be unlatched in either of two ways. The actuator can be used to move the yoke and free link to the open-latch position, or the secondary member can be tilted. Beyond a certain tilt angle, the forces are redirected so that the roller no longer retains the secondary member.

Several variations of the latch mechanism are possible. For example, the latch housing can be a separate part, or it can be an integral part of one of the members. The slot that controls the movement of the main link can be machined in the housing or in the main link. The yoke can be moved by a hydraulic actuator or by a spring, gear motor, or other means. The yoke can be replaced by any other part that rotates about the yoke pivot point and causes movement of the free-link connecting point for clearance removal.

This work was done by William R. Acres of **Johnson Space Center.** *For further information, Circle 73 on the TSP Request Card.*

This invention is owned by NASA, and a patent application has been filed. Inquiries concerning nonexclusive or exclusive license for its commercial development should be addressed to the Patent Counsel, Johnson Space Center [see page 29]. Refer to MSC-20910.

Mobile Remote Manipulator

A turret, roll arm, and trolley enhance manipulator dexterity.

Lyndon B. Johnson Space Center, Houston, Texas

A mobile remote manipulator has seven degrees of freedom. Designed for handling, inspecting, and maintaining the modules of a space station, the manipulator can extend the end effector to points on, around, and under the space-station structure. Manipulators having such capabilities may be useful on Earth; for example, as robots in manufacturing, for the erection of large structures, or for performing complicated tasks in hazardous locations.

The manipulator moves on a vehicle that provides one-degree-of-freedom movement (translation) along the structure and two degrees of freedom by a rotating turret top (yaw) and an arm (roll). A jointed manipulator arm attached to the roll-axis arm provides additional degrees of freedom.

This work was done by Stanis Coryell and Roy E. Olsen of Grumman Aerospace Corp. for **Johnson Space Center.** *For further information, Circle 72 on the TSP Request Card.*
MSC-21051

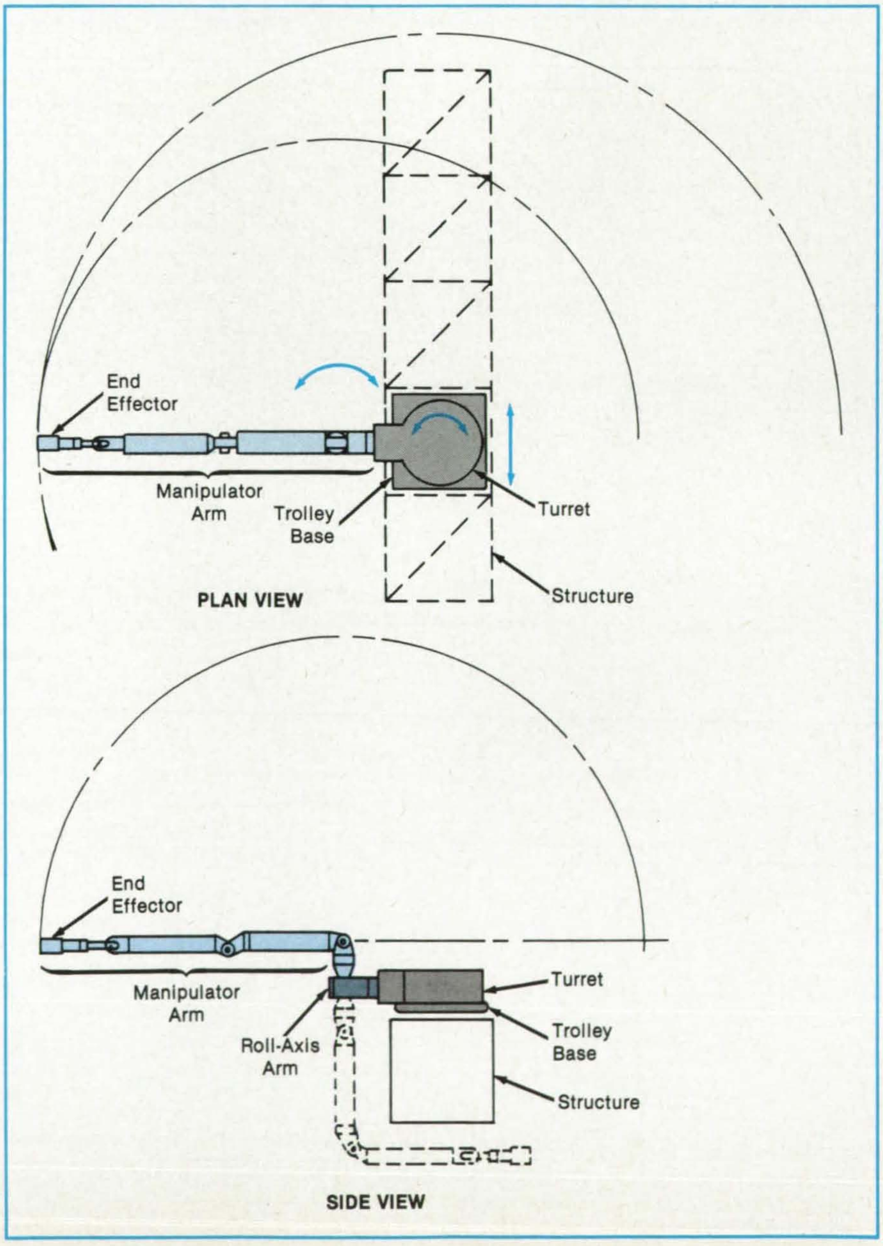

The **Remote Manipulator Moves on a Trolley** base along a structure. The roll-axis arm positions the manipulator arm so that it can extend the end effector under the structure. The yaw-axis rotation gives added reach to the arm above the structure.

Lightweight Motorized Valve

A redesigned actuator assembly weighs 50 percent less than before.

Lyndon B. Johnson Space Center, Houston, Texas

An isolator valve is operated by an ac motor instead of the usual dc solenoid. The valve weighs only 3 lb (1.4 kg) — half the weight of a dc-operated valve. In addition, the new valve functions with either two-phase or three-phase power.

The new valve seals against fluid movement in both the forward and reverse directions. Developed for isolating fluids in the propellant tanks, manifolds, and interconnecting lines of the Space Shuttle reaction control and orbital maneuvering subsystems, the valve is well suited to applications in which leakage must be kept to a minimum at high pressure differences — in petroleum and chemical processing, for example.

The ac motor, gear train, sector gear, and torsion bar operate a finger that opens and closes a ball valve (see figure). The finger extends through a bellows to the ball. The bellows are filled with a material that damps pressure differences across it. The torsion bar ensures that the ball is held open or closed against its stops with a spring force greater than the potential reverse forces of the fluid and, therefore, is not moved substantially by the fluid. Shock absorbers stop the gear train at the designated limits of travel so that the impacts on gears and bearings remain within safe limits. The shock absorbers also prevent the sector gear from bouncing excessively when it reaches its limits of travel.

The ball valve rotates about an axis slightly displaced from its geometrical center. It therefore clears the seals rapidly, causing less seal wear than it would if rotated about the center. The inner seal prevents forward flow, and the outer seal prevents reverse flow. Each seal contains a flat spiral spring that provides a sealing pressure of 200 lb/in.^{2} (1.4 MN/m^2).

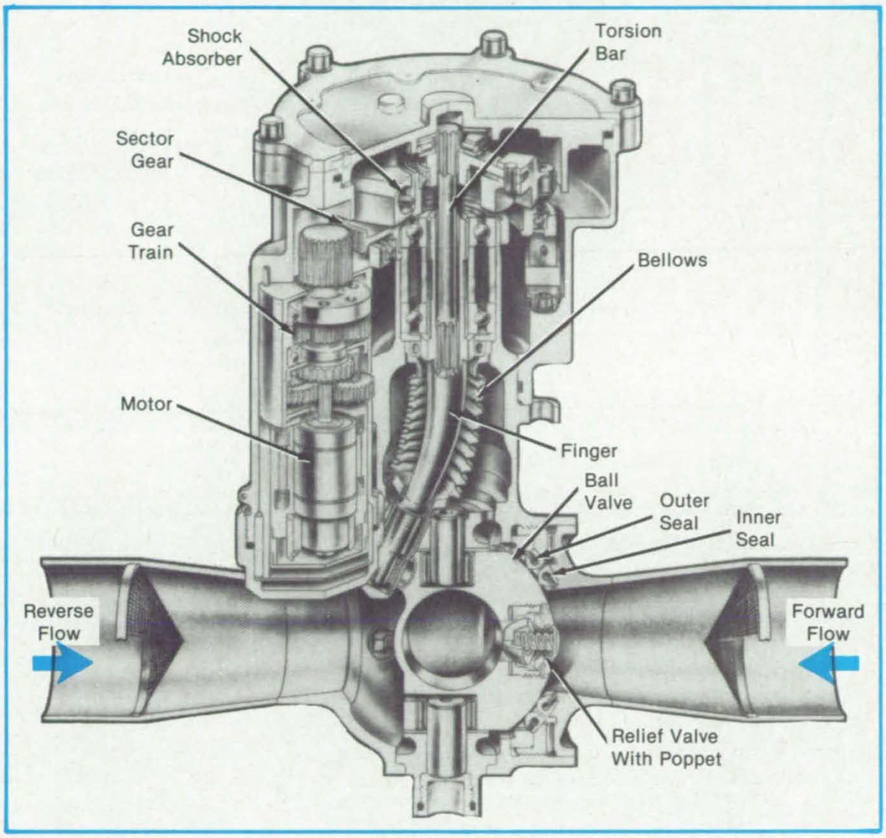

A **Motor Drives a Gear Train**, thereby turning a finger that opens or closes a ball valve. The motor-and-gear actuator assembly can be removed and replaced without removing the ball valve or otherwise invading the unit.

The valve contains a relief valve that automatically releases heat-induced pressure from the outlet to the inlet port. This is a spring-loaded poppet containing a soft spring-loaded seal.

This work was done by Rudy Gonzalez of Rockwell International Corp. and J. M. Vandewalle of Parker-Hannifin Corp. for **Johnson Space Center.** *For further information, Circle 3 on the TSP Request Card. MSC-20848*

Heat Pipes Reduce Engine-Exhaust Emissions

Increased fuel vaporization raises engine efficiency.

Lewis Research Center, Cleveland, Ohio

Heat-pipe technology has increased the efficiency of heat transfer beyond that obtained by metallic conduction. Heat pipes have been used in a variety of ways to move large quantities of heat at high transfer rates. NASA research has examined heat-pipe application in turbine-engine exhaust systems. New techniques have been developed to address three problem areas that generate exhaust emissions in existing gas-turbine engines. These problems are low combustion efficiency at idle (caused by poor fuel vaporization), high NO_x emissions (caused by high-flame-temperature combustion at takeoff condition), and minimal primary-zone combustor life in rich-burn combustion (in ground power applications).

Heat-pipe technology was applied to each of these problem areas with the following results: The low efficiency at idle

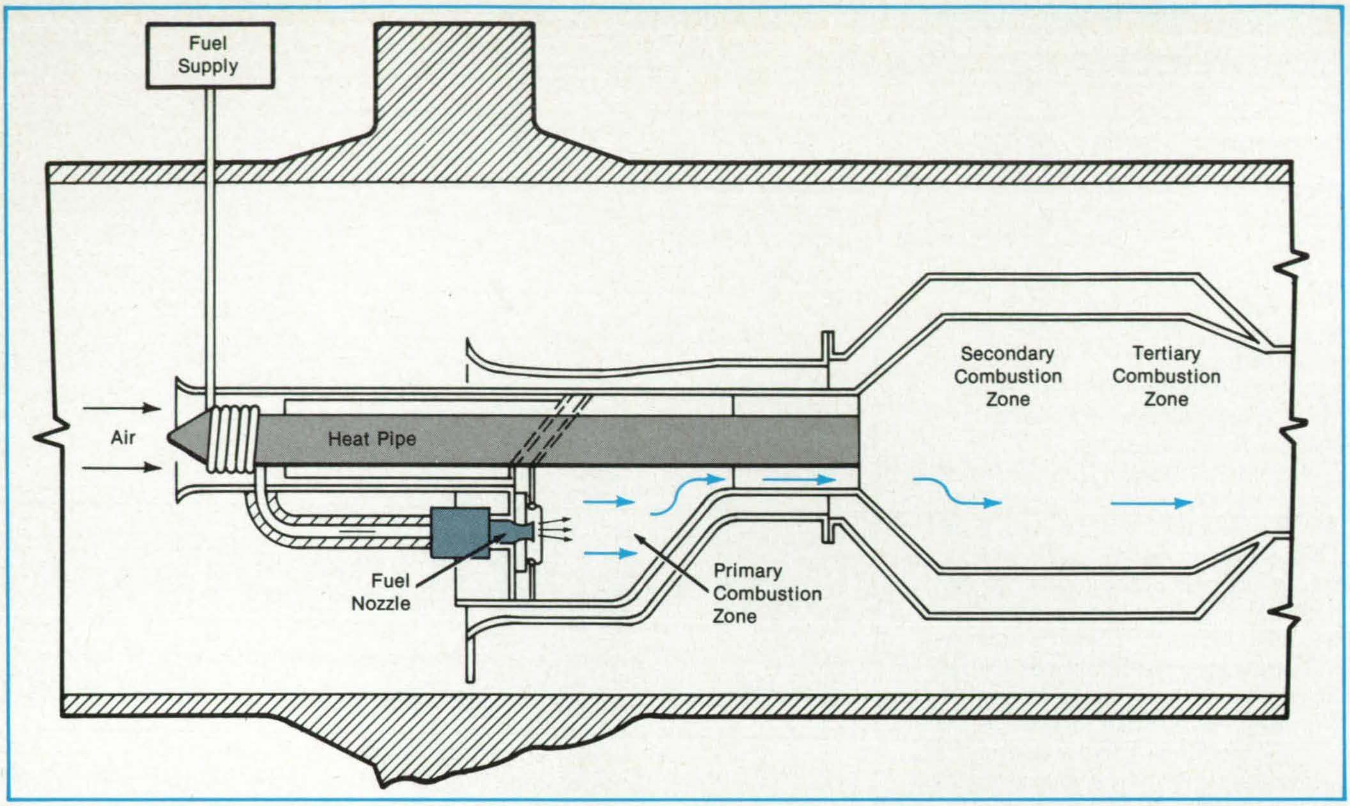

Figure 1. **Heat From the Primary Combustion Zone** of a can-type combustor is transferred by a heat pipe to the fuel and combustion air to increase fuel vaporization.

power was addressed by using heat pipes to warm the combustor inlet air and fuel, thus increasing fuel vaporization. The increased fuel vaporization and resulting combustion increased engine efficiency, thus reducing exhaust emissions of unburned hydrocarbons and carbon monoxide.

Figure 1 shows this technique being applied to the primary zone of a can-type combustor. Note that heat pipe heats only the fuel and primary-zone combustion air. Unheated air is available for cooling the primary-zone walls and the rest of the combustor can. Note also that most primary-zone heat removal occurs at the rear or high-temperature region. This is the same region where NO_x formation is most prevalent at the takeoff-power condition. Therefore NO_x at takeoff is reduced by heat removal in this area.

Figure 2 shows the use of heat pipes to increase liner durability in a fuel-rich primary-zone combustion environment, as is found in the combustion of nitrogenous fuels for the control of NO_x emissions. In this application, heat pipes are used to form the walls of the combustor. The heat pipes in this application have the additional benefit of providing increased fuel vaporization as the fuel again is used as a heat sink. The combustion of No. 4 and No. 6 heating oils can benefit from this increased fuel vaporization.

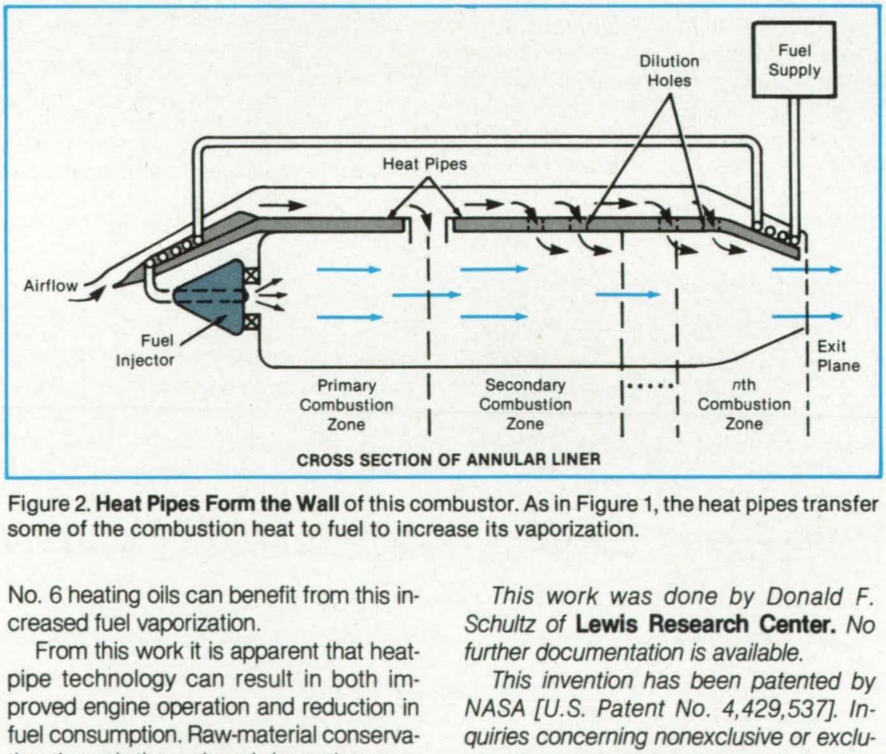

Figure 2. **Heat Pipes Form the Wall** of this combustor. As in Figure 1, the heat pipes transfer some of the combustion heat to fuel to increase its vaporization.

From this work it is apparent that heat-pipe technology can result in both improved engine operation and reduction in fuel consumption. Raw-material conservation through the reduced dependence on strategic materials will also benefit from this type of heat-pipe technology. Future applications will result in improved engine performance and a cleaner environment.

This work was done by Donald F. Schultz of **Lewis Research Center.** *No further documentation is available.*

This invention has been patented by NASA [U.S. Patent No. 4,429,537]. Inquiries concerning nonexclusive or exclusive license for its commercial development should be addressed to the Patent Counsel, Lewis Research Center, [see page 29]. Refer to LEW-12590.

New Alloy for Glass-to-Metal Seals

The coefficient of thermal expansion approximates that of glass more closely.

Lyndon B. Johnson Space Center, Houston, Texas

A new alloy has a coefficient of thermal expansion of only $1.9 \times 10^{-6}(°F)^{-1}$ [$3.4 \times 10^{-6}(°C)^{-1}$]. Because the coefficient is close to that of KG-33 (or equivalent) glass, the alloy can be used in glass-to-metal seals without introducing excessive residual stresses. In addition, the alloy has potential for other applications in which low thermal expansion is important; for example, mechanical measuring devices and precise sliding parts that must function over wide temperature ranges.

The alloy is composed of about 60 percent iron, 40 percent nickel, and traces of six other elements. It was developed as a replacement for Kovar (or equivalent) Fe/Ni/Co alloy in a ferrule-and-tube assembly (see figure). The new alloy has about the same strength, solderability, and compatibility with fuel as does Kovar (or equivalent).

Previously, the ferrule was bonded to a glass preform by soldering and heating the glass until it flowed plastically. After cooling, the assembly had a high residual stress because of the difference in thermal expansion between the metal and the glass. Many assemblies failed because of broken glass during manufacturing, testing, shipping, and even storage.

Changing to the new alloy reduced the residual stress in the glass from 4,500 lb/ in.^{2} (31 MN/m^2) to 1,300 lb/in.^{2} (9 MN/m^2). The new value is well below the allowable maximum of 2,000 lb/in.^{2} (14 MN/m^2). The new alloy forms a hermetic seal with glass at a much lower temperature than does Kovar. Changes in the shapes of the parts reduced the glass stress even further.

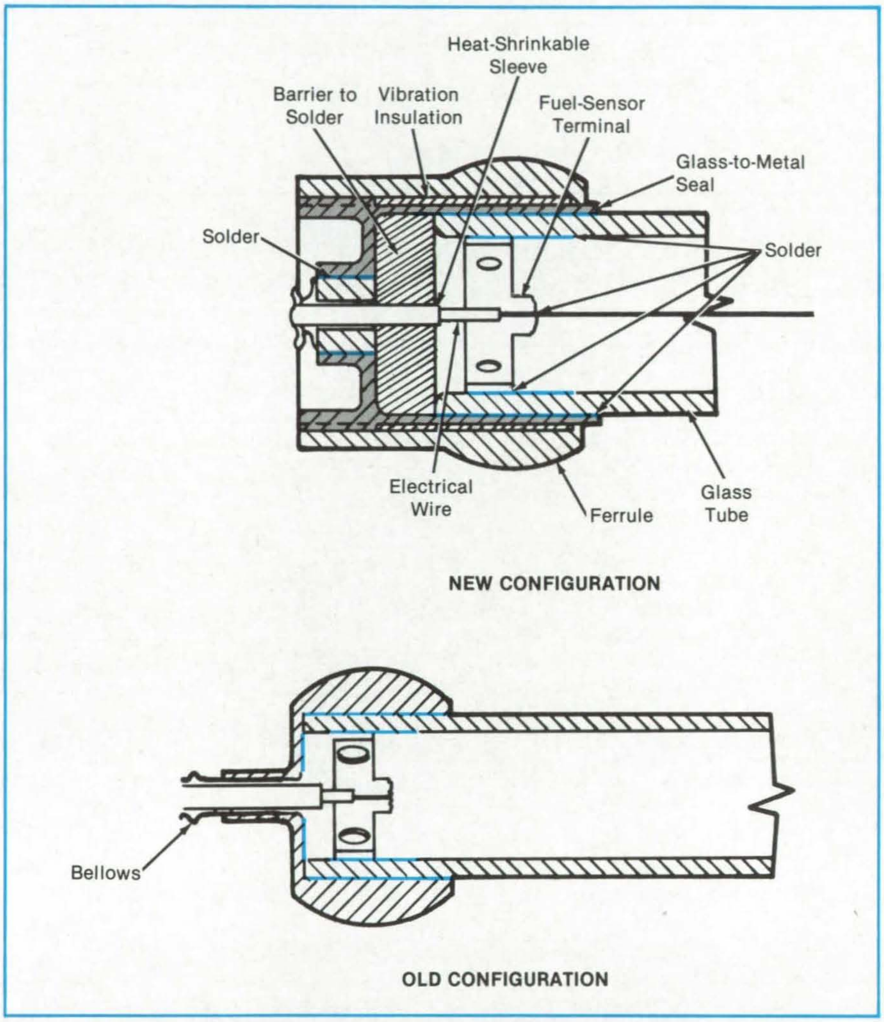

The **Low-Expansion Alloy** is used for the ferrule of a ferrule-to-tube joint in a fuel sensor.

This work was done by Adolph J. Schmuck of McDonnell Douglas Corp. for **Johnson Space Center**. *No further documentation is available. MSC-21023*

Torque-Summing Brushless Motor

Torque channels function cooperatively but are electrically independent for reliability.

Lyndon B. Johnson Space Center, Houston, Texas

A brushless, electronically-commutated dc motor sums the electromagnetic torques on four channels and applies them to a single shaft. The motor can operate with any combination of channels and can continue to function if one or more of the channels should fail electrically. The motor employs a single stator and rotor and so is mechanically simple; however, each of the channels is electrically isolated from the other so that the failure of one does not adversely affect the others.

The motor consists of a samarium/cobalt permanent-magnet rotor and a stator

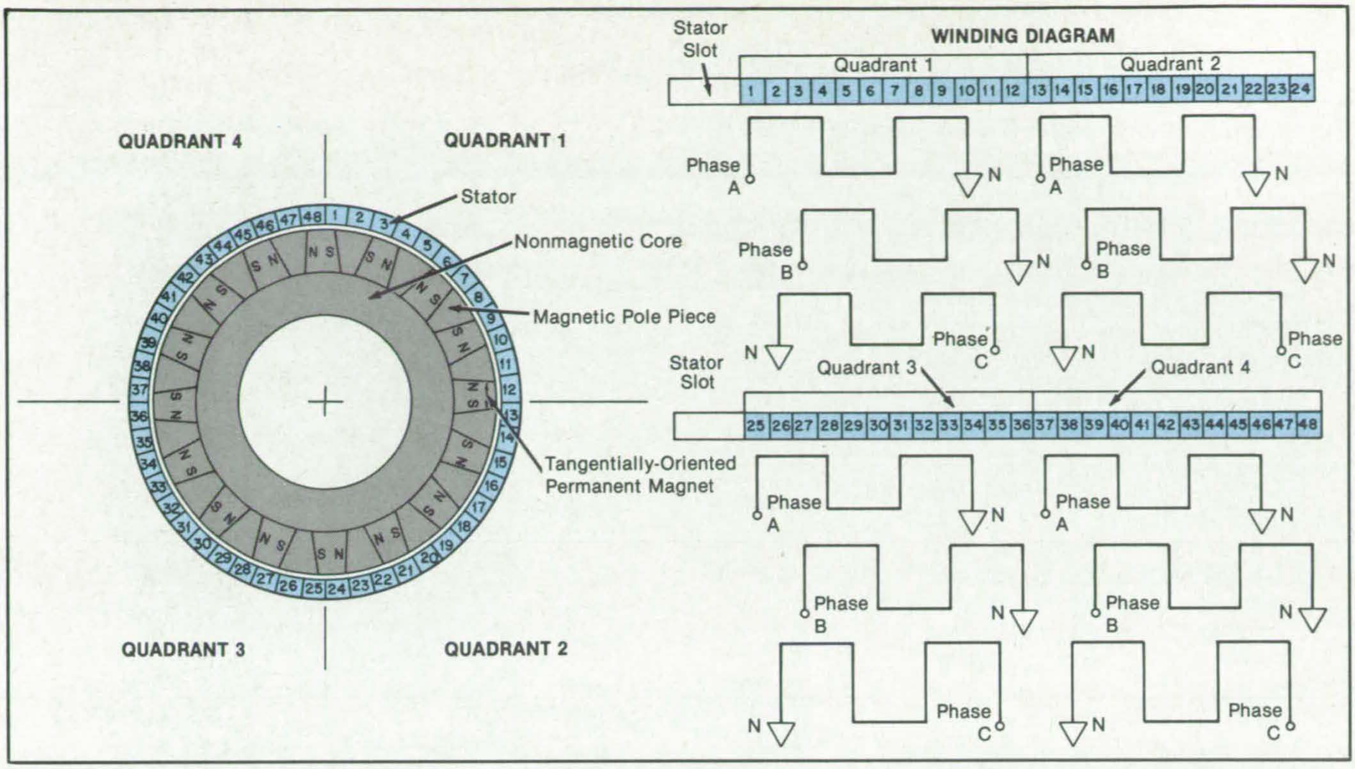

Sets of Windings Occupy Separate Quadrants in a four-channel motor. No two windings share a common slot in the stator. Thus if one winding burns out, it does not harm other windings.

with four sets of windings, each in a separate quadrant electrically isolated from the others (see figure). Each set of windings is wired for three phases. Electrical isolation is achieved by use of consequent-pole, full-pitch windings, in which the number of stator slots is an integral multiple of the total number of poles times the number of phases per quadrant. The total number of poles is four times the number of poles per quadrant. A 16-pole, 48-slot motor was designed, built, and tested to demonstrate the concept.

The four-channel motor offers important advantages over other ways of summing torques on a shaft. Four motors on a common shaft, for example, would be costly, large, and heavy and might be subject to critical-speed problems. A single motor with four parallel windings would not have critical-speed problems and would be lighter, but would not isolate the channels electrically, since the windings would be in the same stator slots.

This work was done by Jayant G. Vaidya of Sundstrand Advanced Technology Group for **Johnson Space Center.** *For further information, Circle 55 on the TSP Request Card.* *MSC-20986*

Cleaning High-Voltage Equipment With Corncob Grit

The high electrical resistance of the particles makes a power shutdown unnecessary.

Lyndon B. Johnson Space Center, Houston, Texas

A new, relatively inexpensive method of cleaning high-voltage electrical equipment makes use of a plentiful agricultural product — corncob grit. The method removes dirt and debris from transformers, circuit breakers, and similar equipment. The method is suitable for utilities, large utility customers, and electrical-maintenance services.

With conventional methods, it is necessary to turn off the power in a substation so that workers can clean high-voltage devices by hand. Meanwhile, the buildings and facilities connected to the substation are without power. The use of the new method, in contrast, makes it possible to proceed with the equipment energized.

The procedure is similar to sandblasting. The corncob grit is fed from a hopper into a 1-in. (2.54-cm) airhose, where air from a compressor forces it through a tapered nozzle onto the surfaces to be cleaned. The abrasive action of the grit quickly removes caked dirt. The high electrical resistance of the grit prevents high-voltage arcing and tracking; a compressor capacity of 600 ft^3/min (0.28 m^3/s) is adequate.

The cost is moderate — about 10 cents per kilovolt-ampere of capacity (1979 prices). For example, it has been estimated that the costs of cleaning a 10^4-kVA power substation are the following:

- $100 for 400 lb (180 kg) of corncob grit;
- $110 for rental of a 600-$ft^3$/min (0.28-$m^3$/s) air compressor; and
- $800 for 32 manhours of labor.

This work was done by C. E. Caveness of Rockwell International Corp. for **Johnson Space Center**. *No further documentation is available.*
MSC-20180

Hydraulic-Leak Detector for Hidden Joints

Slow leakage of fluid is made obvious.

Lyndon B. Johnson Space Center, Houston, Texas

An indicator reveals leaks in hidden fittings on hydraulic lines. It allows fast inspection of joints without disassembly. It can be used in aerospace, petroleum, chemical, nuclear, and other industries where removing covers for inspection is impossible, difficult, or time-consuming.

The indicator consists essentially of a wick wrapped at one end around the joint to be monitored. The wick absorbs hydraulic fluid leaking from the joint and transmits it to the opposite end, which is located outside a cover plate and is therefore visible to an inspector. Leakage is thus manifested as a discoloration of the outside end of the wick.

The wick is Kevlar (or equivalent) aramid sleeving, a material that absorbs and propagates hydraulic fluids. At the end of the wick is a bulb filled with fibrous insulation to make the fluid more evident (see figure). The portion of the wick leading to the bulb is sheathed in heat-shrinkable tubing. The sheathed part is shaped by holding it in position while heat is applied; it retains its new shape when it has cooled. The unsheathed portion of the wick is taped to the joint to be monitored.

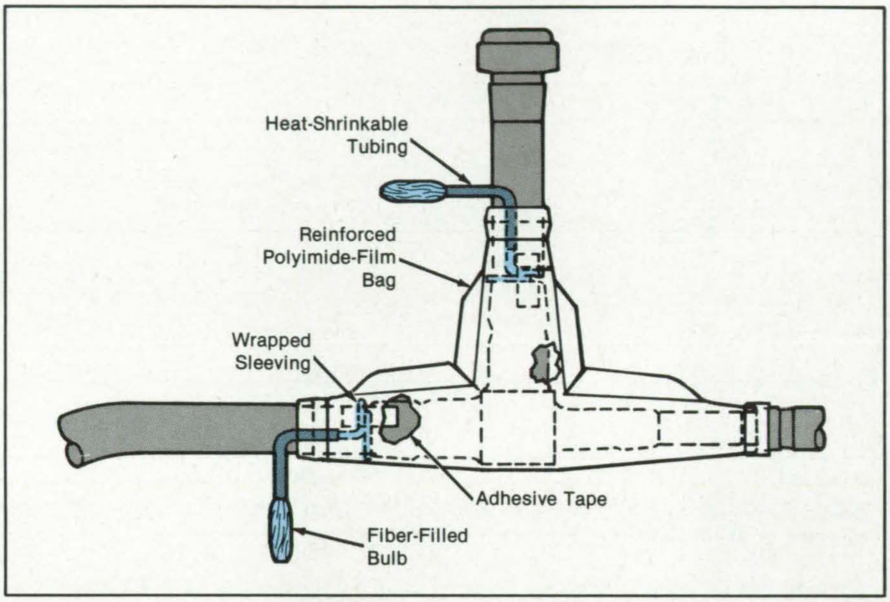

Two Leakage Indicators were wrapped on a fitting for tests in which oil was injected into a polyimide bag surrounding the fitting.

The indicator had been tested to demonstrate its ability to serve as a leak detector and to survive random vibration. It is inexpensive, easily adapted to a variety of fitting shapes, light in weight, and easy to install. On the Space Shuttle, where about 2,000 hydraulic joints must be checked for leakage, it has greatly speeded postflight inspection.

This work was done by George E. Anderson and Shu Loo of Rockwell International Corp. for **Johnson Space Center.** *For further information, Circle 74 on the TSP Request Card.*

This invention is owned by NASA, and a patent application has been filed. Inquiries concerning nonexclusive or exclusive license for its commercial development should be addressed to the Patent Counsel, Johnson Space Center [see page 29]. Refer to MSC-20783.

Measuring Continuous-Path Accuracies of Robots

Sensors yield data on deviation from a predetermined path and speed.

Marshall Space Flight Center, Alabama

The accuracy and repeatability of continuous-path robot motion can be measured with a new test method. Until now, robot performance has been specified on a point-to-point basis. Point-to-point specifications, however, tend to be inadequate in describing such continuous-path operations as welding, sealing, and deburring.

The new method measures accuracy and repeatability at various speeds and loads within ±0.001 in. (25 μm). It determines the ability of a robot to maintain tool orientation. It can be used with almost any type of manipulator arm and with a separate, coordinated part positioner.

The robot end effector is directed to trace the contour of a path plate without contacting it (see figure). The end effector is fitted with a tool containing eddy-current sensors, which determine the separation of the tool or sensors from the path plate.

The robot is programmed to maintain a 0.045-in. (1.14-mm) separation between a sensor and the path plate, and the sensors are calibrated to produce zero output at that separation. A deviation from the programmed displacement appears as a negative or positive voltage at the sensor output terminals. An analog-to-digital converter transforms the sensor outputs (which can vary from −5 to +5 V) to digital form and feeds them to a portable computer for processing and storage.

The sensors are arranged in pairs on two perpendicular plates. They can thus measure the deviation in two perpendicular planes. The tool orientation can be determined from the outputs of the

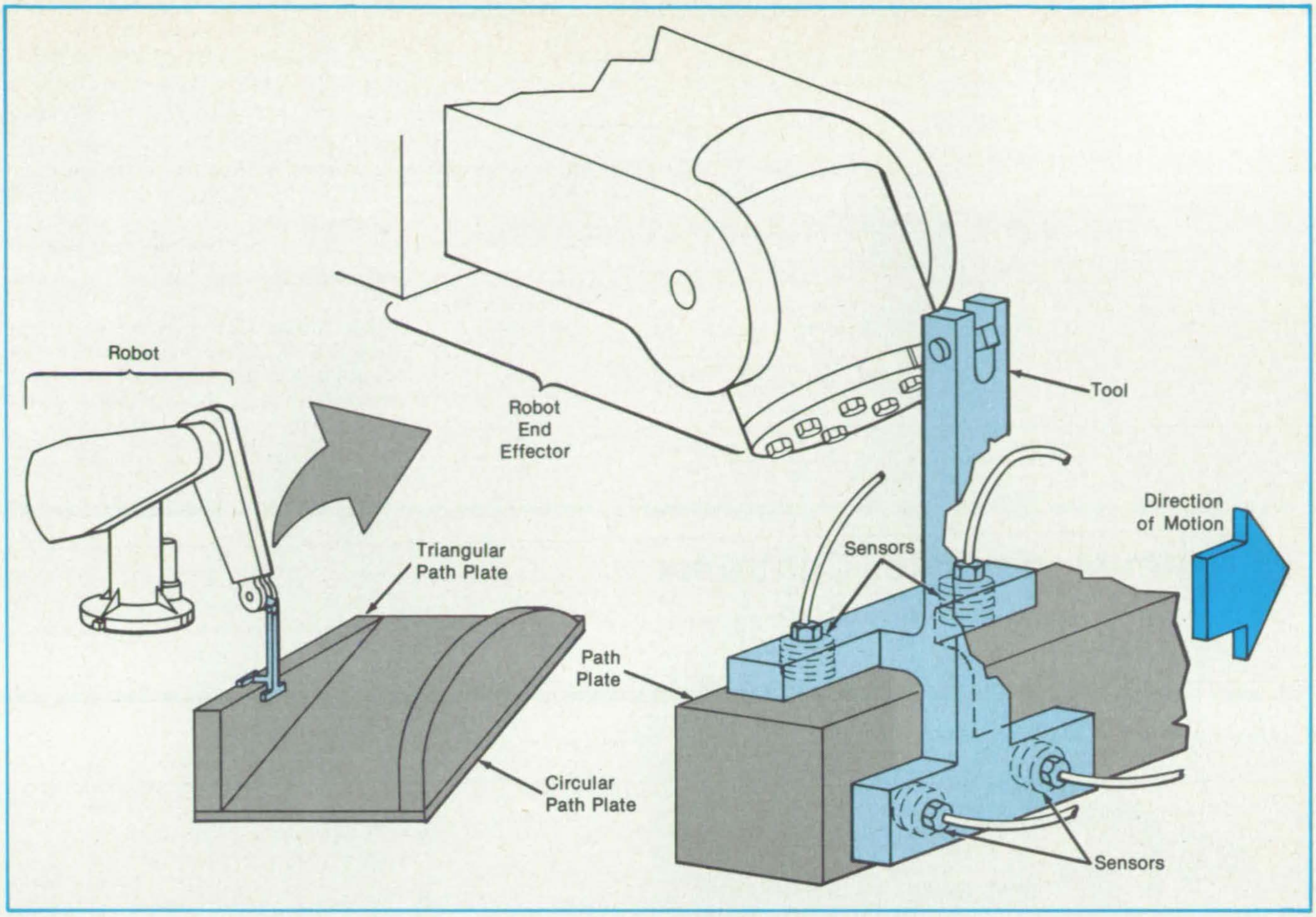

Noncontacting Eddy-Current Sensors measure the distance from a tool to an aluminum path plate as a robot end effector moves the tool at a prescribed distance from the plate. Flat, sloped, curved, and other shapes can be used for the path plate.

two sensors on a given plate; any tendency for the tool to rotate appears as a difference in the two sensor outputs corresponding to the given rotation axis.

Path plates in a variety of shapes can be used. Triangular or circular-segment plates, in addition to the flat horizontal plate in the figure, can test a robot for its response to a variety of contours.

So that the tool speed can be measured, the aluminum path plate contains notches of a different material at precise intervals. The notches produce pulses in sensor output as a sensor passes over them. A deviation in the time between pulses represents a variation in speed.

This work was done by Timothy A. Allison and Gregory A. Arnold of Rockwell International Corp. for **Marshall Space Flight Center**. *For further information, Circle 45 on the TSP Request Card. MFS-29121*

Cleaning of Liquid N_2O_4

This technique is useful in reducing the clogging of fluid lines.

Lyndon B. Johnson Space Center, Houston, Texas

A technique developed for cleaning of liquid N_2O_4 may be adaptable to the cleaning of a variety of industrial fluids, including fuels. Performance studies on the Space Shuttle vernier thrustor showed that the ratio of N_2O_4 oxidizer to fuel decreased during operation because of the deposition of metal (primarily iron) nitrates in the N_2O_4 line. This deposition occurred around the pressure-drop-trim orifice located between the valve outlet and the final injector-tube entrance. The iron nitrates presumably arose from the reaction of N_2O_4 with moisture and with iron from the mild-steel shipping containers. The precipitation of the nitrates apparently was a consequence of the pressure drop—such pressure drops were previously known to be among the factors causing the precipitation of nitrates from propellants saturated or supersaturated with iron.

The process for reducing metal nitrate concentration in liquid N_2O_4 is shown schematically in the figure. After being cooled to less than 40 °F (4 °C) in a heat exchanger, the liquid N_2O_4 is agitated through a hydraulic pump. The resulting precipitated nitrates are then removed by a very fine membrane filter. This process, used in filling the facility storage tank, is repeated several times by the recirculation of the stored N_2O_4 to remove as much of the nitrates as possible.

This system typically lowers the iron content in liquid N_2O_4 from as high as 5.0 parts per million to about 2.0 or fewer parts per million.

This work was done by Gerald R. Pfeifer of The Marquardt Co. for **Johnson Space Center.** *For further information, Circle 97 on the TSP Request Card. MSC-20989*

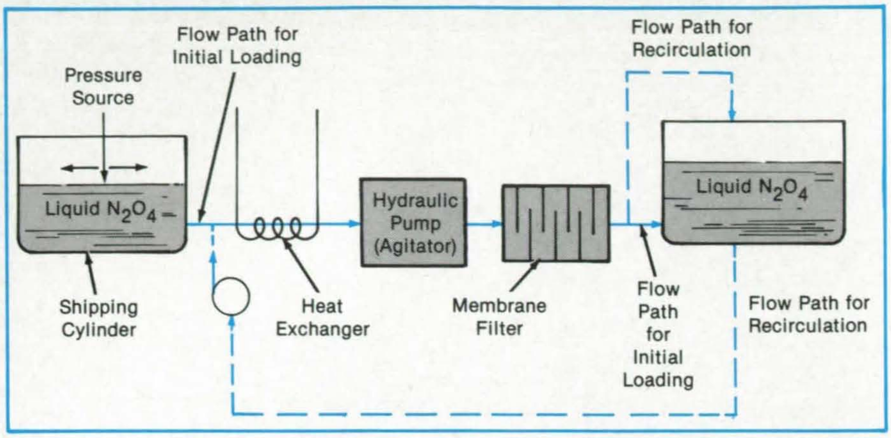

Metal Nitrate Impurities are precipitated from N_2O_4 by cooling the N_2O_4 in a heat exchanger and then passing it through a hydraulic pump. The precipitate is then removed by a fine membrane filter.

Two-Arm-Manipulator Controller

The controller provides 7 degrees of freedom in each arm.

Lyndon B. Johnson Space Center, Houston, Texas

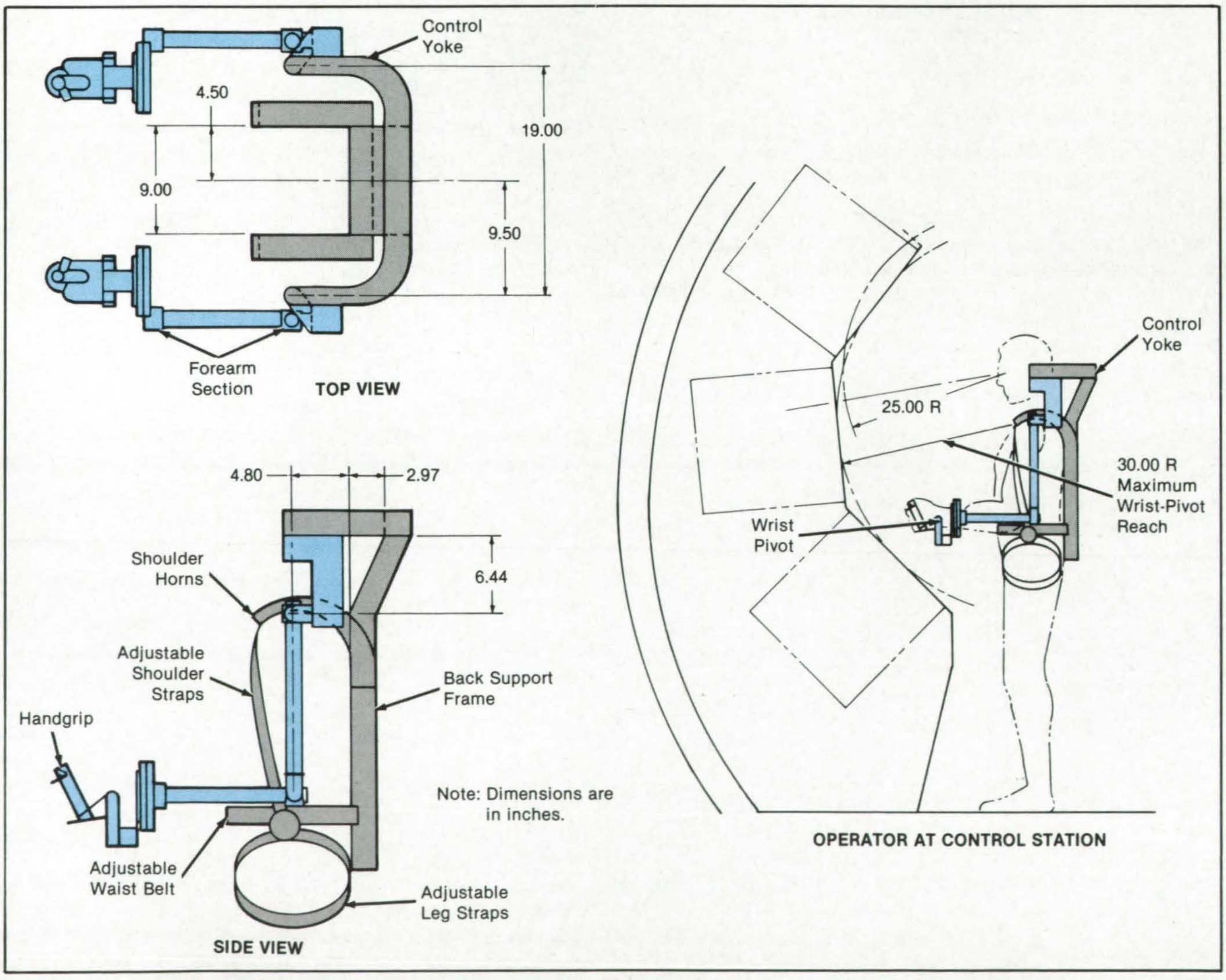

Figure 1. **Two Arm Mechanisms** of the controller are moved by the operator's arms and hands. The remote manipulator, located elsewhere, responds to the operator's arm and hand movements. Adjustable shoulder straps, a waist belt, and leg straps hold the harness securely on the wearer. The mechanisms and harness allow the operator to reach almost normally at a control station.

Master Degrees of Freedom in Angular Degrees

Shoulder	Pitch	+135, −15
	Roll	+90, −30
	Yaw	+50, −20
Elbow	Pitch	±45, −75
Wrist	Pitch	±45
	Roll	±180
	Yaw	±40

Note: Dimensions are in inches.

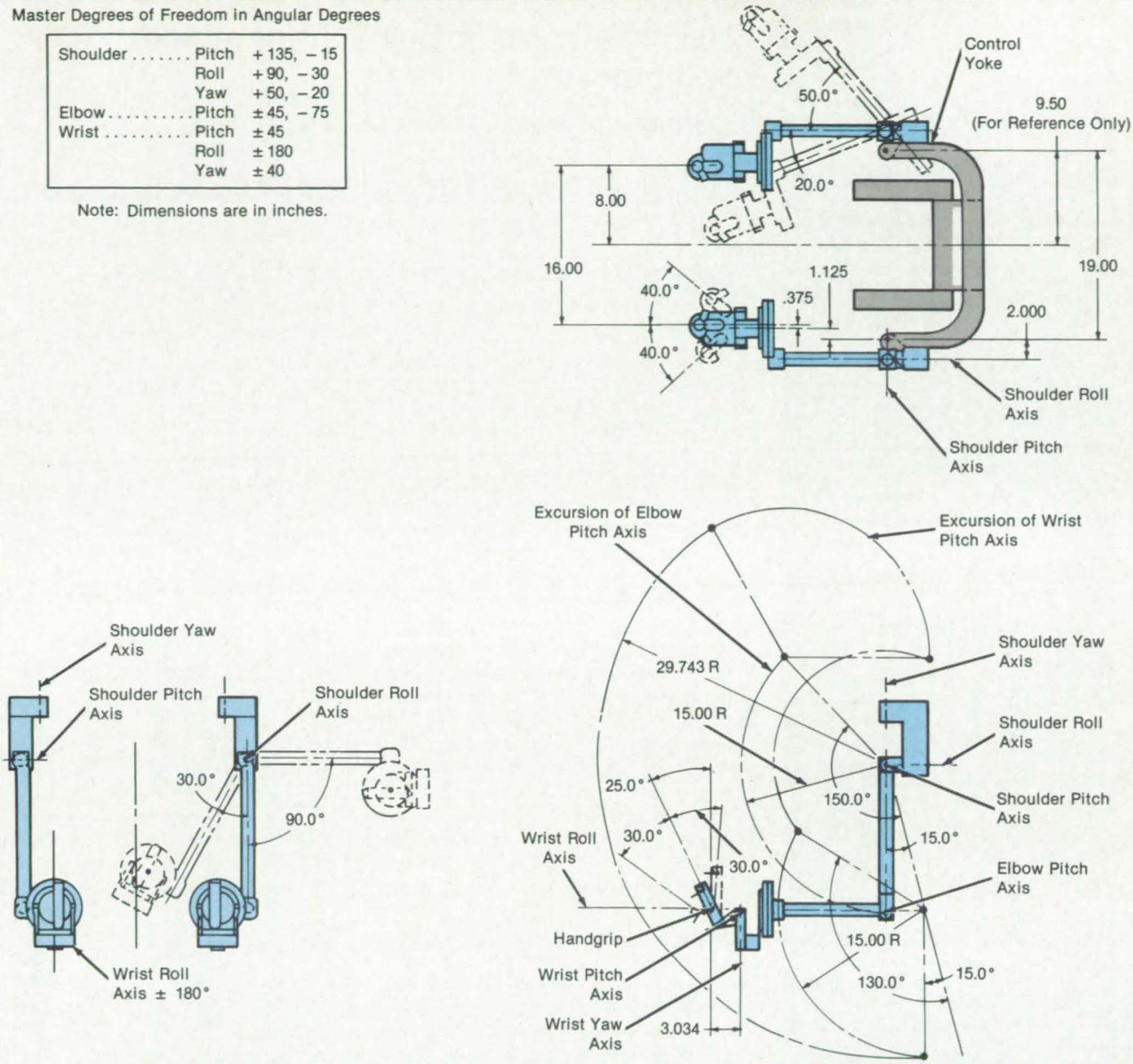

Figure 2. The **Control Motions** have the ranges indicated by the arcs and by the extreme mechanism positions.

A proposed shoulder harness would allow the wearer to control simultaneously and independently two remote manipulator arms and their end effectors. Each manipulator arm would have 7 degrees of freedom.

The harness would support manipulator-arm control mechanisms that are strapped to the operator's arms (see Figures 1 and 2). Each mechanism would include a wrist with 3 degrees of freedom, an elbow with 1 degree of freedom, and a shoulder with 3 degrees of freedom.

The wrist assembly would include a forearm roll ring that fits around the operator's wrist. A handgrip would transmit the operator's hand movements to the end effector. The forearm section may also be strapped to the operator near the elbow. The forearm and upper-arm sections would be adjustable in length to suit individual operators. The harness assembly would consist of a shoulder/neck yoke segment and a lower torso attachment with straps to fix the shoulder points relative to the operator.

This work was done by Stanis Coryell and Roy E. Olsen of Grumman Aerospace Corp. for **Johnson Space Center**. *No further documentation is available.*
MSC-21049

Toxic-Waste Disposal by Combustion in Containers

Chemical wastes would be burned with minimal handling in their storage containers.

NASA's Jet Propulsion Laboratory, Pasadena, California

A proposed technique for disposing of chemical munitions by burning them inside their shells might be applied to the disposal of toxic materials stored in drums. This fast, economical procedure would overcome the heat-transfer limitations of conventional furnace designs by providing direct contact of oxygen-rich combustion gases with the toxic agent. There would be no need to handle the waste material, and the container would also be decontaminated in the process.

When an oxygen-rich oxygen/acetylene torch is inserted into the empty burster well of a chemical-agent shell (see figure), its side jets will cut the thin metal wall of the burster well. As the torch cuts through the metal, the liquid agent is exposed to the hot, excess-oxygen flame, which causes extremely rapid vaporization and combustion of the agent inside the shell.

As the torch moves down, it cuts more off the wall to expose more of the agent to the excess oxygen, thus ensuring complete combustion of the agent. It is envisioned that the reaction will be complete when the temperature of the outside surface of the shell reaches approximately 1,000 °F (540 °C), as indicated by a prepositioned thermocouple.

The side jets that make the initial cut into the burster well also serve as the equivalent of an afterburner, since they present a flame front through which the combustion products must pass before they can leave the shell. A relatively small exhaust scrubber can be used, since oxygen rather than air supports the combustion, resulting in a volume reduction by a factor of approximately 5.

There are many possible variations of the in-shell combustion theme: The vaporization, combustion, or afterburning steps could involve acetylene/air, oxygen/hydrogen, methane/air, plasma, or laser (pyrolysis), while burster-well breaching could involve oxygen/hydrogen or plasma torches, electric discharges, lasers, or mechanical dies.

It is estimated that the agent within a round can be completely burned out in a few minutes. An obvious advantage is that the agent is contained within the munition or other container until the moment of destruction.

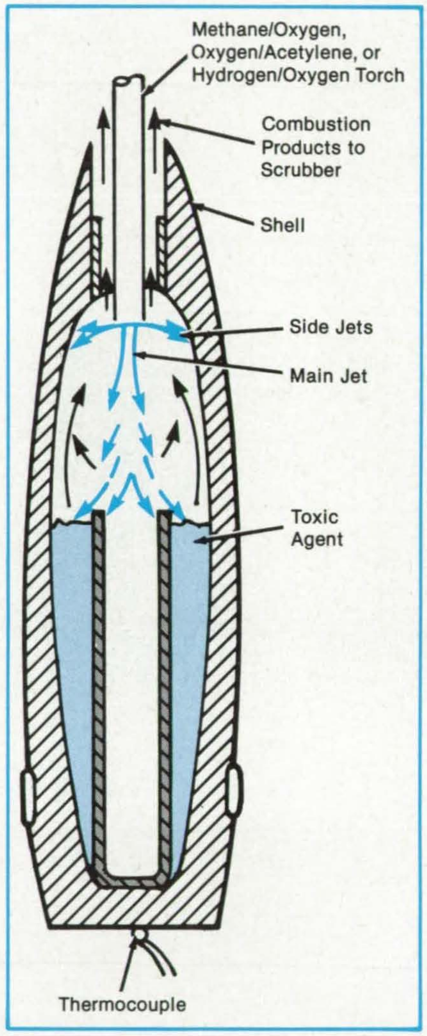

An **Oxygen-Rich Torch Flame** cuts the burster well and then causes the vaporization and combustion of the toxic agent contained in the shell.

This work was done by John Houseman, James B. Stephens, Philip I. Moynihan, Leslie E. Compton, and John J. Kalvinskas of Caltech for **NASA's Jet Propulsion Laboratory.** *For further information, Circle 6 on the TSP Request Card.*

NPO-16710

Toxic-Waste Disposal by Drain-in-Furnace Technique

The compact furnace could be moved from site to site.

NASA's Jet Propulsion Laboratory, Pasadena, California

Toxic industrial wastes could be destroyed using a furnace concept developed for the disposal of toxic munitions. In this procedure, the toxic waste would be drained into the furnace where it would be incinerated immediately.

In the case of chemical munitions, first the burster well would be breached with a perforating mandrel, then temporarily resealed with a low-melting-point wax plug. Then the munition would be inverted in the furnace (see figure), and the gas fires ignited. The hot combustion gases would melt the wax plug, allowing the agent to drain quickly from the munition. The remaining thin liquid film of the agent would be vaporized quickly when the temperature of the shell wall reaches its boiling point.

As the liquid agent flows from the inverted munition onto the lower bed of hot ceramic balls, it would be spread into a thin film of large surface area. Here it would be ignited by hot combustion air and gases rising through the ceramic balls from the natural-gas burner. The resulting flames and hot combustion gases would pass directly upward over the munition, thus causing its own combustion to heat it directly. Eleven percent of the heat of combustion of the 6 lb (2.7 kg) of agent VX in a typical 100-lb (45.4-kg) round would suffice to raise the temperature of the shell to 1,000 °F (538 °C).

Immediately above the main furnace would be an afterburner, which would incorporate hot ceramic balls, possibly coated with a combustion catalyst, to destroy any remaining agent by providing additional residence time at high temperature. Combustion would be continued until the exhaust-gas sampler no longer detects any traces of agent and the shell-wall temperature has reached 1,000 °F (538 °C). The gas flame would then be turned off and the shell transfer fixtures removed from the chamber.

The small combustion chamber would have fireproof doors at its entry and exit side. Between combustions, the munitions set in transfer fixtures would be moved into and out of the chamber by a guideway of powered rollers. Roller guideways are simple and reliable and would not present any sealing problems in the air locks.

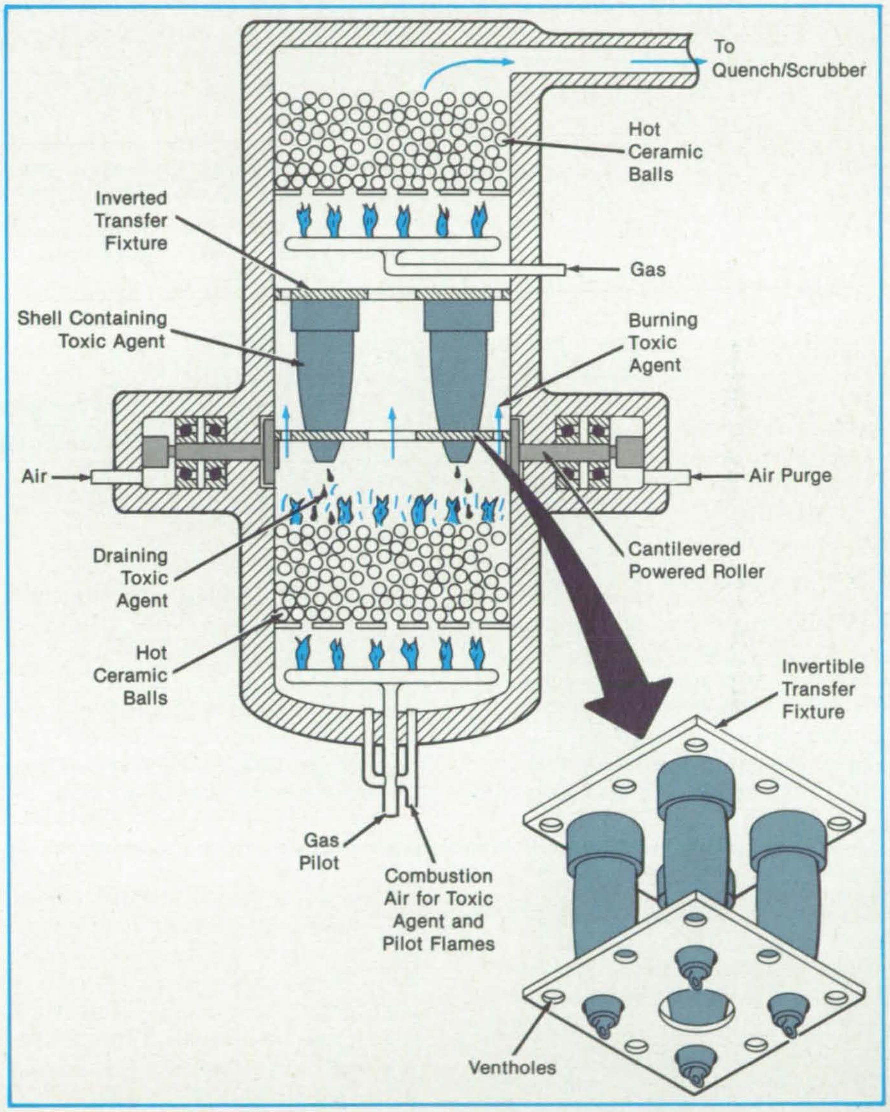

In the **Furnace** the toxic agent is rapidly drained and destroyed in the small combustion chamber between upper and lower layers of hot ceramic balls.

It is estimated that an overall cycle time of 20 min can easily be achieved. A total of ninety 155-mm rounds per batch could be processed in a combustion furnace/afterburner combination 3 ft wide by 8 ft high by 24 ft long (0.9 m wide by 2.4 m high by 7.3 m long). Such a furnace could be mounted on a 10- by 40-ft (3- by 12-m) trailer that could be moved from site to site, as could the deburstering and scrubbing equipment.

This work was done by Leslie E. Compton, James B. Stephens, Philip I. Moynihan, John Houseman, and John J. Kalvinskas of Caltech for **NASA's Jet Propulsion Laboratory.** *For further information, Circle 38 on the TSP Request Card.*

NPO-16579

Nozzle Extension for Safety Air Gun

A conical airstream at the end of the extension protects the operator from blowback.

Langley Research Center, Hampton, Virginia

Safety air guns are used for the removal of chips from machined parts during the machining process to prevent unnecessary heat and wear on cutting tools and to improve the quality of parts. On a numerically controlled machine, an extended nozzle is required on the air gun to remove chips without putting the operator dangerously close to the rotating spindle and cutting tool. Previous modifications to extend the nozzles of the commercially available safety air guns in use at Langley Research Center were considered unsafe because the modifications failed to provide back-pressure relief and a conical airstream to prevent chips from being blown back at the operator.

A new nozzle-extension design overcomes these problems and incorporates the original commercial nozzle, thereby retaining its intrinsic safety features. The components include an extension tube, the length of which can be made to suit the application; the adaptor fitting (which, in place of the safety nozzle, is pinned and sealed into the air gun); and the nozzle adaptor, into which the safety nozzle is repinned to maintain the original safety features. The extension tube is threaded and sealed into the adaptor fitting at one end and into the nozzle adaptor at the other end, as shown in the figure.

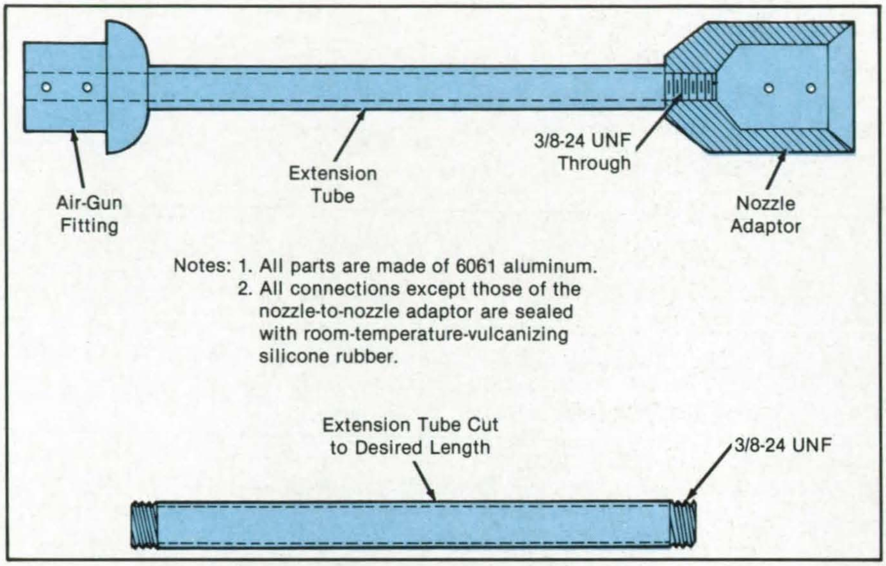

The **Nozzle Extension** helps to blow machine chips away from the operator.

This design moves the conical airstream to the end of the extension to blow machine chips away from the operator. This nozzle-extension modification allows the safe and efficient operation of machine tools while maintaining the integrity of the original safety-air-gun design.

This work was done by Henry N. Zumbrun and Delwin R. Croom, Jr., of **Langley Research Center**. *No further documentation is available.*
LAR-13366

Books and Reports

These reports, studies, and handbooks are available from NASA as Technical Support Packages (TSP's) when a Request Card number is cited; otherwise they are available from the National Technical Information Service.

Coal-Based Fuel-Cell Powerplants

Alternative plant designs are evaluated.

A report assesses advanced technology design alternatives for integrated coal-gasifier/fuel-cell powerplants. Various gasifier, cleanup, and fuel-cell options are evaluated, in part by assessment of the technical assumptions used in the design studies and the status of development of proposed technology alternatives. The evaluation includes adjustments to the assumed performances and costs of proposed technologies where required. The analysis identifies uncertainties remaining in the designs and the most promising alternatives and the research and development required to develop these technologies.

The bulk of the report is a summary and detailed analysis of six major conceptual designs and variations of each. All designs are for a plant that uses Illinois No. 6 coal and produces 675 MW of net power. These plant designs are compared to a reference design that includes an oxygen-blown gasifier, a solvent process for gas cleanup, and a molten-carbonate fuel cell. Power is produced in the expansion turbines, the fuel-cell modules, and a conventional steam cycle. The system efficiency of this design is 48.7 percent.

Of the alternative plant designs, two apparently would generate the electricity cheaper than the reference design would provide. When the entrained-bed gasifier and the low-temperature gas-cleanup system of the reference are replaced by a fluidized-bed gasifier and a hot gas-cleanup system, respectively, the unit cost of electricity is reduced by 4 percent.

The most promising design includes a fluidized-bed gasifier, zinc/ferrite high-temperature gas cleanup, and a pressurized solid-oxide fuel cell. Coal is fed with air and steam to the gasifier. The gasifier effluent is cooled to generate steam, then sent to the gas-cleanup unit. The clean gas is expanded and fed to the fuel cell along with preheated and compressed air.

The fuel-cell exhaust gases are combined in an afterburner that preheats the incoming air. A turbocompressor compresses the fuel-cell and gasifier air and generates power. Turbine exhaust is cooled in steam generators and an economizer before being released to the atmosphere. The steam is used in the steam cycle to produce power.

A plant built according to this design would produce electricity at a unit cost of 91 percent of that of the reference system. A unique feature of this design is the choice of low fuel use in the fuel cell and the ability to use gas turbines at high inlet temperatures.

This work was done by Joseph F. Ferral, Alfred W. Pappano, and Charles N. Jennings of Caltech for **NASA's Jet Propulsion Laboratory.** *To obtain a copy of the report, "Assessment of Technology Alternatives for Coal-Based Fuel Cell Power Plants," Circle 24 on the TSP Request Card.*
NPO-16543

Lifetimes and Reliabilities of Bevel-Gear Drive Trains

Statistical methods are used to predict system lifetimes from component lifetimes.

A NASA-Lewis report presents a life and reliability model for bevel-gear drive trains. Bevel-gear and support-bearing lives are analyzed for each gear and bearing in the drive train, with the results statistically combined to produce a system life for the entire drive train. A numerical example is included.

Experimental testing programs are normally used by industry to evaluate different gearbox designs. These programs include real-time duty-cycle simulation and overload tests. These tests provide an important proof test for proposed designs but are extremely costly in terms of time and resources. Analytical life models are needed in order that only optimal designs are actually tested.

A life and reliability model is presented for bevel-gear drive trains, based on the pitting-fatigue life of the components of the system. The components include the driving and driven bevel gears and the support bearings. The drive train may have a single input gear or dual input gears of equal size. The gears may be straddle mounted or supported in a bearing quill. The loading on the gear train is specified by the use of a mission spectrum consisting of loads and time-at-loads.

The bearing fatigue life is determined using the classical Lundberg-Palmgren theory. The Lundberg-Palmgren theory has been adapted to predict the bevel-gear life. Both the bearing and gear lives follow the Weibull failure distribution. The report shows how to use this information to determine the system life of the drive train, using the methods of probability and statistics. The basic dynamic capacity, defined as the output torque that may be applied for one million output rotations with a 90-percent probability of survival, is also developed.

A numerical example is included in the report. The life distributions for the components are plotted. The system life is plotted on Weibull coordinates and also plotted against the load.

This work was done by D. G. Lewicki and J. J. Cox of **Lewis Research Center** *and M. Savage and C. K. Brikmanis of the University of Akron. Further information may be found in NASA TM-87006 [N85-27227/NSP], "Life and Reliability Modeling of Bevel Gear Reductions."*

Copies may be purchased [prepayment required] from National Technical Information Service, Springfield, Virginia 22161, Telephone No. (703) 487-4650. Rush orders may be placed for an extra fee by calling (800) 336-4700.
LEW-14372

Interchangeable Tools for Remote Manipulators

Remote manipulators could handle a variety of maintenance and assembly jobs.

A report presents concepts and specifications for a set of interchangeable end-effector tools. The tools would be used on a remotely operated manipulator to work on satellites in orbit. Such tools, for example, would make urgent repairs, do routine maintenance, transfer fluids, construct and assemble satellites, and deploy and retract appendages. With modifications, the tool concepts and the systematic approach to tool design should be applicable to such terrestrial uses as industrial robots, manually operated tools, and safety equipment.

The tool set covered in the report includes the following:

- Rotary power tools with attachments,
- A fluid-connector mating and demating tool,
- An explosive-shearing tool,
- An electrical-connector mating and demating tool,
- A general-purpose grappler,
- A power spreader,
- An unpowered pry bar,
- A hole-punching and riveting tool, and
- Special grips and jaws.

The report examines the in-orbit maintenance needs of satellites planned for launching from the mid-1986 through the year 2000. It reviews criteria for selecting members of a set of tools to meet these needs. It describes the tools and tabulates the various operations that each can perform. It presents dimensions and performance specifications for each and explains how each would be operated and controlled. Finally, the report discusses a concept for a tool-storage system that would hold the tools securely when they are not used but kept accessible to the manipulator. Drawings attached to the report illustrate the general shapes and sizes of some of the conceptual tools.

This work was done by Joseph C. Cody of SRS Technologies for **Marshall Space Flight Center**. *To obtain a copy of the report, "Interchangeable End Effector Tools Utilized on the PFMA — Task 1 Final Report," Circle 76 on the TSP Request Card.*

Inquiries concerning commercial use of this invention should be addressed to the Patent Counsel, Marshall Space Flight Center [see page 29]. *Refer to MFS-27125.*

Solar Thermal Rocket Propulsion

Heating a propellant with concentrated Sunlight is considered.

A paper analyzes the potential of solar thermal rockets as a means of propulsion for planetary spacecraft. A solar thermal rocket uses concentrated Sunlight to heat a working fluid, which is expelled through a nozzle to produce thrust.

This paper presents an analysis of solar thermal rocket mission performance on the basis of transfer characteristics, which describe any one of a number of solar thermal thruster concepts. It considers the thermal control of the liquid hydrogen propellant (chosen because it enables the maximum specific impulse), the propellant-feeding system, and the system mass. The report compares the performance of solar thermal rocket propulsion with electric propulsion based on arc-jet or ion engines for the completion of missions to Saturn and Uranus.

The paper finds that solar thermal propulsion can be useful in future missions of planetary exploration. The performance of solar thermal rocket propulsion can be comparable to that of electric propulsion when used with the Space Shuttle and a Centaur G′ upper stage for injecting payloads into transfer trajectories. Both electric and solar thermal propulsion would shorten the travel time to Saturn and Uranus considerably below that for chemical propulsion.

The paper describes a solar thermal propulsion concept based on solar collectors that rotate to orient themselves toward the Sun to enable the generation of thrust in any direction. A planetary spacecraft would be launched from the Space Shuttle with the Centaur and solar thermal stages. The Centaur would provide the initial acceleration and then would separate. The solar thermal stage would then deploy and operate for about a month to place the spacecraft in its final trajectory.

This work was done by Joel C. Sercel of Caltech for **NASA's Jet Propulsion Laboratory**. *To obtain a copy of the report, "Solar Thermal Propulsion for Planetary Spacecraft," Circle 110 on the TSP Request Card.*
NPO-16654

Studies of Pilot-Induced Oscillation

The Total In-Flight Simulator permits reliable evaluation of landing characteristics of aircraft with PIO.

Four types of flight simulators were used to study a pilot-induced oscillation (PIO) that had been observed during one approach and landing test of the Space Shuttle. In addition to describing the test results, a report discusses the simulation requirements for investigating PIO characteristics and includes an evaluation of the relative merits of the simulators. These observations should be of interest to those studying landing characteristics of other aircraft and to those designing pilot-training programs.

The general conclusion is that in-flight simulation is the only reliable method of evaluating the landing characteristics of aircraft with PIO tendencies; even then, some form of artificial task needs to be introduced to produce a pilot workload similar to that encountered in an actual landing. However, the report also describes a simpler fixed-base simulation of a tracking task that correlates well with the landing task and which can be used in the development of control systems.

The Space Shuttle was simulated with a fixed-base ground simulator, two moving-base ground simulators, and an in-flight simulator. The moving-base facilities were the Flight Simulator for Advanced Aircraft and the Vertical Motion Simulator, both at Ames Research Center. The in-flight simulation was performed on the Total In-Flight Simulator. Additional studies on the effect of time delay were performed on the F-8 digital fly-by-wire airplane at Ames.

The report includes diagrams of the rating scales used by the pilots to describe handling characteristics in general. The distribution of pilot ratings under various tests conditions is shown in a series of 18 bar graphs. For the F-8 studies, two graphs show the pilot ratings as a function of time delay over the range of 125 to 300 ms for landings with high- or low-workload tasks and for a tracking task (simulated tracking for in-flight refueling). The tracking test results fall between the lines for the high- and low-workload tasks.

The closed-loop response characteristics in the tracking task are a function of the pilot gain and lead compensation and of the distance from the tracking aircraft to the target. By adjusting the distance variable and the time available for accomplishing the task in the fixed-base simulation, the closed loop PIO frequencies seen on the simulator could be matched to those observed in the Shuttle landing tests. This provides a convenient way to reproduce PIO conditions and makes it possible to evaluate control-system changes with a relatively simple simulation. It should be noted, however, that this technique is useful mainly for evaluating PIO characteristics that have already been observed in flight, inasmuch as the actual oscillation frequencies are required for the simulation. The report includes seven references to previous work in the field.

This work was done by Bruce G. Powers of **Ames Research Center**. *Further information may be found NASA TM-86034 [N84-20566/NSP], "Space Shuttle Pilot-Induced-Oscillation Research Testing."*

Copies may be purchased [prepayment required] from the National Technical Information Service, Springfield, Virginia 22161, Telephone No. (703) 487-4650. Rush orders may be placed for an extra fee by calling (800) 336-4700.

Inquiries concerning rights for the commercial use of this invention should be addressed to the Patent Counsel, Ames Research Center [see page 29]. Refer to ARC-11601.

Properties of Combustion Gases

New reports include graphs to facilitate the use of combustion data.

Computations have been made to determine the equilibrium properties of the gaseous products resulting from the combustion of ASTM Jet A fuel and dry air and natural-gas fuel and dry air. During combustion reseach, it is important that the properties of combustion gases be readily available and in a form that is convenient and useful to the designer and researcher.

In the past, the combustion-gas properties of gas-turbine fuels, as well as of a variety of other hydrocarbon fuels, have been computed and reported. These reports have been used extensively at NASA and throughout industry. The computational schemes that have been developed over the years by Huff, Gordon, Zeleznik, and McBride form the basis for these reports and have been used to compute combustion-gas properties for a wide spectrum of fuel and oxidant combinations. Often, however, the tables and charts have not been prepared for specific fuels. The data, for example, are in a tabular form for hydrogen/carbon ratios of 1.7, 2.0, and 2.1 for a range of assigned pressures, temperatures, and fuel/air mixtures.

In a new series of reports, the computed data also include combustion thermodynamic properties for a range of inlet-air temperatures, but these data are plotted to facilitate their use. The resulting figures have proved to be extremely useful in combustion research, and copies of such figures have been prepared for a wide variety of fuels. A new series of figures and tables, which extend the applicable range of the parameters, has been published. The first report of this series lists data from the combustion of ASTM Jet A fuel and dry air.

The second report presents tables and figures for the combustion-gas properties of natural-gas fuel and dry air for pressures from 0.5 to 50 atm (5×10^4 to 5×10^7 Pa), inlet-air temperatures from 250 to 1150 K, and equivalence ratios from 0 to 2. A complete set of tables and figures is provided on four microfiche films supplied with the report.

This work was done by Jerrold D. Wear, Robert E. Jones, Arthur M. Trout, and Bonnie J. McBride of **Lewis Research Center**. *Further information may be found in:*

NASA TP-2359 [N85-10064/NSP], "Combustion Gas Properties I -ASTM Jet A Fuel and Dry Air" and NASA TP-2435 [N85-21168/NSP], "Combustion Gas Properties II -Natural Gas Fuel and Dry Air."

Copies may be purchased [prepayment required] from the National Technical Information Service, Springfield, Virginia 22161, Telephone No. (703) 487-4650. Rush orders may be placed for an extra fee by calling (800) 336-4700.
LEW-14275

THE FIRST NAME IN DIGITAL SCOPES

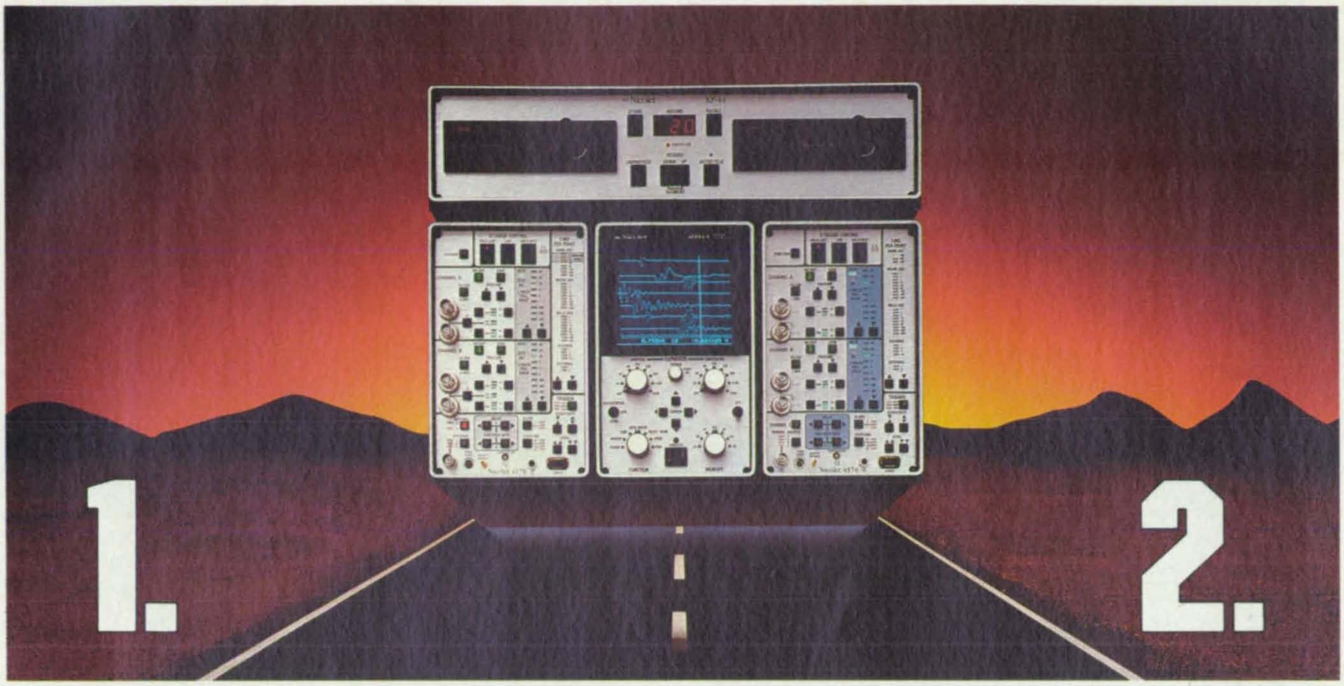

TWO DIGITAL SCOPES IN ONE.

The Acquisition.

With sweep speeds from days to nanoseconds and resolution up to 15 bits, the 4094 digital 'scope can capture the most elusive signals. Every plug-in has 16K of memory, viewable trigger set-up and independent pre- or post-trigger delay on each channel. Signal averaging is standard and our latest 10 MHz/12-bit plug-in even offers real time manipulation of the incoming signals. With two plug-ins the 4094 can record four channels simultaneously. Or even monitor two slow signals and capture high speed glitches at the same time. All under computer control or via manual operation: whatever your application demands.

The Analysis.

Expand and examine any waveform feature in detail. Use the dual cursors and numerics to measure the time or voltage of any point. Compare live or stored waveforms with each other or with pre-recorded references. Store signals on disk manually or automatically. Use pushbutton programs to manipulate the data or send it to your computer via GPIB or RS232 interface. Complete your report with a hardcopy plot using the XY/YT recorder or digital plotter outputs.

First Time, Everytime.

Don't miss important data because of set-up errors. From the World's first in 1973 to the latest models, Nicolet 'scopes are easy to use. Find out how they can be the quickest solution to your signal problems. For more information call 608/273-5008, or write Nicolet Test Instruments Division, P.O. Box 4288, 5225 Verona Road, Madison, WI 53711-0288.

Nicolet

Circle Reader Action No. 438

Fabrication Technology

Hardware, Techniques, and Processes

Books & Reports

Computer Programs

Telescoping Space-Station Modules

The "module-within-a-module" design doubles usable space.

Langley Research Center, Hampton, Virginia

Current plans regarding the construction of a permanently-manned orbiting space station include the use of the Space Shuttle to deliver modules to orbit. These modules will provide living quarters for the space-station crews and will house experimental and fabrication equipment. To minimize transportation requirements, the space-station capability delivered per Shuttle launch must be maximized.

A new telescoping-space-station design for achieving this goal involves essentially a module within a module. After being carried to orbit within the payload bay of the Space Shuttle orbiter, the outer module would be telescopically deployed to achieve nearly twice as much usable space-station volume per Space Shuttle launch as would be otherwise achieved. Also, by retracting the outer module over the inner module, significantly enhanced protection against space debris and radiation could be achieved.

The basic module-within-a-module assemblage is shown in Figure 1. Two such assemblages could fit easily within the Space Shuttle orbiter payload bay with additional volume and payload to spare. There are two options regarding module pressurization. One is to vent the entire assemblage from ground to orbit and then pressurize in orbit. The other is to pressurize the inner module to 30 psia (200 kN/m^2) prior to launch and, through expansion of the assemblage at the station and equalization of the compartment pressures, provide the standard 14.7 psia (100 kN/m^2) initial atmosphere.

Closed-loop or "race-track" space-station configurations (see Figure 2) are possible with this concept and provide additional benefits. One benefit involves making one of the modules a double-walled haven safe from debris, radiation,

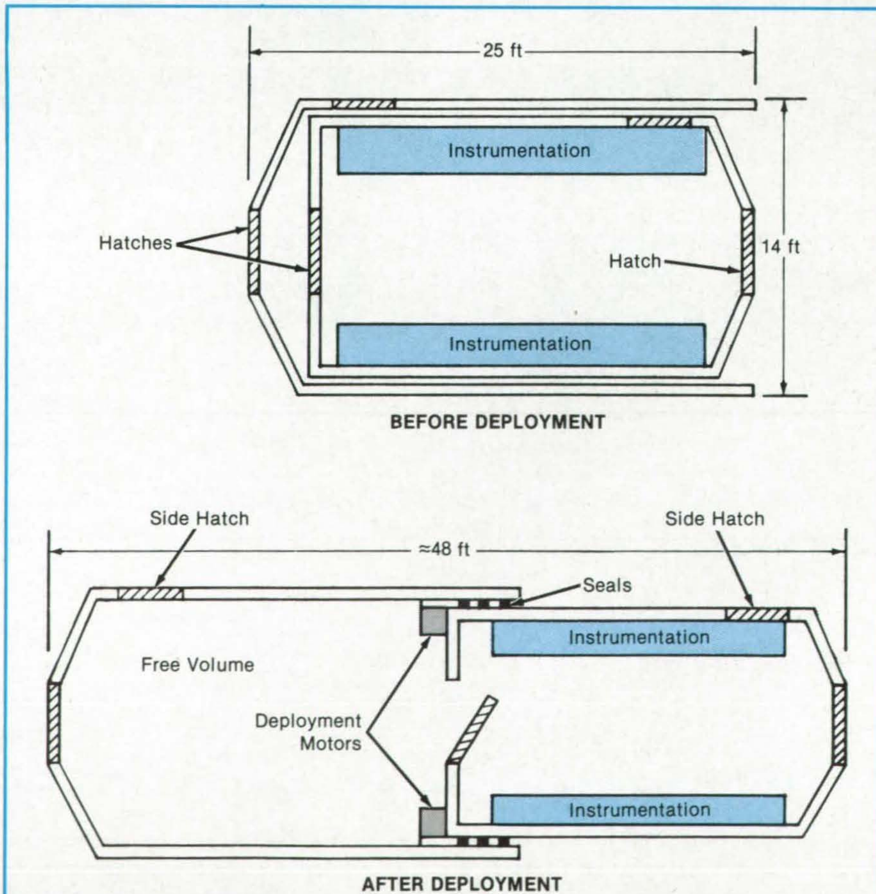

Figure 1. **Before Deployment,** the assembly is essentially a module within a module. After deployment, the available space is approximately doubled.

and the like. This module would be accessible from either end, and hence readily available to all positions in the space station.

The telescoping nature of the modules lends the concept to variations in space-station configuration, assembly, and disassembly. Adaptations of the concept could also provide flexibility in the methods in which the Space Shuttle orbiter is docked or berthed with the space station and decrease the chances of damage because of accidental contact between the station and the orbiter during these maneuvers.

This work was done by Robert D. Witcofski of **Langley Research Center**. *For further information Circle 63 on the TSP Request Card.*

This invention is owned by NASA, and a patent application has been filed. Inquiries concerning nonexclusive or exclusive license for its commercial development should be addressed to the Patent Counsel, Langley Research Center [see page 29]. Refer to LAR-13330.

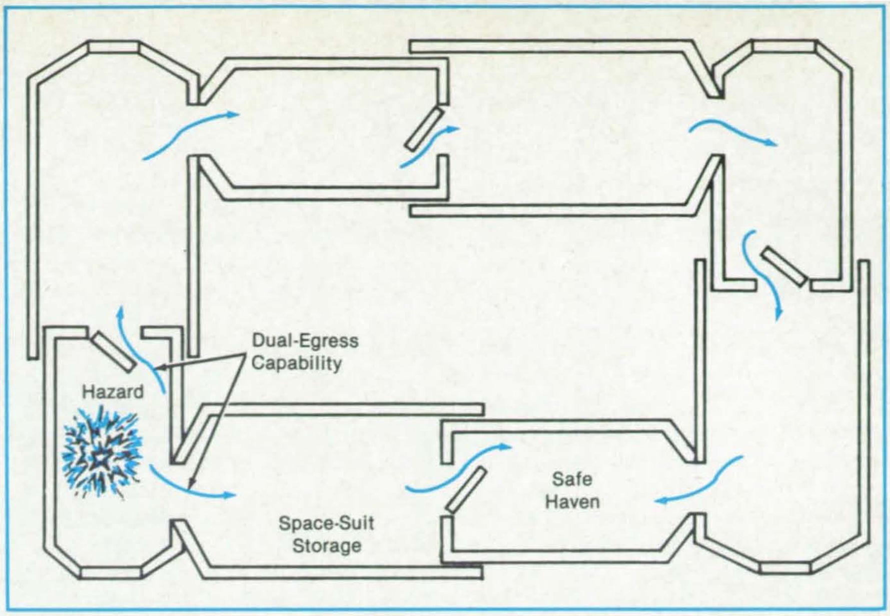

Figure 2. The **"Race-Track" Configuration** provides additional benefits, including an accessible safe haven.

Thermal-Stress-Free Fasteners for Orthotropic Materials

Two-dimensional analysis defines the shapes of interfaces between materials.

Langley Research Center, Hampton, Virginia

A common method of attaching structural components in aerospace systems is by riveting or bolting. If the rivet or bolt is made from a material with a coefficient of thermal expansion substantially different from those of the components being attached, then it is possible to encounter fairly high thermal stresses (or, conversely, a loose joint) if the temperature is increased or decreased significantly. In the case of metal components, this is generally not a problem, because the rivet or bolt is made from the same or a similar alloy. However, with structures made from composite materials, it is difficult to fabricate fasteners from the same material. Also, structural metals are generally isotropic; that is, the thermal-expansion coefficient is the same in all directions. Composite materials, on the other hand, are often anisotropic. Hence, when riveted composite materials heat up or cool down, the rivets can come loose or be subjected to high compressive stresses. Even the state-of-the-art DAZE conical fastener, which by its unique geometry can successfully join isotropic materials with dissimilar rivets, has found only limited application with composites, because most composites are not isotropic.

A theoretical basis for the design of thermal-stress-free fasteners has been de-

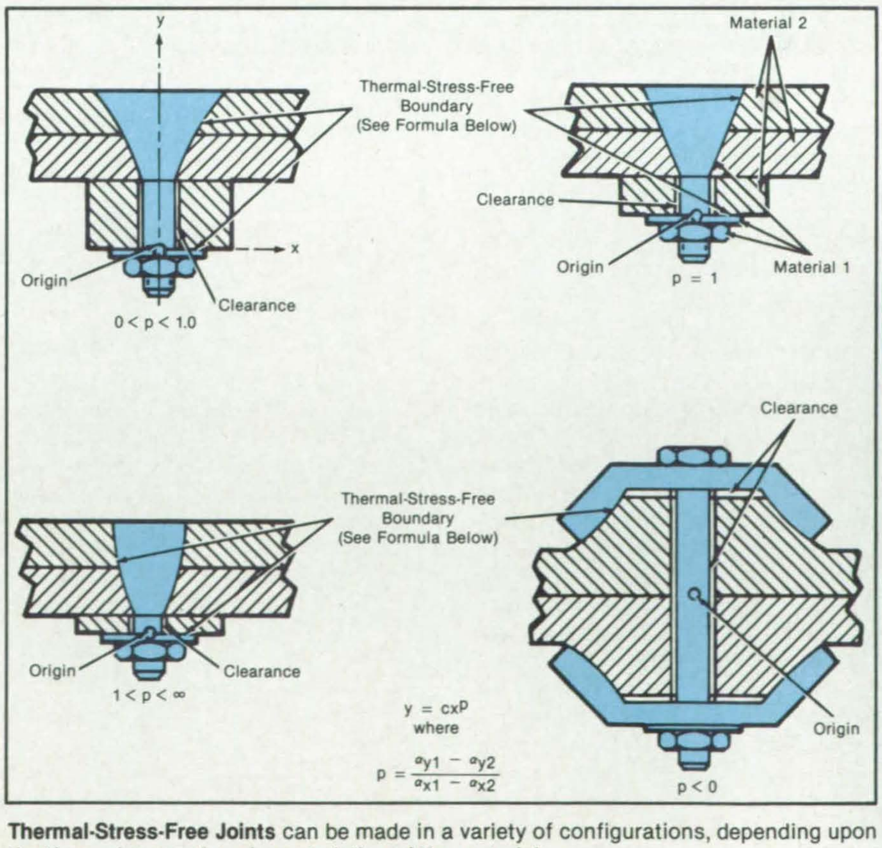

Thermal-Stress-Free Joints can be made in a variety of configurations, depending upon the thermal-expansion characteristics of the materials.

veloped. The analysis yields the equation of a two-dimensional thermal-stress-free interface between two materials with orthotropic coefficients of thermal expansion. If both materials have coefficients of thermal expansion that are isotropic in one plane, the two-dimensional analysis can be used to design thermal-stress-free fasteners, made from one material, which are used to join pieces of the other material. The two materials remain in contact as the temperature increases, forming a tight joint without interference and providing effective shear transfer. The simplest general shape is an axisymmetric, curved-side fastener. If the exact shape of the thermal-stress-free fastener is nearly conical, it can be approximated by a conical fastener with the vertex slightly offset.

Several types of thermal-stress-free joints are shown in the figure. The material being joined (material 2) has unequal thermal coefficients of expansion (COE) in the inplane and thickness directions, denoted in the figure as α_{x2} and α_{y2}, respectively, which also differ greatly from the inplane and thickness COE's of the fastener material (material 1), α_{x1} and α_{y1}, respectively. These conditions will cause adverse thermal stresses or looseness in the joint if conventionally shaped fasteners are used. This design technique determines fastener shapes that will maintain a tight thermal-stress-free joint while the joint undergoes a uniform temperature change.

The equation defining the initial interface shape is shown in the figure as a power curve in which the exponent is dependent on the COE's of the fastener (material 1) and of the structural material (material 2). Suitable minimum and maximum fastener diameters are obtained by varying the washer thickness of material 2 and the coefficient of the power term. Varying the COE values results in shapes having either negative curvature ($0 < p < 1$), conical shapes (the shape of the DAZE fastener with $p = 1$), positive curvature ($p > 1$), or a negative slope with negative curvature ($p < 0$). A steel fastener designed to join pieces of graphite survived four thermal cycles to 1,600 °F (870 °C), whereas a conventional fastener failed after only one cycle, demonstrating the validity of this concept.

This work was done by Max L. Blosser and Robert R. McWithey of **Langley Research Center** *and Thomas F. Kearns of the Institute for Defense Analyses. Further information may be found in NASA TP-2226 [N84-13614/NSP], "Theoretical Basis for Design of Thermal-Stress-Free Fasteners."*

Copies may be purchased [prepayment required] from the National Technical Information Service, Springfield, Virginia 22161, Telephone No. (703) 487-4650. Rush orders may be placed for an extra fee by calling (800) 336-4700.

This invention is owned by NASA, and a patent application has been filed. Inquiries concerning nonexclusive or exclusive license for its commercial development should be addressed to the Patent Counsel, Langley Research Center [see page 29]. Refer to LAR-13325

Modular Firewalls for Storage Areas

Honeycomb ablative structures are assembled in place as needed.

John F. Kennedy Space Center, Florida

A portable, modular barrier withstands the heat of combustion for a limited time and confines the combustion products horizontally to prevent fire from spreading. The barrier absorbs the heat energy by ablation and is not meant to be reused. Designed to keep fires from spreading among segments of solid rocket propellant in storage, the barrier could also be erected between storage units of other flammable or explosive materials — for example, tanks of petroleum or liquid natural gas. Since few common materials have heating values or energy-release rates as high as those of rocket propellants, the barrier should be adequate for most industrial purposes.

For an economy of material and space, the barrier is laid out on a hexagonal floor plan and resembles a honeycomb (see figure). Steel triangular towers are placed at the hexagon corners to support the 8- by 12-ft (2.44- by 3.66-m) steel-skeleton panels of the honeycomb-cell walls. Cells are added horizontally to cover the required floorspace. The structures can also be stacked vertically in 12-ft (3.66-m) units to a maximum cell height of 60 ft (18.29 m).

Each tower is made of three 5-in. (12.7-cm) pipes laterally supported by 6-in. (15.2-cm) I-beams and braced by ¾-in. (19.05-mm) rods. The panels are lattices of variously sized beams braced by rods.

After the steel skeleton is erected, the structure is lined with firebricks. Each brick is about 6 by 9 by 3 in. (15.2 by 22.9 by 7.5 cm) and is molded with tabs that interlock with the steel framework. The bricks are stacked with the 6-in. dimension as the insulating-wall thickness. The bricks can be placed on either or both panel faces and on any or all tower faces.

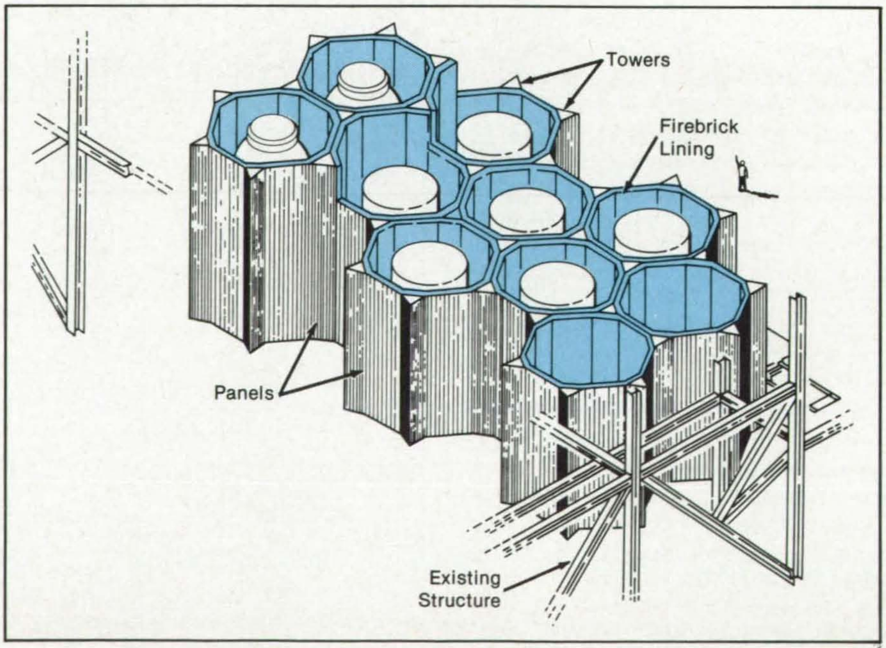

Giant Honeycomb Structures are assembled in modular units. Flammable materials are stored in the cells. The walls are insulated with firebrick to prevent the spread of fire among the cells.

The insulating firebrick material is a porous clay less than half as dense as conventional firebrick. Some types can withstand 1,538 °C for an indefinite time. The hot face can be exposed briefly to 2,760 °C: At this temperature, it ablates; but until ablation is nearly complete, it does not lose strength or transmit excessive temperature to the opposite face. The walls are designed to withstand a maximum combustion pressure of 540 lb/ft^2 (26 kN/m^2).

This work was done by Otto H. Fedor and Lester J. Owens of **Kennedy Space Center.** *For further information, Circle 88 on the TSP Request Card.*

Inquiries concerning rights for the commercial use of this invention should be addressed to the Patent Counsel, Kennedy Space Center [see page 29]. Refer to KSC-11276.

Faster Edge-Defined Silicon-Ribbon Growth

End-cooling may allow faster growth and may yield single-crystal ribbons.

NASA's Jet Propulsion Laboratory, Pasadena, California

A proposed improvement in the edge-defined film-fed process for growing silicon ribbons should increase the speed of growth and improve the quality of the silicon product. The improved process may also produce silicon sheets, webs, or boules.

To maintain the growth of a silicon ribbon, the liquid silicon emerging from the die must be solidified by cooling within the maximum height that the liquid meniscus can extend above the die before collapsing. For a 0.15-mm-thick sheet, this height is more than 8 mm on the sides but only about 1 mm at the ends.

In the current process, the molten silicon emerging from the die is solidified with the help of two cold shoes placed on opposite sides of the ribbon (see Figure 1). The speed of growth is very limited. Experience has shown that whenever the upper pulling-speed limit is reached, the growth of the ribbon is terminated by the collapse of the meniscus at one of the ends. The silicon-ribbon product is mainly polycrystalline.

In the improved process, heat sinks in the form of cooled metal parts are placed at the two ends of the die where the liquid material forms a meniscus. As in the current process, cold shoes are also placed along the two faces of the growing ribbon, approximately 5 mm above the height of the two end cold shoes (see Figure 2). With this modification, solidification of the silicon should start at the ends, and the point of solidification should remain below the 1-mm meniscus height limit, even at high pulling speeds. The cold shoes along the sides of the ribbon will have to be arranged to avoid overcooling of the sheet.

This work was done by Robert Richter of Caltech for **NASA's Jet Propulsion Laboratory.** *For further information, Circle 51 on the TSP Request Card.*
NPO-16692

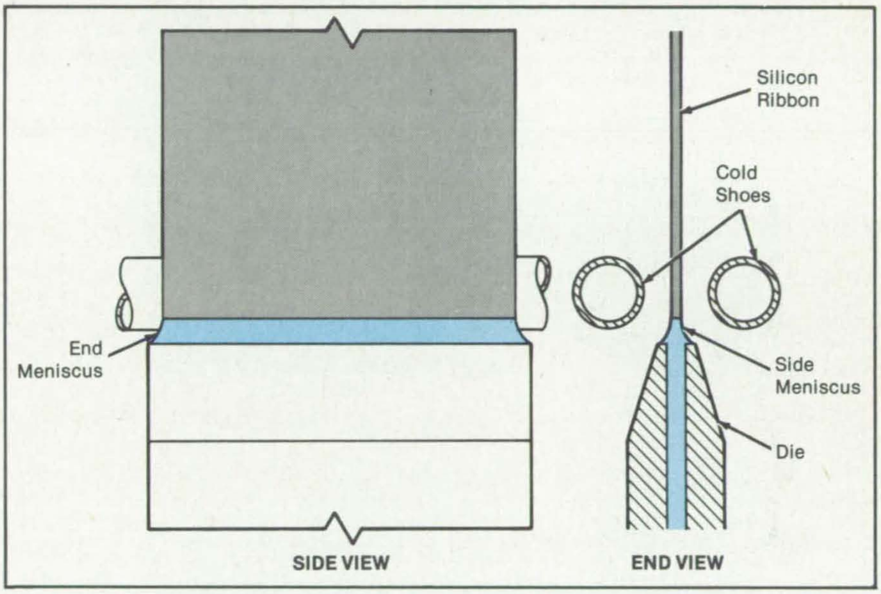

Figure 1. In the **Present Edge-Defined Film-Fed Crystal-Growth Process,** the cold shoes are placed at the sides of the emerging ribbon. The ribbon growth is determined by the maximum height (1mm) that the end menisci can reach before baking.

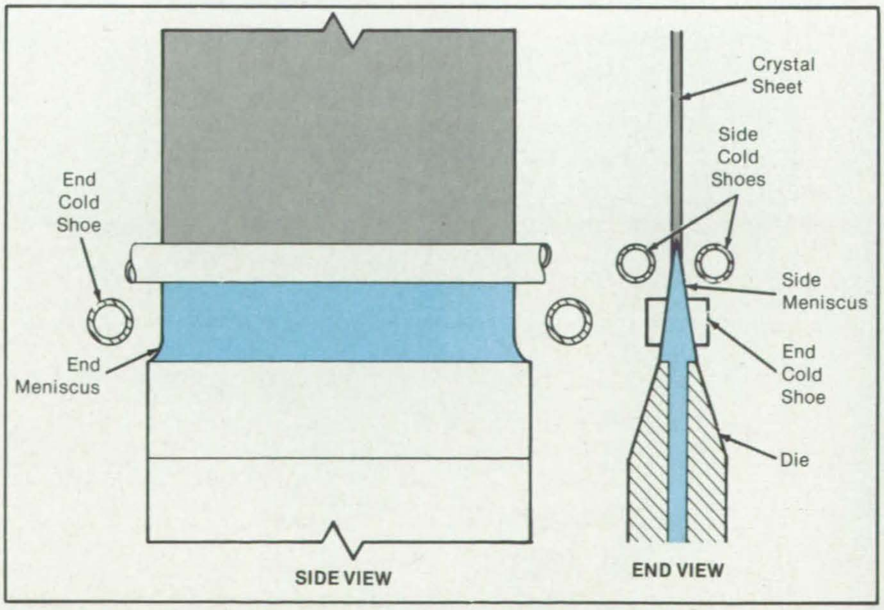

Figure 2. In the **Improved Process,** cold shoes cool the melt at the ends of the emerging sheet. Since solidification at the ends should now occur before the end menisci reach their maximum height, the ribbon could be drawn substantially faster.

Lightweight Forms for Epoxy/Aramid Ducts

Aluminum mandrels are easy to remove.

Lyndon B. Johnson Space Center, Houston, Texas

A lightweight aluminum mandrel for shaping epoxy/aramid ducts simplifies and speeds production. Previously, the mandrel was made of plaster and, therefore, was heavier and more difficult to maneuver into and out of the curing oven than the aluminum tool. In addition, during the cure the plaster mandrel gave off moisture that tended to distort and damage the duct. Most importantly, the plaster mandrel had to be removed by slow and tedious chipping, during which the duct could easily be damaged.

In the new process, glass-reinforced epoxy/aramid cloth is wrapped on the aluminum mandrel. Stainless-steel flanges and other hardware are then fitted on the duct and held by simple tooling. The entire assembly is then placed in an oven to cure the epoxy. After curing, the assembly is placed in an alkaline bath that dissolves the aluminum mandrel in about 4 hours (compared with about 40 hours for removing the plaster form). The epoxy/aramid shell is then ready for use as a duct.

The aluminum mandrel (see figure)

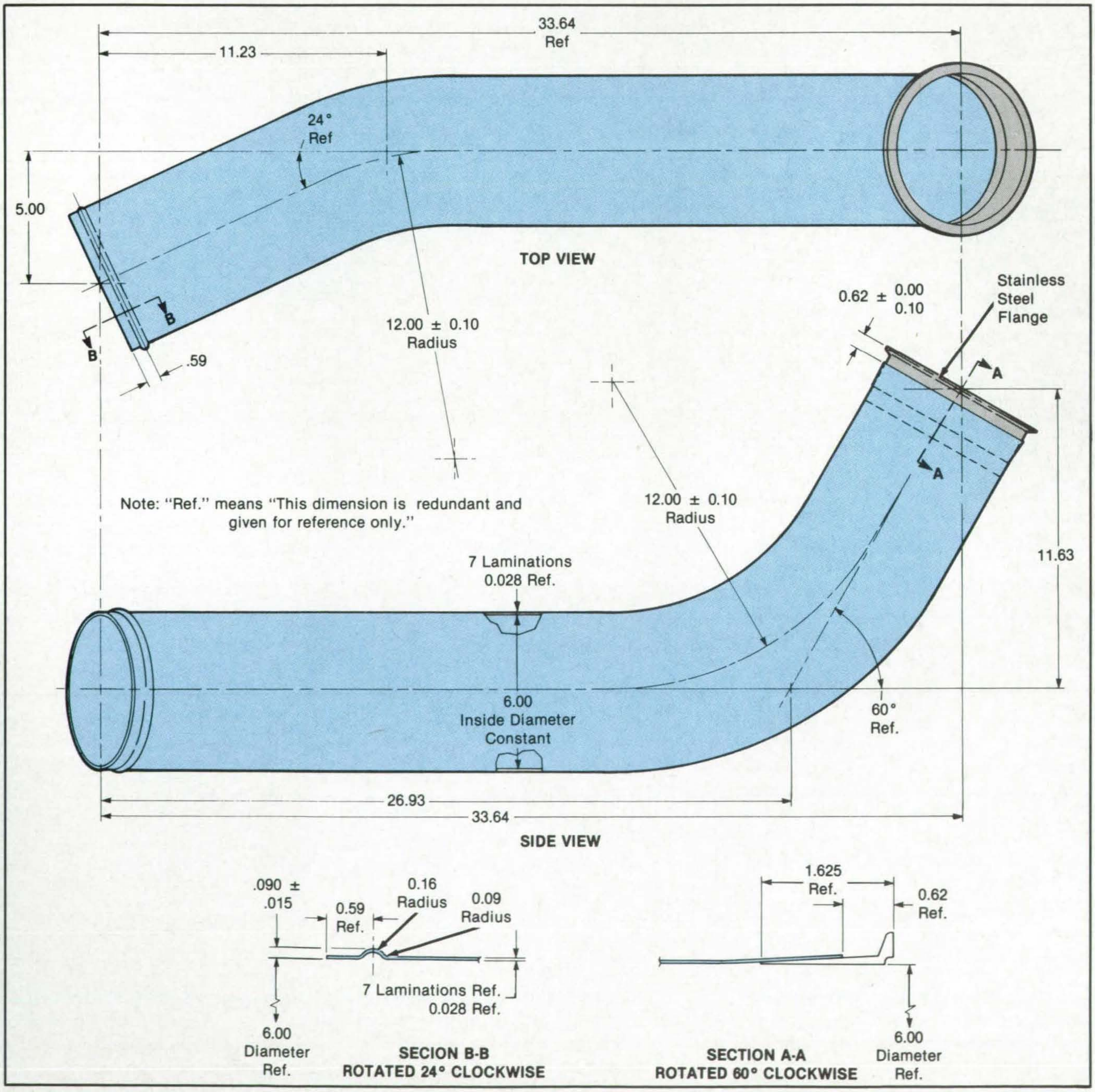

A **Large-Diameter Duct** of glass-reinforced epoxy/aramid material with stainless-steel flanges was formed on an aluminum mandrel. The curvature of the duct is much more easily imparted to the aluminum mandrel than to its plaster predecessor.

has been used to make ducts of various inside diameters up to 6 in. (15.2 cm). Standard aluminum forms can be used; for example, straight tubing, Y-joints, T-joints, and other forms can be sawed and welded into a variety of shapes, ready to be wrapped. Conventional tube-bending equipment produces the requisite curves in the mandrels.

This work was done by Edward W. Mix, August N. Anderson, and Donald L. Bedford, Sr., of Rockwell International Corp. for **Johnson Space Center.** *No further documentation is available. MSC-20957*

Low-Flammability PTFE for High-Oxygen Environments

A modified forming process removes volatile combustible materials.

Marshall Space Flight Center, Alabama

The flammability of cable-wrapping tape has been reduced by altering the tape-manufacturing process. The problem arose when liquid-oxygen-sensor cable assemblies were unable to pass a standard flammability test. Posttest infrared spectrography showed that the polytetrafluoroethylene (PTFE) tape contained small amounts of hydrocarbons.

Previously, the first step in manufacturing was the formation of billets made of PTFE powder and a hydrocarbon extrusion aid, such as naphtha or other petroleum distillates. The newly formed billets were then extruded and calendered into tape. An attempt was made to reduce flammability by sintering. Although sintering was supposed to evaporate the hydrocarbons, it actually sealed them inside the tape; therefore, the hydrocarbons were present and aided combustion during the flammability tests.

In the new manufacturing process, the tape is formed by a proprietary process of screw extrusion (instead of calendering), followed by a washing in a solvent and drying. The tape is then wrapped as before.

Spectrograms of the new tape show that it contains only a small amount of hydrocarbons (see figure). This is borne out by flammability tests, in which flames did not propagate on the tape.

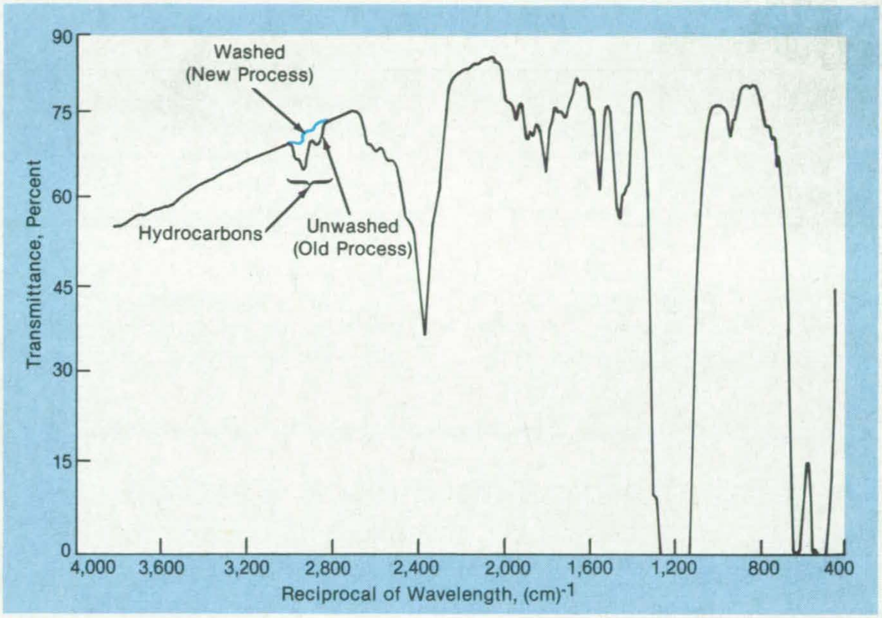

The **New Process Alters the Shape** of the spectrogram. The spectrogram taken after extrusion, washing, and drying shows a lower hydrocarbon content.

PTFE formed by the new process is well suited to oxygen-rich environments. It is safe in the liquid oxygen of the Space Shuttle tank as well as in such medical uses as thin-wall shrinkable tubing in hospital test equipment, surgical instruments, and implants.

This work was done by E. M. Walle, B. M. Fallon, and A. T. Sheppard of Martin Marietta Corp. for **Marshall Space Flight Center**. *No further documentation is available.*

Inquiries concerning rights for the commercial use of this invention should be addressed to the Patent Counsel, Marshal Space Flight Center *[see page 29].* *Refer to MFS-28127.*

Joint for Rapid Structural Assembly

A quickly attaching joint could be used in a variety of truss structures.

Langley Research Center, Hampton, Virginia

Quickly-erecting truss structures have a variety of potential applications, from towers and geodesic-dome structures on Earth to space-station keel beams, antenna masts, and large platforms. These truss structures typically have large numbers of joints, and each joint must have the capability of quick connection at a single visit if the structure is to be erected in a reasonable time.

Other requirements of this type of joint include component simplicity, low cost, inspectability, and the ease of assembly. The joint should have positive latching that will not loosen from vibration or handling, and there should be a direct structural load path through the joint. The joint should have no external protrusion, and the parts should have no sharp edges or pointed ends to endanger the assembler. The joint should feature side-entry attachment to facilitate the removal of a single structural strut for repair without necessitating the removal of additional pieces. It should have a preload capability to remove free play and to provide linear load-displacement response over a prescribed load range. Finally, the joint must be usable with structural members over a large range of sizes.

A new quickly-attaching side-entry joint, shown in the photograph, meets all of these requirements. A split locking ring with tapered internal sides is forced onto a matched taper that is machined on an endbell of each tube. One-half of the split ring is loosely attached to each endbell with screws or pins. When the tubes are slid together to make the joint, a wedged fit develops between the split locking rings and the endbells of the two members.

A collar attached to one member has an internal taper to match an external taper machined on the split ring. The collar is forced over the split ring, forcing the endbells together to load the joint internally. The collar is held in place by connected pins that ride in a groove machined in one of the members. The groove is machined axially along the tube to allow the rapid advancement of the collar and transitions to a spiral around the tube. Locking forces are developed when the collar and split ring are in contact.

Near the end of the groove, the pitch of the spiral goes to zero to form a circumferential groove, which locks the collar against inadvertent rotation during use. The collar may be rotated by hand or with a spanner wrench if large clamping loads are required. Release and removal are accomplished by reversing the assembly procedure.

The split ring is made in one piece and split radially after final machining. The mating tapers on the split ring and endbells are small: approximately 7° on the model shown. Tapers of this range permit high internal preloads to be obtained, yet the parts can be easily separated when the collar is released. Preliminary results from tests on the developmental model indicate that the load-displacement response is linear and that substantial preloading can be accomplished.

This work was done by Marvin D. Rhodes of ***Langley Research Center.*** *No further documentation is available.*

Inquiries concerning rights for the commercial use of this invention should be addressed to the Patent Counsel, Langley Research Center [see page 29]. Refer to LAR-13489.

Split Locking Rings and Endbells combine with the collar to enable the internal loading of the joint.

Welding and Brazing Silicon Carbide

Hot isostatic pressing and conventional furnace brazing are effective under the right conditions.

Lewis Research Center, Cleveland, Ohio

A study was performed that showed the feasibility of welding SiC using several welding and brazing techniques. One of the prime candidate structural ceramic materials for use in advanced gas-turbine and diesel engines is sintered alpha silicon carbide (SiC). The use of SiC would improve engine efficiency by allowing an increase in the operating temperature from 1,700 °F (930 °C) to about 2,450 °F (1,340 °C). Wider and more efficient utilization of SiC would be possible if means were available to weld SiC to itself with elevated-temperature properties of welded joints equivalent to those of the SiC base material.

A literature review by the Lewis Research Center revealed that fusion welding (by melting the base material) was not applicable because SiC tends to vaporize on heating, rather than melt. Since fusion welding was not applicable, feasibility studies at Lewis Research Center on solid-state welding and brazing were initiated. Results were evaluated solely by studying the microstructures of the joints.

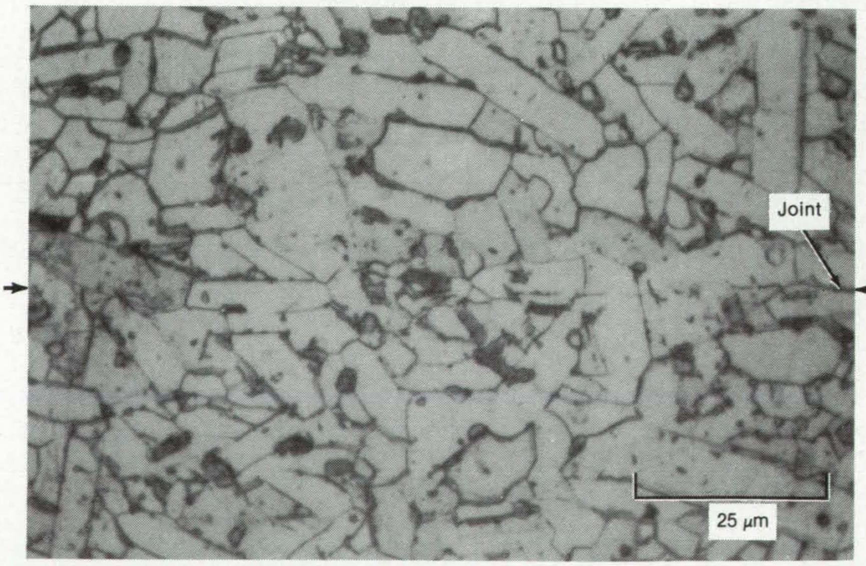

Figure 1. This **Hot Pressure Weld** in SiC was made at 1,950 °C and 138 MPa for 3 h, with 25 percent deformation. Grains have grown across the weld interface. (This sample was etched.)

It was found that SiC could be successfully hot-pressure-welded at 3,550 °F (1,950 °C) in argon (see Figure 1). Welding was possible because the SiC material flowed plastically under uniaxial pressure. Conversely, under hot-isostatic-pressing (HIP) conditions [3,350 °F (1,950 °C), at 20 kpsi (138 MPa) for 2 h], with no plastic deformation, SiC could not be welded at all. However, HIP with AlB_{12}, B_4C, and ZrB_2 interlayers produced diffusion-welded joints successfully, and HIP with SiB_6, Al_4C_3, and $MoSi_2$ interlayers produced successfully brazed joints. The joint produced with the SiB_6 interlayer is shown at the top of Figure 2. Conventional furnace brazing techniques were used to braze SiC using a $TiSi_2$ interlayer and heating to 3,175 °F (1,746 °C) for 5 min in argon, as shown at the bottom of Figure 2.

There are now several options for welding and brazing SiC where otherwise few, if any, were available. Refinements of the solid-state welding and brazing procedures used in this study may be sufficient for some specific industrial applications; but more extensive research, including elevated-temperature strength and property determinations, would be required for most other applications.

This work was done by Thomas J. Moore of **Lewis Research Center**. *For further information, Circle 62 on the TSP Request Card.*
LEW-14251

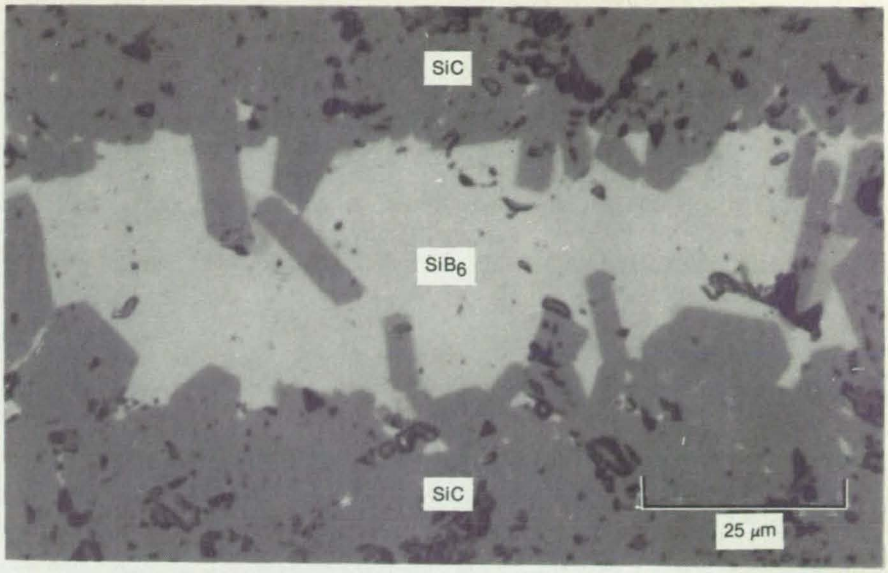

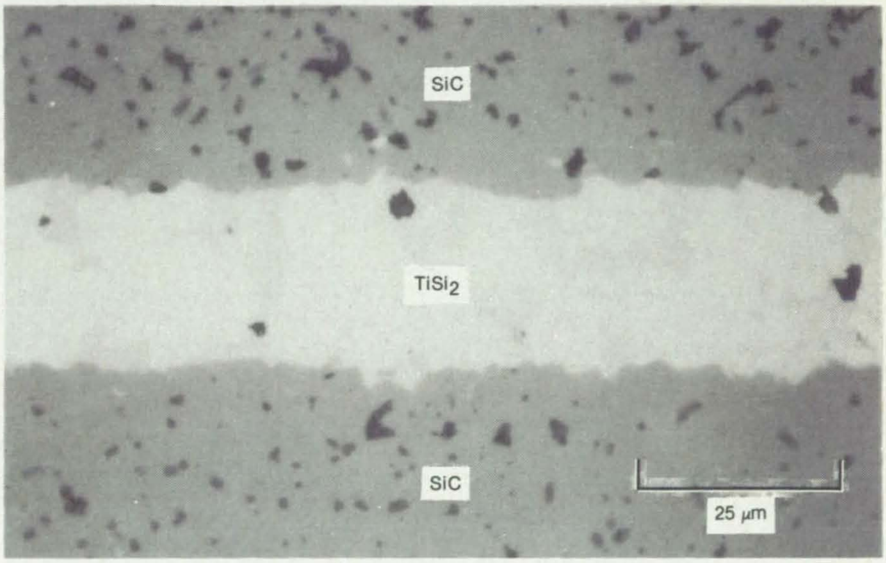

Figure 2. These **Joints in SiC Were Brazed.** In the upper sample, the SiC layers were hot isostatically pressed with an SiB_6 interlayer at 1,950°C and 138 MPa for 2 h. SiC grains appear to have grown into the SiB_6. In the lower sample, the layers of SiC were brazed in a furnace with a $TiSi_2$ interlayer at 1,750°C in argon for 5 min. (Both samples are unetched.)

Making a Lightweight Battery Plaque

The plaque is formed in porous plastic by electroless plating.

Lewis Research Center, Cleveland, Ohio

A lightweight nickel plaque was prepared for use as an electrode substrate for alkaline batteries, chiefly for Ni and Cd electrodes, and for possible use as electrolyte-reservoir plates for fuel cells. The usual commercial nickel plaque is made by sintering nickel powder, sometimes with binders and/or pore formers. This plaque is heavy and uses expensive powdered nickel.

The lightweight plaque is prepared by the electroless plating of a porous plastic that contains an embedded wire or expanded metal grid. The plastic may or may not be filled with a soluble pore former. If the plastic contains a soluble pore former, it is treated to remove the soluble pore former and increase the porosity. The porous plastic is then clamped into a rig that allows the plating solutions to flow through the plastic.

The essential features of the rig are as follows: Vertical walls above and below the porous plastic to allow uniform flow of the plating solutions through all parts of the plastic; a plating rig and a perforated plate made of nonplatable rigid plastic to support the porous plastic; a diffuser plate, directly beneath the porous plastic and above the perforated supporting plate, consisting of nonplatable, porous carbon such that the flow through the carbon is much more rapid than through the porous plastic (this allows more uniform flow than does a perforated plate alone), and provision for pressure or vacuum, if needed, to produce adequate flow.

Commercial electroless nickel-plating solutions prepared according to formulas in the literature may be used. Because of the high surface area of the porous plastic, the plating can be carried out at temperatures lower than those normally used. After plating, impregnation of the plaque with active material is carried out in the usual manner.

An electrode prepared from Amerace A-40® porous plastic extracted with KOH and plated with commercial boride-based electroless nickel solutions (Allied Kelite Division), was subjected to 145 charge/discharge cycles at 100 percent depth of discharge, at current densities from 10 to 100 mA/cm^2, without loss of capacity. At a loading of 1.60 g/cm^3 void, these electrodes have a theoretical energy density of 0.23 A-h/g, compared to 0.12 A-h/g for a typical sintered electrode.

This work was done by Margaret A. Reid, Robert E. Post, and Daniel Soltis of **Lewis Research Center**. *Further information may be found in NASA TM-86861 [N84-32357/NSP], "Development of a Lightweight Nickel Electrode."*

Copies may be purchased [prepayment required] from the National Technical Information Service, Springfield, Virginia 22161, Telephone No. (703) 487-4650. Rush orders may be placed for an extra fee by calling (800) 336-4700.

This invention has been patented by NASA (U.S. Patent No. 4, 439, 465). Inquiries concerning nonexclusive or exclusive license for its commercial development should be addressed to the Patent Counsel, Lewis Research Center *[see page 29]*. *Refer to LEW-13349.*

Pressure Rig for Repetitive Casting

The equipment life is increased by improved insulation.

Langley Research Center, Hampton, Virginia

Conventional pressure rigs are designed for the casting of such low-melting-temperature alloys as aluminum or magnesium. Each casting in conventional rigs requires repreparation of the pressure-rig cavity, and the heat necessary for preparation and casting drastically decreases the life of the expanding rubber diaphragm and other components. A new design uses a commercially-available blanket-type insulator, which overcomes these problems.

The ceramic cavity (see figure) is lined with the insulating material, necessitating only a relining for subsequent use and eliminating the lengthy cavity preparations. In addition, the expandable rubber diaphragm is protected by the insulating material, thereby decreasing its vulnerability to heat damage. Finally, the hazardous asbestos gaskets in the former design are replaced by a nonasbestos material.

The new design, in use at Langley Research Center, has cut the time of preparation for casting from several days to about 1 hour. Most of this saving is due to the elimination of the lengthy heating and drying operations formerly associated with the preparation of the ceramic mold. The quality of the casting is improved because moisture in the cavity is eliminated by use of the insulating material, and a more uniform pressure is applied to the process. The life expectancy of the pressure rig is doubled by this new design, and bursting of the rubber diaphragm due to heat is minimized. Additionally, the improved heat protection has allowed the casting of brass and other alloys with higher melting temperatures in this pressure rig.

This work was done by Peter Vasquez and William R. Hutto of **Langley Research Center.** *No further documentation is available.*
LAR-13485

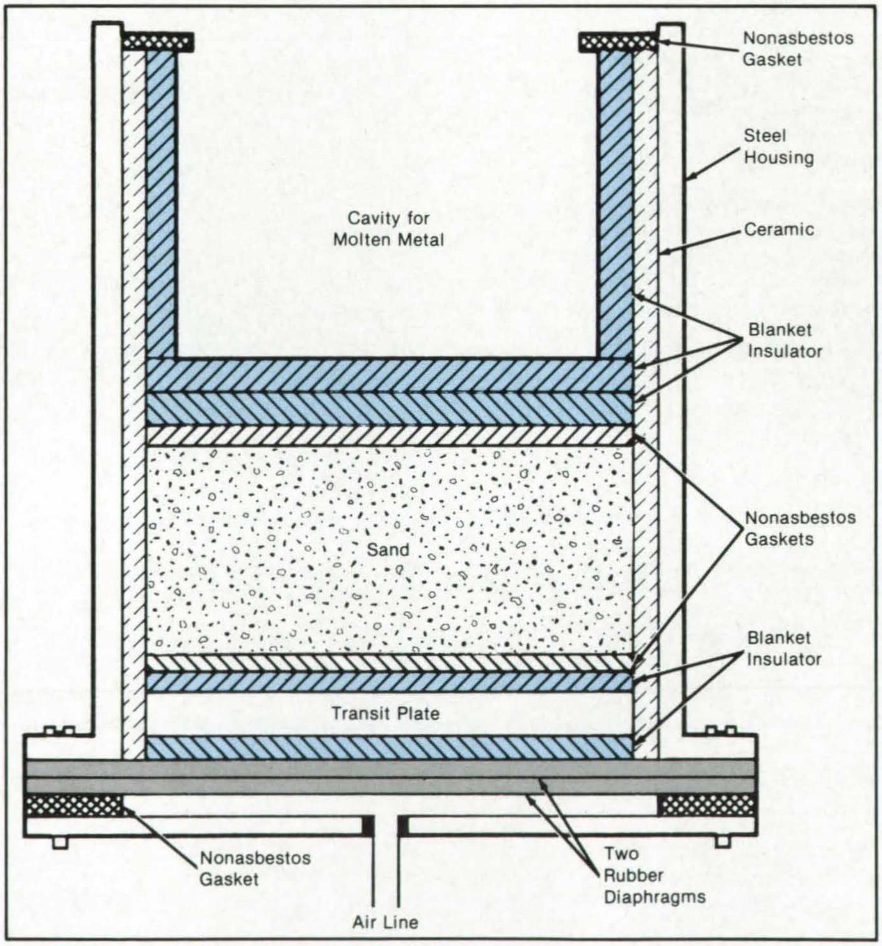

A **Commercial Blanket Insulator** protects components from heat, thereby increasing the life of the pressure rig and enabling repeated use.

Automatic-Control System for Safer Brazing

Integrated unit reduces hazards and improves product quality.

Lyndon B. Johnson Space Center, Houston, Texas

An automatic-control system for radio-frequency (RF) induction brazing of metal tubing reduces the probability of operator errors, increases safety, and ensures high-quality brazed joints. The unit combines the functions of gas control and electric-power control. It minimizes the unnecessary flow of argon gas into the work area and prevents electrical shocks from the RF terminals.

The controller will not allow power to flow from the RF generator to the brazing head unless the work has been firmly attached to the head and has thereby actuated a microswitch. A potential shock hazard is thus eliminated. In addition, the flow of argon for purging and cooling must be turned on and adjusted before brazing power can be applied. This provision ensures that power is not applied prematurely, causing damaged work or poor-quality joints. The controller automatically turns off the argon flow at the conclusion of brazing so that this potentially suffocating gas does not accumulate in confined areas.

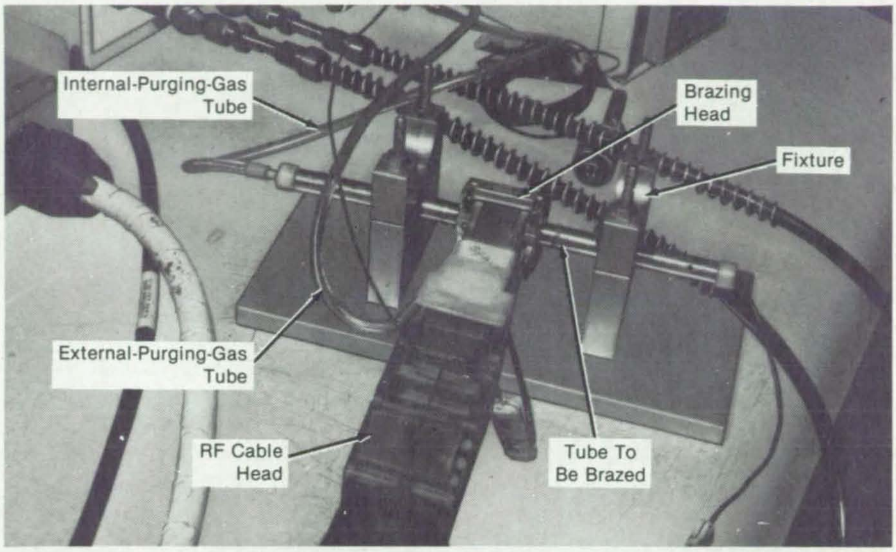

Tubing Is Positioned in a fixture for brazing. The flow of cooling and purging gas and the application of RF power for induction heating are controlled automatically when the operator pushes a button to start the brazing process.

To braze two pieces of tubing together, the operator inserts the pieces in a fixture and places the brazing head over the ends (see figure). The operator then attaches an argon-supply hose for internal purging to an end of the tubing to be brazed and a hose for external purging to the brazing head. The flow of gas to both hoses starts when the operator sets a switch on the flowmeter box. The operator adjusts the purging gas flow to 15 standard ft^3/h (120 standard cm^3/s). The internal and external flows remain on until after brazing, when the thermocouple senses that the workpiece temperature has dropped below 200 °F (93 °C). At that point, the controller turns off the flow.

The flow of argon for cooling the brazing head enters the brazing head through a tube in the RF cable head, removes heat from the head, and exits through another tube in the cable head. The operator presets the cooling-gas supply pressure to 75 to 100 lb/in.^{2} (500 to 700 kPa). The cooling-gas flow starts when the operator presses the "braze start" switch, continues during heating up and brazing, and stops 90 s after brazing has ended.

Before starting the brazing operation, the operator sets the temperature and power controls according to the size and type of joint. The operator then sets the timer to a maximum allowable time. (The timer is a protectively redundant power-shutoff device; normally, the power would be shut off automatically when the workpiece reached the assigned temperature, before the maximum allowable time.) When a light indicates that the work station is ready, the operator presses the "braze start" control, and brazing proceeds automatically.

This work was done by John A. Stein and Maurice A. Vanasse of Rockwell International Corp. for **Johnson Space Center.** *For further information, Circle 49 on the TSP Request Card. MSC-20881*

Books and Reports

These reports, studies, and handbooks are available from NASA as Technical Support Packages (TSP's) when a Request Card number is cited; otherwise they are available from the National Technical Information Service.

Coating Circuit Boards With Silicone

Techniques appropriate to boards containing CMOS circuits are detailed.

A document presents a procedure for applying a thin conformal coating to such electronic assemblies as printed-circuit boards and wire-wrapped boards. The coating is from 1 to 7 mils (25 to 178 micrometers) thick and composed of room-temperature-vulcanizing (RTV) silicone. The document specifies the materials, equipment, spraying method, and quality requirements.

Silicone was selected as the coating material on the basis of its electrical and mechanical properties. It was evaluated, along with other materials, by sectioning, thickness measurements, microscopic examination, electrical tests, and photography.

The procedure takes into account the special needs of circuits made with complementary metal-oxide/semiconductor (CMOS) devices on circuit boards. Previously-developed conformal-coating procedures tend to induce excessive stresses in these chips and ultimately cause failure.

Special attention is given to preventing damage by electrostatic discharge, to which CMOS circuits are especially sensitive; for example, the document notes that equipment, personnel, and assemblies should be fully grounded throughout the procedure.

The coating procedure consists of the following steps:

1. The workpiece to be coated is removed from its protective package and grounded.
2. The areas to be coated are cleaned in specified solvents.
3. The areas not to be coated are masked with tape, temporary coatings, or fixtures.
4. A primer is applied to the unmasked areas and allowed to dry at room temperature.
5. The silicone coating material is diluted with xylene and then sprayed on the workpiece.
6. The coated workpiece is cured at room temperature and humidity for a week or at 75 ± 5 °C and 20 to 40 percent relative humidity for at least 16 hours.
7. The masking materials are removed.
8. The coating is inspected. Acceptance or rejection is based on such criteria as the numbers and sizes of bubbles, the thickness, adherence to the circuit board, completeness of cure, and uniformity.

This work was done by Saverio Gaudiano of **Johnson Space Center**. *To obtain a copy of the document, "Procedure for Spray Application of Thin (1-7 mils) RTV Conformal Coatings for Electronic Assemblies," Circle 8 on the TSP Request Card.*
MSC-21020

Investing in a Large Stretch Press

A press for forming large aluminum parts from plates would provide substantial economies.

A study has assessed the advantages and disadvantages of investing in a large stretch-forming press of about 5,000 ton (4.4×10^7 N) capacity per jaw. The study also developed a procurement specification for the press.

The press would be of a longitudinal-and-transverse design with a 1½-in. (3.8-cm) jaw opening and a die-table ram force of 10,000 ton (8.9×10^7 N). It would process 2219-T37 aluminum alloy plates measuring 1 by 210 by 480 in. (2.5 by 533 by 1,219 cm).

The press would be used for fabricating gores and dome segments for Space Shuttle fuel tanks. Currently, these pieces are stretch formed and chemically milled before heat treatment and final machining. Dome caps could also be made on the press — these parts are now spun-formed and machined. The pieces would be premachined (skin milled) before stretch forming, to reduce detail fabrication costs and assembly costs and eliminate the need for chemical milling.

The study found from parametric cost estimates that a large stretch press could pay for itself in fewer than 100 tank units. The major advantage of premachining and large-stretch-press forming is the saving of time through the elimination of the lengthy process currently required for chemical milling. In addition, these techniques enable the production of larger lots and thereby reduce setup costs. The study also found that increasing the size of tank gores would reduce the costs of final assembly, setup, welding, and inspection by at least 30 percent.

The study examined the question of location for the large stretch press. Water access from major producers of large aluminum plates would be essential. Without direct water access, transportation costs become prohibitive. A site in the southeastern United States is recommended on the basis of low-cost electrical power, favorable business climate and labor market, and convenience of access to suppliers.

This work was done by M. W. Choate, W. P. Nealson, G. C. Jay, and W. D. Buss of Boeing Aerospace Co. for **Marshall Space Flight Center**. *To obtain a copy of the report, "NASA/MSFC Large Stretch Press Study," Circle 79 on the TSP Request Card.*
MFS-27126

Exploiting the Vacuum of Space

Molecular-beam epitaxy and other processes could be tested with minimal contamination.

A proposed vacuum experimental facility for outer space would create vacuums higher than those available in terrestrial vacuum chambers, according to a report. The facility would minimize contamination of the work from walls and would allow the rapid removal of gases and heat generated by the experimental processes. The facility would be used for such processes as molecular-beam epitaxy (for growing semiconductor superlattices, for example), for metal/organic chemical vapor deposition, for coating mirrors and other optical components, and for ultrapurification.

The facility would include a spherical-segment shell raised on a boom above the Space Shuttle, concave side facing forward. Positioned near the apex of the shell on the convex side, the experimental apparatus would be exposed to the high vacuum of the Space Shuttle orbit but would be shielded from contaminating atmospheric molecules in the Shuttle wake. The shell would also shield the work from material outgassed by support equipment mounted on the concave side. Even most of the molecules given off by the downstream wall of the shell would not contaminate the work because this wall is not within the view of the experimental apparatus.

The remaining source of contamination, the factor that limits the attainable vacuum level, is the backscattering of atmospheric molecules by collisions with molecules outgassed from the convex wall. Backscattering would be reduced to a minimum by the choice of a low-outgassing shell material and by the use of a novel bakeout procedure in orbit. When the facility is deployed from the Shuttle, the convex side of the facility would be initially aimed in the forward direction, where the flow of rare atomic oxygen would help to remove traces of hydrocarbons that might later outgas. After this exposure, the concave side of the shell would be pointed toward the Sun. In that position, the polished metal surface would heat up; in effect, it would be baked out by the Sun to reduce outgassing further. At the end of the bakeout period, the shell would be turned to the forward-concave orientation. These cleaning and baking provisions should enable the attainment of vacuums of 10^{-12} to 10^{-14} torr (about 10^{-10} to 10^{-12} N/m^2) in the experimental apparatus.

The device to be processed would have to be degreased and cleaned on Earth. It would be shrouded against contamination during launch and deployment. The finished vacuum-processed work would be stored in protective containers and returned to Earth on the Space Shuttle. The concept can readily be adapted to service on the Space Station as well as on the Space Shuttle. It will then be more economical, since the facility will not have to be transported back and forth between Earth and orbit.

An important feature of the facility not shared by ordinary vacuum chambers is that emissions from a process would be less able to contaminate it, thereby making it unsuitable for use with other materials. For example, although experimenters are strongly interested in building mixed lattices of groups III/V and II/VI elements by molecular-beam epitaxy, they are reluctant to risk contaminating expensive vacuum chambers, dedicated to III/V work with II/VI materials, and vice versa. With the new ultra-vacuum device, however, most of the emissions would disappear into space.

This work was done by Robert J. Naumann of **Marshall Space Flight Center**. *To obtain a copy of the report, "Space Ultra-Vacuum Facility," Circle 40 on the TSP Request Card.*

Inquiries concerning rights for the commercial use of this invention should be addressed to the Patent Counsel, Marshall Space Flight Center [see page 29]. Refer to MFS-28139.

Physics of Fusion Welding

The applicabilities and limitations of three techniques are analyzed.

A NASA technical memorandum discusses the physics of electron-beam, gas/tungsten-arc, and laser-beam welding. From a comparison of the capabilities and limitations of each technique with regard to various welding conditions and materials, it is possible to develop criteria for selecting the best welding technique in a specific application.

All three techniques are classified as fusion welding; that is, a small volume of the workpiece (the weld puddle) is melted by an intense heat source. The heat source is moved along the seam, leaving in its wake solid metal that joins the seam edges together.

Gas/tungsten-arc welding is usually done manually, especially on parts that are too complicated for automated welding. Electron-beam welding is not suitable for manual operations because it must be done in a vacuum. Both electron-beam and laser welding are best done by robots because these processes are difficult to control safely by hand.

The broad, rounded puddle usually produced in gas/tungsten-arc welding must either melt a lot of metal with consequent damage to the workpiece and high power consumption, or else its penetration must be limited. A weld is typically built up in multiple passes, each contributing a small fraction of the total weld cross section. The use of many passes raises the cost and increases the incidence of defects.

Both electron-beam and laser welding are capable of greater penetration with less damage to the surrounding material. Both are capable of "keyholing"; that is, forming a vapor cavity that pushes the molten metal aside and aids the penetration of the beam. An electron beam can readily penetrate the vapor in the keyhole, while a laser beam is defocused and stopped by a plume of ionized gas issuing from the keyhole. In cases in which either technique might be used, a laser may be preferable if there is a risk of overpenetration.

Both gas/tungsten-arc and electron-beam welding are sensitive to magnetic fields. Because a ferromagnetic workpiece can become ionized by welding currents, it may cause the welding beam to wander. When dissimilar metals are welded, thermoelectric currents are generated and these, too, may cause erratic behavior of the beam. The effect is especially severe if one of the dissimilar metals is ferromagnetic.

The three techniques differ somewhat with regard to internal and external defects. The straighter, narrower holes produced by keyholing in electron-beam and laser welding result in less thermal distortion of the workpiece than is observed in gas/tungsten-arc welding. Porosity is more likely to occur in gas/tungsten-arc welding than in the other types. Most of the common external defects in all three cases can be eliminated with appropriate automation.

The following is an example of the selection of a welding technique: It is necessary to have the deep penetration and relatively low distortion afforded by keyholing. This excludes gas/tungsten-arc welding. It is also necessary to operate in air, and magnetic fields may be present. This excludes the use of an electron beam. In this case, only laser-beam welding is acceptable.

This work was done by A. C. Nunes, Jr., of **Marshall Space Flight Center**. *Further information may be found in NASA TM-86503 [N86-11473/NSP], "A Comparison of the Physics of Gas Tungsten Arc Welding (GTAW), Electron Beam Welding (EBW), and Laser Beam Welding (LBW)."*

Copies may be purchased [prepayment required] from the National Technical Information Service, Springfield, Virginia 22161, Telephone No. (703) 487-4650. Rush orders may be placed for an extra fee by calling (800) 336-4700. The report is also available on microfiche at no charge. To obtain a microfiche copy, Circle 41 on the TSP Request Card.
MFS-27138

Properties of VPPA-Welded 2219-T87 Aluminum

Metallurgical properties and effects of welding are described.

A report describes an investigation of the welding of 2219-T87 aluminum alloy by the variable-polarity plasma-arc (VPPA) process. The purposes of the research were to determine the highest strength attainable with this alloy and process and to estimate the changes in weld properties caused by variations of process controls.

Alloy 2219 is strong and heat treatable and retains its structural integrity up to 600 °F (316 °C). This is the principal structural alloy of the Space Shuttle external tank. The VPPA process offers many advantages and is now replacing the tungsten/inert-gas process that was used initially. In over 24,000 in. (610 m) of welds on the tank, there has been no internal defect requiring manual repair.

In the VPPA process, the current, voltage, and polarity are changed with time in a controlled manner. The primary advantage is in the 4-ms reverse-polarity portion of the welding cycle, during which argon ions bombard the workpiece and remove the oxide layer. During the 19-ms forward-polarity interval, the alloy is heated by the impingement of hot electrons. The plasma (of which the argon ions and the electrons are principal components) acts as a constraint that reduces the sensitivity of the weld to the distance between the welding torch and the workpiece.

VPPA welding can be done in the "keyhole" mode, in which the weld penetrates through the total thickness of the workpiece. By the appropriate control of the electrical current and the gas-flow rate, the plasma pressure can be increased to form a stable keyhole that moves with the weld. The hole is filled as the weld moves on. The liquid layer in the keyhole is so thin that gases released during freezing are swept away rather than being entrapped to form porosity in the final joint.

In the investigation, welded and unwelded specimens of the alloy were subjected to tensile tests and examinations by scanning-electron microscopy. Microchemical analysis was also performed in the scanning electron microscope by examination of the X-ray spectra produced by bombardment of the sample surfaces with 5-keV electrons.

The strength of welded panel was found to depend on a number of interacting factors. The composition of the base metal and modifications of this composition by the filler metal govern the dimensions of microstructural features, which in turn influence the weld strength. Other factors that affect the microstructure and strength include the heating and cooling rates, preheating, and the angle between the weld and the direction in which the alloy plate was rolled during manufacture.

Interdendritic particles in the fusion zone contribute to void formation, which controls the ultimate tensile strength. A variation of 150 μm in size was found to correspond to a variation of 10 kpsi (69MPa) in ultimate tensile strength. All fracture surfaces were of the dimple-rupture type, with fracture beginning in the fusion zone. Welds were found to be stronger when aligned with the rolling direction. The application of water-cooled blocks along the weld track produced a small increase in the strength and toughness of the weld.

This work was done by W.A. Wilson of **Marshall Space Flight Center** *Wartan A. Jemian of Auburn University. To obtain a copy of the report, "The Strength and Characteristics of VPPA Welded 2219-T87 Aluminum Alloy," Circle 50 on the TSP Request Card.*
MFS-27105

Deployable Construction Platform

A structure folds compactly for transportation but opens into a large work and storage area.

A report describes a concept for a deployable platform for the construction of large structures. Developed for use on a space station, the concept includes folding structural parts that may be adaptable to portable or field-assembled terrestrial structures.

The platform would be a central location for building structures, storing equipment and parts, and servicing and checking out space vehicles. The platform would provide electrical power, lighting, and tools.

The deployed platform would consist of a truss structure attached to a transfer tunnel at a docking port on the space station. A pair of rails, supported by truss members, would brace large modules delivered to the space station. Compartments installed within truss members would store such small items as tools, holddown mechanisms, and auxiliary lights. A lightweight hangar would protect astronauts while they work on the platform; it would allow them to move about untethered on the platform and would contain small objects that happened to float free.

According to current plans, the platform floor area would measure 18 by 28 m. The truss would be composed of graphite /epoxy tubes typically about 2 m long.

Knee joints in the centers of the surface struts and pin joints and the clustered ends of the struts allow the truss to fold compactly for transportation to orbit. The entire truss would fold into a package measuring 2.72 by 1.75 by 2.24 m.

This work was done by Richard M. Gates and Kenneth P. Hernley of Boeing Aerospace Co. **Marshall Space Flight Center.** *To obtain a copy of the report, "Deployable Construction Platform," Circle 58 on the TSP Request Card.*

Inquiries concerning rights for the commercial use of this invention should be addressed to the Patent Counsel, Marshall Space Flight Center (see page 29). Refer to MFS-28117.

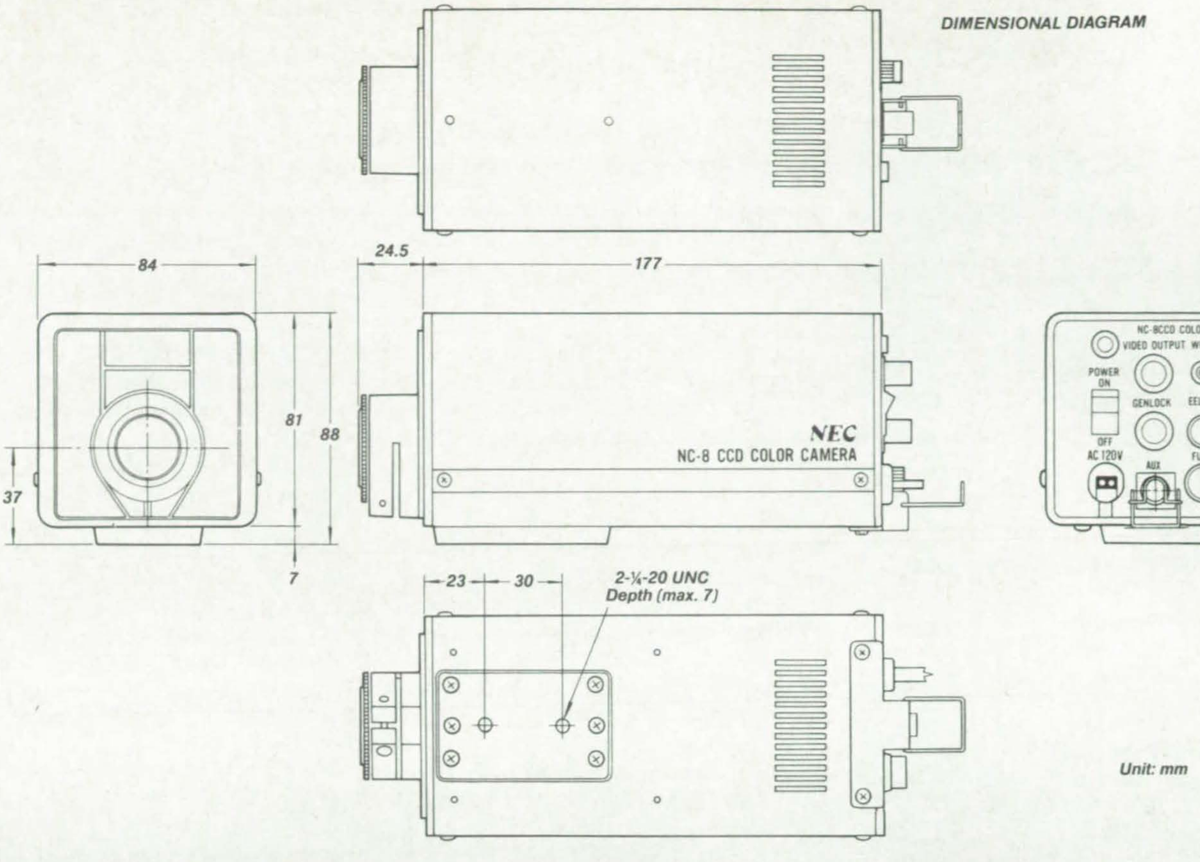

OUR DESIGN FITS YOUR SPECS.

NEC invites you to take a look inside the NC-8 single chip color camera — the camera designed with your specifications in mind. With the lightweight, flexible NC-8, you get high definition and resolution, very low lag and no burn in. It resists shocks, is immune to magnetic distortion, and because its pixels are arranged in a high precision matrix, there is no geometric distortion. It includes Gen Lock as a standard feature. It is equipped for any C-mount lens including auto iris.

This durable little camera is a match for any of your toughest video camera requirements and is easily adaptable to a wide variety of settings.

NEC, the world's largest manufacturer of semiconductors, offers an entire line of solid state industrial cameras—all high quality, hard-working products from a respected source.

C&C
COMPUTERS AND COMMUNICATIONS

Specifications

Pickup	Interline transfer type CCD x1
Number of picture element	H427xV492
S/N ratio	47dB (illuminance channel, standard recording conditions, AGC: off)
Resolution	Horizontal: 280 lines Vertical: 350 lines
Sensitivity	1,600 Lux F4.0
Minimum illumination	10 Lux F1.4 AGC: ON (20% signal output level)
White balance adjustment	Manual/Remote
Lens mount	C-Mount
Power consumption	Approx. 6.5W (less than 9VA)
Weight	Approx. 1.4kg [3.1 lbs] (excluding lens)

NEC

IMAGINE WHAT WE'LL DO FOR YOU

For more information about the NC-8, TI-22AII, TI-22PII and TI-26A industrial cameras, contact the Industrial Video Group, Broadcast Equipment Division, NEC America, Inc., 1255 Michael Drive, Wood Dale, IL 60191 Toll free 1-800-323-6656. In Illinois phone 312/860-7600.

Circle Reader Action No. 369

Mathematics and Information Sciences

Hardware, Techniques, and Processes

Books & Reports

Computer Programs

Function-Keypad Template Filer

Each page of this filer shows various keypad designations corresponding to a variety of software packages.

NASA's Jet Propulsion Laboratory, Pasadena, California

Microcomputer operators using a variety of software packages can be assisted by a simple filer that illustrates various keyboard functions corresponding to different software packages. Keyboard functions can change, depending on the selected software. The filer has a set of templates showing keyboard functions for various software packages. The templates can be set up quickly as desktop references to the key functions.

Usually, overlay templates have been placed over the function keys, indicating only their function with a particular software package. If each template corresponds to one software package, the user frequently has to swap one template for another (since templates do not stack easily on the keyboard), losing time in locating the desired template. Alternatively, the same template can indicate different sets of functions for each key. This can be confusing. Moreover, if eyestrain is to be avoided, the print on the templates has to be sufficiently large so that no more than four or five different sets of functions could be indicated on a single template.

These difficulties are avoided by the function-keypad template filer. The filer has the various templates bound together so that they can be indexed easily and stood up for ready viewing. Template filers are made of inexpensive materials. Templates of various manufacturers can be added in pages appropriately die cut to receive them.

The template filer comprises several rigid sheets of material arranged in hinged or jointed binding; for example, a spiral-ring binding (Figure 1). The filer rests on a base page. The page next to the base page is scored to be folded into a triangular support for the assembly of

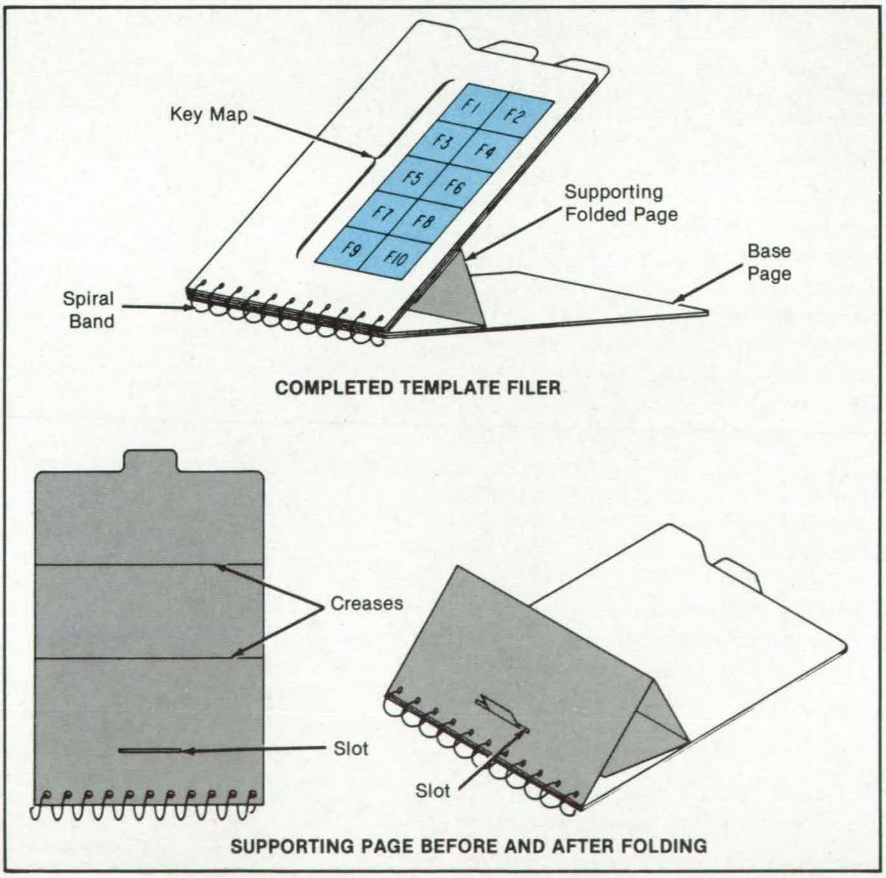

Figure 1. The **Inner Pages of the Function-Keypad Template Filer** are maintained at a convenient viewing angle by a triangular support constructed from the page above the base page.

inner pages. A tab and tab slot are provided to secure the triangular base.

As shown in Figure 2, some of the inner pages are printed to represent a particular key map, while slotted pages are used to hold the plastic templates that are popular in software applications. Index tabs at the tops of the pages allow the function-keypad templates to be located quickly.

This work was done by Paul A. Headley of Caltech **NASA's Jet Propulsion Laboratory.** *For further information, Circle 77 on the TSP Request Card.*
NPO-16676

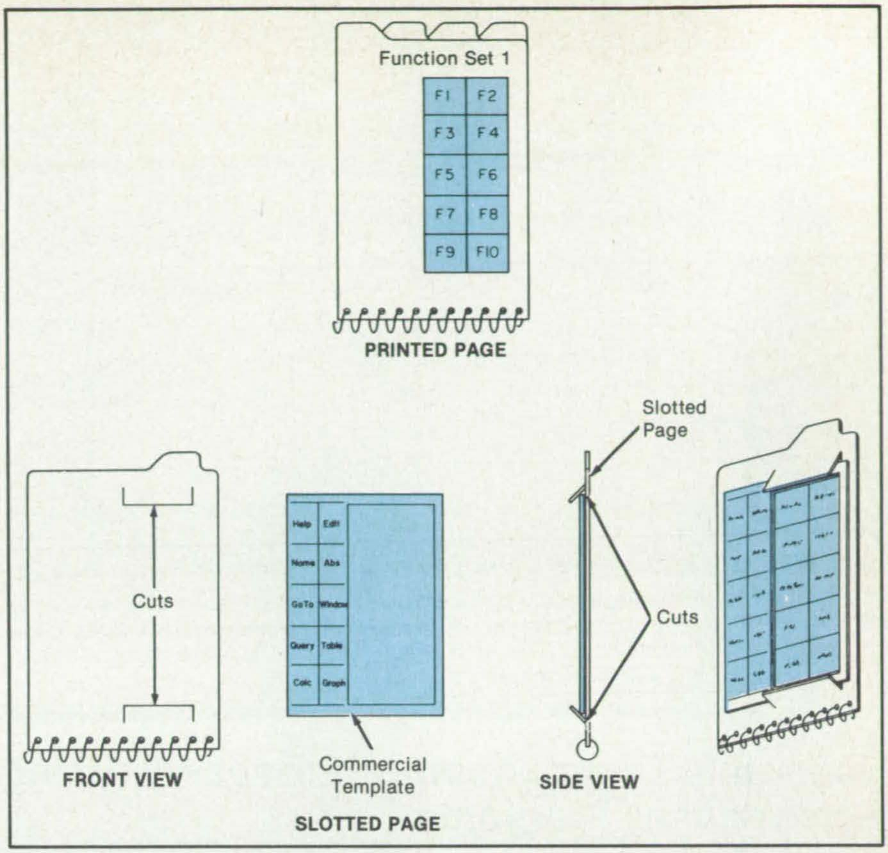

Figure 2. **Printed Inner Pages** represent a particular keyboard. Alternatively, slotted pages hold the commercial templates indicating the key functions.

Solving Nonlinear Coupled Differential Equations

A harmonic balance method gives useful results fairly easily.

Lewis Research Center, Cleveland, Ohio

A harmonic balance method has been developed to obtain approximate steady-state solutions for nonlinear coupled ordinary differential equations. Such equations arise, for example, in determining the motion of an unbalanced, rigid disk in a shaft system. Although the nonlinear terms are commonly neglected in rotordynamic calculations, order-of-magnitude analysis indicates that they are significant in geared shaft systems.

Up to now, suitable techniques have not been available for solving the complete nonlinear equations. However, the method of harmonic balance is a suitable solution technique. Moreover, the method is usable with transfer matrices, which are commonly used to analyze shaft systems. The solution to the nonlinear equation, with a periodic forcing function, is represented as the sum of a series similar to a Fourier series but with the form of the terms suggested by the equation itself. As an example, if one considers the equation for the two-degree-of-freedom spring-mass pendulum system shown in Figure 1

$$\ddot{r} - r\dot{\theta}^2 + C_R/m\dot{r} - g(1 - \tfrac{1}{2}\theta^2) + k/m(r - l) = 0$$

$$r^2\ddot{\theta} + 2r\dot{r}\dot{\theta} + (C_\theta/m)\dot{\theta} + gr(\theta - \theta^3/6) = T_0/m \sin(\omega t)$$

where a two-term Taylor series has been substituted for the usual trigonometric terms on the left sides of the equations.

Examination of the equations suggests the following form of solution

$$\theta(t) = \theta_{11} \sin(\omega t) + \theta_{12} \cos(\omega t)$$

$$r(t) = r_0 + r_{21} \sin(2\omega t) + r_{22} \cos(2\omega t)$$

These assumed solutions are substituted into the differential equations. By ignoring harmonic terms not in the assumed solution and applying the principle of harmonic balance, one produces five nonlinear polynominals in the five unknowns r_0, r_{21}, r_{22}, θ_{11}, and θ_{12}. The nonlinear algebraic equations thus produced are solved by an iterative method.

Figure 2 shows the θ response obtained for an example problem, with the

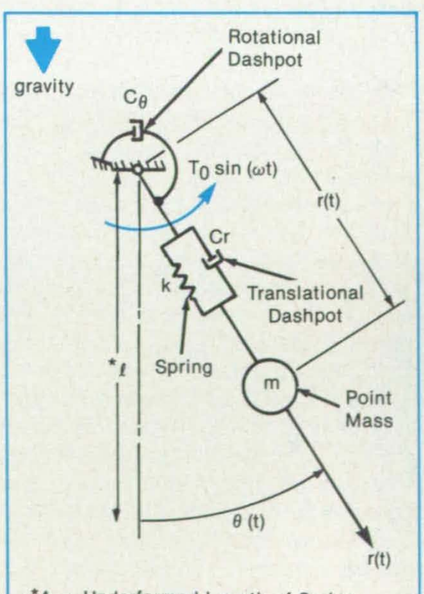

Figure 1. A **Pendulum** includes a point mass suspended on a spring. Both the spring flexing and pendulum rotation are damped by dashpots.

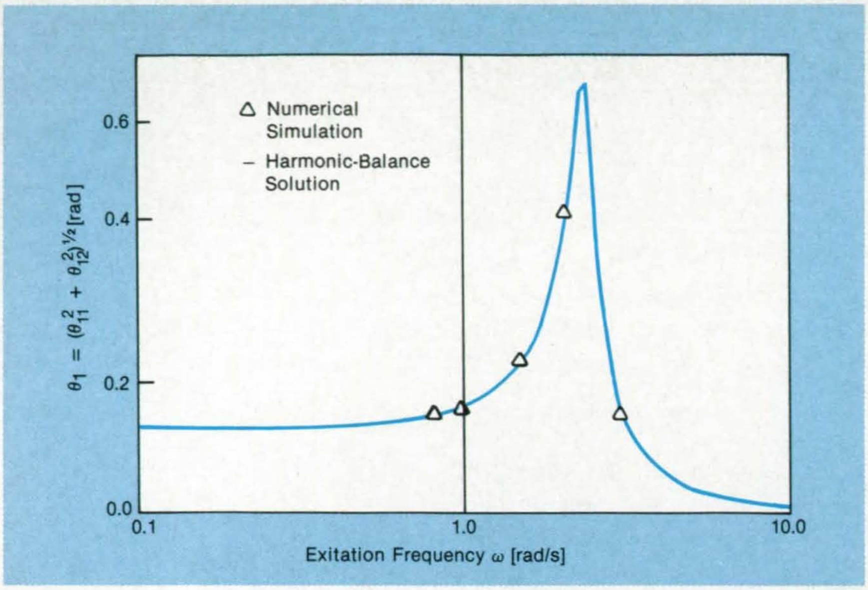

Figure 2. **Solutions to the Equations of Motion** for the pendulum of Figure 1 were obtained by the harmonic-balance method and numerically from the original differential equations. These are steady-state solutions for m = 10 kg, k = 100 N/m, C_R = 10 N·m/s, C_θ = 10 N·m-s, T_0 = 25 N·m, l = 1 m, and g = 9.81 m/s^2.

approximate solution compared to a precise numerical solution of the original differential equations. The system parameters were such that the response was fairly large. In light of the large nonlinearity in the differential equations, the agreement between the harmonic-balance and numerical solutions is considered good. The solution precision could be improved further, if necessary, by using higher-order harmonic terms in the assumed solution form.

This work was done by L. D. Mitchell and J. W. David of the Virginia Polytechnic Institute for **Lewis Research Center**. *For further information, Circle 14 on the TSP Request Card.*
LEW-14165

Economic Comparison of Processes Using Spreadsheet Programs

An inexpensive approach can aid plant-design decisions.

NASA's Jet Propulsion Laboratory, Pasadena, California

Commercially available electronic spreadsheet programs can aid the economic comparison of different processes for producing a particular end product. This can facilitate plant-design decisions without requiring large expenditures for powerful mainframe computers.

To estimate plant performance, data for process feeds, yields, and utility requirements are first entered in the spreadsheet "baseline" (first) column (see table). Performance parameters can then be calculated and displayed in the second column. Using the performance parameters, the process analyzer can quickly compare the baseline parameters and adjust the performance parameters as desired.

The adjusted performance parameters (placed in the third spreadsheet column) and mathematical functions that describe the interactions of unit operations in a simplified block flow diagram of the plant then yield adjusted baseline values, which are displayed in the fourth column. Repeating these procedures for the different plants allows their adjusted baseline performance data to be compared.

For each plant, stored, adjusted baseline-performance data enable the estimation and tabular display of costs for each plant component and for the entire plant. After the "adjusted" baseline performance is calculated, the cost of each plant component is estimated by use of calculated values stored in the spreadsheet cells. A cost-estimate template can be made from unit costs and scaling exponents. Then installed-unit costs are scaled according to the following:

		PLANT DESIGN A			
		BASELINE	Performance Parameter	Adjusted Performance Parameter	Adjusted Baseline
9	Coal feed (TPD)	4607.0			4746.5
10	Coal feed (MMBtu/hr)	4697.2			4839.4
11	Coal feed (MW)	1376.3			1417.9
12	Pipeline gas feed (MMBtu/hr)	36.9			0.0
13	Oxygen [or air] feed (TPD)	3860.0	0.838	0.813	3859.5
15	Gasifier gas (MMBtu/hr)	3630.0	0.773	0.750	3629.6
16	Gas as fuel to cleanup (MMBtu/hr)	36.9	0.008	0.005	24.2
17	Treated gas (MMBtu/hr)	3593.1			3605.4
19	POWER GENERATORS:				

Process Feeds, Yields, and Power Requirements of a coal-gasifier/fuel-cell powerplant are summarized from design data and displayed on a spreadsheet, a small section of which is shown here. These input data are used for technical and economic performance estimates.

Multiple Pages Intentionally Left Blank

$$\text{installed cost of unit B} = \text{installed cost of unit A} \times \left(\frac{\text{capacity of unit B}}{\text{capacity of unit A}}\right)^n$$

where n is a scaling exponent between 0 and 1.

From plant costs and the appropriate economic assumptions, the required product selling price can be estimated and displayed. The spreadsheet approach also allows the quantification of the uncertainties in the estimates of performance and cost, and for the pictorial presentation of the results of sensitivity analyses and comparisons, by use of the graphic routines built into the spreadsheet software package.

This work was done by Joseph F. Ferrall, Alfred W. Pappano, and Charles N. Jennings of Caltech for **NASA's Jet Propulsion Laboratory.** *For further information, Circle 46 on the TSP Request Card.*
NPO-16660

Computer Program To Transliterate Into Arabic

A computer would be used as an Arabic typewriter.

John F. Kennedy Space Center, Florida

A conceptual program for the TRS-80, Model 12 (or equivalent) computer would transliterate from the English letters of the computer keyboard to Arabic characters in the output of the associated printer. The program would automatically change the character sequence from the left-to-right of English to the right-to-left of Arabic. It would be easy to use and involve minimal shifting. (Current Arabic typewriters require much shifting because almost every letter has four forms: one used at the beginning, one in the middle, one at the end of a word, and one standing alone.)

The figure gives an example of how the program would function, using the Arabic phrase for "the Arabs and the Moslems." Of course, a dot-matrix printer would have to be used in the absence of a printing head with Arabic characters. Since graphics are used to create the cursive characters, the user can virtually create any "font" desired by making alterations in the "basic" program.

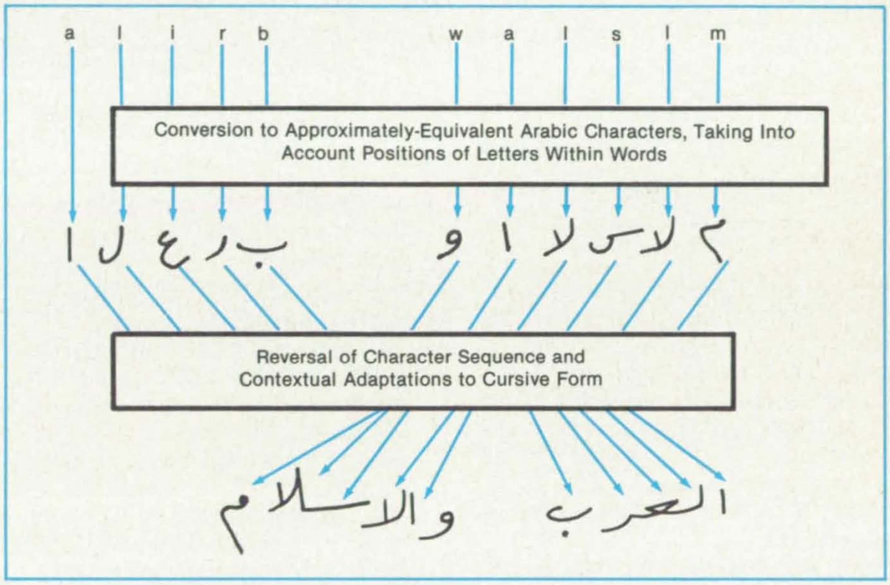

An **English-to-Arabic Transliteration Program** would provide a printed Arabic output from a keyed-in English transliteration.

The program would leave 16 keys unused with the shift. These could be used for Arabic punctuations that lack, or look different from, English equivalents. These keys might also be used for commands if a word-processing program is developed.

This work was done by Emile Stephan of **Kennedy Space Center.** *No further documentation is available.*

Inquiries concerning rights for the commercial use of this invention should be addressed to the Patent Counsel, Kennedy Space Center [see page 29]. Refer to KSC-11342.

Larger Convergence Zones for Newton's Method

An iterative technique applies over a wider range of initial guesses.

Marshall Space Flight Center, Alabama

A new theorem describes the convergence zone of Newton's iterative method for finding the zeros of a real function. A previous theorem, called the contraction mapping theorem, was overly restrictive in that it guaranteed convergence over only a portion of the new, larger convergence zone.

In using Newton's method, one makes an initial guess, x_0, of the solution to the equation $f(x)=0$. If x_0 lies in the convergence zone, then the first iterate, $x_1 = x_0 - f(x_0)/f'(x_0)$ lies closer to the solution than does x_0. Similarly, one can calculate the second iterate, $x_2 = x_1 - f(x_1)/f'(x_1)$. If this process is repeated many times, the *n*th iterate approaches the exact solution, x_z.

The new theorem involves two points, x_p and x_p^*, called the primary conjugate points. If the exact solution lies between these points ($x_p < x_z < x_p^*$) and there are no other conjugate points in this interval, then according to the theorem, subsequent iterations will converge upon the exact solution if the initial guess lies in the interval.

Newton's method diverges (or at least fails to converge properly) for x_0 outside the convergence zone. If x_0 lies at one of the primary conjugate points, the method neither converges nor diverges; instead, x_1 is the other conjugate point, and x_2 is the initial guess, x_0. Thus, the subsequent iterations oscillate between the primary conjugate points if x_0 is one of these points.

The associated function, A(x), is useful in finding the conjugate points and analyzing the convergence properties of f(x). It is defined as the difference between the second iterate and the initial guess

$$A(x_0) = x_2 - x_0 = [f(x_0)/f'(x_0) + f(x_1)f'(x_1)]$$

Since $x_2 = x_0$ for an initial guess at x_p or x_p^*, and since all iterations give x_z for an initial guess at x_z

$$A(x_p) = A(x_p^*) = A(x_z) = 0$$

Another useful property is that $A'(x_z) = -1$ so that A(x) must be positive in the part of the convergence zone below x_z and negative in the part above x_z. These properties are illustrated in the figure, which shows f(x) and A(x) for the inverse sine of x.

The proof of the convergence theory depends on the following restrictive assumptions:

- $f(x_0)$, $f(x_1)$, and their first and second derivatives must be continuous on an interval that includes the primary conjugate points.
- $f(x_p)f''(x_p)$, $f(x_p^*)f''(x_p^*)$, and $f''(x_p)f''(x_p^*)$ must all be negative.
- $f'(x_0)$ and $f'(x_1)$ must be nonzero between the primary conjugate points.

These assumptions may be overly restrictive; future research on A(x) may result in a more general convergence criterion.

This work was done by C. Warren Campbell of **Marshall Space Flight Center**. *Further information may be found in NASA Technical Paper 2489 [N85-28656/NSP], "Convergence of Newton's Method for a Single Real Equation."*

Copies may be purchased [prepayment required] from the National Technical Information Service, Springfield, Virginia 22161, Telephone No. (703) 487-4650. Rush orders may be placed for an extra fee by calling (800) 336-4700. The report is also available on microfiche at no charge. To obtain a microfiche copy, Circle 17 on the TSP Request Card.
MFS-27124

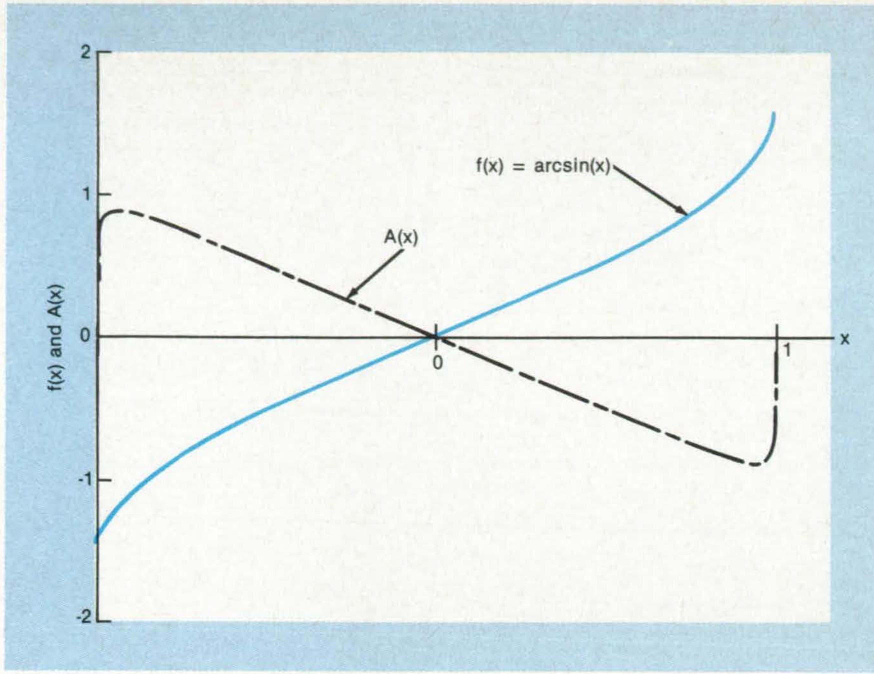

The **Function and Associated Function** for the arcsin(x) illustrate the convergence of Newton's method in the interval between $x_p = -1$ and $x_p^* = 1$.

Books and Reports

These reports, studies, and handbooks are available from NASA as Technical Support Packages (TSP's) when a Request Card number is cited; otherwise they are available from the National Technical Information Service.

Five-Parameter Bivariate Probability Distribution

Theory and applications are discussed.

A NASA technical memorandum presents four papers about the five-parameter bivariate gamma class of probability distributions. With some overlap of subject matter, the papers address different aspects of the theory of these distributions and the use of them in forming statistical models of such phenomena as wind gusts.

The first paper, "A Note on the Ratio of Positively Correlated Gamma Variates," derives the density and the distribution functions for the ratio of positively-correlated gamma variates using a modification of Jensen's bivariate gamma distribution. The expressions for the moments differ from those given by some previous authors, but all the expressions are identical when the variates are uncorrelated. One advantage of this representation lies in the ability to compute the cumulative distribution function of the ratio. In addition, this function has potential for use in testing for the equality of shape parameters in a particular family of bivariate gamma distribution functions.

The second paper, "A Method for Determining If Unequal Shape Parameters Are Necessary in a Bivariate Gamma Distribution," describes a procedure to help an experimentalist in deciding between four and five parameters in a Jensen-type bivariate gamma distribution. The procedure is based on the properties of the cumulative distribution function for the ratio of correlated gamma-distributed variates. A preliminary evaluation showed promise, even though the procedure is not universally applicable.

The third paper, "A Differential Equations Approach to the Modal Location for a Family of Bivariate Gamma Distributions," gives analytical and numerical methods for determining the location of the mode as a function of the parameters of a class of bivariate gamma distributions. The authors derive new theorems and use them to calculate modal-location functions in numerical examples.

The fourth paper, "Analysis of Wind Gust Data," summarizes the analysis of wind-gust magnitude and length data, using mathematical and statistical procedures developed for bivariate gamma

distributions. The data were partitioned according to altitude and analyzed by univariate and multivariate techniques. Neither the normal nor the bivariate gamma class of distributions was found acceptable at all altitudes for all wind components. However, both classes may provide acceptable results for defining constraints in such problems as designing aircraft and spacecraft to withstand large wind-gust loads.

This work was done by J. D. Tubbs, D. W. Brewer, and Orvel W. Smith of **Marshall Space Flight Center**. *Further information may be found in NASA TM-82550 [N84-15866/NSP], "Some Properties of a Five-Parameter Bivariate Probability Distribution."*

Copies may be purchased [prepayment required] from the National Technical Information Service, Springfield, Virginia 22161, Telephone No. (703) 487-4650. Rush orders may be placed for an extra fee by calling (800) 336-4700. The report is also available on microfiche at no charge. To obtain a microfiche copy, Circle 20 on the TSP Card.
MFS-27061

Codes With Parity Conditions on Subsets of Coordinates

New theorems aid the search for efficient code alphabets.

A paper discusses the theory of finding the largest binary codes 2k bits in length, in which all words differ from each other in at least d places and in which words truncated by ignoring certain subsets of bit positions belong to shorter linear codes. This theoretical work was motivated by the search for binary codes for the American National Standard Code for Information Interchange (ASCII) control characters used in simple protocols for transferring files between microcomputers.

The general codes are characterized by the functions A, B, and C, that specify the size (that is, the number of code words) of a given code. Specifically, A (2k,d) = the largest size of a binary code of length 2k and minimum distance ≥d. If each code word is required to contain an even number of ones in its first k and in its last k bits, then the size of the code is given by B (2k,d). If each code word is required to contain an even total number of ones (regardless of position), then the size of the code is given by C (2k,d). Because case B is included in case C and case C is included in case A, B (2k,d) ≤ C (2k,d) ≤ A (2k,d).

The codes of case B are of principal interest in the solution of the ASCII problem, in which control characters are to be transmitted as pairs of 8-bit ASCII characters. Relying heavily on matrix and vector-space theory, the authors derive several theorems and lemmas about these codes, including notably the following:

- When the integer k is even, B (2k = 4n, d = 2n) = 8n, provided that a 4n-by-4n Hadamard matrix exists.
- When k is odd, then B (2k = 4n, d = 2n) ≤ 8n − 4, or = 8n − 4 if a 4n-by-4n Hadamard matrix exists.

The latter theorem is the main one and is applied to the construction of a code incorporating two eight-bit ASCII characters. Two bits are constants of the desired set of characters and are therefore discarded, leaving a total of 2k = 12 bits, of which two are parity bits. Since 4n = 12, n = 3, and the maximum number of words in such a code is given by B_{max} = (8 × 3) − 4 = 20. This type of code enables the correction of up to 2 erroneous bits and the simultaneous detection of a third erroneous bit in two characters transmitted together.

This work was done by Ed Posner and Zinovy Reichstein of Caltech for **NASA's Jet Propulsion Laboratory**. *To obtain a copy of the report, "Codes With Parity Conditions on Subsets of Coordinates," Circle 21 on the TSP Request Card.*
NPO-16572

LEADER

Sometimes it's hard to go back for a scope!

LBO-325 CRT is shown actual size.

60-MHz full-function field-service Attache Case Oscilloscope is so light and small it will be taken everywhere, every time.

LBO-325 packs all the power and performance of a cumbersome, backbreaking, 60-MHz workbench oscilloscope into an easy-to-carry, ultra-compact, featherweight unit. Although its 3½-inch CRT is as big and clear as screens on large field-service scopes– LBO-325 weighs only 9 lbs. So it won't weigh field-technicians down, no matter how far afield they go! LBO-325 is so small it fits inside a 3-inch deep attache case with room to spare for a multimeter, service manuals and some tools. The ideal full-function scope for a cramped work area or crowded bench.

Reduces the cost of service calls.

Time is money. A scope left in the vehicle takes time to retrieve. One kept in the shop causes repeat service calls. The LBO-325 Attache Case Oscilloscope is so easy to carry and use, techs will take it everywhere, every time. And the time saved translates into extra profits for years to come.

Outperforms all other portables:

• 60 MHz • Dual channel • ALT TIME BASE simultaneously displays main waveform and any expanded portion • ALT TRIG for stable display of. 2 asynchronous signals • Bright, sharp 12-kV trace • Large 3½-inch PDA CRT • Illuminated graticule • Comprehensive triggering • TV-V and TV-H sync separators • Variable trigger hold-off • Delay line shows sharp leading edges • CH-1 output drives low-sensitivity instruments • Measures only 3 x 9 x 11⅜ inches • Weighs 9 lbs.

Two-year warranty.

Built tough to provide long use, LBO-325 is backed by Leader's 30-year reputation for reliability and by factory service depots on both coasts.

Call toll-free
(800) 645-5104
In NY State
(516) 231-6900

Request an evaluation sample, our latest Test Instrument Catalog with over 100 outstanding products, the name and address of your nearest "Select" Leader Distributor, or additional information.

For professionals who know the difference. LEADER Instruments Corporation

380 Oser Avenue
Hauppauge, New York 11788
Regional Offices: Chicago, Dallas
Los Angeles, Boston, Atlanta
In Canada call Omnitronix Ltd.
(514) 337-9500

For Product Demonstration Circle RAC No. 443
For Product Information Circle RAC No. 444

Life Sciences

Hardware, Techniques, and Processes

Books & Reports

Filter Bed of Packed Spheres

Spheres are sized and treated for the desired sieve properties.

NASA's Jet Propulsion Laboratory, Pasadena, California

A proposed filter would be constructed from densely packed spheres restrained by screens (see figure). Hollow gas-filled plastic or metal spheres would normally be used. These can be manufactured within one percent or better diameter tolerance. Normally, all the spheres in a filter would be of the same nominal diameter.

The spheres could be sintered together, thereby eliminating the need for screens. In most cases, however, it is better to retain the spheres by screens alone, thereby making it possible to remove the spheres for cleaning, chemical treatment, or replacement.

The passages formed by the interstices between the packed spheres have well-defined widths due to the close control of sphere diameters. Therefore, such a filter could be used as a sieve to pass only particles smaller than a given size or to retain particles larger than that size. In the case of cells or other biological materials, the new filter may be preferable to older screen-type filters, which can damage the cells or other filtrate particles.

The spheres could be given special surface treatments, depending on the intended use. Coatings that have affinity for certain constituents (for example, blood or blood fractions) could be applied. Palladium could be used to filter hydrogen out of an effluent gas mixture. Catalytic coatings or multilayer, multipurpose coatings are also possible.

Given such design constraints as the maximum tolerable differential pressure, the desired flow rate, and the anticipated

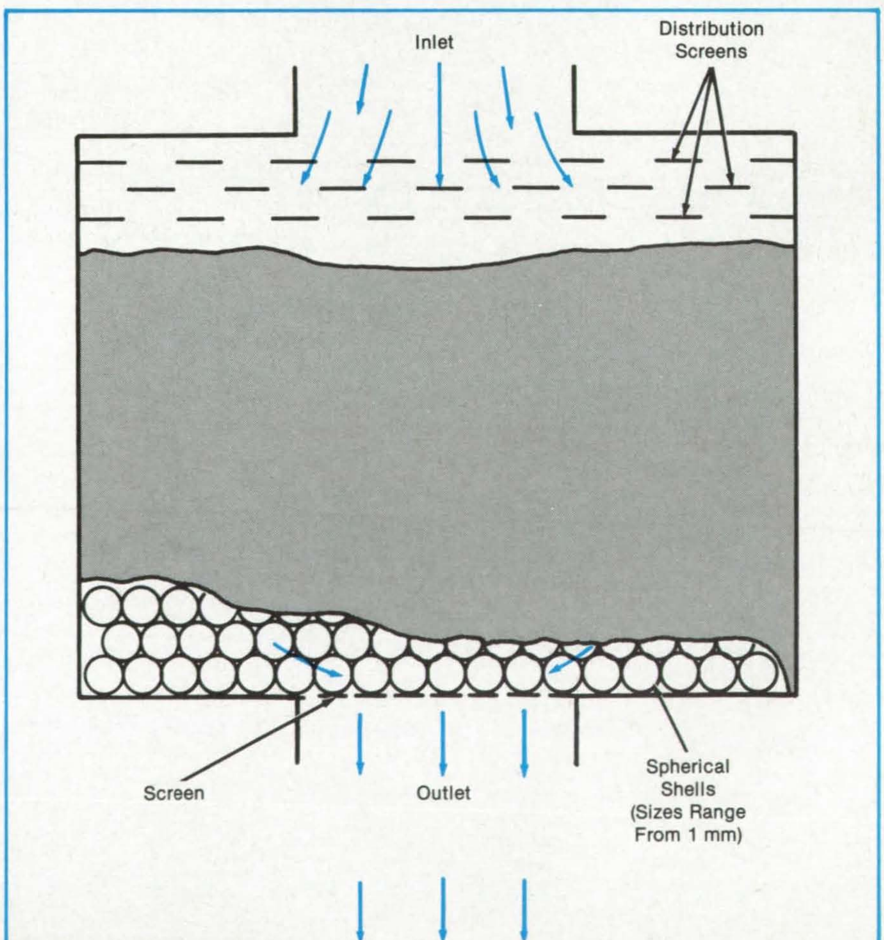

Packed Spheres Retained by Screens form a filter or sieve. The dimensions and surface coatings of the spheres are selected to provide the desired physical and chemical properties.

particle-size distribution in the fluid, a filter might be designed by a suitable choice of the number of layers of spheres, the size of the spheres, and the dimensions of the container. The options available under the filter concept make it fairly easy to design for a specific application.

This work was done by Daniel D. Elleman and Taylor G. Wang of Caltech for **NASA's Jet Propulsion Laboratory**. *For further information, Circle 47 on the TSP Request Card.*

Inquiries concerning rights for the commercial use of this invention should be addressed to the Patent Counsel, NASA Resident Office-JPL [see page 29]. Refer to NPO-15906.

Books and Reports

These reports, studies, and handbooks are available from NASA as Technical Support Packages (TSP's) when a Request Card number is cited; otherwise they are available from the National Technical Information Service.

Contrast-Sensitivity Research

The spatial-frequency spectrum of patterns changes the visibility of spatial phase differences.

A report presents a study of the visual effects of the frequencies of luminance patterns and particularly how frequency components affect the visibility of spatial phase differences over several octaves. The study should be of interest to researchers engaged in the development of algorithms relating to visual processing in robots, the incorporation of human factors in the design of visual displays, and the development of a set of rules the visual system uses to reconstruct a three-dimensional perception from a two-dimensional neural representation.

The psychophysical study made use of a visual-testing instrument (VTI), a minicomputer to control the VTI, and a cathode-ray tube to display the visual stimuli. The cathode-ray tube was surrounded by a light-green cardboard. The tests were governed by a two-interval, forced-choice paradigm. Both intervals contained test gratings of the same frequency added to the same background grating and differed only in the spatial phases between the test and background gratings. The difference between the spatial phases was fixed at 90° throughout the study. This difference was set by shifting the peak luminance of the test grating one-eighth of a period of the fundamental frequency of the background to the left (left-shifted stimulus) or one-eighth of a period to the right (right-shifted stimulus). Both single- and multiple-frequency backgrounds were used.

In the experiments, the spatial-frequency components over a four-octave range affected the visibility of spatial phase differences. When the spatial frequency of the test and background gratings differed by one octave or less, phase differences were more visible (in certain frequency combinations) than they were when the frequencies differed by more than an octave. Phase differences were visible at low contrasts over a three-octave range of test frequencies when the test and background frequencies were harmonically-related and when the spatial period of the background was wide.

Practice increased the ability of the test subject to discern the phase differences, primarily for test and background frequencies within one octave of each other. When such practice consisted of scrutinizing spatial windows of different widths, monitoring the directions of shifts in the positions of small luminance differences, and memorizing several different orderings of light and dark bars, it facilitated phase discrimination for multiple-frequency gratings, spanning a much wider range of frequencies than would otherwise be possible. These results are consistent with the notion that the visibility of phase differences is processed by some combination of even and odd symmetric cells in the striate cortex tuned to a wide range of different spatial frequencies.

This work was done by Teri A. Lawton of Caltech for **NASA's Jet Propulsion Laboratory.** *To obtain a copy of the report, "The Spatial Frequency Spectrum of Patterns Changes the Visibility of Spatial Phase Differences," Circle 39 on the TSP Request Card.*
NPO-16643

Subject Index

BEI's LED-equipped Optical Encoders. Proven thru Time and Space.

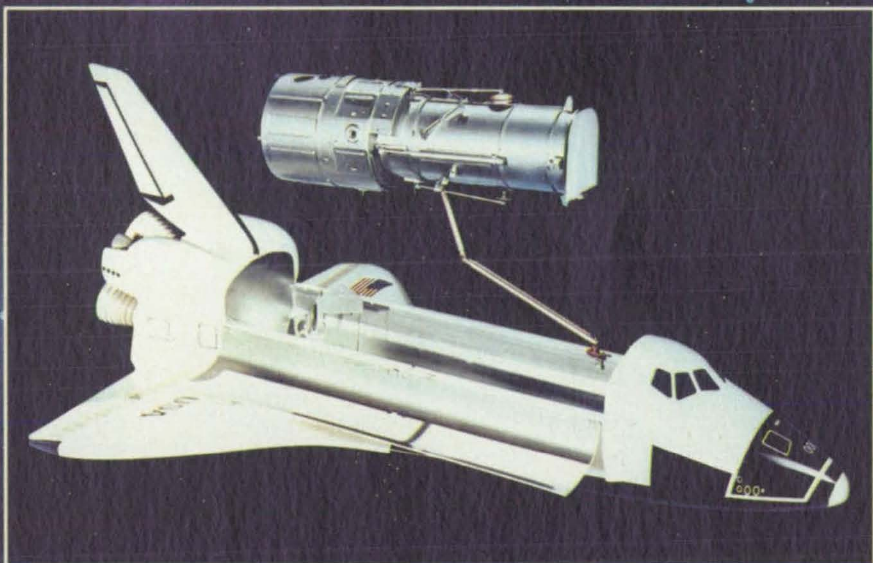

BEI's LED-equipped optical encoders help position the space shuttle arm and provides guide star position data on NASA's Hubble Space Telescope.

This totally integrated motor-encoder system for the Hubble space telescope provides resolution and accuracy to 21 bits.

The space shuttle's remote manipulator arm uses high-reliability BEI encoders.

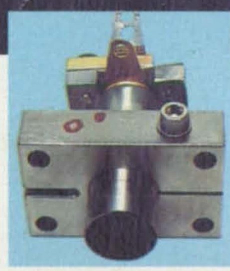

LED read station with optics.

Our remarkable code disk, unequaled for accuracy in the world ... and beyond.

BEI introduced the first 19-bit LED light source encoder design to NASA almost twenty years ago. We've both traveled a long way since then.

Our LED-equipped "pancake" encoders designed for the space shuttle in 1974 have reliably helped position the remote manipulator arm on many successful missions. Only 1.6" thick including electronics, they offer a direct read of 16-bits resolution and accuracy.

In 1979, BEI's Ultra-Loc® precision drive with LED-equipped motor-encoders were selected for the space telescope's fine guidance system. This lightweight beryllium motor-encoder is totally integrated including motor commutation. It provides resolution and accuracy to 21-bits — with rotational drive speeds varying from 0.5 arcseconds/second (one revolution every 30 days), to 16384 arcseconds/second. The design life is ten years.

Our long established systems and procedures are in compliance with quality criteria NHB-5300.4 (1B) and MIL-Q-9858A, and high reliability criterion MIL-STD-785. Contact BEI for more details.

BEI Motion Systems Co.

BEI

Digital Products Division

BEI Motion Systems Co. • Digital Products Division • P. O. Box 3838 • Little Rock, Arkansas 72203 • (501) 851-4000

Circle Reader Action No. 337

Letters

The "Letters" column is designed to encourage a wide exchange of ideas among *NASA Tech Briefs* readers. To contribute a request for information or to respond to such a request, use the feedback cards in this issue, or write or call: Manager/Technology Transfer Division, P.O. Box 8757, Baltimore/Washington International Airport, MD 21240; (301) 859-5300. While we can print only a small number of letters, we will endeavor to select those that are of varied and wide interest.

IDEAS WELCOME

I feel that, working for a NASA contractor, I should be able to submit items to Tech Briefs. *May I?*

Clark Dunson
Payload Engineer
Lockheed Space Ops.
VAFB, CA

A number of *NASA Tech Briefs'* readers have inquired about the procedures for submitting items of technical interest to the journal. If the item you're referring to is part of the work you did under a NASA contract, then you should speak to your project manager about reporting the item to NASA under the contract's new technology reporting clause. In this case, your project manager would forward the item to the NASA contract manager, who would in turn report it to the technology utilization officer at the NASA field center that sponsored the contract. The technology utilization officer would then determine whether the item is appropriate for publication in *Tech Briefs*.

If you're referring to items of technological interest that have been developed, either at work or on your own time, independently of NASA contracts, you can submit them directly to the editor of *NASA Tech Briefs* in the form of a letter. (You might need to obtain your company's approval if the item was developed as part of your job.) *NASA Tech Briefs* would like to establish a forum for readers to exchange ideas, and feels the "Letters" column is the best place to start. Please send your letters to the Editor, NASA Tech Briefs, 41 E. 42nd Street, Suite 921, New York, NY 10017, and include a phone number where you can be contacted for follow-up purposes.

PATENT COMMENTS

Information in Tech Briefs *has more than once pointed out ways to improve our products—aerosol and particulates sampling equipment. Our experience has been that the summaries in* Tech Briefs *are themselves sufficient to point the way. More detailed support packages often turn out to be of no additional help, because key details are usually missing. Beyond that point, it becomes nebulous on how further details may be obtained—who really has the information that counts and whether the originator is truly willing to pass on the information.*

That situation casts a great shadow on whether it's worthwhile to pursue any licensing possibility. Oftentimes, the originator may want to start his own business on the side using the technology and is silently a potential competitor. NASA should, as a policy, caution the people submitting tech briefs that they themselves are not expected to exploit it commercially while still working for NASA.

William Chiang
President
California Measurements, Inc.
Sierra Madre, CA

Tech Briefs *needs to inform clearly which briefs are available for licensing and which briefs are not.*

Dr. C. Fernandez
President
TWT Co.
Tempe, AZ

The fastest way to obtain clear information about the possibilities of licensing a technology published in *NASA Tech Briefs* is to contact the Patent Counsel at the NASA field center that sponsored the research. The names, addresses and phone numbers of these individuals are listed in every issue (page 29, this issue).

Before a technology is published in *Tech Briefs*, NASA has already assessed its "patentability." Preliminary information concerning the patent status of various inventions appears in italics at the end of each brief. If no mention is made of patent or licensing rights, then you can assume it's legal to apply the technology without obtaining NASA's permission.

In any case, if you still have further questions, contact NASA's Patent Counsels. They have more timely information and are available to answer your questions.

Advertiser's Index

***RAC** stands for **Reader Action Card.** For further information on these advertisers, please circle the RAC number on the Reader Action Card elsewhere in this issue. This index has been compiled as a service to our readers and advertisers. Every precaution is taken to ensure its accuracy, but the publisher assumes no liability for errors or omissions.

Circle Reader Action No. 378

ABOUT THE NASA TECHNOLOGY UTILIZATION PROGRAM

Thumb Index

This document was prepared under the sponsorship of the National Aeronautics and Space Administration. NASA Tech Briefs is published quarterly and is free to engineers in U.S. industry and and to other domestic technology transfer agents. It is both a current-awareness medium and a problem-solving tool. Potential products. . . industrial processes. . . basic and applied research. . . shop and lab techniques. . . computer software. . . new sources of technical data. . . concepts. . . can be found here. The short section on New Product Ideas highlights a few of the potential new products contained in this issue. The remainder of the volume is organized by technical category to help you quickly review new developments in your areas of interest. Finally, a subject index makes each issue a convenient reference file.

Further information on innovations—Although some new technology announcements are complete in themselves, most are backed up by Technical Support Packages (TSP's). TSP's are available without charge and may be ordered by simply completing a TSP Request Card, found at the back of this volume. Further information on some innovations is available for a nominal fee from other sources, as indicated. In addition, Technology Utilization Officers at NASA Field Centers will often be able to lend necessary guidance and assistance.

Patent Licenses—Patents have been issued to NASA on some of the inventions described, and patent applications have been submitted on others. Each announcement indicates patent status and availability of patent licenses if applicable.

Other Technology Utilization Services—To assist engineers, industrial researchers, business executives, Government officials, and other potential users in applying space technology to their problems, NASA sponsors Industrial Applications Centers. Their services are described on pages 28-29. In addition, an extensive library of computer programs is available through COSMIC, the Technology Utilization Program's outlet for NASA-developed software. See special section on computer programs on page 70.

Applications Program—NASA conducts applications engineering projects to help solve public-sector problems in such areas as safety, health, transportation, and environmental protection. Two applications teams, staffed by profesionals from a variety of disciplines, assist in this effort by working with Federal agencies and health organizations to identify critical problems amenable to solution by the application of existing NASA technology.

Reader Feedback—We hope you find the information in *NASA Tech Briefs* useful. A reader-feedback card has been included because we want your comments and suggestions on how we can further help you apply NASA innovations and technology to your needs. Please use it; or if you need more space, write to the Manager, Technology Transfer Division, P.O. Box 8757, Baltimore, Maryland 21240-0757.

Advertising Reader Service—Reader Action Card (RAC): For further information on the advertisers, please circle the RAC number on the separate Reader Action Card in this issue.

Change of Address—If you wish to have *NASA Tech Briefs* forwarded to your new address, use the Subscription Card enclosed at the back of this volume of *NASA Tech Briefs*. Be sure to check the appropriate box indicating change of address, and also fill in your identification number (T number) in the space indicated.

Mission Accomplished

Through the technology transfer process, many of the systems, methods and products pioneered by NASA are re-applied in the private sector, obviating duplicate research and making a broad range of new products and services available to the public.

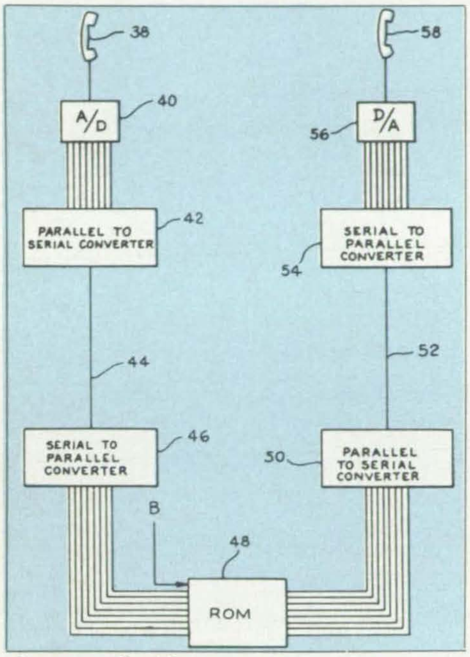

A new method for transmitting high quality audio signals over long distances has been developed at Kennedy Space Center.

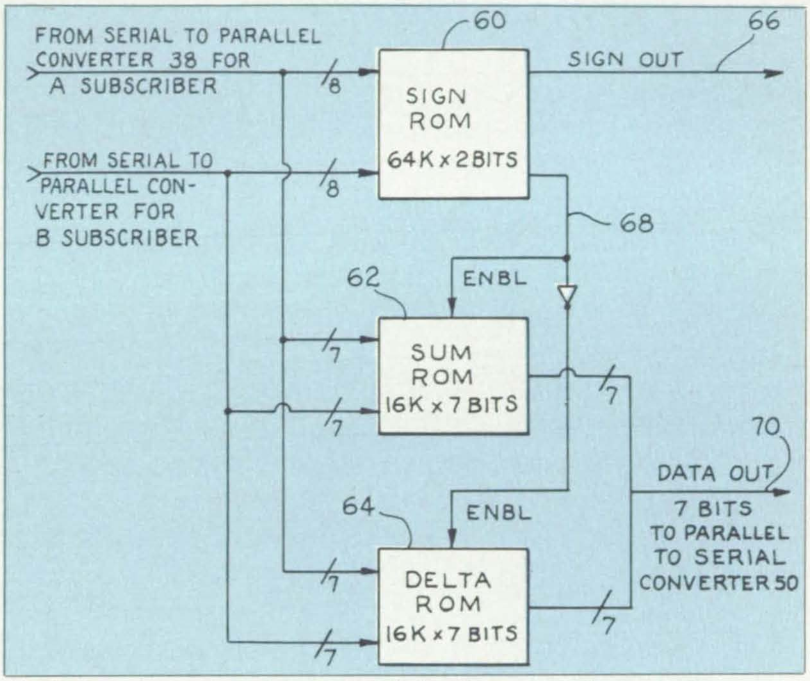

To eliminate redundant data and minimize storage requirements, the conference calling system utilizes a sign ROM, a sum ROM and a delta or difference ROM to determine the output-sign bit.

Kennedy Space Center's approach to technology development differs from that of its NASA counterparts. Compared to Langley, Lewis and Ames, for example, where research and development are longstanding traditions, Kennedy Space Center's programs are much more operations-oriented. And because the nature of these operations—spacecraft assembly and launch—is somewhat unique, Kennedy's technology development programs tend to result in similarly unique applications.

A case in point is the recently patented conference calling system developed by Frank Byrne, Kennedy Space Center's deputy director of information systems. Byrne's "Method and Apparatus for Operating on Companded PCM Voice Data" has the potential to link up to 2,000 people in a single conference call. While it's true that few organizations need to simultaneously involve 2,000 people in a conference call, it's also true that, for Kennedy's purposes, commercially available conference call systems are not quite up to par. For one thing, the transmitted audio signals tend to degrade in relation to noise when a large number of parties are involved, and secondly, this effect is heightened when the signal must be transmitted over long distances.

Ongoing commercial development efforts have addressed the signal-to-noise degradation, resulting in innovative digital signal-transmitting devices. While these devices reduce the amount of signal interference for a limited number of parties and over short distances, they still fall short of Kennedy Space Center's requirement to link a large number of people at varying distances with minimum interference.

Frank Byrne's development efforts addressed these particular requirements and resulted in a method for combining a multiplicity of signals with a minimal amount of noise. The heart of his invention is an innovative read-only memory (ROM), which both reduces the number of signal-processing steps and eliminates redundant data, minimizing the ROM's storage requirements and resulting in a clearer signal.

To further minimize interference and to facilitate transmission over long distances, Byrne incorporated a multiplying-ROM subsystem which compensates for differences in signal amplitude between system subscribers. The subsystem multiplies the signal's amplitude prior to processing to increase its volume, and enables subscribers at varying distances to receive signals of equal clarity.

The new conference calling system will advance Kennedy's already sophisticated communications network. In addition, it's expected that the signal-combining technology will be licensed and adapted for commercial purposes, eventually replacing current systems and enabling the general public to talk shop along the leading edge of technology. □


HONEYWELL AEROSPACE AND DEFENSE
This photograph has been retouched to safeguard proprietary information.
©1984 Honeywell Inc.